APPLICATION OF SEISMIC MONITORING IN CAVING MINES - CASE STUDY OF TELFER GOLD MINE

by

Yousef Abolfazlzadeh

A thesis submitted in partial fulfillment
of the requirements for the degree of
Master of Applied Science (M.A.Sc.) in Natural Resources Engineering

The School of Graduate Studies
Laurentian University
Sudbury, Ontario, Canada

THESIS DEFENCE COMMITTEE/COMITÉ DE SOUTENANCE DE THÈSE

Laurentian Université/Université Laurentienne
School of Graduate Studies/École des études supérieures

Title of Thesis Titre de la thèse	APPLICATION OF SEISMIC MONITORING IN CAVING MINES - CASE STUDY OF TELFER GOLD MINE
Name of Candidate Nom du candidat	Abolfazlzadeh, Yousef
Degree Diplôme	Master of Applied Science

Department/Program Département/Programme	Natural Resources Engineering	Date of Defence Date de la soutenance	September 20, 2013

APPROVED/APPROUVÉ

Thesis Examiners/Examinateurs de thèse:

Dr. Marty Hudyma
(Supervisor/Directeur de thèse)

Dr. Ming Cai
(Committee member/Membre du comité)

Dr. Shailendra Sharan
(Committee member/Membre du comité)

Dr. Xiaolin Yao
(External Examiner/Examinateur externe)

Approved for the School of Graduate Studies
Approuvé pour l'École des études supérieures
Dr. David Lesbarrères
M. David Lesbarrères
Director, School of Graduate Studies
Directeur, École des études supérieures

ACCESSIBILITY CLAUSE AND PERMISSION TO USE

ABSTRACT

Comprehensive and reliable seismic analysis techniques can aid in achieving successful inference of rockmass behaviour in different stages of the caving process. This case study is based on field data from Telfer sublevel caving mine in Western Australia. A seismic monitoring database was collected during cave progression and breaking into an open pit 550 m above the first caving lift.

Five seismic analyses were used for interpreting the seismic events. Interpretation of the seismic data identifies the main effects of the geological features on the rockmass behaviour and the cave evolution. Three spatial zones and four important time periods are defined through seismic data analysis.

This thesis also investigates correlations between the seismic event rate, the rate of the seismogenic zone migration, mucking rate, Apparent Stress History, Cumulative Apparent Volume rate and cave behaviour, in order to determine failure mechanisms that control cave evolution at Telfer Gold mine.

Keywords: sublevel caving, mining-induced seismicity, caving mechanics

ACKNOWLEDGEMENTS

I would like to take this opportunity to acknowledge and thank those who made this work possible.

I sincerely thank Newcrest Mining Limited for making available the rock mechanics data, seismic data and technical documents associated with the Telfer sublevel caving mine.

I would like to acknowledge the Australian Centre of Geomechanics for use and support of their MS-RAP software.

Sincere thanks to Dr. Ming Cai, Dr. Shailendra Sharan, and Dr. Mike Yao for their constructive comments on my research and for their efforts in reviewing this thesis.

My utmost gratitude to my supervisor, Dr. Martin Hudyma, associate professor and academic advisor for Mining Engineering at Laurentian University, whose sincerity and encouragement I will never forget. Dr. Hudyma has been my inspiration as I hurdle all the obstacles in the completion this research work.

I would like to express my sincerest appreciation to my family, my father and mother, Ghaffar and Sari, and to my brother and sister, Emad and Mehrnaz.

Last but not the least, I thank my friends, especially Emad J, Pooneh T, Mehdi F, Peyman A, Sina T (R.I.P), Hesam E and Omid M, for their support during the dark and cold days.

TABLE OF CONTENTS

LIST OF FIGURES

LIST OF TABLES

1 INTRODUCTION

1.1 Background

1.1.1 Sublevel Caving

Sublevel caving is a bulk underground mining method based on fracturing the mineralized and surrounding rocks under controlled massive caving. In sublevel caving, the ore is divided into sublevels with planned spacing. Development in sublevels is achieved with drifts that cover the entire orebody. The orebody is drilled with longholes in an uphole fan shaped pattern. A slice of ore is fragmented by blasting of the fan holes. The blasted ore falls into the drift where it is loaded and transported to orepasses.

The ore extraction creates a caved-in area in the region above the sublevel. A complete and continuous fracturing process is necessary in the caved area since underground cavities run a high risk of sudden collapse with severe after-effects to the mining operation. Understanding of rockmass behaviour is an essential factor for managing the risks associated with caving methods.

There are few effective means of monitoring rockmass behaviour in caving mines. In recent years, interpretation of rockmass behaviour has been inferred from mining-induced seismicity occurring with the rockmass caving.

1.1.2 Rockmass Monitoring

Rockmass monitoring gives information about the local state and stress conditions. This monitoring can help in better understanding of the rockmass behaviour and in identifying of mining activities that affect the overall mine structure. Finding the location of seismic events provides an insight into the relation between the events and active workplaces conditions, and additionally an insight into the variations of these conditions over the time.

Conventional monitoring methods such as visual observation, geotechnical methods (extensometers and TDR), and stress monitoring can be used for better understanding of the rockmass behaviour. These techniques are only somewhat reliable in caving because of the limited access to install in above the cave, limitations of point measurements in a large volume, and a frequent short life of the instruments.

Some advantages and disadvantages of the seismic monitoring are described in Table 1.1.

Table 1.1 Advantages and disadvantages of the seismic monitoring.

	Advantages	Disadvantages
Seismic Monitoring	Volume monitoring	Not a direct displacement or stress measurement
	Better access	Event parameters interpretation is needed for displacement and stress measurement
	Cave evolution monitoring	Still an evolving technology
	Failure mechanism monitoring	Interpretation techniques are largely empirical
		Uncertainty in interpretation

1.1.3 Seismic Monitoring in Mines

A seismic event is a dynamic stress wave caused by the fracture or deformation of a rockmass. Generally, seismic events can be divided into microseismic and macroseismic events according to their magnitude. Microseismic and macroseismic events are the events with a magnitude less than and larger than 0, respectively. Analysis of the mining-induced seismic data provides four-dimensional information about the rockmass behaviour that helps in better understanding of trends in caving mechanisms. Thus, seismic monitoring can be applied as a tool to monitor rockmass failure processes and interpret the failure mechanism.

Seismic source parameters can present information about:

- Failure mechanism (Domanski and Gibowicz, 2008; Legge and Spottiswoode, 1987),
- Failure process (Glazer and Hepworth, 2004),
- Rockmass damage (Dunlop et al., 2010),
- Caving mechanisms (Duplancic and Brady, 1999),
- Caving rate and cave performance (Glazer and Hepworth, 2007; Trifu et al., 2002; Giovinozzo and Singh, 2010; Hudyma et al., 2007b).

Among the different case studies of rockmass behaviour applying the interpretation of the seismic events, only Trifu et al. (2002) and Giovinazzo and Singh (2010) used seismic interpretation for the sublevel caving mines. Furthermore, only in the Telfer mine did the sublevel cave propagate into an open pit (Giovinazzo and Singh, 2010).

In most past studies, caving analysis has largely been based on event location and event time. Seismic monitoring data is rich with information about seismic source parameters; however, this has been rarely investigated in past caving mining seismic analysis.

1.2 Thesis Objectives

The objective of this thesis is to provide information about cave mechanisms in different stages of the cave evolution using seismic data analysis. This information helps in a better understanding of the rockmass behaviour and predicting caveability with respect to opening of the first lift, mucking rate, seismogenic zone migration, event rates and magnitudes.

This thesis focuses on analysis of the variations in event magnitude, frequency, Apparent Stress, Energy Index, Cumulative Apparent Volume, energy and moment of the seismic data from Telfer Gold mine. These analyses provide meaningful information about rockmass failure, the level of mining-induced stress, and the relative level of deformation related to one or many seismic events.

1.3 Thesis Structure

The purpose of this thesis is to present the rockmass behaviour during the initial blasting, cave initiation, cave propagation and breakthrough. An overview of the thesis chapters is given in Table 1.2.

Table 1.2 Overview of the thesis chapters

Chapter	Title	Summary
1	Introduction	Thesis introduction and scope are presented.
2	Literature Review	A review of literature on history of seismic monitoring, general objectives of seismic monitoring in caving mines and contributions of seismic monitoring towards understanding rockmass performance in different mines is provided.
3	Seismic Analysis for Telfer Gold Mine	A summary of Telfer Gold mine geology, orebody geometry, mining methods, seismic data assessment and different cave evolution periods is provided.
4	Caving Mechanisms	Results from analysis of Magnitude-Time history, Frequency- Magnitude, S:P energy ratio, Apparent Stress History(ASH), Energy Index, Cumulative Apparent Volume (CAV) and Energy-Moment of seismic events during the four major cave evolution periods are assessed.
5	Relation between Event rate/ Mucking rate/ CAV rate and ASH	Strong/Weak correlations in the variations of the Event/ Mucking/ CAV and ASH rates are discussed with respect to the caving mechanics.
6	Conclusions and Recommendations	The thesis conclusions with recommendations for further developments in the area of seismic monitoring applications in caving mines are discussed.

2 LITERATURE REVIEW

> "There are two main reasons for monitoring: safety, and optimization of mine layout and sequence. Monitoring usually pays for itself by saving lives, reducing accidents, and preventing dilution of ore, and costly delays."
>
> John Franklin (1990)

2.1 Introduction

Excavation of large volumes of rock at a depth disturbs the equilibrium of *in situ* stresses. As cracks are generated and movement of a rockmass initiates along pre-existing fracture planes, these movements can be recorded with a monitoring system.

Time Domain Reflectometry (TDR), extensometers, open holes, caving measurement, and seismic monitoring are the five major geotechnical methods which are routinely used for monitoring cave initiation and propagation. These methods are often used together. TDR is an electrical pulse testing technique to monitor both local extension and local shearing (Dowding et al., 1988). TDR has been applied for the last 30 years in different mines. Extensometers measure the displacements along the axis of the drill hole. Extensometers are divided into single-point and multiple-point extensometers according to their application (Brady and Brown, 1993). Open holes are used for measuring the location of cave back, especially where there is an air gap above the caved ore. A caving measurement system, as a laser-based monitoring system, may be used to measure the cave back profile where access is available (like open void or air gap) and also used to examine undercuts or any unnecessary residual pillars (e.g. de Nicola and Fishwick, 2000).

In order to study the seismic source mechanism and eventually evaluate the rockburst hazard caused by the source mechanism, different seismic analysis methods have been conducted. They all make use of at least one of the independent seismic source parameters such as seismic energy, seismic moment, size, and time or location of event.

2.2 Seismic Monitoring History in Australian and Canadian Mines

In the late 1930's, two researchers L. Obert and W.I. Duvall from the U.S. Bureau of Mines (USBM) carried out sonic studies in a deep hard rock mine. They discovered that a stressed rock pillar appeared to emit micro level sounds (Obert, 1977). A short history of seismic monitoring in Australian and Canadian mines is described in below.

2.2.1 Australian Mines

Australia's first seismic monitoring system was commissioned in May 1994 at Mount Charlotte mine due to occurrence of rockbursts and seismicity over several years. That seismic monitoring system which was a PSS model supplied by CSIR, South Africa, was described by Mikula and Poplawski (1995). In 1996 two other mines, Broken Hill and Northparkes, installed seismic monitoring systems. In contrast with Broken Hill, Northparkes seismic system was used for monitoring the cave evolution (Potvin et al., 2000). Seismic events recorded at Australian mines after 1970's shows that Mount Charlotte mine has experienced 16 large events with Richter magnitude 2.0 or greater (Mikula, 1998). This early monitoring was undertaken with regional earthquake systems, as in-mine seismic monitoring had not yet been established.

In early 2000s, numerous mines in Western Australia started to install seismic monitoring systems. Generally there are two kinds of seismic monitoring systems set up in mines, minewide (MW) and temporary (or portable). Minewide systems can have more than 20 sensors and all are connected to the surface data analysis system. Temporary systems often have up to six sensors and are connected to a remote data collection system in underground (Hudyma et al., 2003).

Pre-mining stress level is one of the great indicators of seismic prone rockmasses. In Western Australian mines, fractures around mining excavation resulting from stress concentration start to appear below 300 m in weaker rocks and below 600 m in stronger rocks (Turner and Beck, 2002). For example, 6000 events were recorded at Broken Hill mine just in two years. Rauert and Tully (1998) described the Broken Hill mine as one of the most frequently occurring of microseismic activity recorded in the Australian Mining Industry. Deep Copper Mine at Mount Isa is located about 1.4 km below the surface. A seismic monitoring system was installed in this mine although no large seismic events recorded in such a deep mine (due to low local stresses).

In Western Australian mines, stresses are high and highly deviatoric (Lee et al., 2001). In several mines like Kundana, Big Bell, Kanowna Belle, and Black Swan the major principal stress is more than 60 MPa. Large numbers of seismic events have been reported from these mines during their mining processes (particularly where the stresses are high).

2.2.2 Canadian Mines

The first use of sub-audible noises for predicting rockbursts was conducted with E.A. Hodgson in Canada in 1923 (Franklin, 1990). By the 1950s, the U.S. Bureau of Mines (USBM) monitoring equipment was considered more of a novelty or "crystal ball" approach than a practical ground control tool (Blake, 1987). More complex monitoring systems (broad-band multichannel tape recorder) which had the ability to locate the source of microseismic events and consequently areas with high concentration of stresses, have been utilized since the 1960s. After ten years, these systems were substituted with computer-based systems. As early as the 1980s, computers which could give the results faster and could produce graphs and plots of microseismic activity that showed the rockmass behaviour (Franklin, 1990).

In Canadian mines, high frequency (HF) systems were tried in conjunction with minewide microseismic systems. HF systems have fewer transducers to monitor local areas for smaller events, from which, larger events may be inferred. The results of monitoring events after development blasts at Creighton and Kidd Creek mines showed that HF systems could indicate high resolution transient of stress changes in local areas in comparison with MW microseismic systems (Butt et al., 2000).

Sudbury in province of Ontario, Canada, is one of the areas of interest for seismic monitoring because of existence of several deep underground mines. Sudbury has more than a 70-year history of large seismic events. Mining-induced stresses, major geological structures are the major sources of seismic events in Sudbury (Hudyma and Beneteau, 2010).

Figure 2.1 shows the number of events with magnitude larger than 2.0, during 2004-2008 at six Vale mines in Sudbury (Thibodeau, 2009).

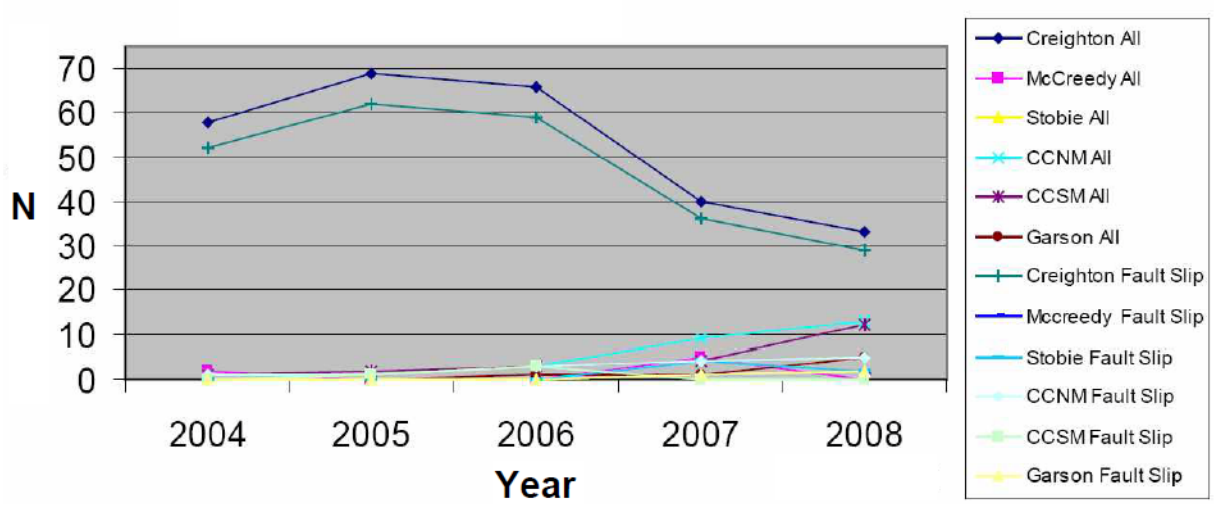

Figure 2.1 Events with magnitude larger than 2, during 2004-2008 at six Vale mines in Sudbury (Thibodeau, 2009).

2.3 Summary of Caving Mechanics

Caving mechanics can be divided into four important categories (Brown, 2003): gravity or release caving, stress caving, subsidence caving, and the combination of these mechanisms. These categories differentiate according to induced stresses types (compressive or tensile), strength of the rockmass, and geometry of the discontinuities.

Gravity or stress release caving happens when the compressive tangential stresses induced in the undercut crown are low or tend to be tensile. Also, when the horizontal *in-situ* stresses are low or decreased as a result of pre-conditioning (slot cutting or blasting), the condition for gravity caving is more favorable. A three dimensional distribution of discontinuities or a low-dip discontinuity with two steeply dipping sets are desired conditions for vertical displacement or sliding on discontinuities.

With ***stress caving***, the tangential stresses are high in comparison with compressive strength of the rockmass and the shear strength of the discontinuities. In this case, brittle fracture of the intact rock occurs.

Where the normal stresses develop on vertical boundaries of a block or the shear strength of the interface is very low, ***subsidence caving*** will happen. In this mechanism, large masses of rock fall down rapidly and the possibility for an air blast increases.

In some situations, the horizontal *in-situ* and tangential stresses induced in the crown of the undercut or cave are high enough to develop clamping forces that inhibit the gravity induced caving. However, such horizontal *in-situ* and tangential stresses are not high compared with the compressive strength of the rockmass. In this situation, caving may be inhibited and a stable arch may develop. Some form of cave induction may be required to weaken the rockmass, relieve the tangential stresses, or induce slip on discontinuities (Kendricks, 1970; van As and Jeffrey, 2000).

In a process named pre-conditioning, hydraulic fracturing or drilling and blasting methodologies are used to alter the inherent characteristics of the rockmass to increase the caving and fragmentation. Furthermore, in block and sublevel caving, caving inducement can be used to assist initial caving or to induce caving where cave propagation is stopped. Boundary slot, boundary weakening and pre-splitting are the common inducement caving techniques.

The first conceptual model of stress caving was described by Duplancic and Brady (1999), using seismic data of Northparkes Mines' E26 Lift 1 block cave, New South Wales, Australia. The model includes the following five regions (Figure 2.2):

Cave Zone: Fallen rock blocks are located in this region. Material in the caved zone provides support to walls of the cave.

Air gap: In continuous caving, the height of the air gap is a function of the caved material and extraction rate.

Zone of loosening: Large-scale displacements of rock occur in this area. Since rocks are highly fragmented, they cannot support the overlying rockmass. No seismicity is recorded within this region. This region at Northparkes Lift 1 (Duplancic and Brady, 1999) was estimated to extend to 15 m from the boundary of cave crown.

Seismogenic zone: An active seismic front occurs due to slip on discontinuities and failure of the rockmass. This behaviour results from the changing stress conditions caused by advancing undercut and the progress of the cave.

Pseudo-continuous domain: Elastic deformation occurs in the rockmass ahead of seismogenic zone.

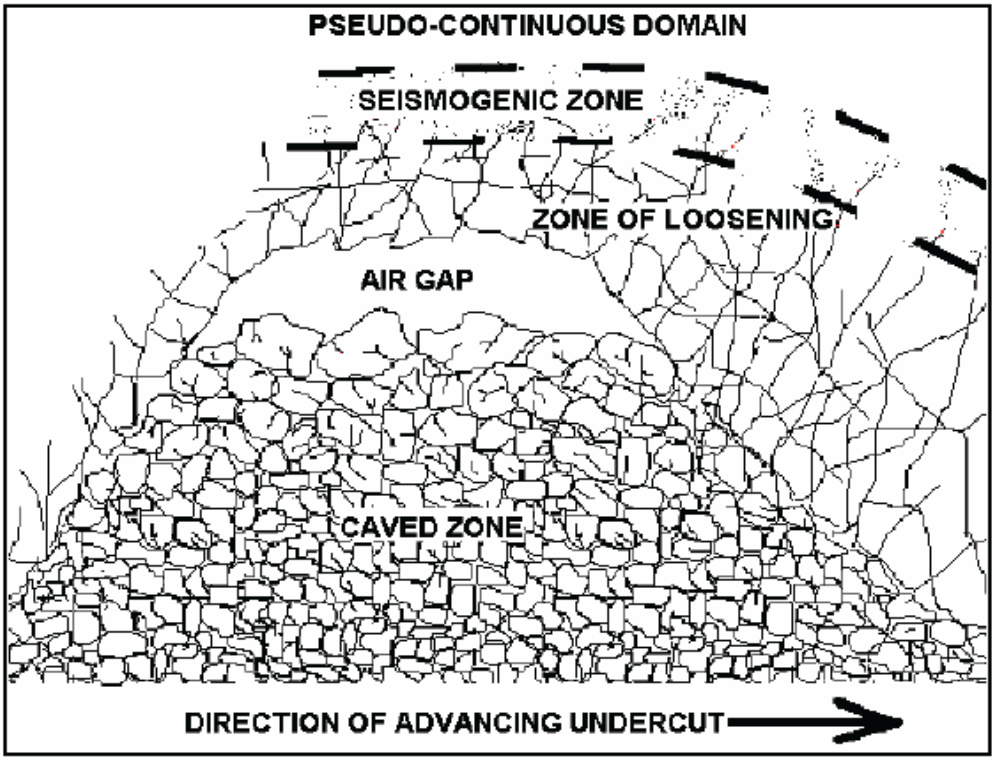

Figure 2.2 Different zones of stress caving conceptual model (after Duplancic and Brady, 1999).

2.4 General Objectives of Seismic Monitoring in Mines

Different mines may have different objectives for seismic monitoring. These objectives may include evaluating the mining process by improving stope sequencing, destress blasting, and ground support. Mendecki et al. (1999) defined several objectives which can be generally realized from seismic monitoring:

Location of Potential Rockbursts: Control areas with an increased risk for rockbursts by identification or analysis.

Prevention: Checking some assumptions during the mine design. For example, proving some sensitive stability parameters such as the orientation of shear and principal stresses.

Control: Verify variations in location and time of seismic parameters. This helps in control measures and managing the re-entry time for personnel.

Warnings: Detect unexpected strong changes in spatial and temporal behaviour of seismic parameters or certain defined characteristic patterns that could lead to dynamic instabilities affecting working places.

Back Analysis: Relating to pillars, mining plans, rates and ways of excavating. It is an important tool for safer and more productive mining.

Seismic monitoring's objectives also can be described in a different way as shown in Figure 2.3. In this description, the goal of seismic monitoring is to find the location of rockmass failure and to understand seismic source mechanism and hazard.

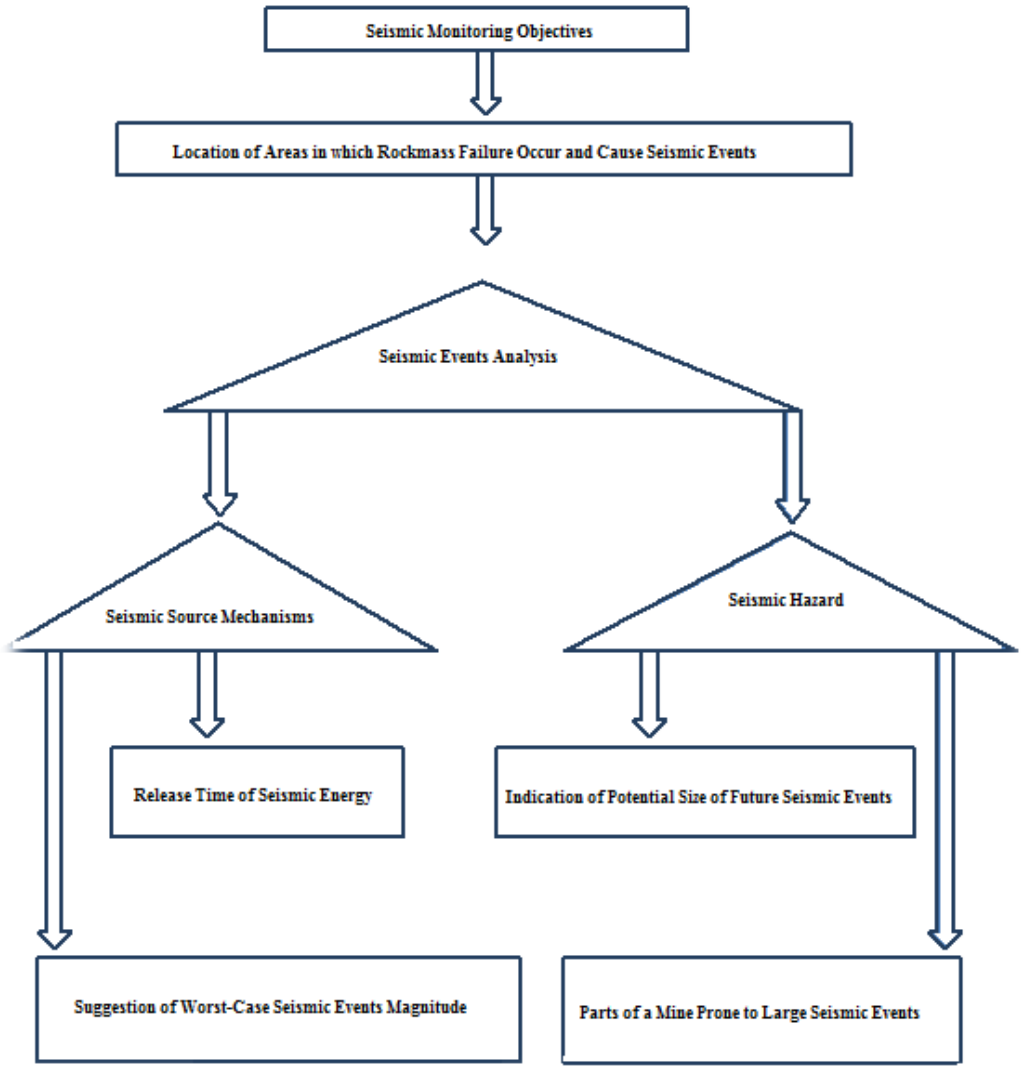

Figure 2.3 Seismic monitoring different objectives (Hudyma, 2010).

In this methodology, there are some important conditions required for success of seismic data analysis (Hudyma, 2010):

- Analysis is much more effective if logical groups of seismic events are analyzed together. By data filtering, some spatial groups of data can be formed according to their common source mechanism. If data are collected from a very wide area such as the entire mine or if more than one failure mechanism is involved, analysis results are more likely to be ambiguous or indeterminate.
- The number of recorded events over a specific period must be adequate to result in reliable conclusions from data analysis. The number of required events depends on the time period that is being investigated.
- The analysis should not depend one or a couple of large seismic events. Seismic monitoring is a means to collect the majority of occurring seismic events that. Large and important seismic events do occur during blasts and are frequently not captured or are poorly captured. Any analysis that is highly dependent upon collecting and interpreting all of the large seismic events is likely not going to give consistent results.

Some of the issues that are particularly related to the seismic monitoring in caving are detailed as follows (Mendecki et al., 1999):

- Limited understanding of radiation processes at seismic sources and incapability of useful information recovery
- Processing of good quality waveforms
- Low sensitivity of seismic instrumentation which results in loss of rock stress and strain information
- Low reliability of a seismic source due to its complexity
- Proper location of seismic sensors around the seismic source
- Inadequate number of triaxial and uniaxial sensors
- Direct waveform techniques that lead to ambiguous results
- Limitations of sampling (event clustering) and quality of seismic data
- Uncertainty regarding the event location and source parameters

2.5 Contribution of Seismic Monitoring towards Understanding Rockmass Behaviour

2.5.1 Event Magnitude

Magnitude is a measure of a seismic event size. Magnitude scales have generally been based on amplitudes recorded over a particular spectral band (Duplancic, 2001).

Some of the commonly used magnitudes are as follows:

- Local magnitude (Richter, 1935) as a measure of the strength of a natural earthquake
- Nuttli magnitude scale (Nuttli, 1973) defined for earthquake and large induced seismic events in Eastern Canada
- Moment magnitude (Hanks and Kanamori, 1979) used for describing the size of a seismic event based on the measured seismic moment.

2.5.2 Frequency Magnitude Analysis

Gutenberg and Richter (1944) proposed a power law relation between frequency and magnitude of events as follows:

$$\log (N(\geq M)) = a - b \times M; \qquad [2.1]$$

where,

$N(M) = \text{Total no. events with magnitude} \geq (M)$

$M = \text{magnitude}$

$a, b = \text{constants}$

As shown in Figure 2.4, the slope of the Gutenberg-Richter frequency-magnitude relation can be used for identifying the seismic source mechanism (b-value). For large populations of seismic events, the b-value is typically close to 1.0. Gibowicz and Kijko (1994) described the x-intercept of the relation (a/b) as the largest magnitude seismic event which could be expected for a given population of seismic data. Fault-slip related seismicity typically has low b-value (often less than

0.8). However, the b-value related to stress change seismic source mechanisms is commonly between 1.2 and 1.5 (Legge and Spottiswoode, 1987).

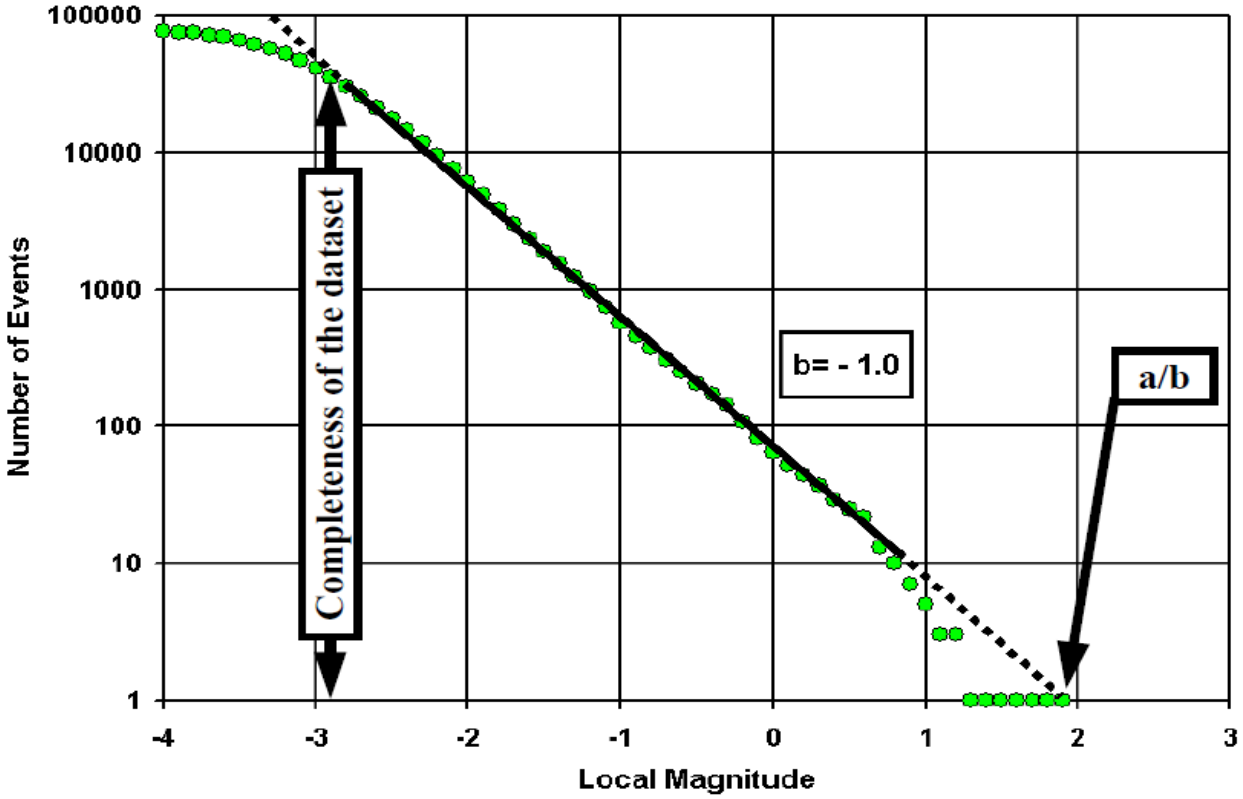

Figure 2.4 Frequency- Magnitude chart and b-value (Hudyma, 2010).

2.5.3 Magnitude –Time History

Plotting magnitudes of events on the y-axis and time on the x-axis can give a good indication of both seismic hazard and seismic source mechanism. In other words, this graph chronologically orders the events as shown in Figure 2.5. Hudyma et al. (2007a) noted that cumulative number of events helps to measure the variations in the event rate (changes in slope of cumulative number of events line).

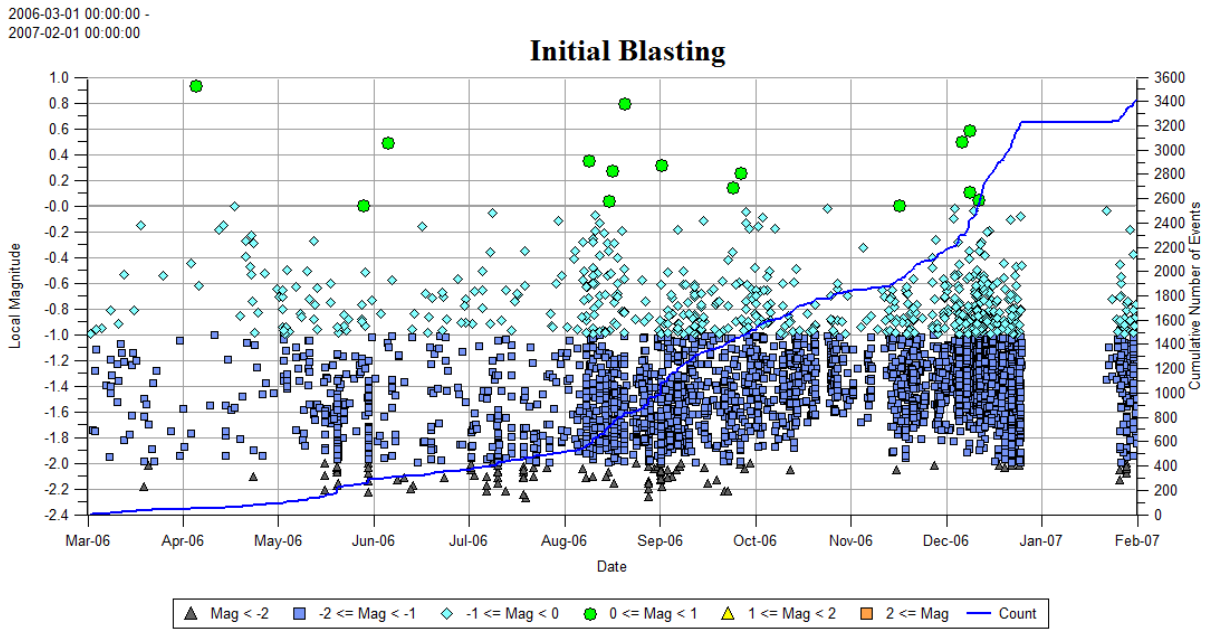

Figure 2.5 Magnitude- Time history and cumulative number of events during initial blasting at Telfer gold mine.

2.5.4 Seismic Energy

The energy release during rock fracturing and frictional sliding comes from the transformation of elastic strain into inelastic strain (Mendecki et al., 1999). This transformation may occur at different rates ranging from slow creep-like events to very fast dynamic seismic events. The average velocity of deformation at the source is up to a few metres per second. Unlike the dynamic sources of the same size, the slow type events have long time duration at the source and thus radiate predominantly lower frequency waves. In terms of fracture mechanics, the slower the rupture velocity is the less energy the event radiates. A quasi-static rupture would radiate practically no energy. Similarly for blasting, smaller blasts make smaller changes to the rockmass or more gradual stress changes so that the response is less dynamic (Mendecki et al., 1999).

Radiated seismic energy is the energy released from the source of the seismic. According to Gibowicz and Kijko (1994), the radiated seismic energy can be calculated for as follows:

$$E = 4\pi\rho_0 c_0 \langle F_c \rangle^2 \left(\frac{R}{F_c R_c}\right)^2 J_c \quad [2.2]$$

where,

E= radiated energy (joules)

ρ_0= rock density (kg/m^3)

c_0= velocity of the wave in rock (m/s)

R= the distance from the seismic source (m)

J_c= the integral of the square of the ground velocity

F_c= an empirical radiation pattern coefficient

Observations from South African mines indicated that most of the seismic energy is contained in the S-waves (Hedley, 1992). Therefore, it was concluded that shear is the predominant failure mechanism. When a seismic event occurs, only about 10% of seismic energy is contained in P-wave. Therefore, this part of energy is often neglected and analysis is based on the S-wave.

2.5.5 S:P Energy Ratio

There are several seismic phases, but only S-waves and P-waves are commonly recorded in mining-induced seismicity. P-waves, or compressive waves, are the first ones which arrive at receivers (accelerometers or geophones). P-waves are the fastest which their velocity depends on medium. They typically travel at speed at 6000 m/s in hard rock (Hudyma et al., 2003). Secondary or S-waves (also called “Shear” waves) move through the body of object like P-waves but they are slower (Figure 2.6). S-waves, in contrast with P-waves, result in transverse ground motion in which they propagate. Typical S-waves propagation speed is in the order of 3500 m/s in hard rock (Hudyma et al., 2003).

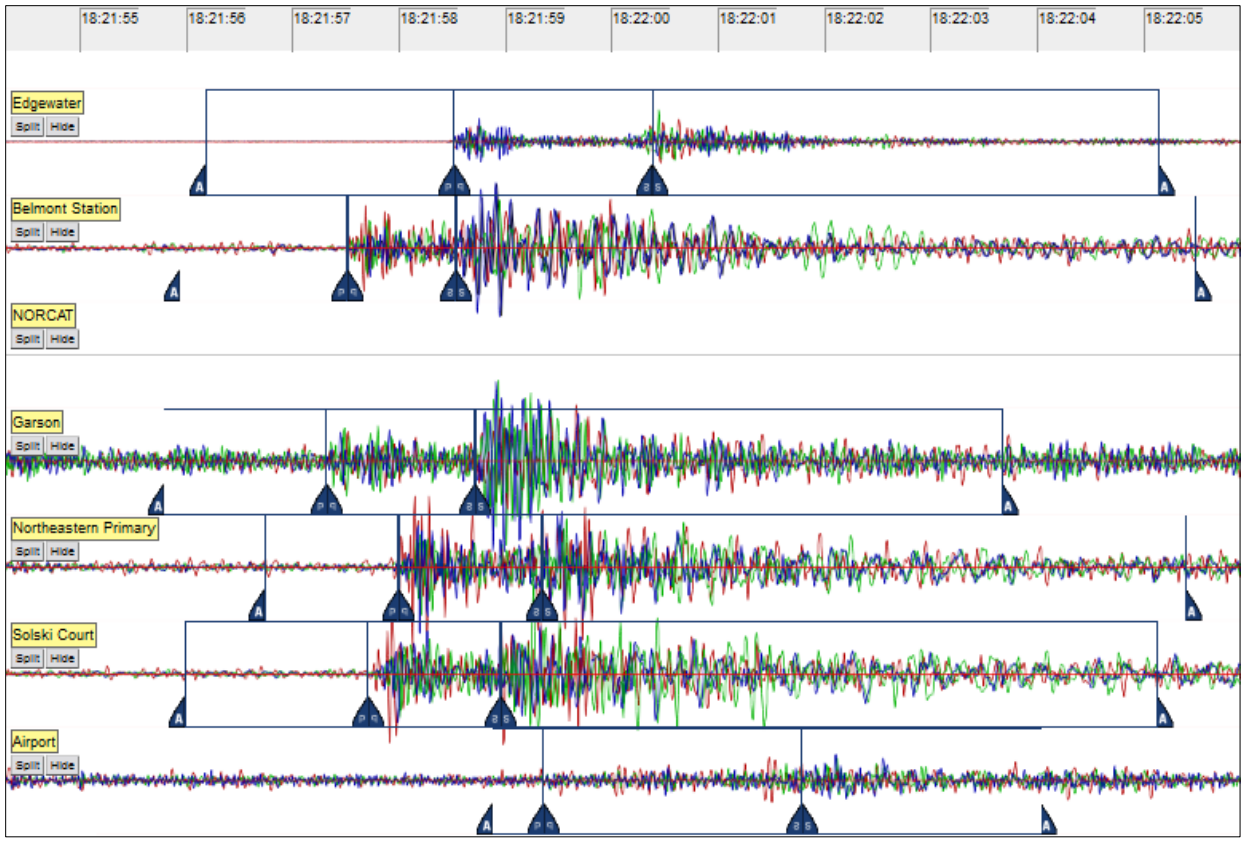

Figure 2.6 The S-wave and P-wave for an event near Sudbury, Ontario, Canada, 2013.

When seismic waves propagate, they carry energy from the source of the shaking outward in all directions. The ratio between S-wave energy and P-wave energy can be an indicator of seismic source mechanism (Urbancic et al., 1992). Seismic energy is proportional to the integral of the square of the vectoral sum of the velocity waveform and can be calculated separately for the P-wave and S-wave (Hudyma et al., 2003). For fault-slip type events, there is considerably more energy in the S-wave than in the P-wave (Boatwright and Fletcher, 1984) with the ratio of the S-wave energy to the P-wave energy frequently greater than 10. Urbanic et al., (1992) noted that for non-shear seismic source mechanisms, there would be a deficiency in S-wave energy or relatively more P-wave energy than for shearing events. For non-shearing event mechanisms such as strain-bursting, tensile failure, and volumetric rockmass fracturing, the ratio of S-wave energy to P-wave energy is frequently in the range of 3 or less (Urbancic et al., 1992).

Generally, S-wave to P-wave energy is plotted as scatter plots on logarithmic charts. Difficulty in interpreting these diagrams leads to the use of cumulative distribution plots. Cumulative distribution plots make it easier to find the percentage of shear and non-shear seismic source

mechanisms for populations of events for comparing different seismic event populations. Scale dependence, or the influence of event size, is a fundamental consideration in analyzing seismic source mechanism. It is important to realize that the smaller and larger events could have different seismic source mechanism. Events directly induced by mine blasting may be the source of the scale dependence problems. Smaller events are potentially caused by stress change due to blasting. Larger events usually have seismic source mechanisms that are different that blast-related mechanisms. However, case studies on Big Bell fault at Big Bell mine in Western Australia and high stress abutment show that the scale dependence of S:P energy ratio always has a high S:P energy ratio for larger events cannot be generalized (Hudyma, 2008).

2.5.6 Seismic Moment

The seismic moment is a quantity to measure the strength of a seismic event by considering the double couple, shear dislocation source model parameters (Duplanic, 2001). The seismic moment can be calculated from the following formula (Gibowicz and Kijko (1994):

$$\mathrm{Mo} = 4\pi\rho_0 {c_0}^3 R \frac{\Omega o}{\mathrm{Fc}} \qquad [2.3]$$

where,

Mo = seismic moment (Nm)

ρ_0 = rock density (kg/m^3)

c_0 = velocity of the wave in rock (m/s)

R = the distance from the seismic source to the receiver (m)

Ωo = the low frequency plateau of the frequency spectrum of a seismic waveform

Fc = an empirical radiation pattern coefficient

2.5.7 Cumulative Apparent Volume

Apparent Volume, introduced by Mendecki (1993), is a parameter expressing the relation between the energy and the moment of an individual event. It is defined as an estimation of the rock volume with co-seismic inelastic strain. The spatial distribution of this parameter can be understood as a measure of co-seismic deformation. Apparent Volume is defined by the following formula (Mendecki, 1997):

$$V_A = {M_o}^2 / 2\mu E_R \qquad [2.4]$$

where:

$V_A =$ Apparent Volume (m^3)
$M_o =$ Seismic Moment (N m)
$E_R =$ Radiated Energy (Joules)
$\mu =$ Modulus of Rigidity (Pa)

Because of its scalar nature, Apparent Volume can be easily manipulated to provide information about the rate and the distribution of co-seismic deformation in the rockmass. When using Apparent Volume, it is necessary to calibrate it according to observed deformation damage. Therefore, a correlation may exist between the spatial distribution of the Cumulative Apparent Volume (the sum of the Apparent Volume of all of the events in a population) parameter and the progression of caving. For instance, high values of Cumulative Apparent Volume may identify a damaged rockmass (Mendecki, 1997).

A practical use of Apparent Volume is described by Dunlop et al., 2010. "For a given period of time, a set of seismic events in the vicinity of the plane is selected as representative of the parameter values on that plane. The individual values of Apparent Volume parameter of each event are collapsed in the plane of interest. Then, a mesh is created in the plane. By griding the parameter, iso-contours can be achieved on the plane. Consequently, the resulting values of the Apparent Volume parameter are cumulative values for the time period of analysis. The use of radius of the equivalent sphere is a practical method to avoid very large number of the Apparent Volume values."

Figure 2.7 shows the evaluation of Apparent Volume parameter in June 2006 for the P1 cross section (Paraaquez). It also displays the observed subsidence damage particularly the strong damage to the galleries in the Teniente 5 level (2,287 m), Teniente Sub 4 (2,320 m) and Teniente 4 (2,358 m) levels at EI Teniente Mine in Chile (Dunlop et al., 2010).

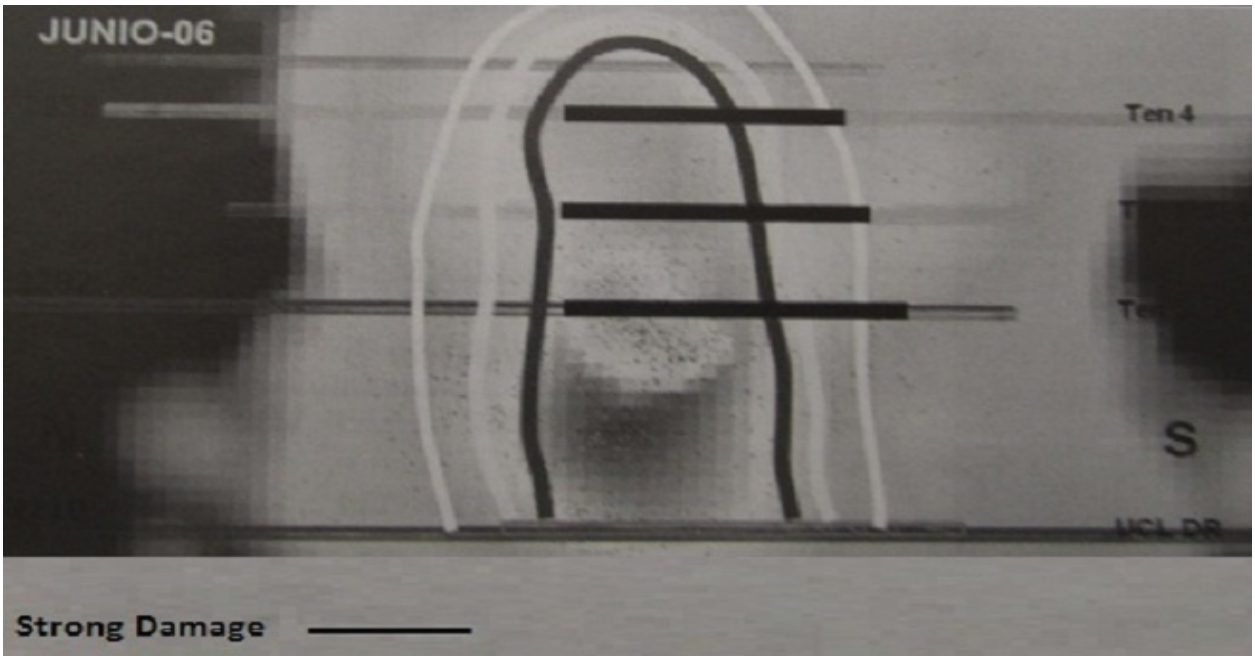

Figure 2.7 P1 cross section displaying the distribution of the Cumulative Apparent Volume parameter (contours in the middle of the diagram) in June 2006 (Redrawn from Dunlop et al., 2010).

2.5.8 Energy Index

Energy Index (EI) is defined as the ratio of the energy released for a seismic event to the amount of energy that is expected for the event (Figure 2.8). As concentration of stress increases in an area, the EI for related seismic event will increase (van Aswegen and Butler, 1993).

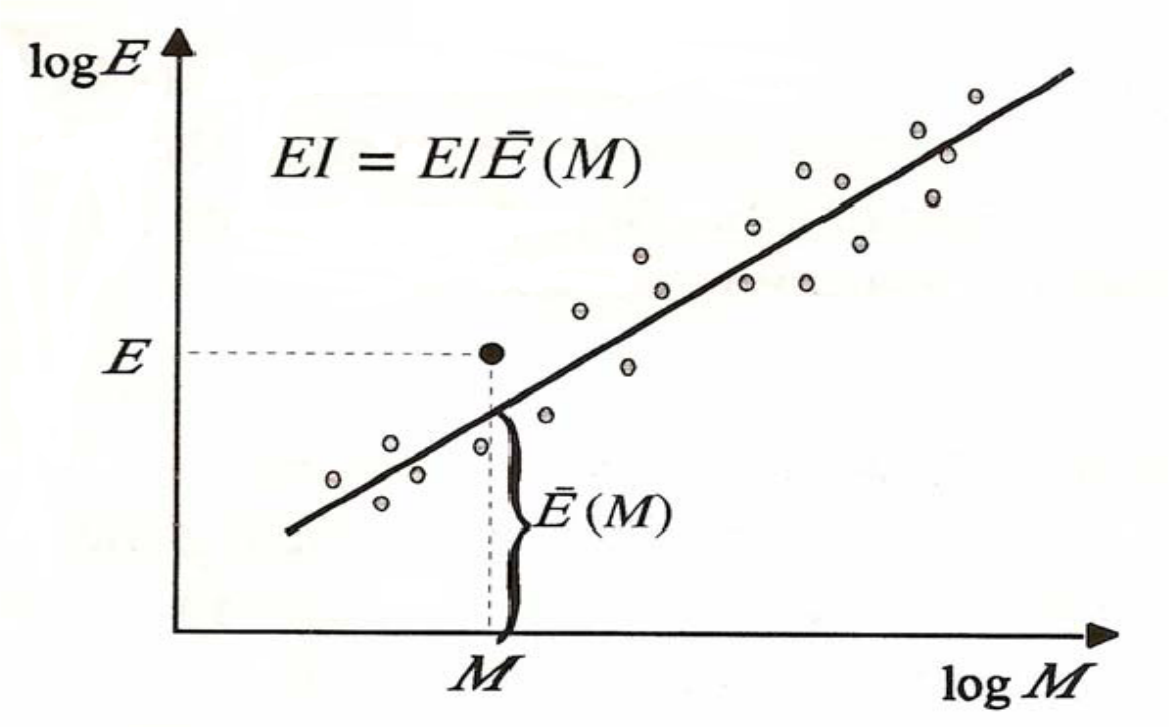

Figure 2.8 Calculation of Energy Index (After Mendecki et al., 1999).

One method of stability analysis of a rockmass uses EI and Cumulative Apparent Volume (CAV). EI (a measure of the relative stress) and CAV (a measure of rockmass deformation) are plotted together on a time history chart. Different case studies in South African "reef-style" gold mines show that EI drops (shedding away of stress) coincides with increase in CAV (deformation) (Hudyma, 2010).

Figure 2.9 is an example of events in a Western Australian mine from mid-September to early December 2002 in which a drop in Energy Index coincides with a significant increase in Cumulative Apparent Volume. Two events with magnitudes larger than Richter +1 occurred coincidentally (Australian Centre for Geomechanics, 2005).

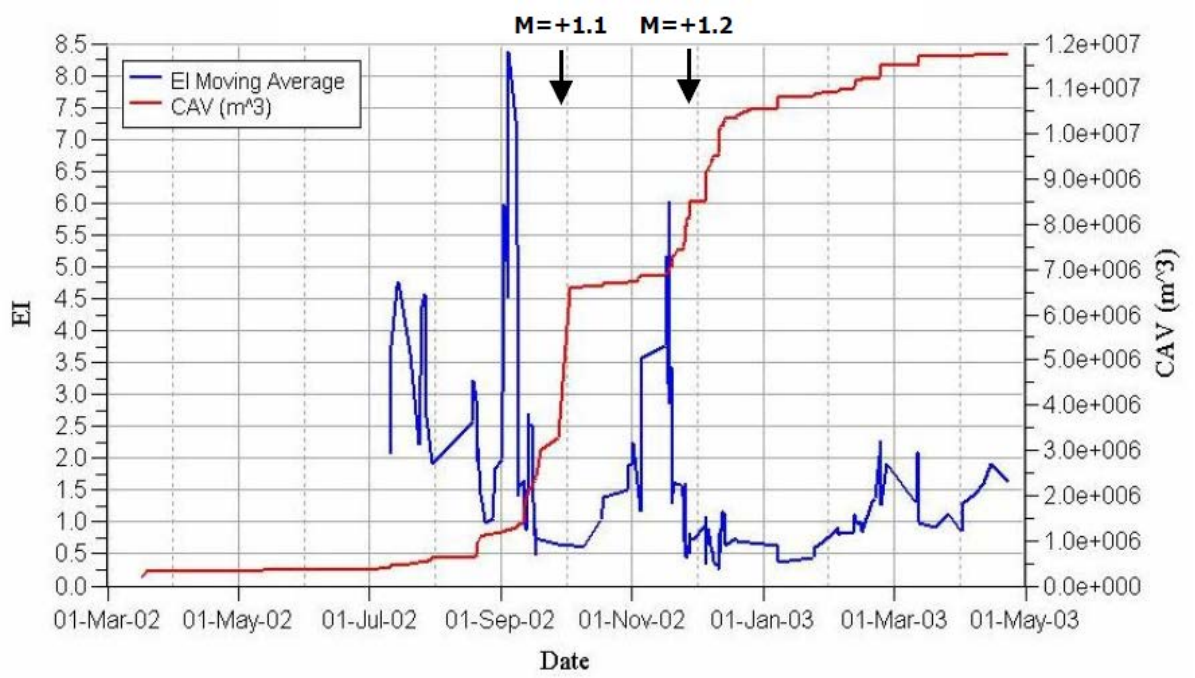

Figure 2.9 In mid-September and early December 2002, a drop in Energy Index coincides with significant increase in Cumulative Apparent Volume and consequently two events larger than Richter +1 (ACG, 2005).

2.5.9 Apparent Stress

Many of the seismic source parameters, that are derivatives of energy and moment, calculated from seismic traces. Seismic energy is the portion of the energy released in the form of seismic waves, and seismic moment is a measure of the permanent deformation at seismic source (Mendecki and van Aswegen, 2001).

Stress state is one of the most important parameters for describing the physical processes of seismicity. In particular, learning the temporal variation of induced stress in seismic source regions, prior to seismic events, is essential for understanding seismic related failures.

Apparent Stress is a model independent measure of the stress change at a seismic source (Mendecki and van Aswegen, 2001; Domanski and Gibowicz, 2008). The formula to define the Apparent Stress as follows (Wyss and Brune, 1986):

$$\sigma_a = \mu E / M_O \quad [2.5]$$

where

σ_a = Apparent stress

μ = The shear modulus of rigidity of the source material,

E = Seismic energy, and

M_O = Seismic moment.

High stress regions tend to release more seismic energy while they tend not to allow as much deformation due to high clamping forces (Simser et al., 2003). This results in comparatively higher Apparent Stress events. Low Apparent Stress events may be due to lower stress areas, or areas that have shed load due to prior rockmass fracturing. It is possible to track the relative stress levels using seismic data.

Simser et al. (2003) noted at Brunswick Mining that it is common to see well-developed stress fracturing around openings in the massive sulphide material, particularly in sill pillar situations. The more fractured the rockmass is the more mobile it becomes, and relatively higher seismic moments are characteristics of this seismicity. Low Apparent Stress events may be results of lower stress areas, or areas that have shed load due to rockmass fracturing (Figure 2.10).

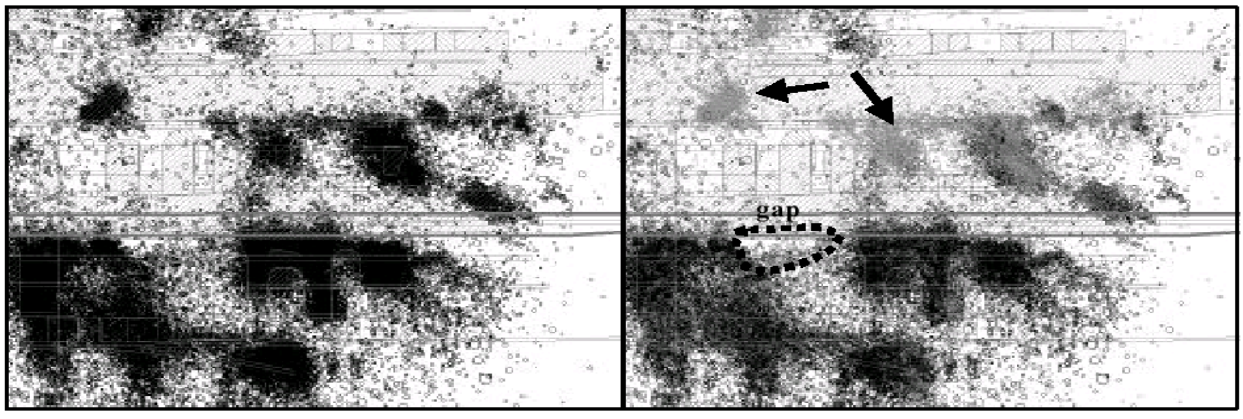

Figure 2.10 On the left are events at Brunswick Mining from 1999 to 2002 (Simser et al., 2003). On the right are the same data but coloured in grey according to Apparent Stress. The light grey areas denoted by arrows represent low Apparent Stress sill pillars that are shedding load due to rockmass fracturing.

Seismic events are caused by sudden failures within the rockmass which result in stress drop. The most significant seismic events should normally be associated with a stress reduction.

Consequently, higher Apparent Stress seismic events usually occur in areas where the stress levels are still relatively high (Andrieux et al., 2008).

Seismic events associated with areas where significant stress occurs due to blasting (change in geometry), often have a higher than expected seismic energy that results in a higher than normal Apparent Stress (Simser et al., 2003; van Aswegen and Butler, 1993). In several case studies, Hudyma (2008) also noted in that blasting often triggers increases in the number of high Apparent Stress events, specifically in proximity to where stress increase would be caused by the blast.

Apparent Stress Time History (ASTH) is a seismic data analysis technique, in which the daily number of events with an Apparent Stress equal or greater than a threshold in a trailing (preceding) time period. ASTH is a method for investigating variations of Apparent Stress. Apparent Stress is a potential indicator of elevated temporal seismic hazard (Hudyma, 2010). Figure 2.11 shows ASTH for a group of events. In this group, all 8 of the large events (local magnitude > 0) occur during or very close to period in which the Apparent Stress Frequency exceeds 5 events per day. In this example, Apparent Stress frequency is averaged over 7 days and the Apparent Stress threshold is 10,000 Pa (Hudyma, 2010).

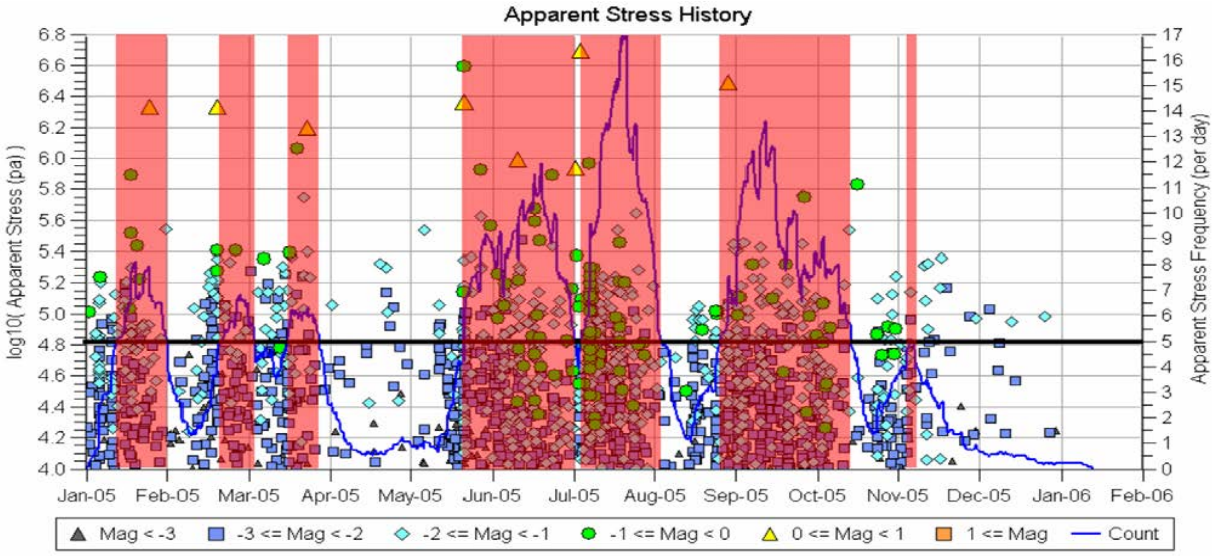

Figure 2.11 In this group of events, all 8 of the large events (local magnitude >0) occur during or very close to period in which the Apparent Stress Frequency exceeds 5 events per day (Hudyma, 2010).

2.6 Case Study of Seismic Monitoring at Palabora Mine

Glazer and Hepworth (2007) discuss one of the first applications of seismic event analysis in caving mines, monitoring the block cave at Palabora copper mine near Limpopo, South Africa. The open pit operations were between 1966 and 2002. A block caving operation was used under the open pit. The undercut at Palabora mine was located 400 m below the open pit bottom (elevation of -820). The production level was 18 m below the undercut and an exploration level was approximately 100 m below the open pit bottom (900 m below the surface).

At Palabora, 26 triaxial geophones were used in the seismic monitoring system. The first seismic event was recorded on 16/09/1999. The initial seismic network (it was flat) was installed in one of the development levels. Thus recorded seismic data during 1999 and 2000 had poor quality. The distribution of sensors was changed in 2001. At this time, sensors were located throughout the mine, especially around the cave extraction level. The geometry of Palabora mine and spatial distribution of the seismic network are shown in Figure 2.12.

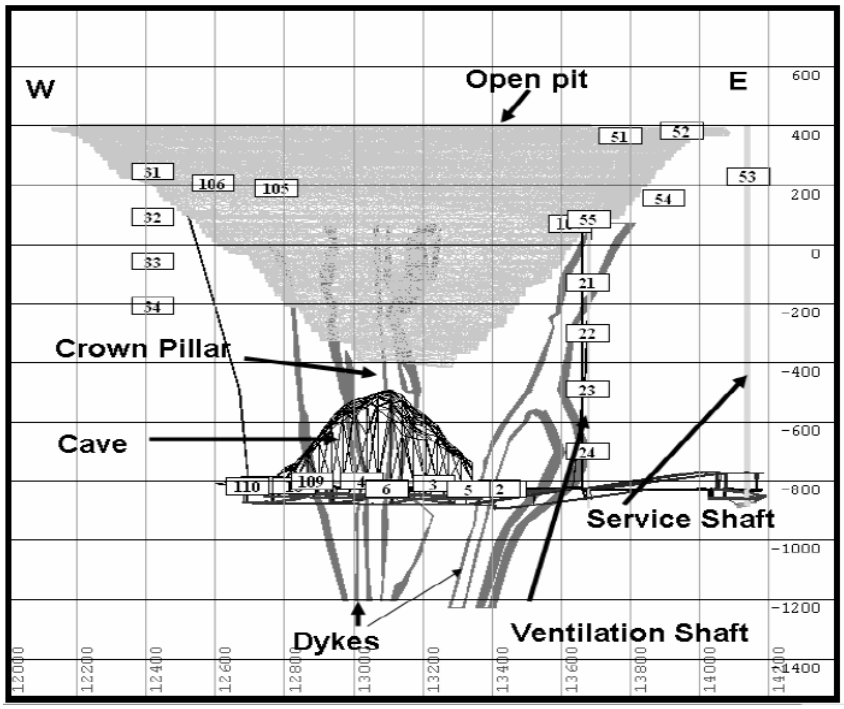

Figure 2.12 Geometry of Palabora mine and spatial distribution of seismic network (Glazer and Hepworth, 2004).

Ten years seismic event analysis (2001 to 2010) at Palabora mine had different objectives such as study of the relation between different seismic event parameters, analysis of the crown pillar failure, production rate, and caving processes. Important periods at Palabora mine from the mine development to cave through into open pit are listed in below (HR refers to the Hydraulic Radius = undercut area/undercut perimeter):

1. Development mining for the block cave – Early 2002
2. Last blast in open pit – April 2002
3. End of ramp mining in the open pit – October 2003
4. Start of gravity caving – HR 35 m October 2001
5. Initiation of the stress caving processes – HR 45 m April 2002
6. Crown pillar failure – end of 2002
7. Initial cave breakthrough into open pit – May 2004
8. Failure of open pit North wall – October 2004
9. East cave breakthrough – May/June 2008

A crown pillar with 200 m thickness between the open pit bottom and cave back was established for two reasons. Firstly, to provide a safe environment for the open pit operations. Secondly, to protect underground operations from ingress of rainfall. Eventually the pillar became fractured and de-stressed to the extent that there was a hydraulic connection between surface and underground (Glazer and Hepworth, 2004).

Cave propagation was strongly related to the drawing rate of caved rock. A zone of loosening (aseismic zone) was located about 60 to 80 m above the cave back at Palabora. The thickness of this zone almost did not change during 2002. As shown in Figure 2.13 seismic events occurred in seismogenic zone of the cave, above the yield (loosening) zone.

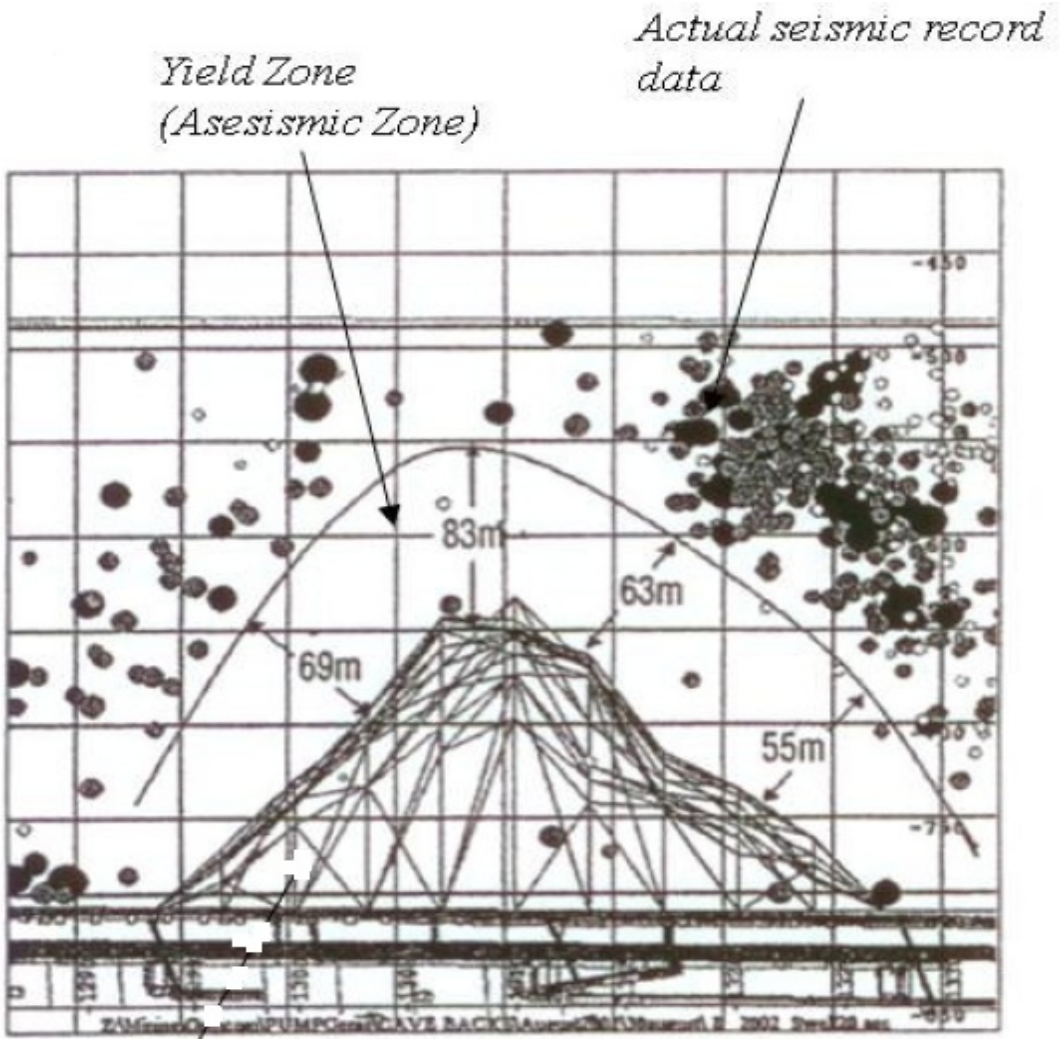

Figure 2.13 Seismic events in seismogenic zone of cave (Glazer and Hepworth, 2007).

An increase in the average elevation of recorded seismic events was identified that showed an increase in the cave back height. Monitoring the seismic zone also helped in management of the air blast risk, a potential risk due to the natural cave expansion rate (Glazer and Hepworth, 2007).

The progression of the cave generated fractures in the more component rock immediately ahead of the fracture zone, which changed the rock properties and lowered its load carrying ability. As the cave back approached the fractured rock, it would yield under the increased load. Increased shear movement between the blocks of rock would create further propagation of fractures (Glazer and Hepworth, 2007).

Two types of seismic data were recorded at Palabora mine (Glazer and Hepworth, 2007):

1. Events related to rockmass fracturing immediately ahead of undercut and in propagating cave back. They were in range between 0.0 to 0.5 local magnitude. They had a positive effect on the cave propagation by aiding cave propagation.
2. Events related to geological discontinuities happened in far distances from the mining area. They were related to stress change in undercut abutment. These events had magnitudes up to 2.1. Due to their locations and related rockmass damage, these events were considered as a negative effect to the mining (Gibowicz and Lasocki, 2001).

A detailed back analysis of the crown pillar failure at Palabora is based primarily on seismic data. From July 2001 to December 2002, average elevation of seismic events above the cave changed from -750 to -460 m (a rate of 15 m per month). Since the zone at the bottom of open pit was fractured, the average elevation of seismic events could not migrate upward. It was interpreted that the crown pillar between the cave and the pit bottom was preconditioned (weakened) by the open pit mining (Figure 2.14) (Glazer and Hepworth, 2007).

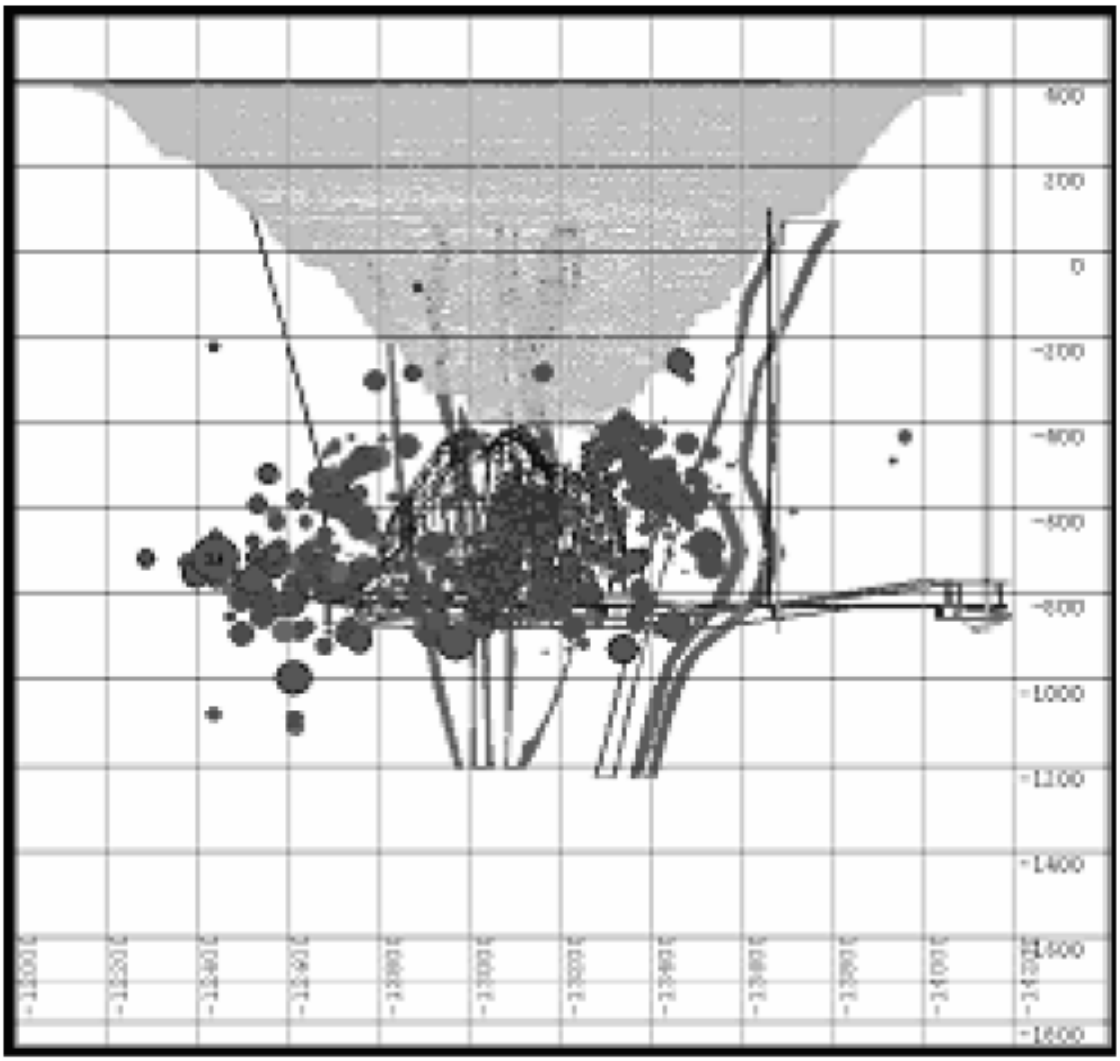

Figure 2.14 Low concentrations of seismic events beneath open pit bottom (Glazer and Hepworth, 2007).

At the end of June 2002, the energy index of the events in the seismogenic zone began to increase. It was attributed to the onset of fracturing processes. The rockmass was intact enough to release high seismic energy events. After four months (end of October 2002), the rockmass below the crown pillar had fractured. The more fractured the rockmass, the more mobile it becomes, resulting in lower energy release (higher seismic moment). Thus the energy index became flat. The slight difference between the lowest and the highest energy index values indicated that the seismic fracturing processes would be in already relatively fractured rockmass (Figure 2.15) (Glazer and Hepworth, 2007).

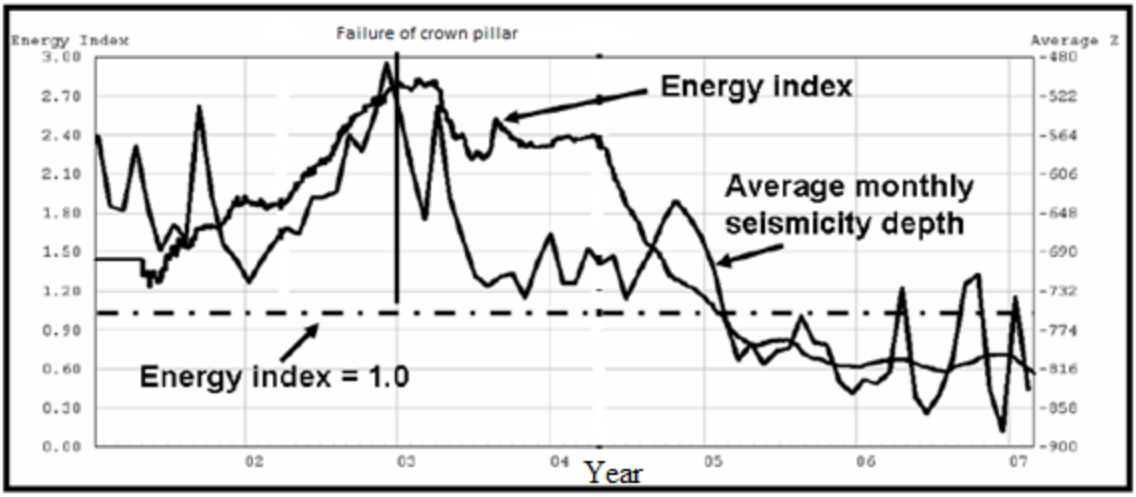

Figure 2.15 General trend of Energy Index, highest value in failure of crown pillar (Glazer and Hepworth, 2007).

A sharp increase in the seismic deformation rate (cumulative seismic moment) started after crown the pillar failure and did not stop even after the energy index started to decrease (Figure 2.16) (Glazer and Hepworth, 2007).

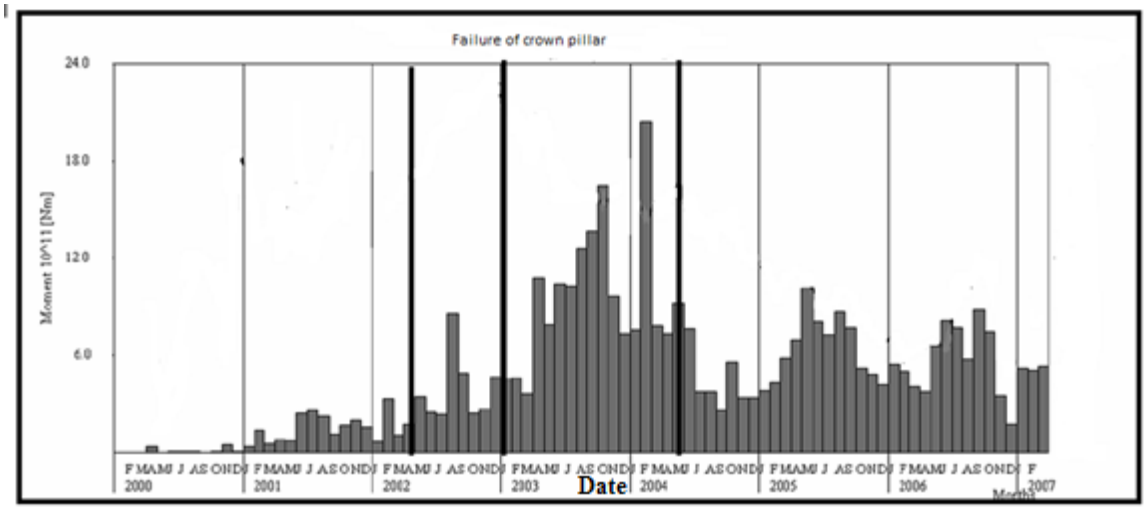

Figure 2.16 General trend of seismic moment, increase in seismic moment after crown pillar failure (Glazer and Hepworth, 2007).

To study the mechanism of crown the pillar failure, two volumes of rockmass were considered (Glazer and Hepworth, 2007):

1. First volume (length: 400 m, width: 300 m, height: 600 m), the larger one, was based on the cave footprint as it existed by the end of 2002. Cave mining and development activities were the sources of seismic events in this volume.
2. Second volume (length: 200 m, width: 200 m, height: 500 m) where caving and open pit activities were the sources of seismic events.

The first volume was divided into three layers, each 200 m in height. A short summary of failure mechanism are described in below (Glazer and Hepworth, 2007):

- With time, seismicity migrated upward.
- A decrease in seismic activity in deepest layer (-600 m to -800 m) was identical to increase in seismic activity in middle layer (-400 m to -600 m).
- The largest magnitude events and also most of seismic energy were released in middle layer.
- An increase in stress was due to cave initiation.
- The seismic data indicated that when the stress release process was completed in shallowest layer, stresses migrated downwards below the cave undercut.

Also a short summary of the failure mechanism based on analysis of seismic history of smaller rockmass volume is as follows (Glazer and Hepworth, 2007):

- The horizontal stress caused the rockmass to fail below the open pit to 100 m below to the open pit base.
- An upward migration of seismic activity accelerated with time.
- The reason for the observed acceleration upward of seismicity was the redistribution of the mining induced stresses.

Seismic monitoring, in contrast to other cave mentoring methods, can provide not only point measurement information but also information around the cave. This makes seismic monitoring a more reliable and powerful monitoring tool than other methods. A limitation of the seismic analysis is that it only provides information on the medium (rockmass) in which the seismic event occurs (Duplancic and Brady, 1999, pseudo-continuous domain and seismogenic zone). However, no information is given on the caved mass or the zone of loosening. Seismic

tomography can potentially provide extra information from within the cave. As seismic tomography allows for monitoring time related changes taking place outside and inside of the cave, this analysis should periodically be repeated. Seismic tomography imaging involves the generation of maps for spatial variation of seismic velocity through a rockmass. The aim of this approach is to use all possible information on what happens to the seismic energy along its path from the seismic source to the seismic receiver. Figure 2.17 shows an east – west section of the cave. The solid shapes represent high velocity areas.

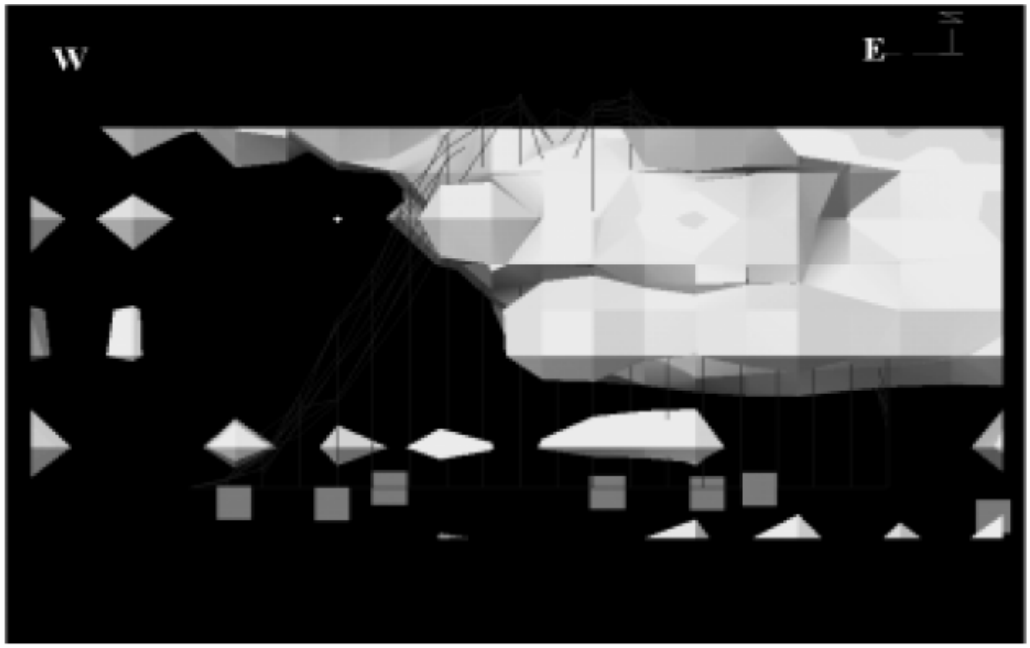

Figure 2.17 The East-West section of the cave. The solid shapes represent higher velocity areas (Glazer and Hepworth, 2007).

Based on Glazer and Hepworth (2007), results on data interpretation using seismic tomography include:

- Distributions of the energy index values indicate the variation of stress level (high or low) in different places.
- High velocity volume in abutment represents either a solid rockmass, rockmass under higher stress, or compact coarser cave material.
- The reasons for coarse fragmentation in the cave are complex. Probably, at this stage the cave has not yet reached a critical height at which the secondary fragmentation is induced. The other factor influencing the fragmentation is the geology.

- The stress increase due to development mining was very low compared with the stress increase induced by the caving process.
- When the seismic velocities in the whole volume of the mine are lower, it means that the rockmass properties have changed.
- Tomography can show that the cave inside the caved zone is not homogenous.
- Velocity images obtained for the inside of the cave are valid representations of what is taking place in the cave.

Reyes-Montes et al. (2007) developed a method to extract information on fracturing mode and orientation from existing microseismic catalogues. The method is based on the statistical analysis of event locations to determine the dominant structure defined within the seismic event cloud. The interpretation is completed with analysis of temporal evolution of the energy content and growth patterns of the yielded volumes (Reyes-Montes et al., 2007). This analysis forms the basis of the Synthetic Rockmass Model for jointed rock (Pierce et al., 2009).

Sainsbury (2010) developed a model for a ubiquitous jointed rockmass (UJRM). The purpose of UJRM was to represent rockmass strength, anisotropy, and scale effects using FLAC3D, as determined from synthetic rockmass (SRM) testing. Applying these techniques showed that the location of the yield zone (or aseismic zone) was from 50 to 80 m above the cave zone. It was in good correlation with previous seismic data analysis (Figure 2.18).

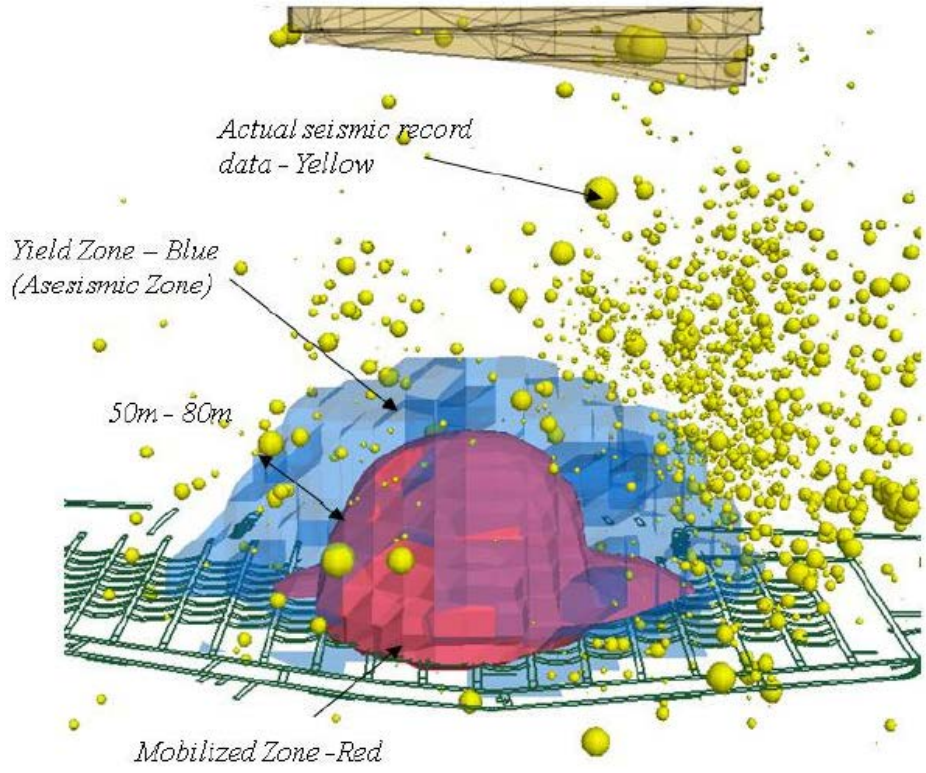

Figure 2.18 Location of yielded zone (or aseismic zone), 50-80m above the cave zone (Sainsbury, 2010).

Figure 2.19 shows that in early stages of mining, seismic events happened under the open pit bottom. After the crown pillar failure, seismic events migrated to the perimeter of mining footprint. Continued production changed the location of seismic events to the area under extraction level. All results are consistent with seismic data interpretation of Glazer and Hepworth (2007).

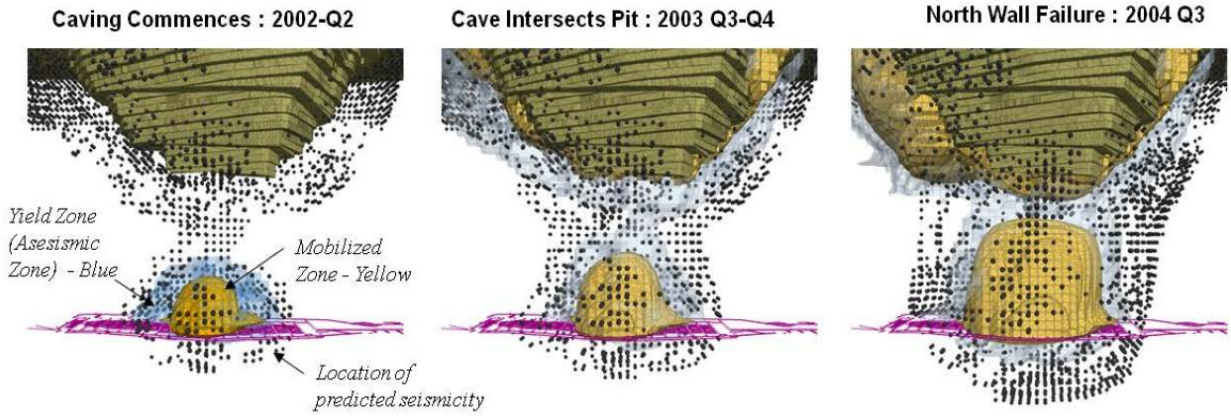

Figure 2.19 Seismic event different locations at different periods in cave (Sainsbury, 2010).

General conclusions after 10 years of seismic monitoring at Palabora mine are described as follows (Glazer and Townsend, 2010):

- Mining induced seismicity is directly related to the mining rate (increase in the mining rate resulted in increased seismicity, energy release, and increased deformation).
- It seems that seismicity induced by cave mining is related to the production rate and the caving process (at some stages of the caving process the seismicity is independent on the production rate).
- The rapid response of seismicity to changes in the production rate suggests that mining is pulling at a rate lower than natural cave expansion rate.
- Seismicity above and below the mine has different seismic trends.

2.7 What other Caving Mines have Achieved with their Seismic Monitoring Systems

2.7.1 Big Bell Mine (Turner and Player, 2000)

Big Bell mine is located in the Murchison Province of Western Australia and started its operation in 1913. The mining method used (from 1996 to 2003) was longitudinal sublevel caving. The Big Bell deposit is situated between a greenstone and sedimentary sequence within the Murchison Province of the Archaean Yilgarn cratonic block (Turner and Player, 2000).

In early 1999, large seismic events and associated rockbursts began at the Big Bell deposit. In August 1999 and in February 2000, an eight-channel CSIR-Miningtek (GMM) seismic system and an 18-channel ISS system were installed, respectively. From August 1999 to June 2000, twelve rockbursts happened including five large seismic events (Richter magnitude > 1.5). Monitoring relative activity and determining spatial temporal trends were the objectives of seismic monitoring at Big Bell. As shown in Figure 2.20, shear failure of intact rock and the tight foliation surface were common sources of seismic events at Big Bell.

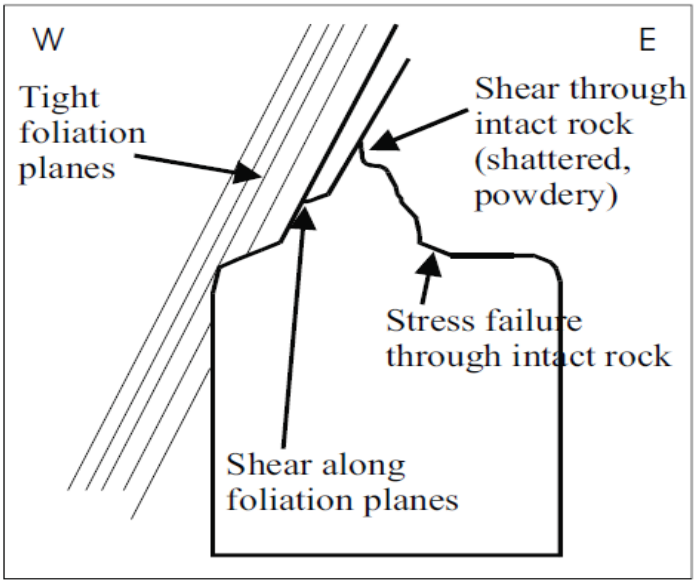

Figure 2.20 Shear of intact rock and the tight foliation surface were the main sources of seismic events at Big Bell (Turner and Player, 2000).

Seismic event interpretation helped in:

- Defining optimum re-entry times (first restrictions were precautionary, later it was reduced to 12 hours).
- Modifying the design such as locating development of footwall drives further away from orebody.
- Identifying areas with a higher risk of rockbursts.
- Replacing the strong but relatively stiff rock reinforcement which was ineffective in rockburst conditions.

Since the focus was on understanding of the rockburst related risks, no substantial analysis was conducted on caving mechanisms.

2.7.2 EI Teniente Mine (Rojas et al., 2000)

EI Teniente mine is an underground copper mine in Chile. It is one of the largest deposits of porphyry copper in the world. The mineralization at EI Teniente can be divided into two distinct parts, primary and secondary. Primary mineralization is located at depth, while the secondary is closer to the surface. Geotechnical investigations have shown that the primary rockmass is harder and is more prone to large fragmentation and violent failures. Also, investigations showed that

defined rockmass behaviour was independent of cave column height. Hence, mine engineers changed the mining method from block caving to panel caving with a higher rockmass column. Mining induced seismicity started with primary rock exploitation. A new sector, Teniente 4 South, was developed with a total column height of 180 m. After 10 years, this height reached to 280 m. Another sector, Sub 6, for reaching the deepest production area was developed. Six months after beginning of production in Sub 6, seismic events and related rockbursts became evident.

Dunlop and Gaete (1995) developed a framework for finding the relation between mining parameters and rockmass response characteristics. As fractures relate to the disruption of joint rockmass, induced seismicity can be associated to the rupture process in a rockmass. Generally, caving processes make large ruptures that can cause significant seismic events and consequently severe damages. Table 2.1 shows four large seismic events in different months at EI Teniente mine.

Table 2.1 Four large seismic events in different months at EI Teniente mine (Rojas et al., 2000).

Date	Events (Richter scale)	Damage Area
18/01/1990	3.6	Transport Gallery
02/07/1990	3.2	Sub6 Sector
23/05/1991	4.0	Production Level
25/03/1992	3.7	Production Level

Figure 2.21 shows cave height increase in the Sub 6 section causing four large seismic events.

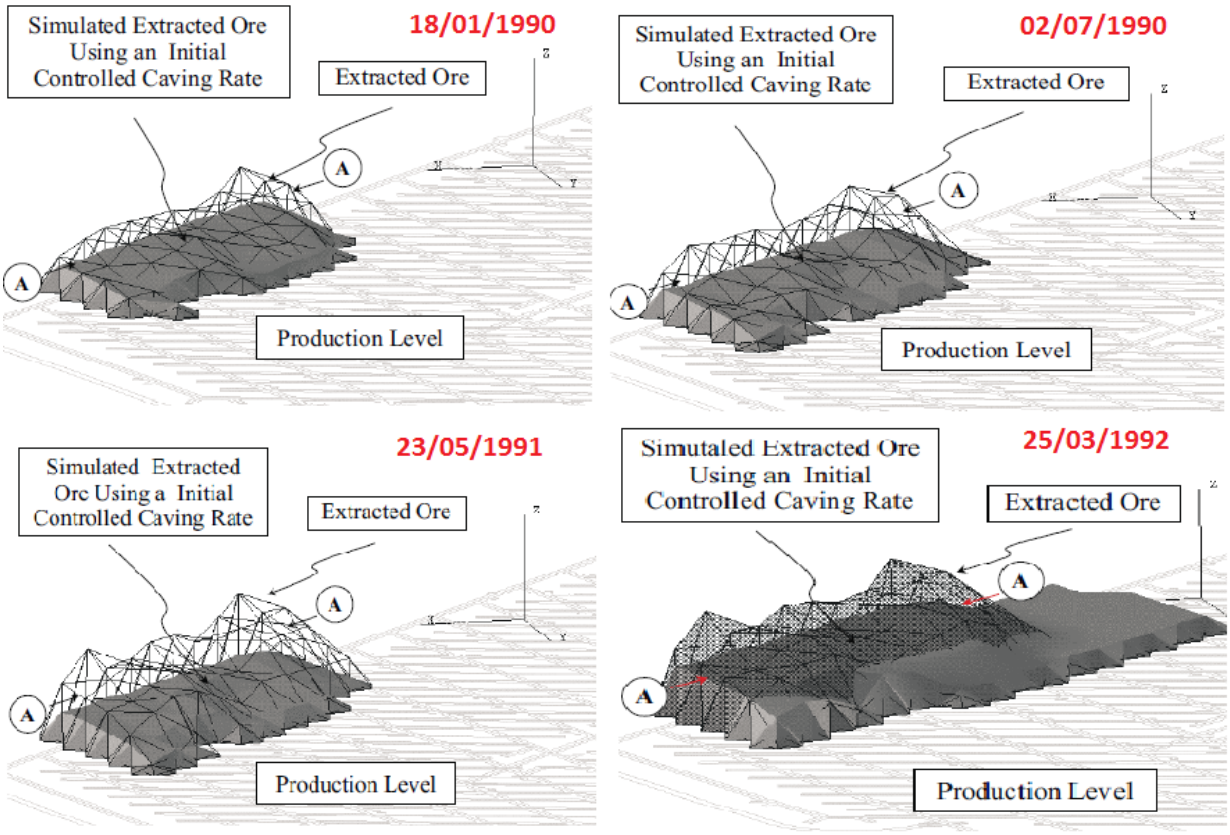

Figure 2.21 Cave height increase in Sub 6 section causing 4 large seismic events (Rojas et al., 2000).

Empirical evidence defined cave initiation, in the process of cave evolution, as the source of the greatest seismic risk. Modifying mining parameters such as controlling undercut and extraction rates helped to decrease the seismic risk resulted from caving (Dunlop and Gaete, 1997).

The cave evolution concepts helped the mine engineers to develop a production plan to connect the Sub 6 to the upper undercut level, Teniente 4. After this development from 1997 to 2000, only minor damaging events occurred (Rojas et al., 2000).

No substantial analysis of caving mechanisms was undertaken at EI Tenient. The focus was on understanding and managing the rockburst related risk on the undercut and extraction levels.

2.7.3 Ridgeway Mine (Woodward, 2011)

Ridgway mine is located in Cadia Valley, in central west New South Wales, Australia. Forest Reefs Volcanics and Weemalla Sediment Formation are the two main geological domains which host a porphyry copper-gold deposit (Burgio and Diering, 2008). The mining process at Ridgeway started in 2000 with sublevel caving (560 m below the surface). In 2011, with development of the Ridgeway Deeps (located approximately 250 m below sublevel cave operations), the mining method changed to block caving. Figure 2.22 shows Claudia, Delphin, North, Purple and Red faults which are the dominant structures in the Ridgway Deep block cave mining area. Using Laubscher's Mining Rockmass Rating system, the minimum hydraulic radius for the cave initiation is determined to be 35 m.

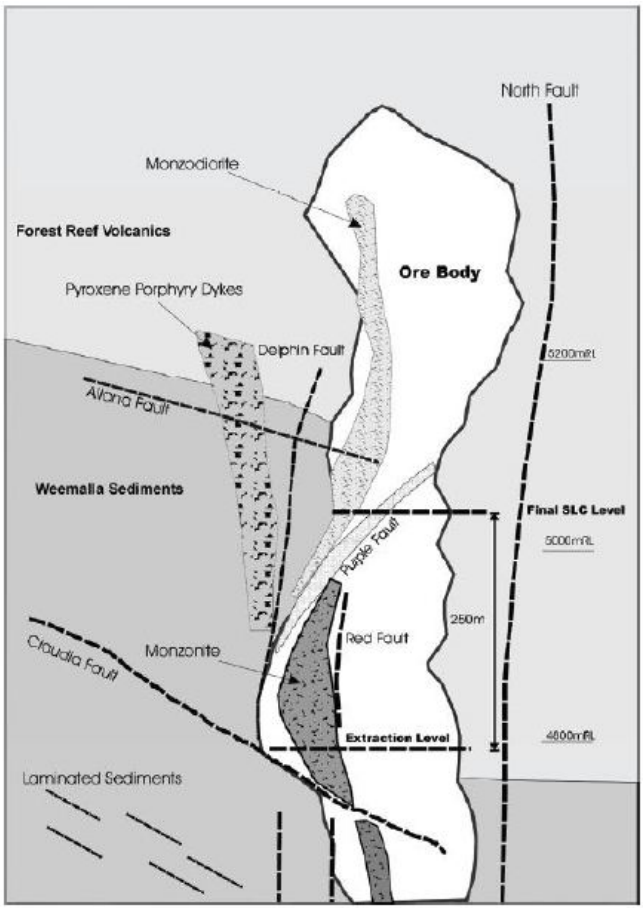

Figure 2.22 Claudia, Delphin, North, Purple and Red fault dominant structures in Ridgeway mine (Woodward, 2011).

For seismic monitoring 39 sensors (five uniaxial and 34 triaxial) were used. As shown in Table 2.2, the mining process in Ridgeway Deep can be divided into five periods.

Table 2.2 Five important periods from undercutting until cave propagation (Woodward, 2011).

Period	Date (Start)	Date (Finish)	Event Count	Blast Count	Ave. Events per Day	Ave. Blasts per Day
Period 1	01/08/2008	1/04/2009	5,568	1,005	22.9	4.1
Period 2	1/04/2009	08/05/2009	1,137	13	28.4	0.4
Period 3	08/05/2009	1/10/2009	12,426	634	85.1	4.3
Period 4	1/10/2009	18/11/2009	2,393	10	49.9	0.2
Period 5	18/11/2009	20/05/2010	75,482	348	412.5	1.9

The first four periods belong to the initial undercutting and the last period is the cave propagation period. Four general analyses such as Magnitude - Time History, Frequency - Magnitude, Energy ratio between S and P wave, and Instability Analysis were conducted for interpretation of data. Below are the some of the important conclusions at Ridgeway (Woodward, 2011):

- Shearing was the dominant rockmass failure mechanism.
- The proportion of shear failure was increasing as the cave was propagating.
- Blasting had a greater influence on seismicity early in the caving.
- Seismicity became increasingly independent with relation to blasting as caving progressed.
- In contrast to the trends in Energy Index, Cumulative Apparent Volume were insensitive to the blasting and event rate.

2.7.4 Northparkes Lift 2 (Hudyma et al., 2007a)

Northparkes mine is located near Parkes, New South Wales, Australia. Block caving is used for extracting copper and gold. It has four major rock types: Quartz Monzonite Porphyry, Volcanics, Biotite Quartz Monzonite and Diorite (Duffield, 2000). As shown in Table 2.3, four important periods were defined in the history of seismic monitoring of Lift 2 at Northparkes.

Table 2.3 Four important periods in history of seismic monitoring at Northparkes (Hudyma et al., 2007).

Time Period	Mining Activity
01 Sept 2002	Start of seismic record for Lift 2. Development mining in the crusher and undercut.
25 Feb 2003 – 21 Jan 2004	Undercut blasting and crusher development
21 Jan 2004 – 21 Aug 2004	Development of production level
21 Aug 2004 – Dec 2004	Initial cave production and propagation

A zone of loosening was 50 to 70 m in height above the cave. Conclusions of different seismic analysis are detailed as follows:

- **Frequency-Magnitude:** Northparkes showed smaller events had different source mechanisms compared with larger events.
- **Magnitude-Time history:** In early stages of undercutting at Lift 2, seismicity was strongly related to blasting. This became weaker in later stages.
- **S:P Energy Ratio Analysis:** The predominant seismic source mechanism was shear (60 to 80% of events had an S:P energy ratio greater than 10).
- **Apparent Stress Time history:** Several spikes were observed but generally it was divided into 17 main periods such as start of undercutting, undercutting widening, cave production period, and etc. During undercutting higher and lower Apparent Stress occurred in the apex shape and along the sides of failure zone, respectively.

The Ridgeway and Northparkes case studies were among the first to use seismic monitoring to investigate at caving mechanisms in block caving mines.

3 SEISMIC ANALYSIS FOR TELFER GOLD MINE

3.1 Telfer Gold Mine Overview

3.1.1 Location

Telfer gold mine is located approximately 1300 km north of Perth, in the Peterson Province, northwest of Western Australia. Newcrest Mining Ltd is the owner of the mining operations.

3.1.2 Geology

Telfer mine is located within a belt of metamorphosed Palaeoproterozoic to Neoproterozoic sedimentary and igneous rock (Gionvinazzo and Singh, 2010). The Main Dome is a dome which trends north-south and has been traced more than 6 km. Telfer lithology from surface to the bottom (Telfer Deeps) is divided into three major parts Telfer Formation, the Malu Quartzite Member, and the Isdell Formation which are concentrically folded (Trenning, 2002). Figure 3.1 shows the stratigraphic column of the mine area.

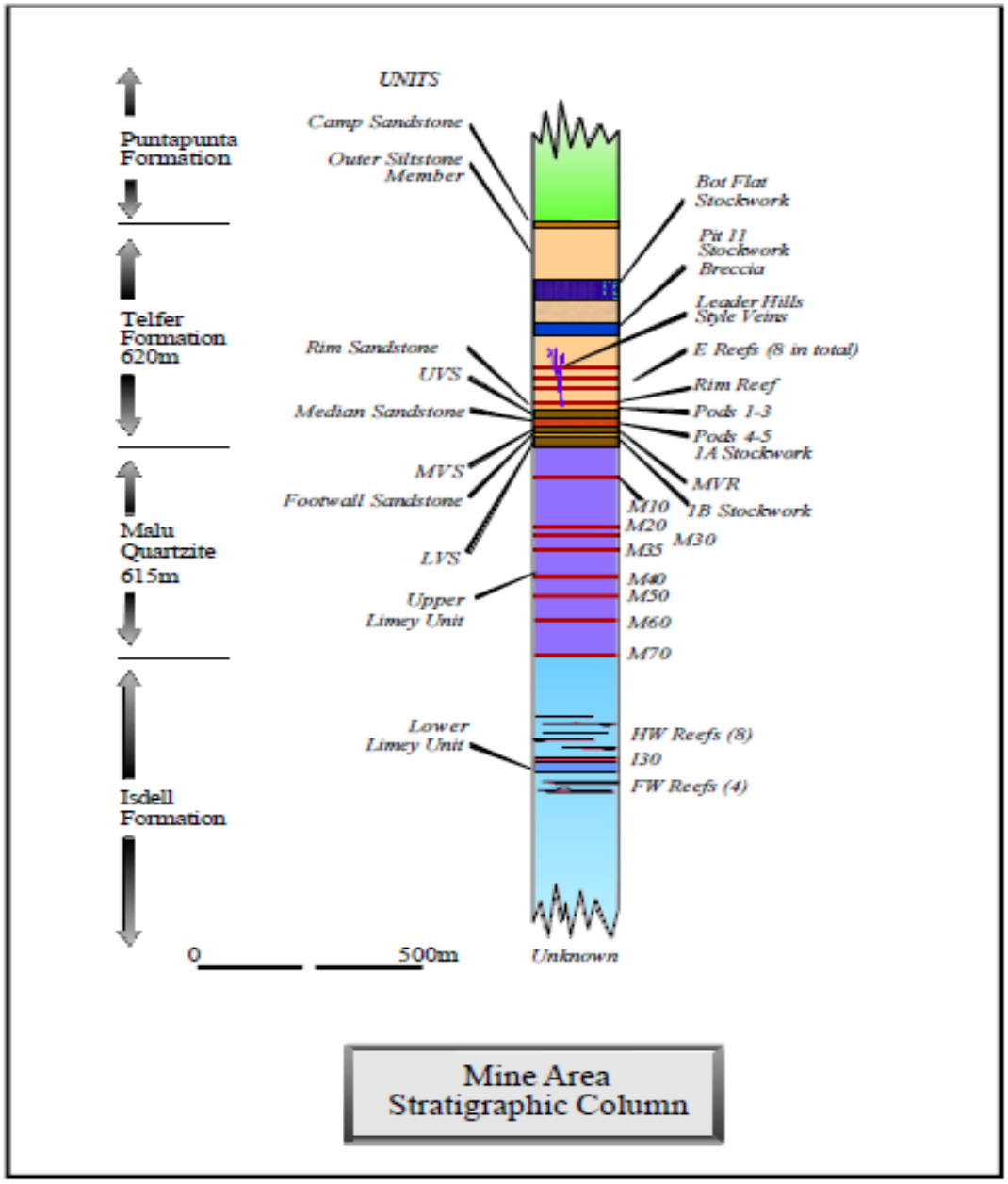

Figure 3.1 Stratigraphic column of mine area (SRK, 2002).

Malu Quartzite Member consists of a massive quartz sandstone to finely laminated carbonaceous siltstones and quartz pyrite reefs. According to the distribution of these minerals, Malu Quartzite Member is divided into Upper, Middle, and Lower Malu Members (Gionvinazzo and Singh, 2010). The SLC (sublevel cave) was immediately initiated beneath the Middle Malu Member (Figure 3.2).

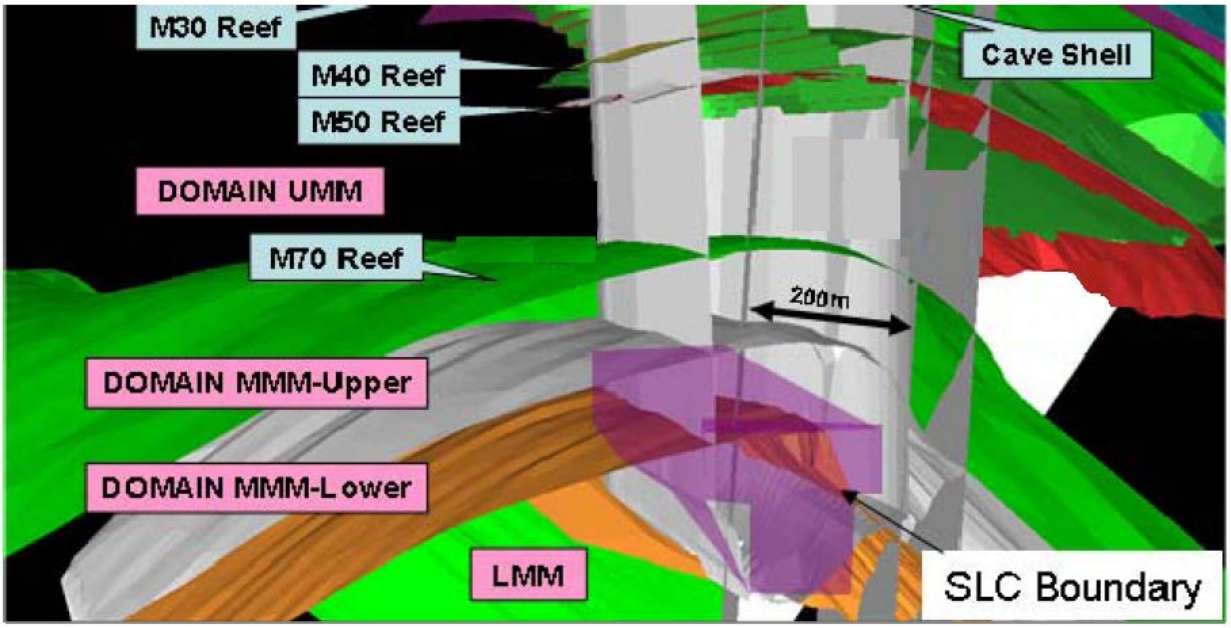

Figure 3.2 Main Dome folding geotechnical domains and the SLC boundries, looking NE (Maxlow, 2007).

The majority of the Telfer Deeps ore is in the Isdell Formation. At the bottom of Telfer mine, the Isdell Formation is divided into three main stratigraphic units Upper Isdell Formation, the Lower Limey Unit, and the Lower Isdell Member (SRK, 2002).

The largest structure in the Main Dome is the Graben fault. It trends NE-SW and is located in the southeast of Main Dome. Graben fault is sub-vertical with an average width of 20 m. The fault includes fracture zones with varying orientation from north-south to northeast-southwest. A series of sub-horizontal thrust, pervasive joint sets, a number of low angle joints sets, and beddings are the main structures in the mine (Gionvinazzo and Singh, 2010).

3.1.3 Orebody Geometry

The Telfer Deeps resource is almost 1000 m long, changing between approximately 120 and 200 m in width and 100 and 180 m in height. The resource is cigar shaped, being widest and highest in the middle, which tapers towards the ends. It is located at a depth of 800-1000 m below the surface (SRK, 2002).

3.1.4 Mining Method

According to the SRK report (2002), the Telfer Gold mine operation includes the Main Dome open pit and the Telfer Deeps underground Mines. The underground operations commenced in 2006 with the sublevel caving approximately 850 m below the surface. The first lift of the sublevel cave (SLC) was opened on the 4650 m level with a production drive orientation perpendicular to the long axis of the orebody. The subsequent production levels, 4625 and below, were each 25 m high. The 42 Mt underground reserve, at 1.6 g/t Au, 0.35% Cu containing 2.2 Moz Au and 140 kt Cu, is extracted with a production rate of six million tonnes per annum from the sublevels.

The caveability of the rockmass at Telfer was assessed using Laubscher's Mining Rockmass Rating system (MRMR) and the hydraulic radius with exceeding dimensions required to induce continuous caving (Burgio and Diering 2008; Laubscher 1994). Table (Table 3.1) shows the RMR and MRMR values for different domains at Telfer.

Table 3.1 RMR and MRMR ratings for each domain (SRK, 2002).

Domain	RMR (25%- 75%)	MRMR (25%-75%)	RMR (Mean)	MRMR (Mean)
Host	52.9 – 61.2	42.9 – 49.6	56.8	46.0
Thrust	49.4 – 59.7	40.0 – 48.4	54.3	44.0
Stockwork	52.7 – 61.1	42.7 – 49.5	56.9	46.1

It was found that the host rock would cave at a hydraulic radius (HR) of between 25 m and 35 m. As of 2006, the HR of the production footprint on 4650 level was approximately 25 m and corresponded with the minimum predicted HR required for caving (Giovinazzo and Singh, 2010).

3.1.5 Seismic Data Assessment

The Integrated Seismic Systems (ISS) for capturing the mining-induced seismicity at Telfer was installed in two phases, the first phase (Figure 3.3), in August 2005 for monitoring the cave initiation, and the second phase, in March 2006 for monitoring the cave propagation. This system consisted of an array of 26 operating 3D geophones (Giovinazzo and Singh, 2010). Monitoring and analysis during the life of the mine facilitated interpretation of rockmass response to caving and managing of risks associated with the cave evolution. Telfer Gold mine case study is extraordinary because it is a high quality seismic data set associated with a sublevel cave into an open pit.

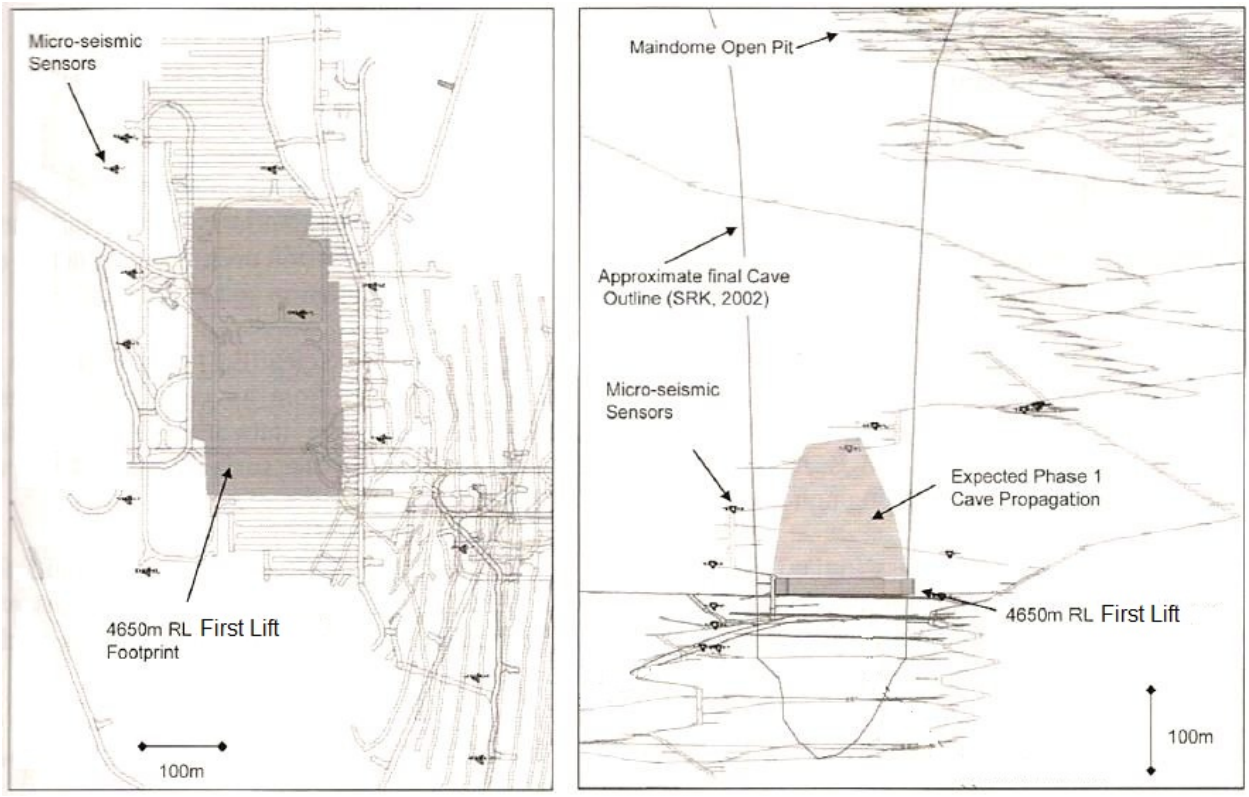

Figure 3.3 Plan (left) and section (right) views of Phase 1 microseismic array (Giovinazzo and Singh, 2010).

During the first five years (2006 to the late 2010) of underground mining operations at Telfer mine, more than 425,000 seismic events were recorded. The largest event with local magnitude +2.2 occurred on January 24, 2008. Telfer mine experienced two temporary shutdown periods in December 2008 and March 2009. The history for all events can be divided into four major time periods (Table 3.2).

Table 3.2 Four major time periods during 5 years mining operations.

		From	To
1	Initial Blasting	2006/03/01	2007/02/01
2	Cave Initiation	2007/02/01	2007/11/01
3	Cave Propagation	2007/11/01	2009/10/01
4	Breakthrough and Breakback	2009/10/01	2010/11/01

A summary of the four important periods during the Telfer cave development is written in the follow section.

3.2 Cave Evolution

According to the SRK (2002) report, crosscuts were oriented in the east-west direction while the blast development was oriented in the North-South direction from 4650 mRL level. From this level, the cave had to enter the Stockwork Domain (25-55 m), the Thrust Domain (up to 20 m) and the Host Domain (600 m) up to the pit bottom. The rockmass in the Host Domain (from the surface to the upper part of the orebody) can vertically be divided into three domains as follows (Figure 3.4):

Zone 1: Due to weathering, the rockmass quality is poor to fair.

Zone 2: This area is more competent than Zone 1. It has a fair quality rockmass.

Zone 3: This zone is reasonably competent and has a mostly fair quality rockmass.

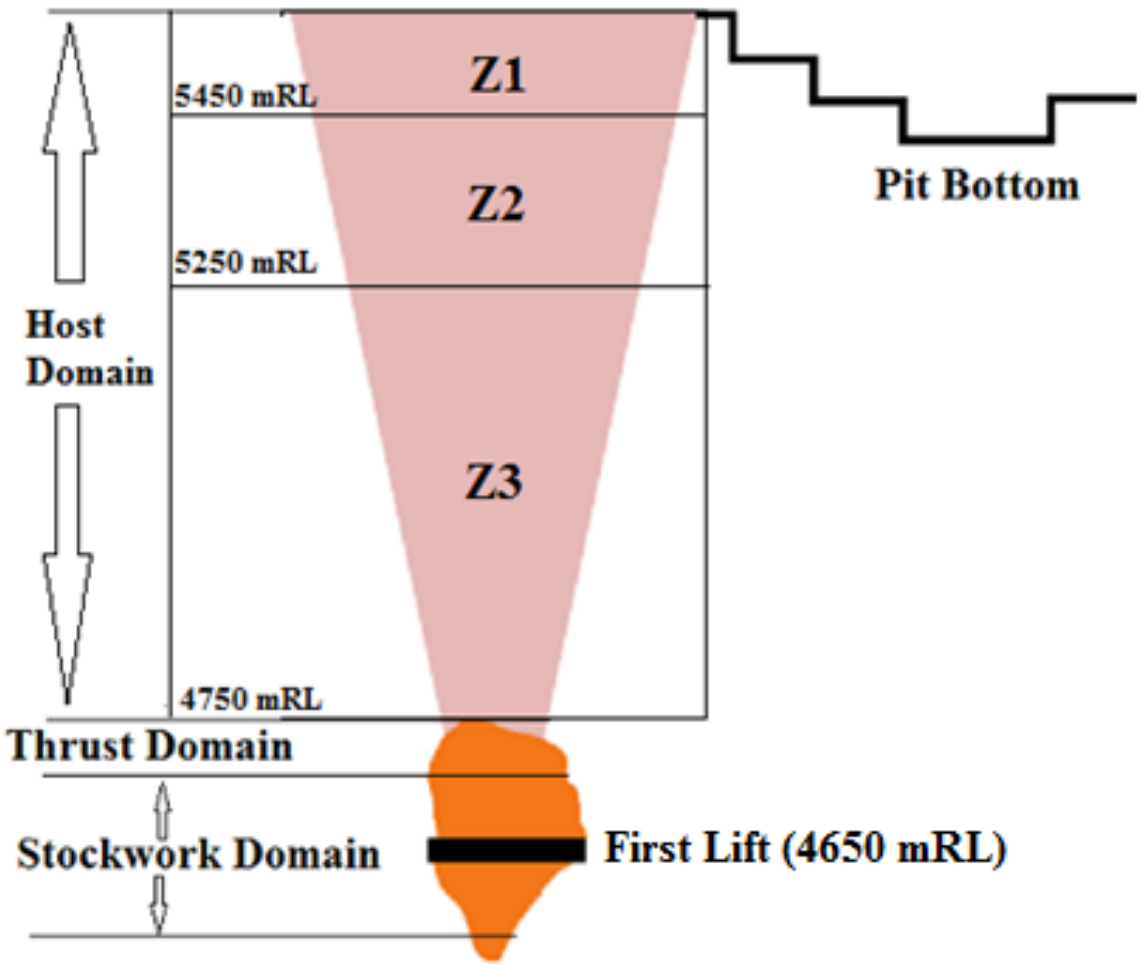

Figure 3.4 Three main zones through which the cave progressed (SRK, 2002).

3.2.1 Initial Blasting

The cave development plan is shown in Figure 3.5, with initial blasting starting in the middle of the orebody on the west side in early March 2006, expanding to the initial undercut to the north and south, then retreating transversely to the footwall in the east.

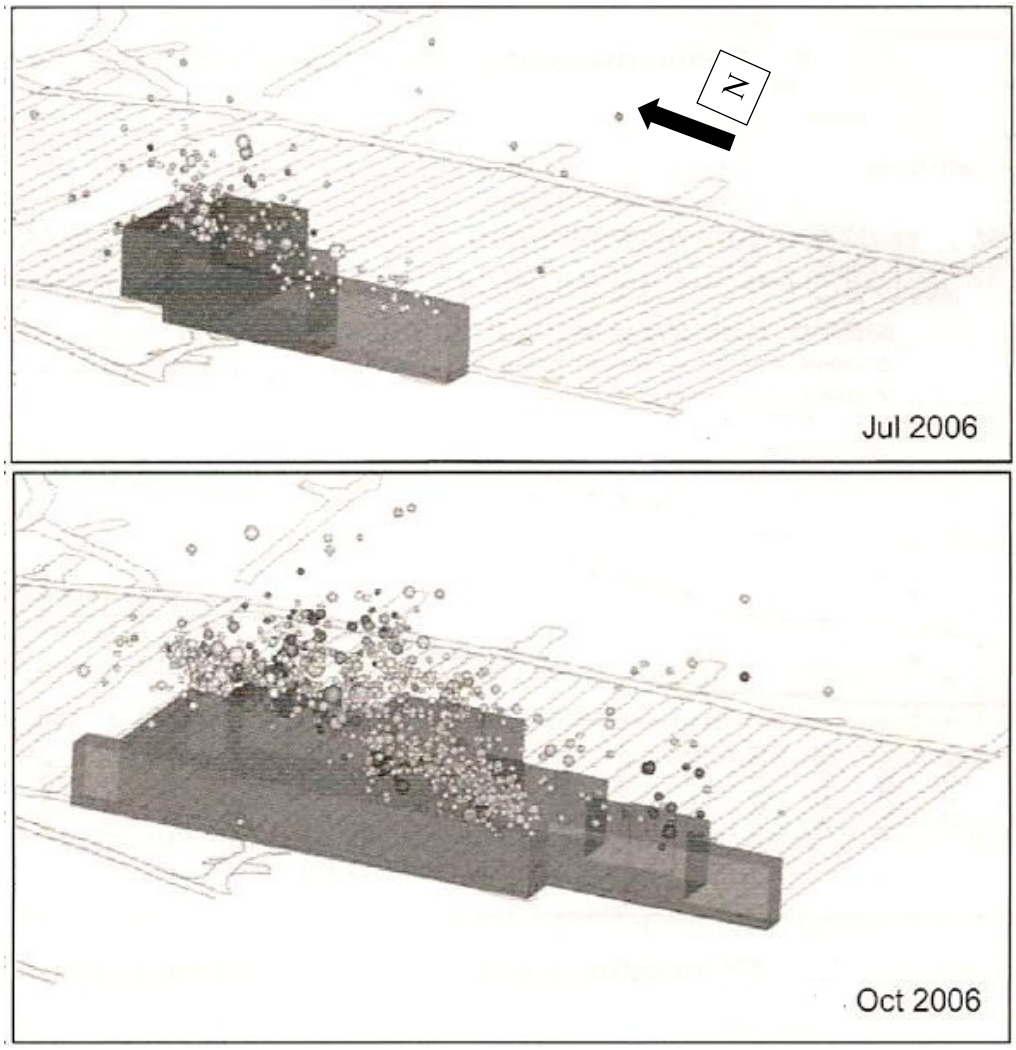

Figure 3.5 Direction of mining of the first lift (Giovinazzo and Singh, 2010).

During the 11 months of the initial blasting, more than 3400 events were recorded. This number of recorded events was relatively low compared with other periods of mining. The seismogenic zone was not clearly defined in the first few months of blasting. However, a distinct seismogenic zone was recognizable above the blasting area by June 2006. Two months before the cave initiation (in December 2006), the seismogenic apex zone was located approximately 60 m above the initial level (4720 mRL) with 20 m thickness (Figure 3.6). The orange line shows the bottom of the apex of the seismogenic zone. It is show as a reference to compare to other time periods.

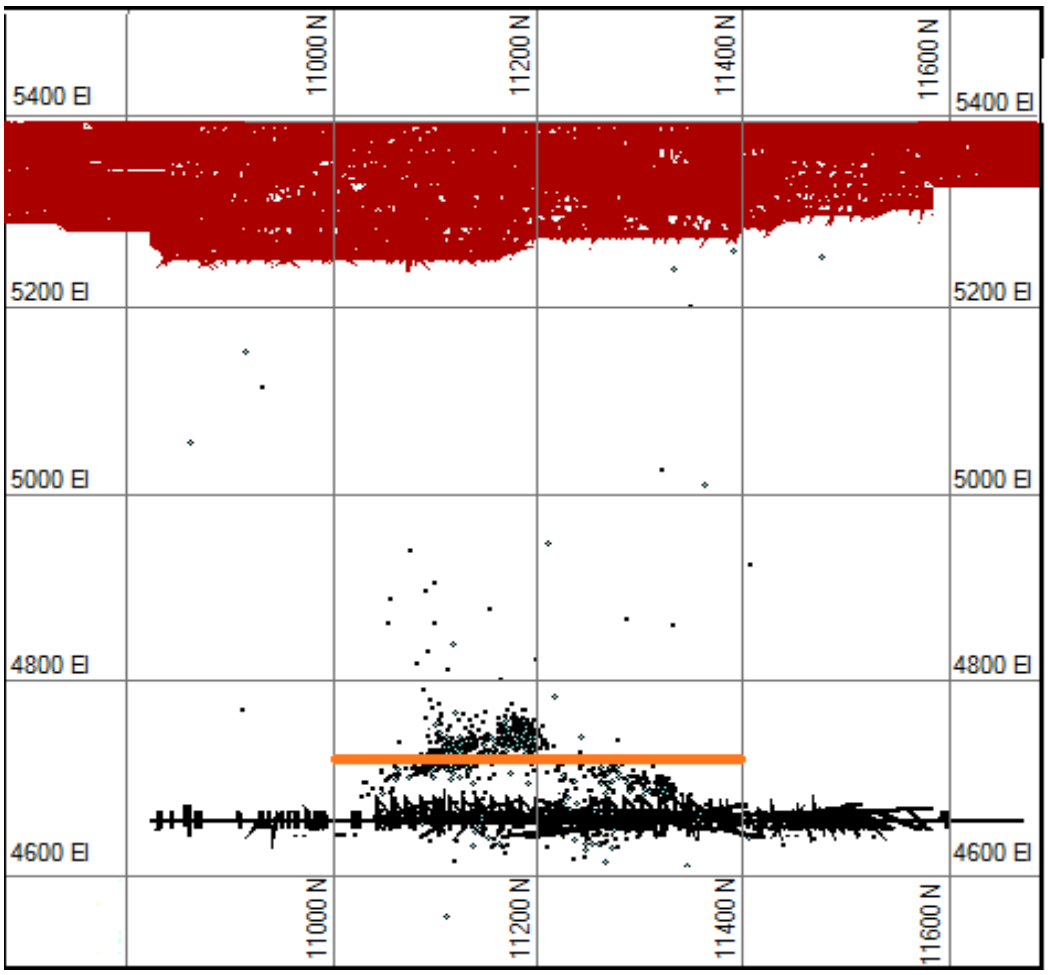

Figure 3.6 Distinct seismogenic zone during initial blasting period events, December 2006.

3.2.2 Cave Initiation

During the cave initiation, a progression of fracturing and rockmass weakening occurs in the cave back due to blasting and primary ore extraction (Mawdesley, 2002). This period can be identified from variations (increases) in the event rate. At Telfer mine, the cave initiation began in February 2007 and continued until November 2007. Almost 10,000 events, including 11 large events ($+1< M_L <+2$), were recorded in 9 months. In the beginning of the cave initiation, the cave apex was approximately at the 4760 mRL and reached to 4850 mRL by the end of the period (with a thickness average of 60 m). The location of the cave apex moved upwards many times during this period (Figure 3.7). The details of the cave initiation mechanisms would be investigated further in the next chapter.

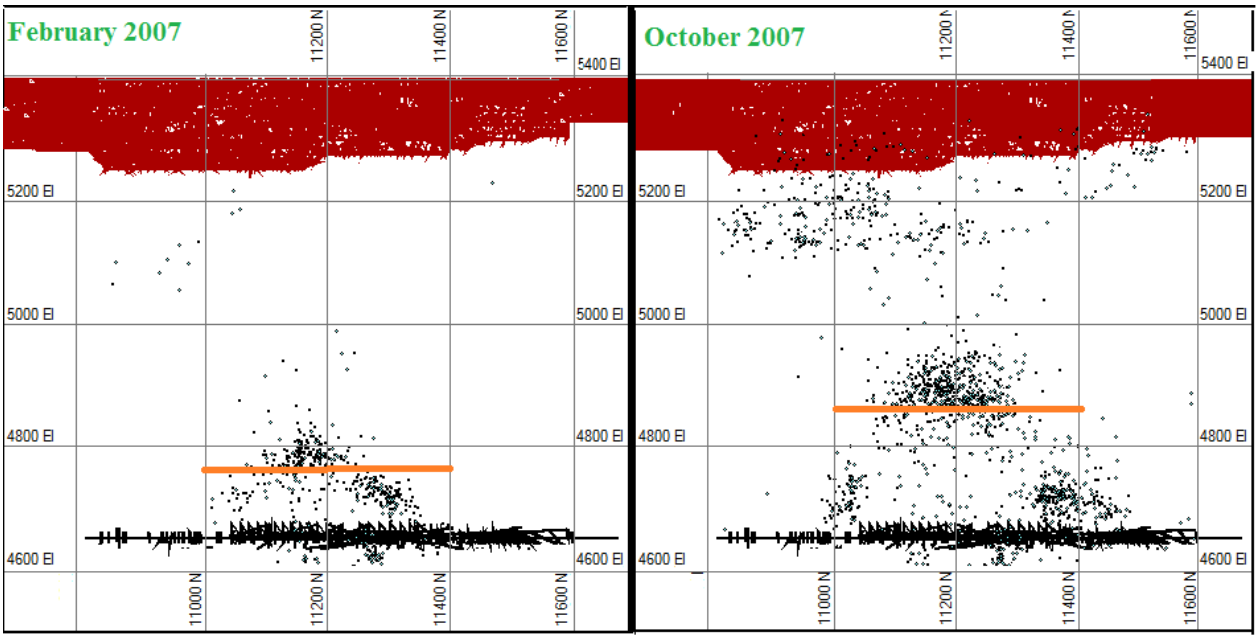

Figure 3.7 Location of the seismogenic apexes in the months of February 2007 (left) and October 2007 (right) during cave initiation.

3.2.3 Cave Propagation

Cave propagation is a continuous rockmass failure process in which the cave back moves rapidly upward as the caved material is mucked from below. During this process, the seismogenic zone migrates because of rockmass failure ahead of the cave back. Cave propagation at Telfer mine was from November 2007 to October 2009. Almost 300,000 events including five very large events ($+2 < M_L < +3$) were recorded during these 23 months. At the beginning of the cave propagation, the cave apex was located approximately at 4860 mRL. By April 2009, the cave apex was located at 5260 mRL, when splitting of the cave apex seismogenic zone occurred. After this time, two separate seismogenic zones were detectable. After another five months, breakthrough into the pit happened in October 2009 (Figure 3.8).

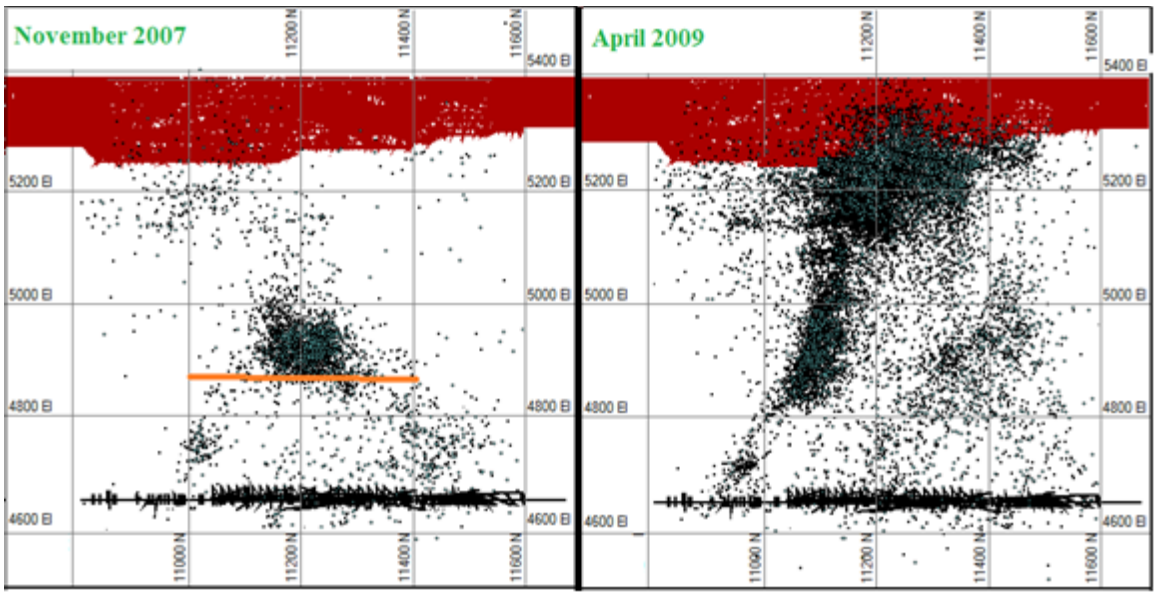

Figure 3.8 Location of the seismic apex in the months of November 2007 (left) and the April 2007 (right) during cave propagation.

The time period of the cave propagation was divided into four periods. The seismogenic zone progressed in the Host domain and passed the M50 and M30 reefs (Figure 3.9). The rate of seismogenic zone movement was significantly affected by M50 and M30 reefs (further details are in Section 4.3).

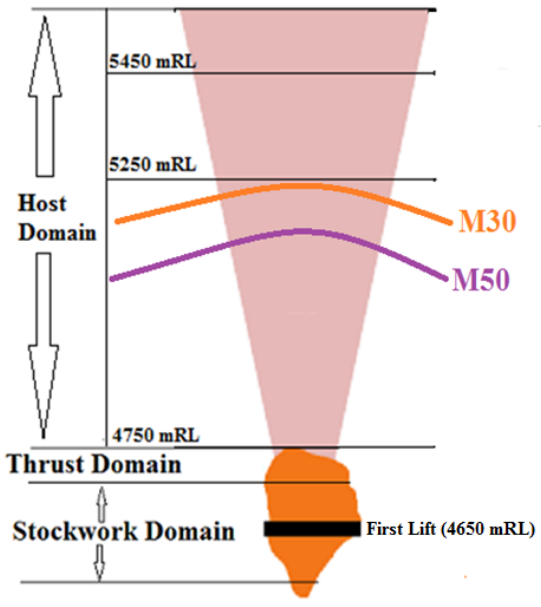

Figure 3.9 Location of M50 and M30 reefs in the Host domain (redrawn from SRK, 2002).

3.2.4 Breakthrough and Breakback

The cave breakthrough is defined by major subsidence in the open pit bottom. This significant subsidence is a vital period of the caving process because of safety and production reasons. Cave breakthrough happened in October 2009 in the west wall of the Telfer open pit at 5380 mRL (Figure 3.10). From October 2009 to December 2010 (the last month of the seismic data collected for this project), more than 120,000 events were recorded. No events larger than local magnitude 2.0 were recorded in this period.

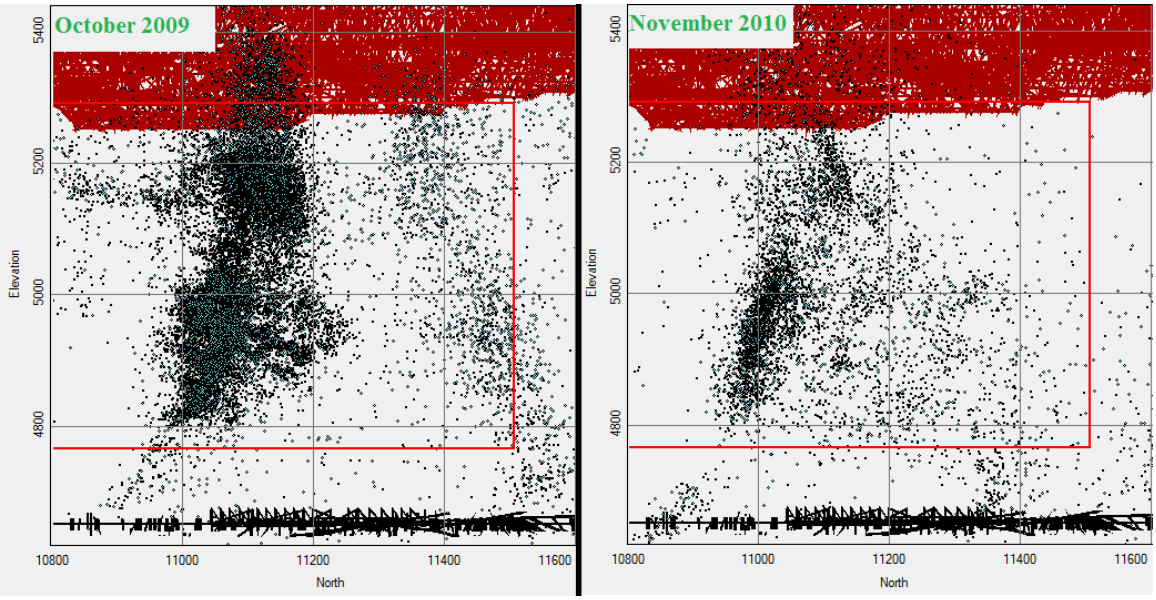

Figure 3.10 Location of the two different seismogenic zones in the months of October 2009 (left) and November 2010 (right) during breakthrough.

In this period, episodes of subsidence-type caving occurred in which sudden displacement of the rockmass between the cave back and bottom of the pit were recorded.

In the breakthrough and breakback period, the average event rate changed three times each of which is analyzed in Section 4.4.

3.3 Identifying and Tracking a Seismogenic Zone

One of the primary objectives in seismic monitoring a sublevel cave (or block cave) is to identify and track the location of the seismogenic zone. Duplancic and Brady (1999) define the seismogenic zone as "an active seismic front occurs due to slip on discontinuities and failure of the rockmass." This behaviour is due to changing stress conditions.

Particular challenges with identifying the seismogenic zone include:

- The zone is three dimensional, with significant variations in elevation,
- The zone moves vertically over time at varying speeds,
- The zone can be quite thin or thick, with the thickness varying over time, and
- Definition of the zone is dependent on the event location accuracy of the seismic system and the sensitivity of the seismic system.

3.3.1 Example of the Seismogenic Zone at Telfer

The seismic events in the month of May 2007 were chosen as an example of a typical seismogenic zone. A plan view, cross sectional projection and longitudinal projection of the 1704 seismic events recorded in this month are shown in Figure 3.11, Figure 3.12, and Figure 3.13.

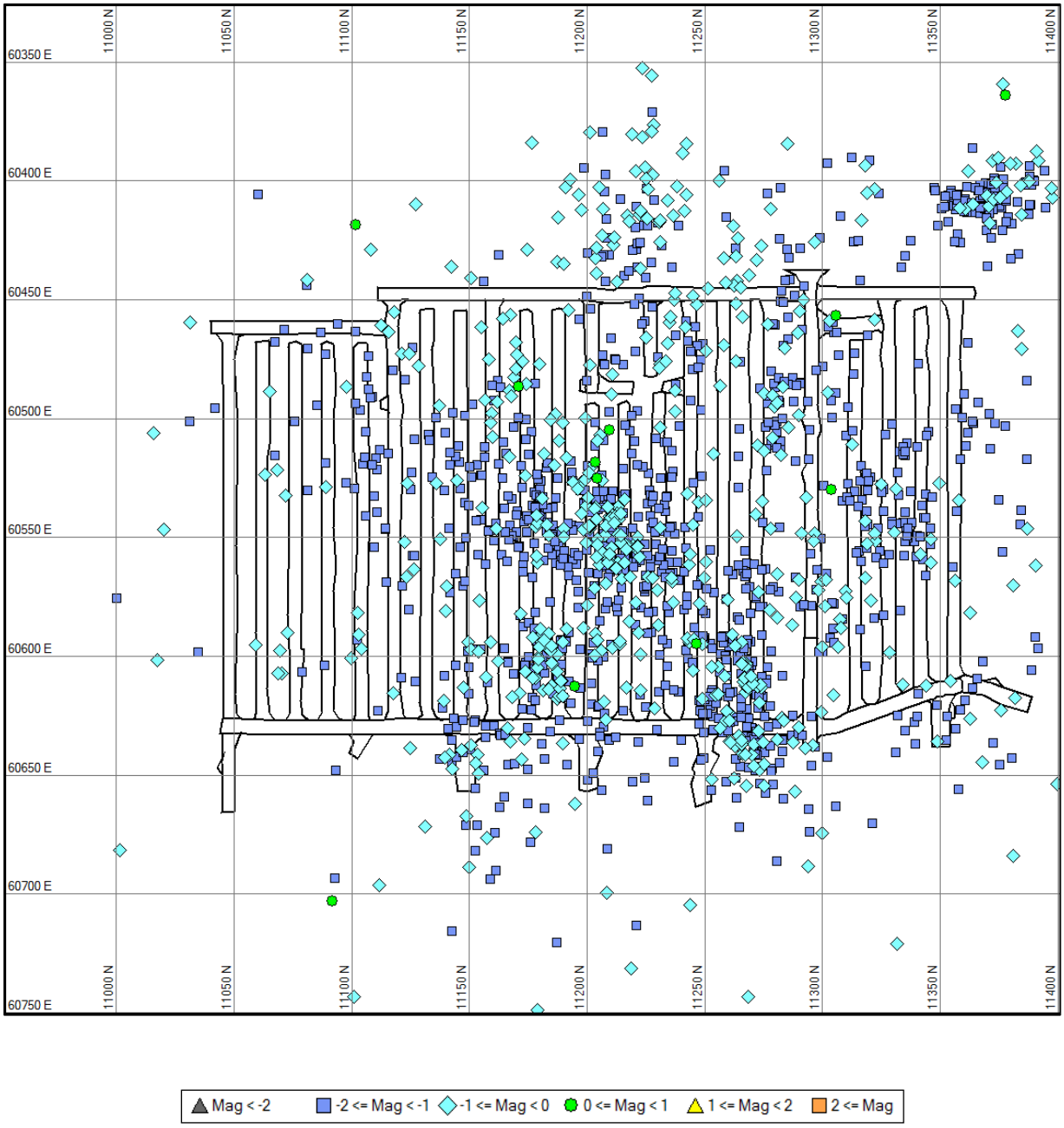

Figure 3.11 Plan view of the locations of the seismic events recorded in May 2007.

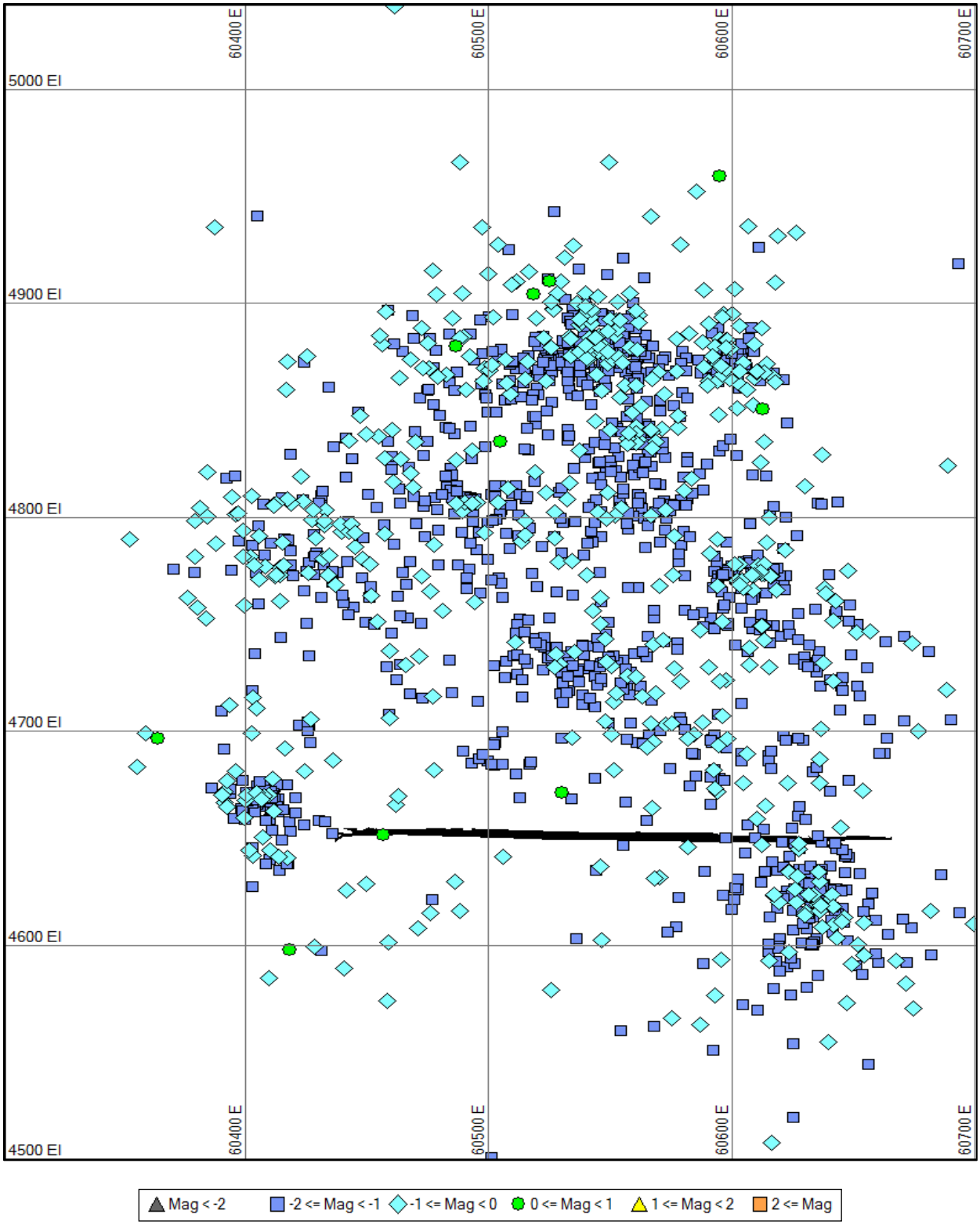

Figure 3.12 Cross-sectional projection looking North of the locations of the seismic events recorded in May 2007. The top extraction level (first lift) is shown at elevation 4650 EL.

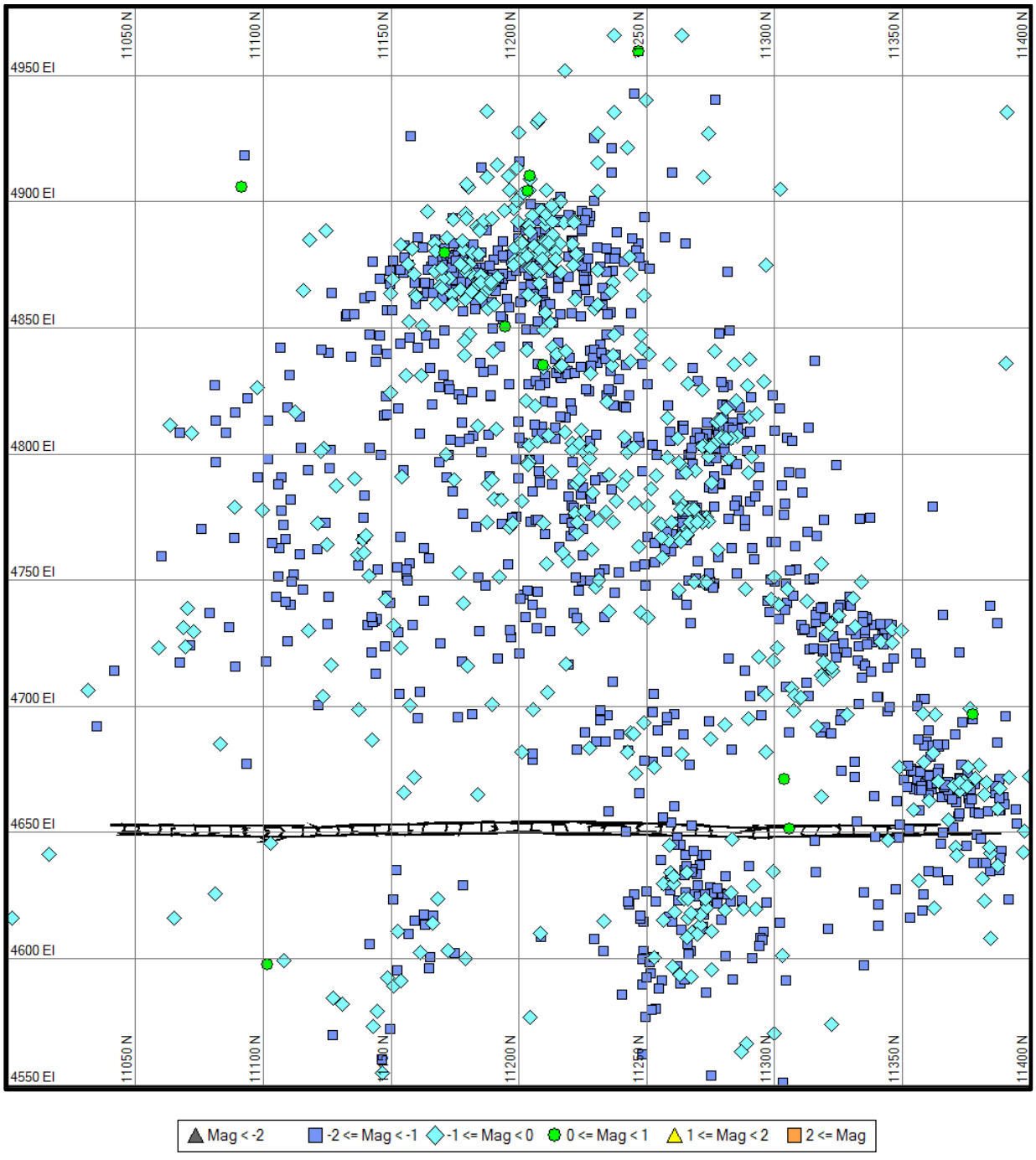

Figure 3.13 Cross-sectional projection looking West of the locations of the seismic events recorded in May 2007. The top extraction level (first lift) is shown at elevation 4650 EL.

There are a number of important observations of the event locations in Figure 3.11, Figure 3.12, and Figure 3.13:

- The events occur over the cave footprint.

- There is a grouping of events around 60640E, 11270N below the first lift level, between elevations 4580EL and 4650EL. This population is not real seismic events, but rather broken muck being tipped into a footwall orepass. There is a similar group of orepass noise events at about 11150N.
- Real seismic events that represent the seismogenic zone are located between 4650EL and 4950EL.
- None of the views can be used to clearly identify the limits of the seismogenic zone. The event locations need to be considered in three dimensions.

A series of North looking sections have been cut every 50 m with the events within 25 m of each section plotted (Figure 3.14 and Figure 3.15). Observations from the North sections in Figure 3.14 and Figure 3.15:

- There are few events at the north and south ends of the cave on the 11050N and 11400N sections. A seismogenic zone of events cannot be identified on these two sections.
- On each of the sections between 11100N and 11350N, there is considerable variation in the elevation of the events.
- On each of the sections between 11100N and 11350N, a zone of high event rates can often be identified. However, there is considerable scatter in the event locations.

To further delineate a seismogenic zone, events within 25 m of the Eastings of 60450E, 60500E, 60550E and 60600E will be grouped. This is shown diagrammatically in Figure 3.16. The average elevations are shown in Figure 3.16 with a black dot. The median event elevations are shown in Figure 3.16 with a red dot. Observations from the four sections in Figure 3.16 are:

- For some sections, there may be events up to 100 m above or below the average elevation.
- The average elevation can be affected by a small number of distant events.
- The median elevation is less affected by a small number of distant events.
- The median elevation appears to be reasonable for a centre line for the seismogenic zone. However, there needs to be a means of defining the top and bottom of the seismogenic zone.

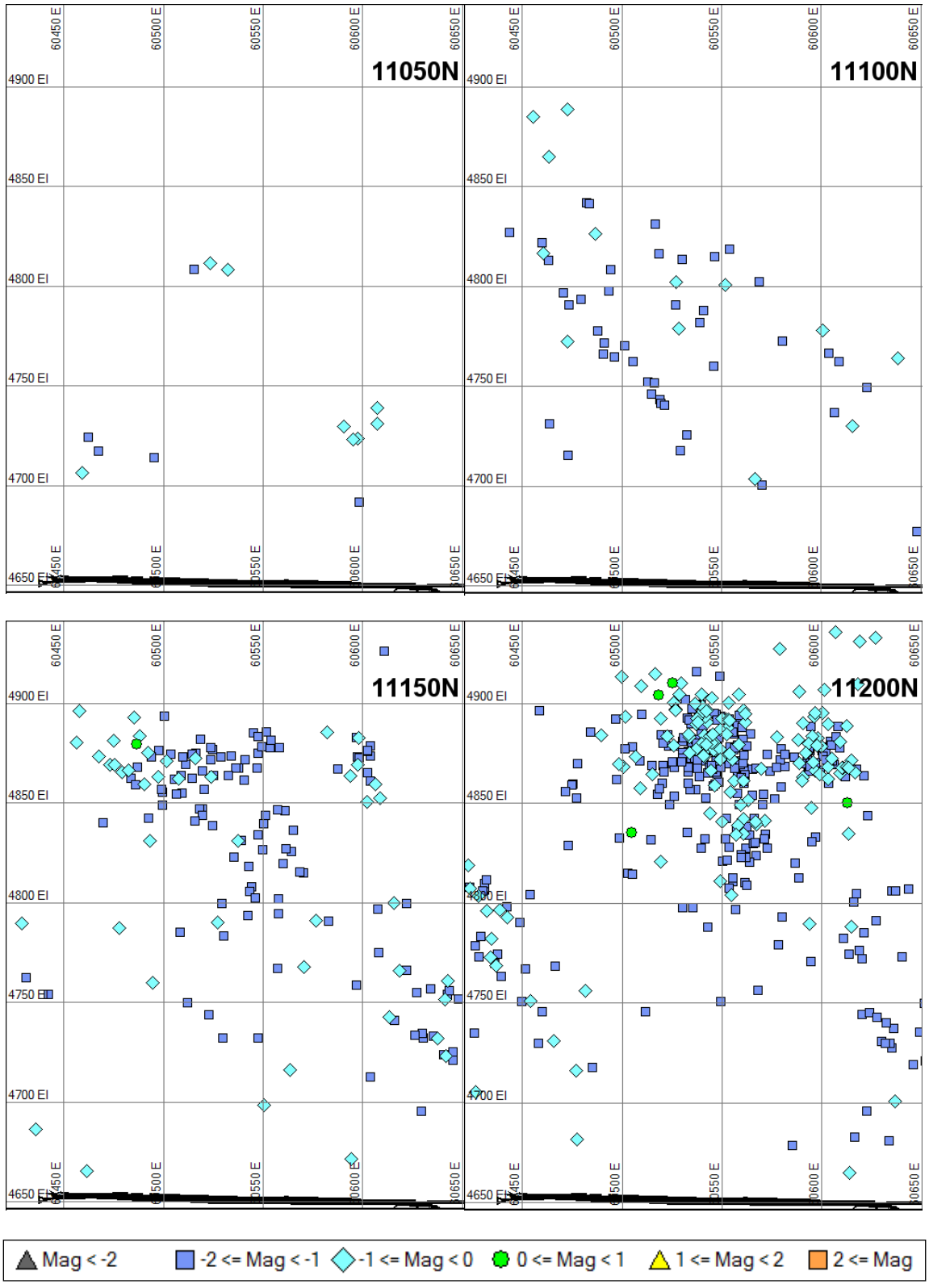

Figure 3.14 Cross-section projections on 11050N, 11100N, 11150N and 11200N. The events shown have a northing within 25 metres of the section.

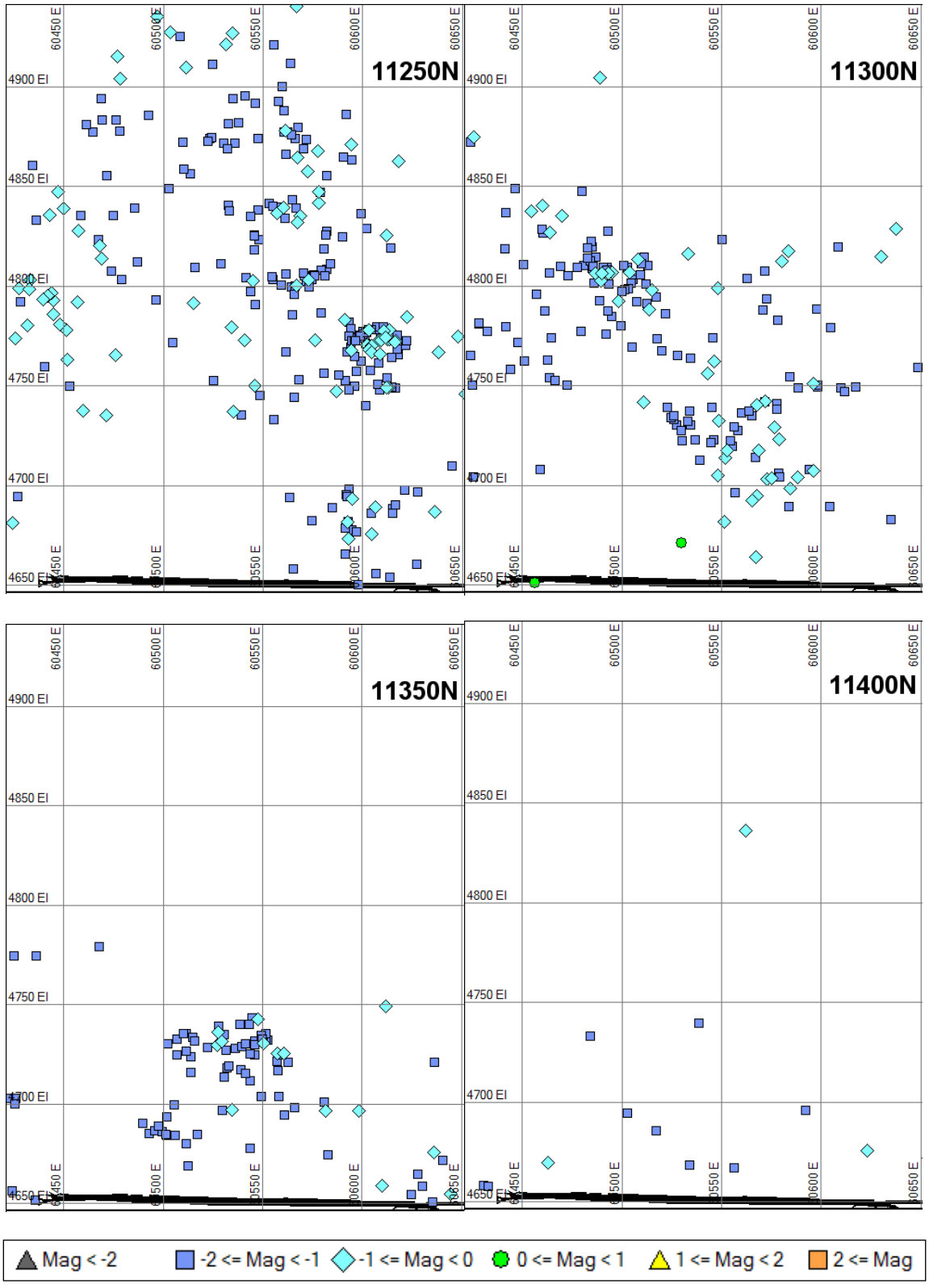

Figure 3.15 Cross-section projections on 11250N, 11300N, 11350N and 11400N. The events shown have a northing within 25 metres of the section.

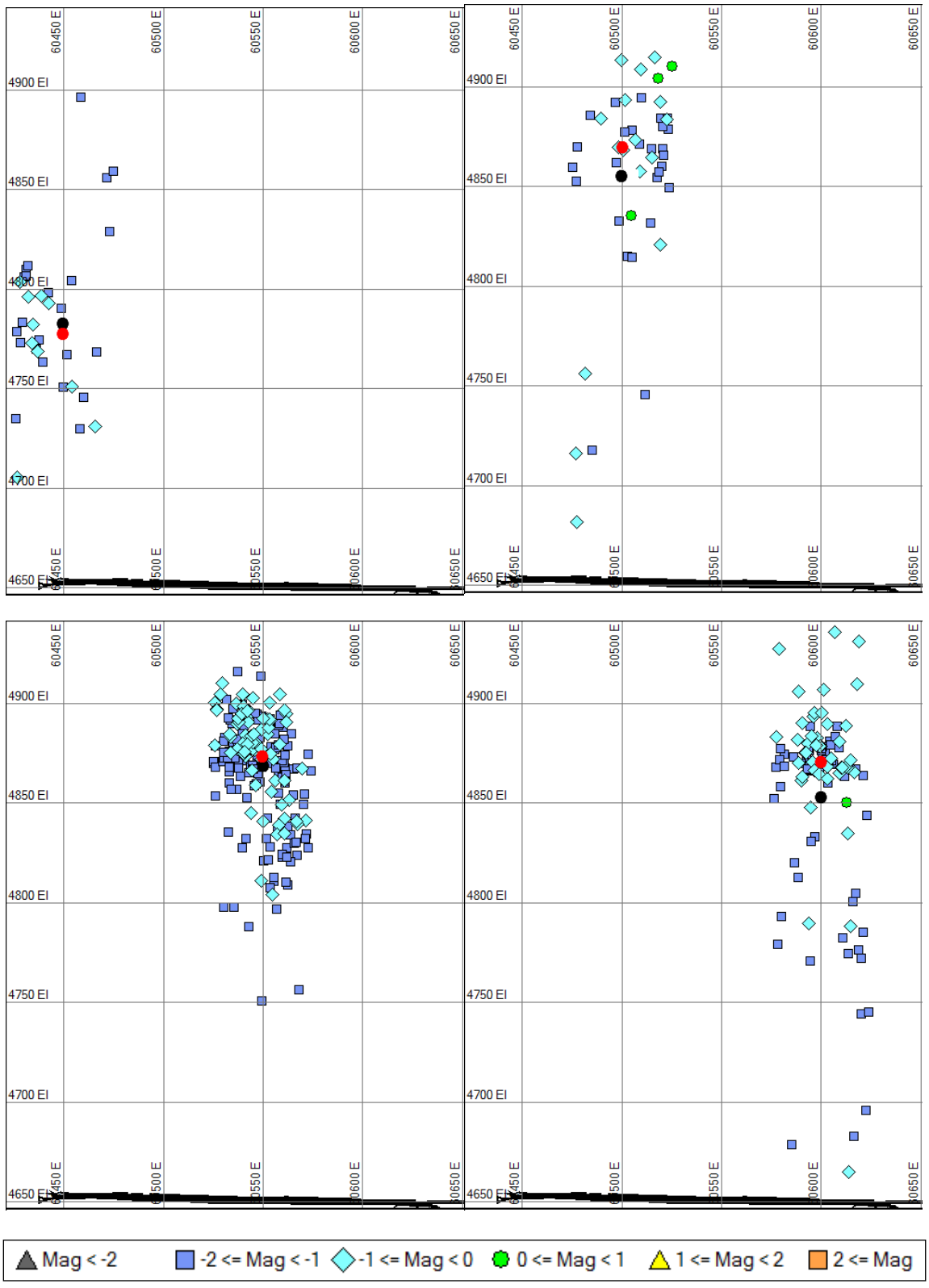

Figure 3.16 On the North section 11200N, events within 25 m of the Eastings 60450E, 60500E, 60550E and 60600E are shown individually. The median elevation is shown with a red dot. The average elevation is shown with a black dot.

A simple method is to incorporate a percentage of the events above and below the median elevation. An arbitrary 40% above and 40% below the median, and 25% above and 25% below the median are shown in Figure 3.17. Observations from Figure 3.17 are:

- Using the median plus or minus 25% defines a reasonable narrow seismogenic zone, but 50% of the events are outside the seismogenic zone.
- Using the median plus or minus 40% defines a much wider seismogenic zone, only 20% of the events are outside the seismogenic zone.
- The seismogenic zone does not continue beyond the 60600E, which is the footwall limit of the cave footprint.

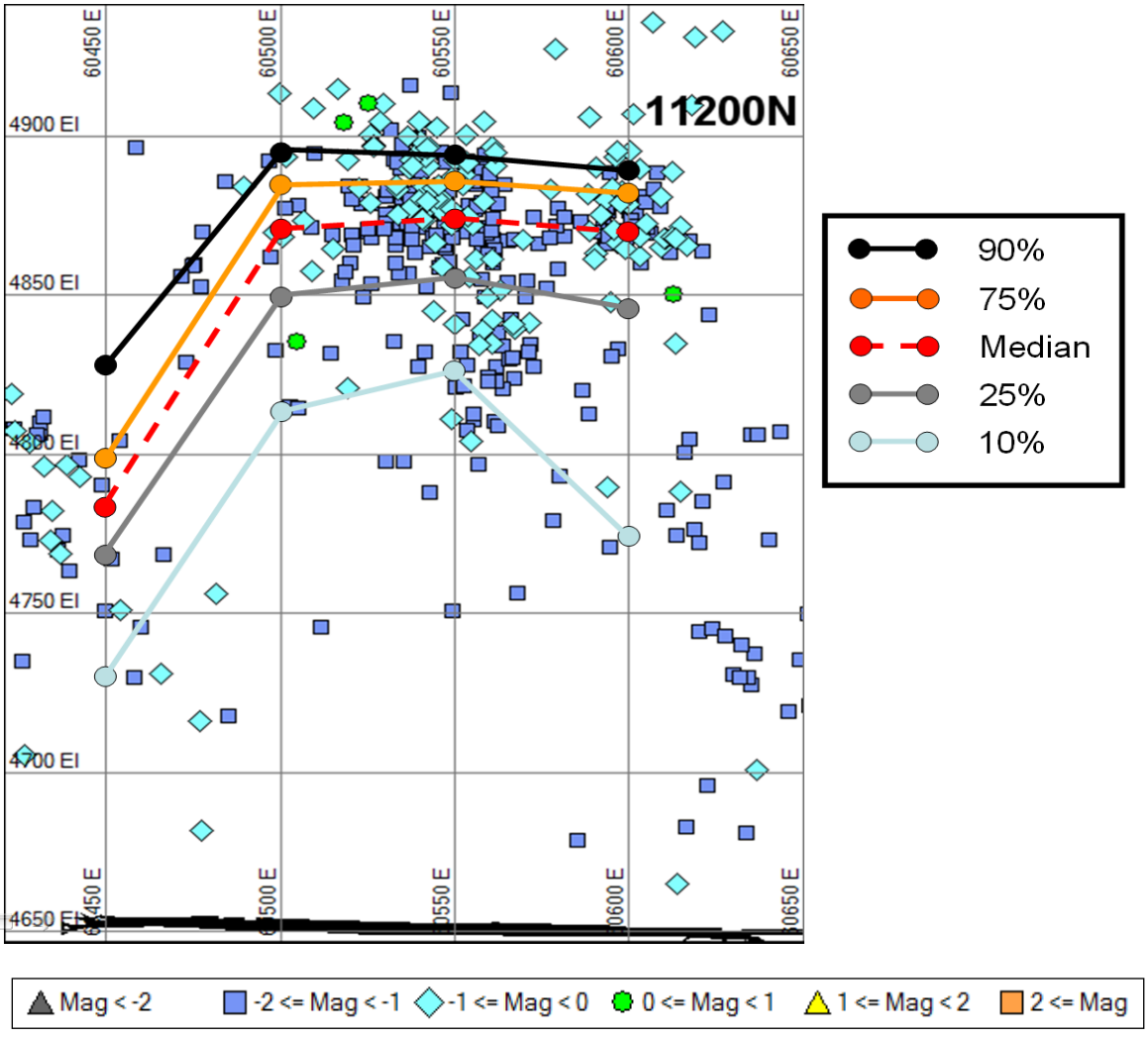

Figure 3.17 The median event elevation is shown with a line for 60450E, 60500E, 60550E and 60600E. The 10 percentile elevation, 25 percentile elevation, 75 percentile elevation and 90 percentile elevations are also shown with lines.

An example of the varying elevation of the seismogenic zone at Telfer is shown in Figure 3.18. This is the median elevation of the seismogenic zone for the seismic data collected in May 2007.

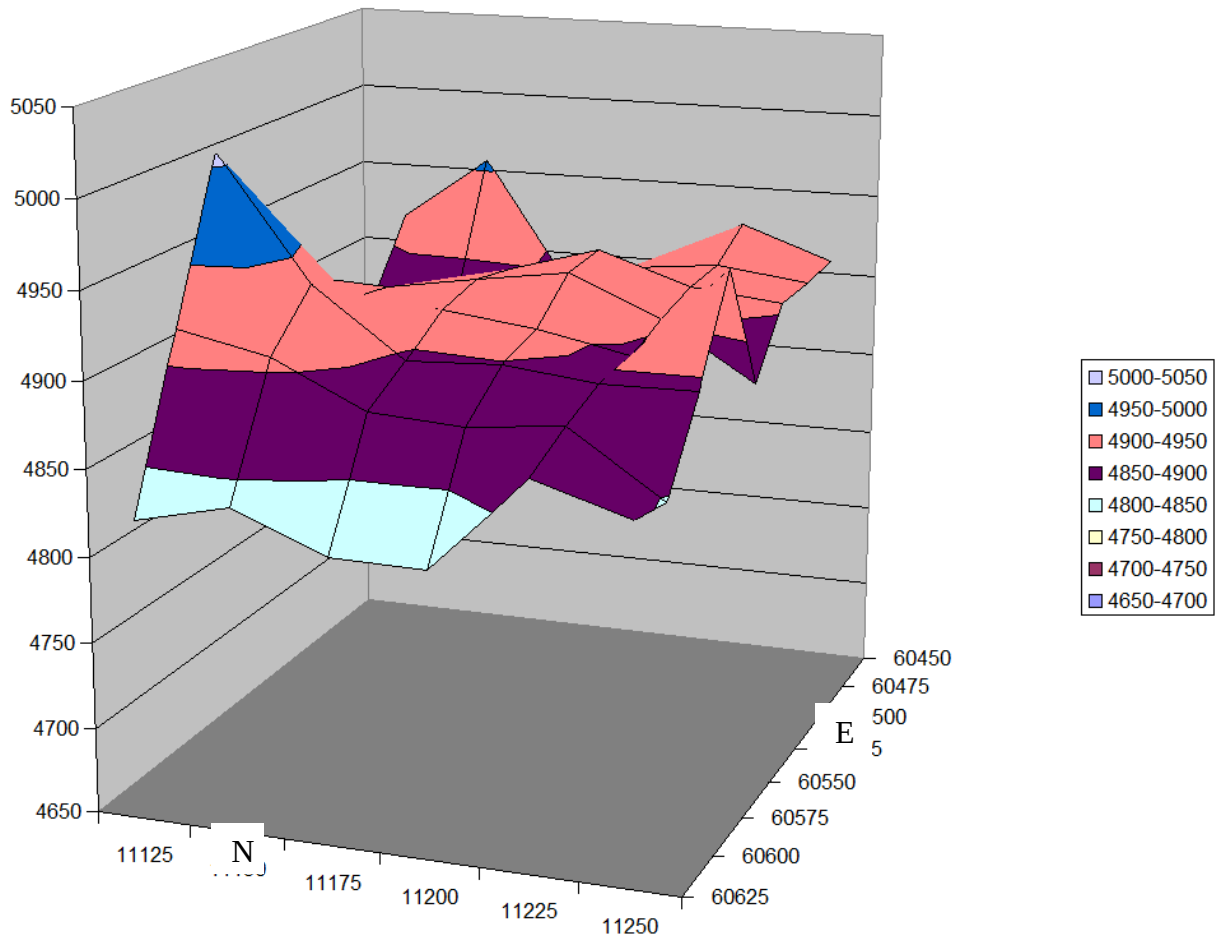

Figure 3.18 Median RL of the Telfer seismogenic zone for May 2007.

Using this methodology, a grid has been created on a 50 m by 50 m spacing in the Northing and Easting direction. Using the events closest to each grid point, the median event elevation gives the effective middle of the seismogenic zone. Ultimately, there is no ideal methodology to define the seismogenic zone. There are a number of considerations:

- A tighter grid spacing gives more detail in the seismogenic zone location. However, this creates more variability in the seismogenic zone location over time.

- The shorter the time span that is considered, the smaller the vertical height of the seismogenic zone.
- If the seismogenic zone moves upwards quickly, a shorter time span will define a tighter zone.
- For a seismic system with high event location accuracy, the seismogenic zone is likely tighter and better defined.
- The 25%, 50%, and 75% elevations divide the event into quartile groups which may be useful to further investigate variations in the seismogenic zone.
- The 10% and 90% elevations could be viewed as effective limits of the top and bottom of the seismogenic zone.

3.3.2 Seismogenic Zone Movement at Telfer

Using the above methodology on a fortnightly basis (every two weeks), the median elevation, lower 25 percentile elevation and upper 25 percentile elevation has been determined for the apex (top) of the seismogenic zone at Telfer. This data is shown graphically in Figure 3.19.

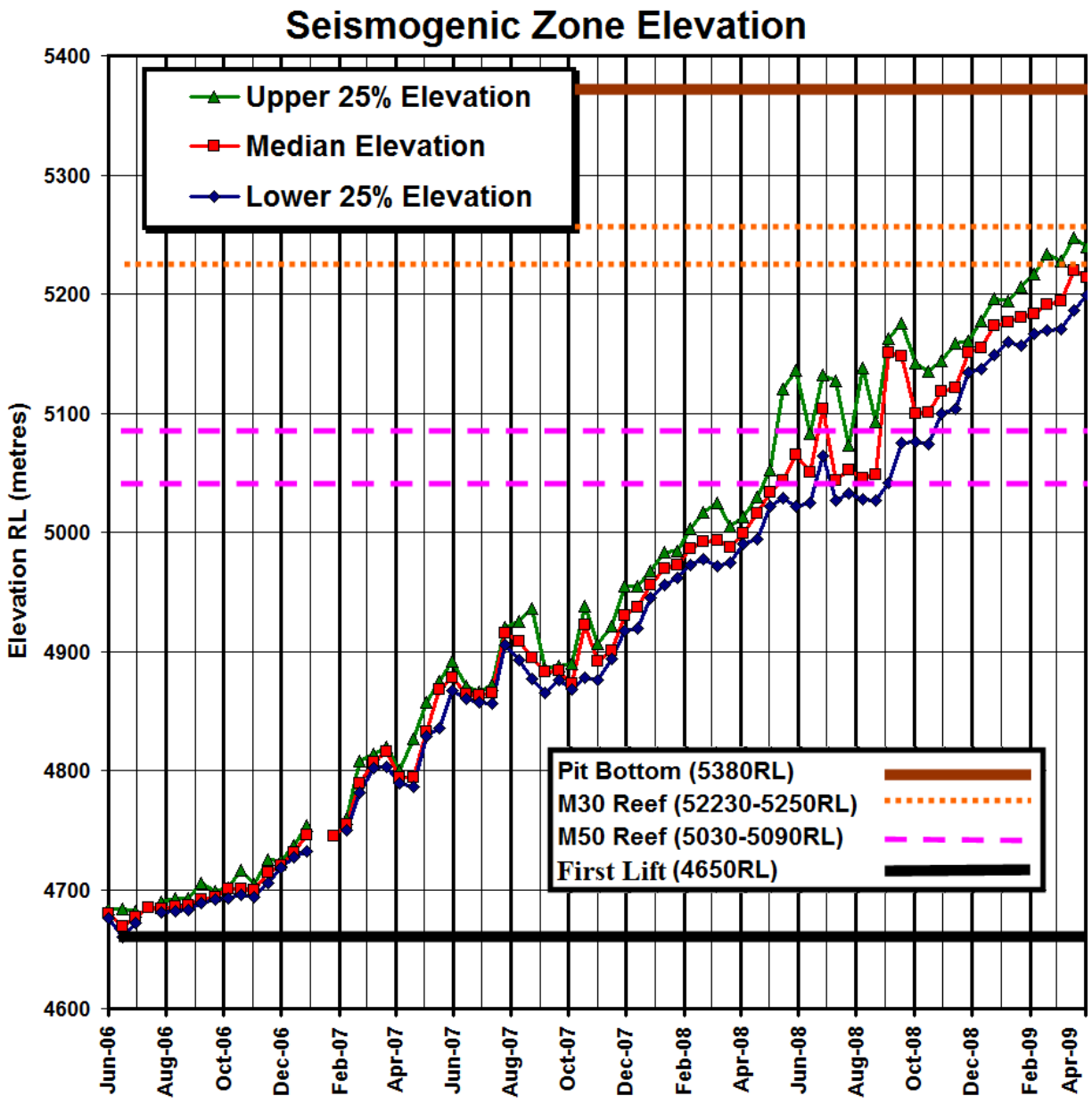

Figure 3.19 Median elevation and the lower 25% and upper 25% elevation of the seismic events in the Telfer seismogenic zone.

There are a number of interesting observations from Figure 3.19:

- The seismogenic zone is relatively narrow at the start of the cave and gradually gets quite thick as the cave approaches the pit.
- Upward movement of the seismogenic zone is at relatively consistent rate until November 2006. This rate is 20 m in 5 months, or 4 m per month, or 130 mm per day.
- The rate of upward movement increases in November 2006, with a roughly constant rate until May 2008.
- Movement of the seismogenic zone slows and stalls as the seismogenic zone approaches the M50 reef in May 2008. For the next few months, the seismogenic zone does not move upward at a constant rate and the thickness of the seismogenic zone increases significantly. The cave apex passed the M50 reef in April 2008.
- Movement of the seismogenic zone slows, becomes thick and moves erratically as it approaches the M30 reef in about January 2009.
- Variability within the data can result in slight decreases in the median elevation of the seismogenic zone.

3.3.3 Characteristics of the Seismogenic Zone Movement at Telfer

A typical seismogenic zone is shown in Figure 3.20 (December 2007). The median elevation, lower 25 percentile elevation and 75 percentile elevations are shown in Figure 3.20. There are distinct trends in the source parameters of the seismogenic zone:

- The larger magnitude events tend to be between the 25 and 75 percentile elevations. Most of the events with an event magnitude of greater than -1 are found in this area.
- The largest events also tend to occur in the apex, or highest part, of the seismogenic zone.
- The higher Apparent Stress events tend to be located above the median elevation. This would suggest that there is induced higher stress acting in the upper part half of the seismogenic zone.
- In the lowest 25% of the events, the Apparent Stress is much lower than that in the rest of the seismogenic zone, with almost all events having and Apparent Stress less than 10 kPa.
- The highest Apparent Stress events also tend to occur near the apex of the seismogenic zone. Almost all of the events with an Apparent Stress greater than 30 kPa occur near the seismogenic zone apex.
- Proportionally, the events with the highest S:P energy ratio occur in the upper 50% of seismogenic zone, and in particular in the upper 25% of the seismogenic zone. This would suggest that a shearing seismic source mechanism is the most common failure mode at the top of the seismogenic zone.
- In the lowest 25% of the seismogenic zone, there are proportionally fewer high S:P energy ratio events, or the events are more related to stress fracturing.

While these are generalizations about event source parameters in the seismogenic zone, the generalizations tend to be consistent for all of the caving periods at Telfer.

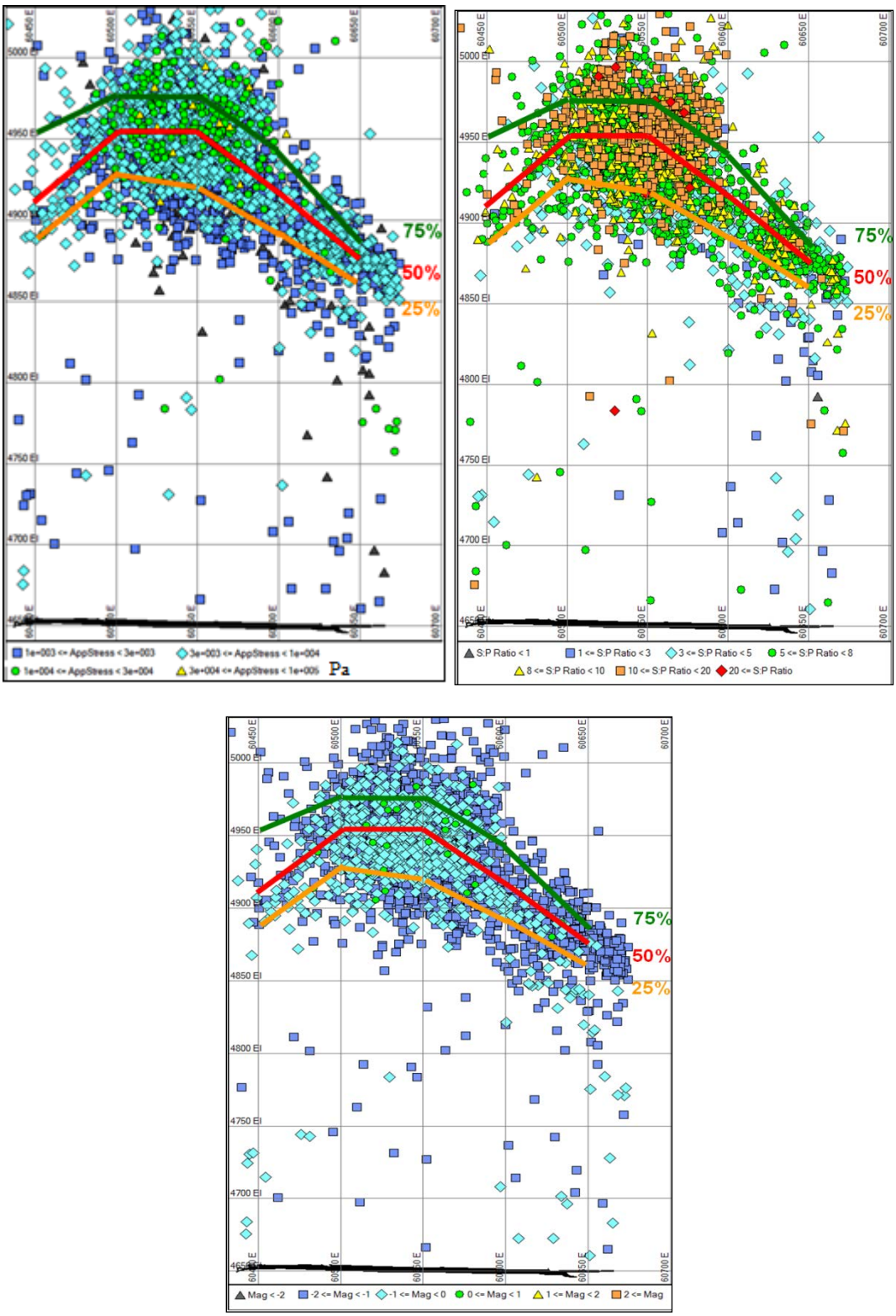

Figure 3.20 Telfer seismogenic zone for December 2007 showing variations in Apparent Stress in Pa (top left), S:P energy ratio (top right) and event magnitude (bottom).

3.4 Comparison of the Seismogenic Zone and Physical Instrumentation

Extensometers at Telfer mine were installed in three different phases. The extensometers were spatially distributed in a way to cover the area above the first lift for measuring the cave back level (Giovinazzo and Singh, 2010).

During the phase 1, seven extensometers were installed at different elevations above the first lift. As shown in Figure 3.21, three of these extensometers (Stations number 1, 2, and 3) were located on the west side of the first lift, one is located on the middle (Station number 5), and the remaining three Stations (number 4, 6, and 7) were placed on the east side. These extensometers were installed in the period of the initial blasting and all of them had failed before the first period of the cave propagation (Giovinazzo and Singh, 2010).

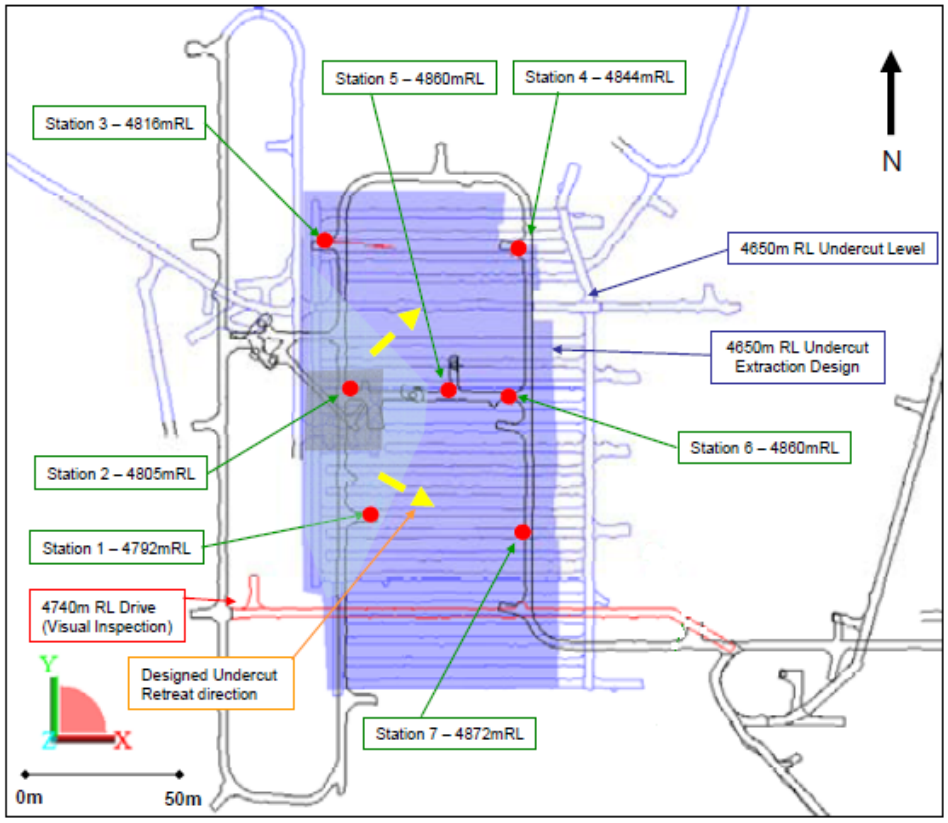

Figure 3.21 Plan view of the distribution of the extensometers during phase 1 (Giovinazzo and Singh, 2010).

According to the locations of the phase 1's extensometers and Table 3.3, the progression of the cave on the west side of the first lift is lower than the cave progression on the east side. This can be related to the lower quality of the rockmass on the east side compared with the west side (due to Graben fault).

Table 3.3 Location of the cave back in phase 1 for different extensometers (Giovinazzo and Singh, 2010).

	Station 1	Station 2	Station 3	Station 4	Station 5	Station 6	Station 7
Cave Back RL (m)	4792	4805	4700	4680	4860	4850	4838

Comparing the cave progression rate (using extensometers) and the average seismogenic zone upward movement shows that there is a stronger relation between these two rates on the west side compared with the east side. In other words, the cave progression rate was faster than the upward movement of the seismogenic zone in the east side (Table 3.4).

Table 3.4 Comparison of the cave progression rate and seismogenic zone upward movement during the phase 1 for the Telfer extensometers (Giovinazzo and Singh, 2010).

	Seismogenic zone upward movement (m/d)	Caving Rate for Station (m/d)
Station 1 (Dec 2006 to Oct 2007)	0.7	0.7
Station 2 (Dec 2006 to July 2007)	0.6	0.5
Station 3 (May to Nov 2007)	0.6	0.06
Station 4 (NA)	NA	NA
Station 5 (March to August 2007)	0.7	1.2
Station 6 (April to Nov 2007)	0.3	0.7
Station 7 (March to Nov 2007)	0.5	0.6

As a result of incomplete data, the exact locations of the extensometers are not defined during phase 2. However, the cave progression rate can be compared with the seismogenic zone upward movement during the phase 2. As shown in Table 3.5, there is a poor correlation between cave progression rate and seismogenic zone upward movement. This poor relation can be attributed to

the effect of the M50 and M30 reefs because the seismogenic zone was migrating in the areas between M50 and M30 in this period.

Table 3.5 Comparison of the cave progression rate and seismogenic zone upward movement during the phase 1 for different extensometers (Giovinazzo and Singh, 2010).

	Seismogenic zone upward movement (m/d)	Caving Rate for Station (m/d)
Station 1 (Feb to Nov 2008)	0.6	0.1

In the phase 3, extensometers are not applicable because of the split in the seismogenic zone after early April 2009.

4 CAVING ANALYSIS

4.1 Initial Blasting Rockmass Failure Mechanisms

Trenning (2002), using geotechnical investigations at Telfer, defined 6 sets of discontinuities (including a bedding) within the Telfer Deeps orebody (Table 4.1).

Table 4.1 Discontinuity set data at Telfer Deeps (Trenning, 2002).

Discontinuity	Dip (Average)	Dip Direction (Average)
J1	85	315
J2	90	40
J3	30	215
J4	30	35
J5	30	310
Bedding	45	270

The joint sets J1 and J2 are almost vertical and orthogonal while the discontinuity sets J3, J4, and J5 dip at shallow to moderate angles towards the SW, NE, and NW, respectively. The J3, J4, and J5 discontinuities are pervasive within the caving zone. Existence of the sub-horizontal discontinuities generally assists the caving progression. The bedding planes occur on average every 2-3 m. A set of thrust faults is more widely and less regularly spaced from the first lift level to the surface. The bedding and thrusts are pervasive and continuous while the J3, J4, and J5 are less continuous (Trenning, 2002).

As mentioned in the previous chapter, the first lift was opened in the Stockwork domain (4650 mRL). The Stockwork domain consisted of Limey and I30 Domains. The Limey was comprised of calcareous sandstone and I30 was a quartz reef (Trenning, 2002). During the blasting of the first lift, cave back had to pass through the Limey and I30 domains above the first lift (Figure 4.1).

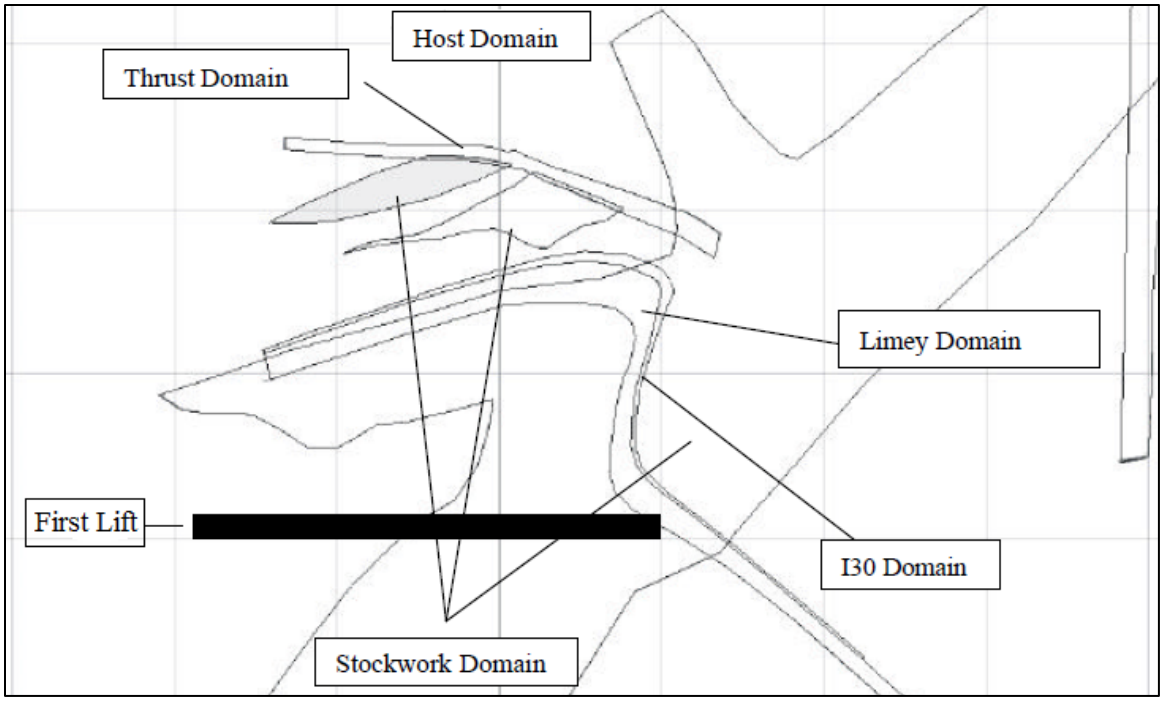

Figure 4.1 Three important domains through which the cave should progress (Trenning, 2002)

Blasting started from the west side of the orebody in a location approximately 200 m from the Graben fault. Investigations into the early initial blasting location indicated that the cave face was directed along with SW-NE. This direction was perpendicular to the direction of the maximum horizontal principal stress. Table 4.2 shows the magnitudes and orientation of the major, intermediate and minor principal stresses.

Table 4.2 *In-situ* stress field in Telfer Deeps (SRK, 2002).

Principal Stresses	Magnitude (MPa)	Orientation	
		Dip (°)	Bearing (°)
Major	6 + 0.046D[1]	20	130
Intermediate	0 + 0.032D	40	22
Minor	0 + 0.019D	43	240

1. D = depth below surface in metres.

Figures 4.2, 4.3, and 4.4 show longitudinal cross sections (top of the each picture) and plan views (bottom of the each picture) of the first lift, and the seismic events (color dots) during the initial blasting from March 2006 to January 2007. A seismogenic zone was distinguishable in June 2006 at an elevation between 4670 EL and 4680 EL. The largest thickness of the seismogenic zone in this period was approximately 20 m.

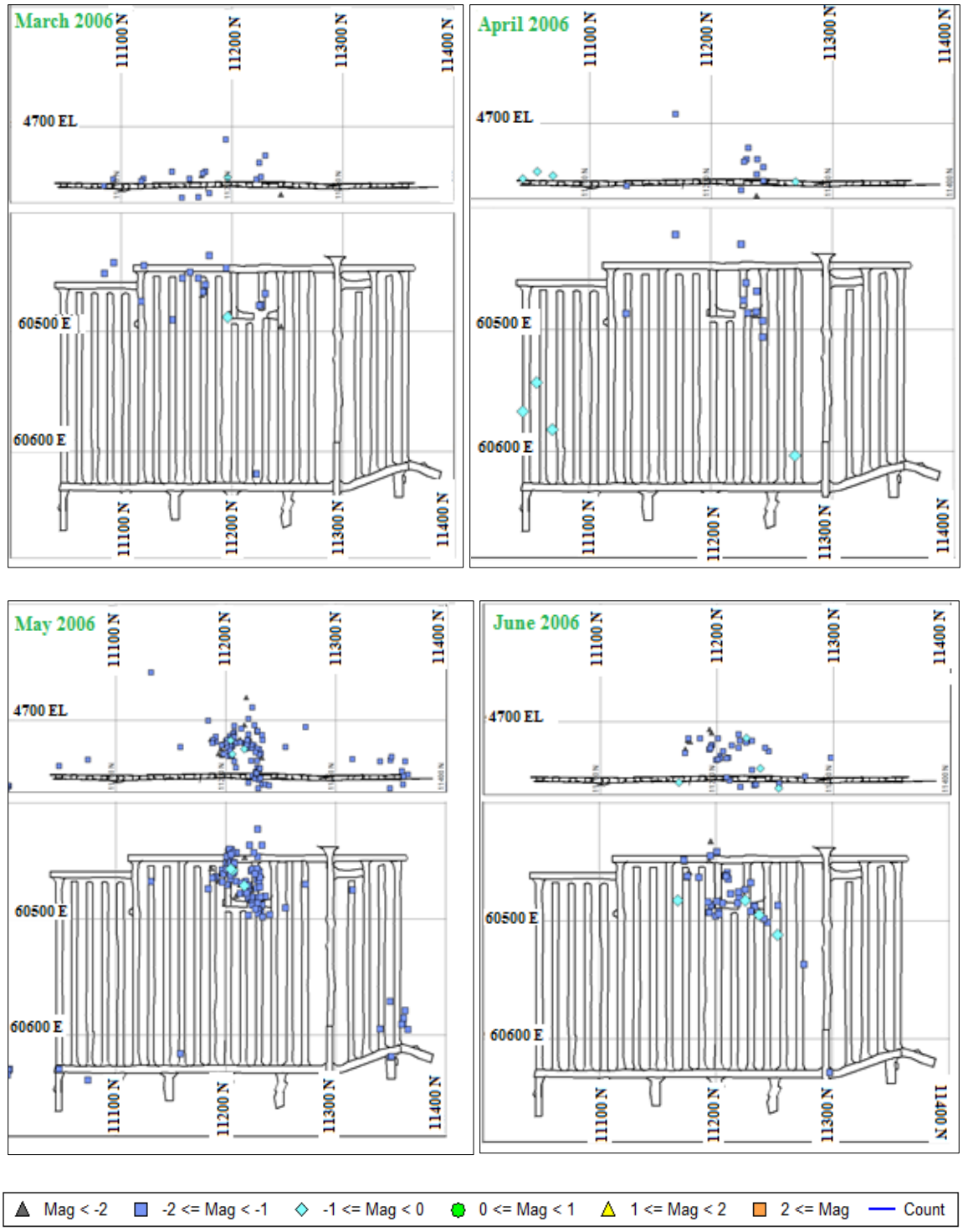

Figure 4.2 The section (top of the each picture) and plan view (bottom of the each picture) of the first lift and also the seismic events (color dots) during the initial blasting from March to June 2006.

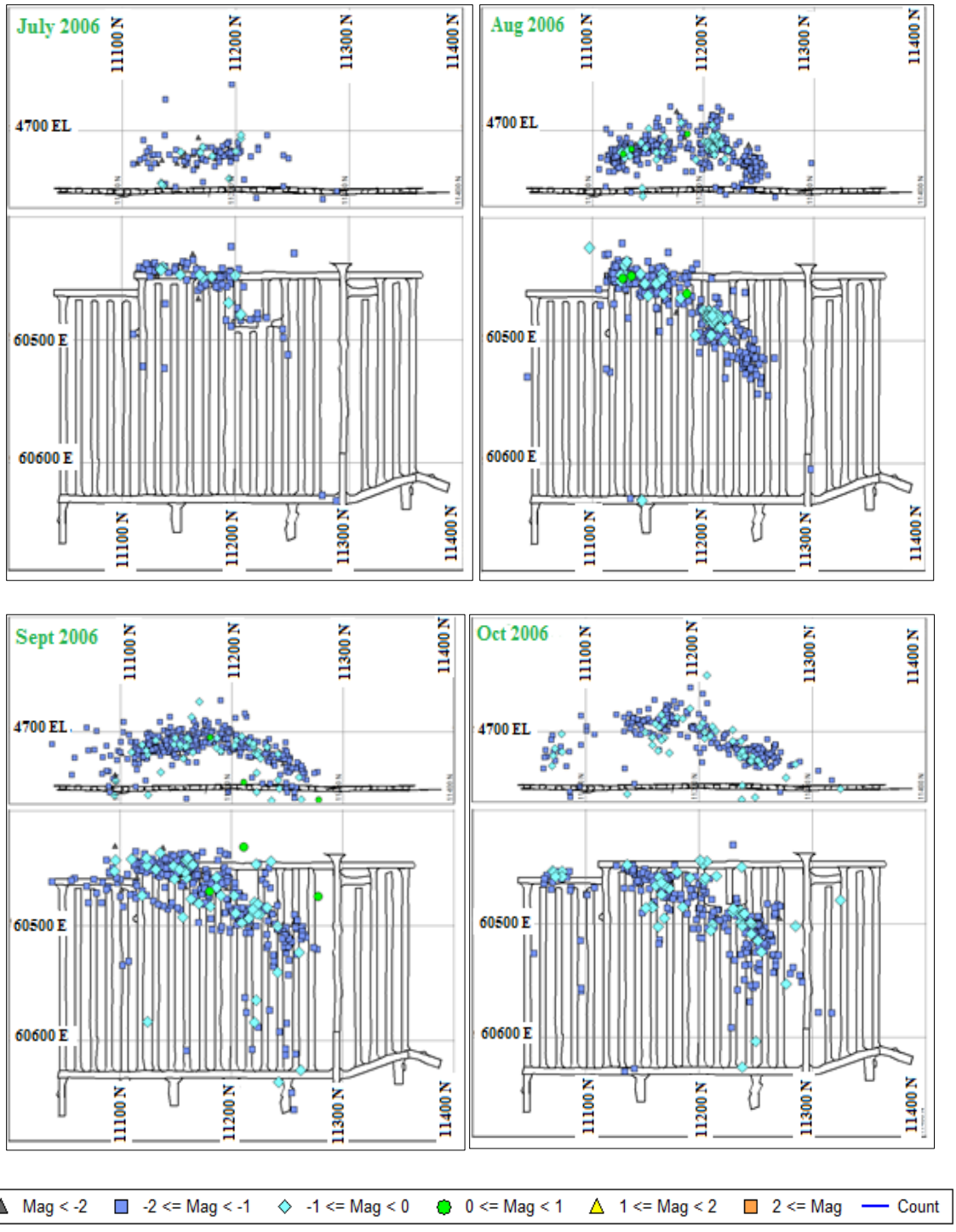

Figure 4.3 The section (top of the each picture) and plan view (bottom of the each picture) of the first lift and also the seismic events (color dots) during the initial blasting from July to October 2006.

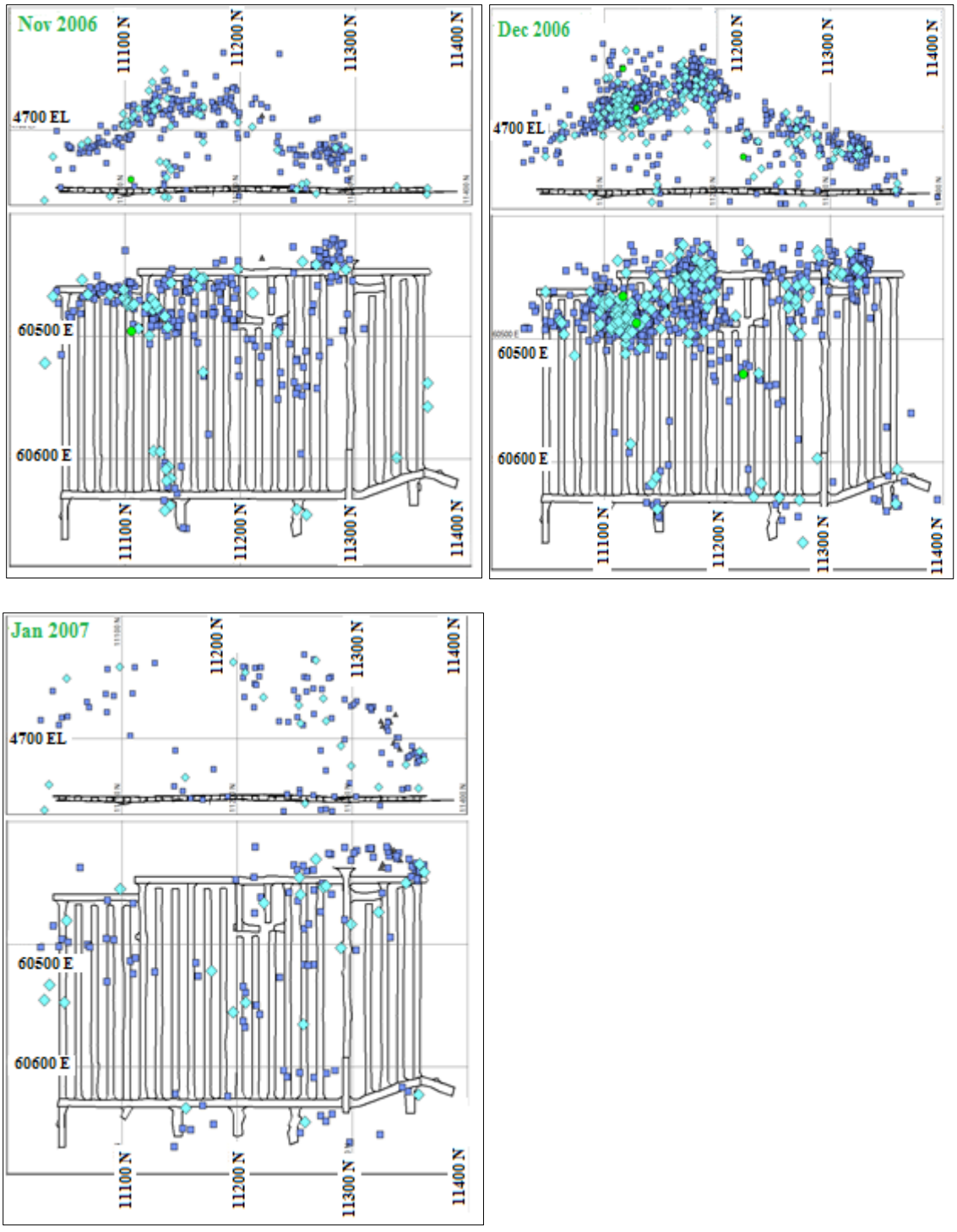

Figure 4.4 The section (top of the each picture) and plan view (bottom of the each picture) of the first lift and also the seismic events (color dots) during the initial blasting from November 2006 to January 2007.

4.1.1 Magnitude- Time History Analysis During the Initial Blasting

As shown in Figure 4.5, the timing and number of the large and significant events are good indicators of the strong relation between the blasting times and the number of events. The events are direct result of the mine blasting and all events have a local magnitude less than 1.0, typical of blast induced seismicity (Hudyma, 2008). The sensitivity of the seismic monitoring system decreased slightly between October 2006 and mid-November 2006. Also, there is about one month data loss between late December 2006 and late January 2007.

The event rate from March to early August 2006 was almost constant. After period, the event rate accelerated until mid-September 2006. Between mid-September and mid-November 2006, the event rate appeared to decrease. However, this was an effect of the decreased seismic system sensitivity. After mid-November 2006, the event rate increased noticeably. The highest rate of events was recorded in December 2006 (average of 109 events per day).

From the elevation, the location, and the thickness of the seismogenic zone (from March to mid-September 2006), it can be inferred that the seismogenic zone was progressing in the Stockwork domain (Figure 4.1). During the progression of the seismogenic zone in the Stockwork domain, the seismogenic zone passed through the Limey and I30 domains. The sudden increase in the number of events between early August and late August 2006 is likely due to widening of the first lift and the change in the lithology (the seismogenic zone entered the Limey domain).

The seismogenic zone passed through the Thrust domain from mid-September to mid-November 2006. In this period, more than 55% of the events had an S:P energy ratio greater than 10 that implied shearing as the primary seismic source mechanism. The low number of recorded events between October 2006 and mid-November 2006 was related (at least partially) to the change of seismic system sensitivity. After this period, the seismogenic zone entered the Host domain and progressed in this domain until the end of monitoring period (2010/10/01).

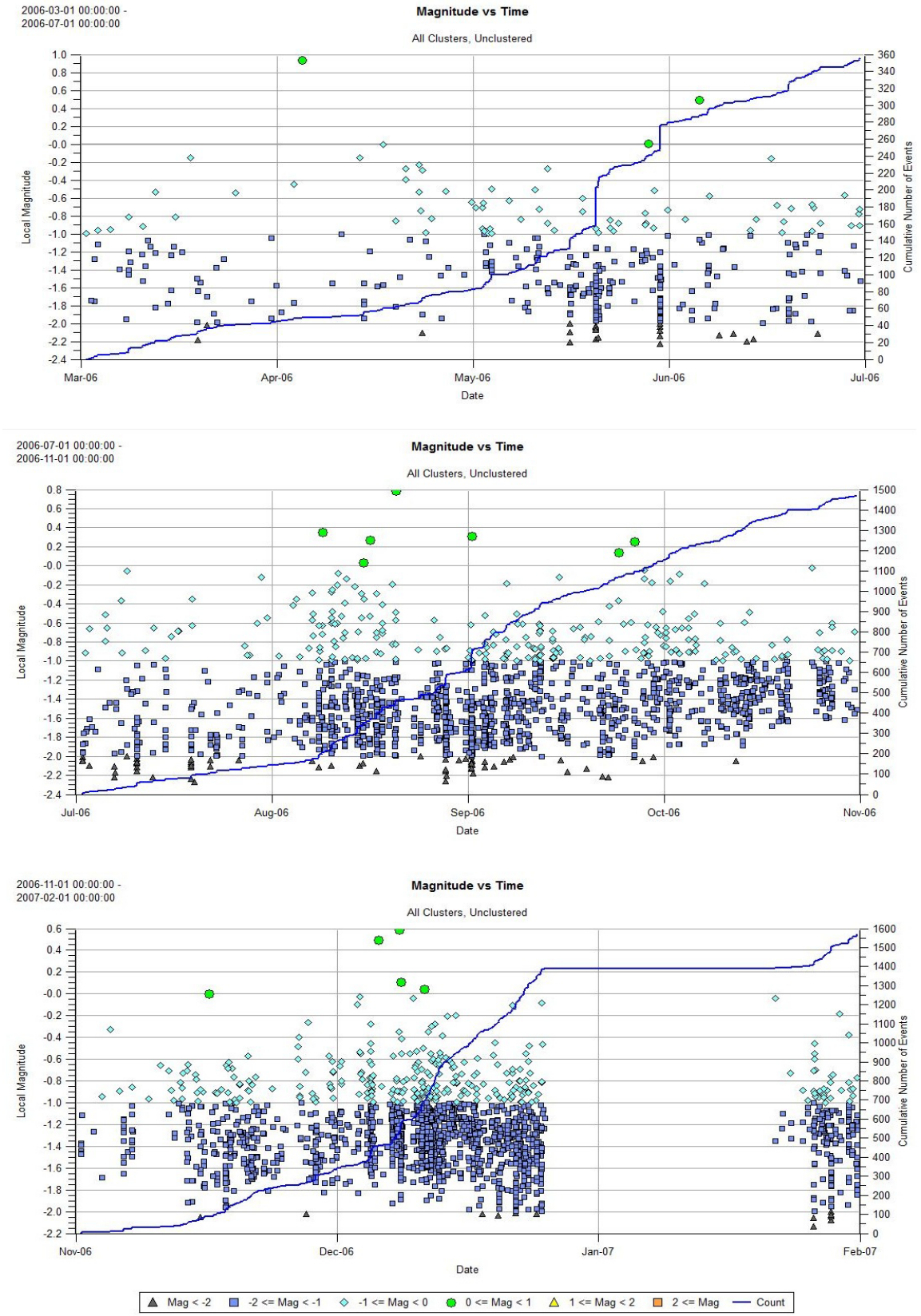

Figure 4.5 Magnitude- time history and cumulative number of events during initial blasting.

4.1.2 Frequency Magnitude Analysis

Frequency-Magnitude analysis for the events during initial blasting shows that the events are a relatively well-behaved data set (Figure 4.6). The b-value for these events was 1.4. The largest expected event from this data set also was 0.9 which was in a good agreement with the events recorded.

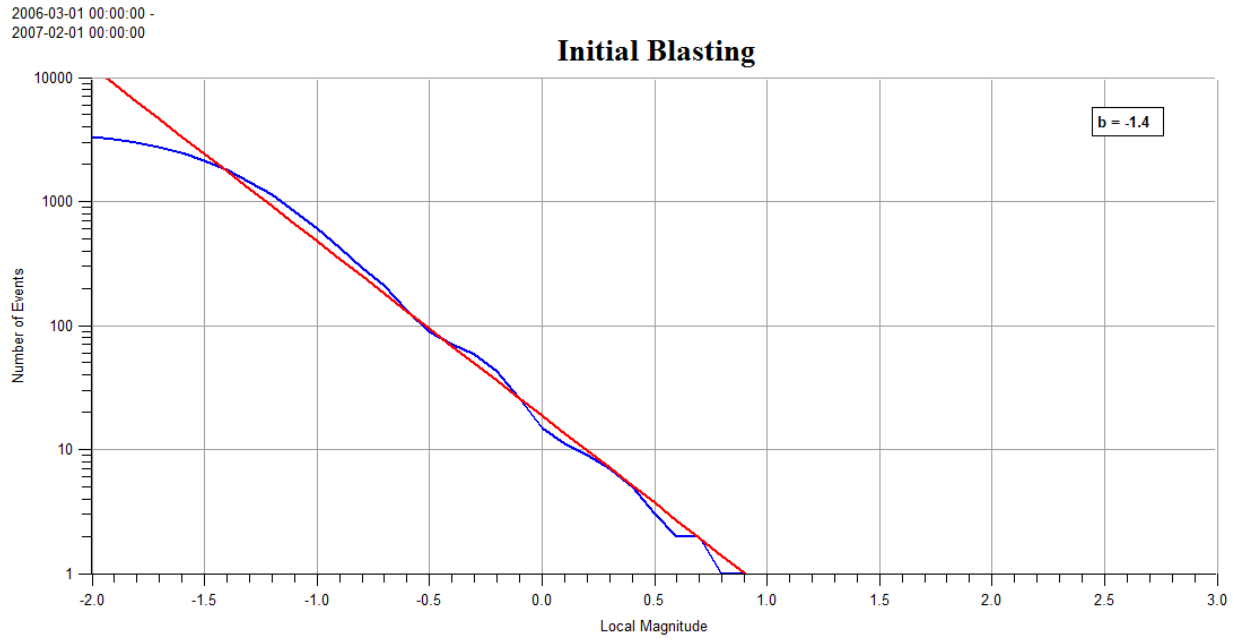

Figure 4.6 The Frequency- Magnitude of the events during Initial Blasting

4.1.3 S:P Energy Ratio Analysis

In the events during initial blasting, 5% of the events have an S:P energy ratio less than 3, and 52% of the events have an S:P energy ratio greater than 10 (Figure 4.7). A shear type source of mechanism is the dominant mechanism. Stress change source mechanisms typically have a non-shearing seismic source mechanism (Urbancic et al., 1992) or a low S:P energy ratio. The Telfer initial blasting events are not following above mentioned generalization.

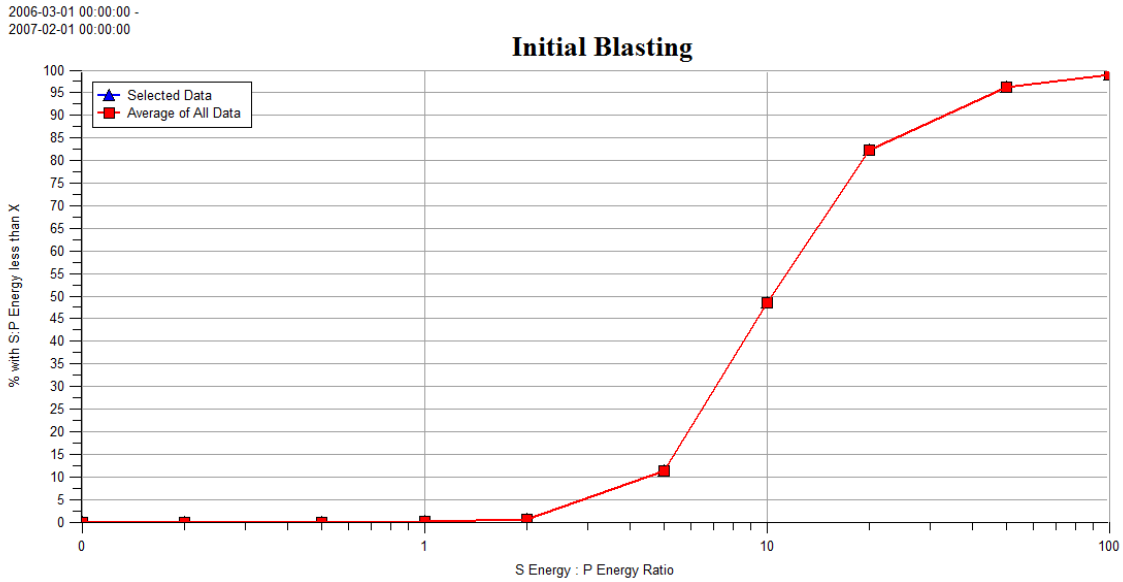

Figure 4.7 The comparison in S:P energy ratio between the all events during initial blasting.

Comparing the S:P energy ratio of the events according to their magnitude (Figure 4.8) shows that the larger events are more related to non-shear type source of mechanisms while smaller events are related to shear type sources. In other words, when the initial blasting occurred, only the large events with low S:P energy had a non-shear mechanism, and the events with low magnitude but high S:P energy ratio were related to the sliding on the discontinuity sets (presumably J1 and J2 sets).

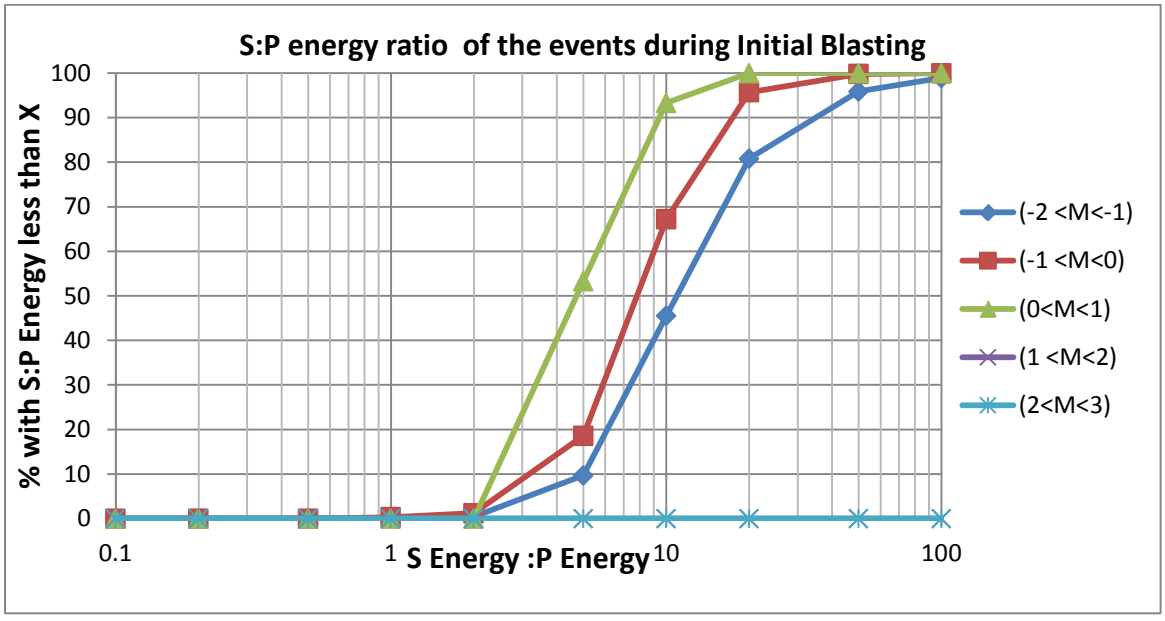

Figure 4.8 S:P energy ratio according to events magnitude during initial blasting.

Plotting the initial blasting events, according to their weekly median S:P energy ratio, percentage of shearing events, and the event rate (Figure 4.9) shows the in most weeks of this period, the median of the S:P energy was greater than 10. This also indicates that a shear mechanism was the dominant source mechanism. The percentage of shearing events was generally highest from March to early August 2006. Weekly increases in the event rate seemed to result in a decrease in the percentage of the shearing events. Between the early August and late August 2006, the percentage of the shearing events decreased while the overall event rate was increasing. As mentioned, this could be related to the effect of the Limey domain. There were no seismic data recorded from December 2006 to January 2007.

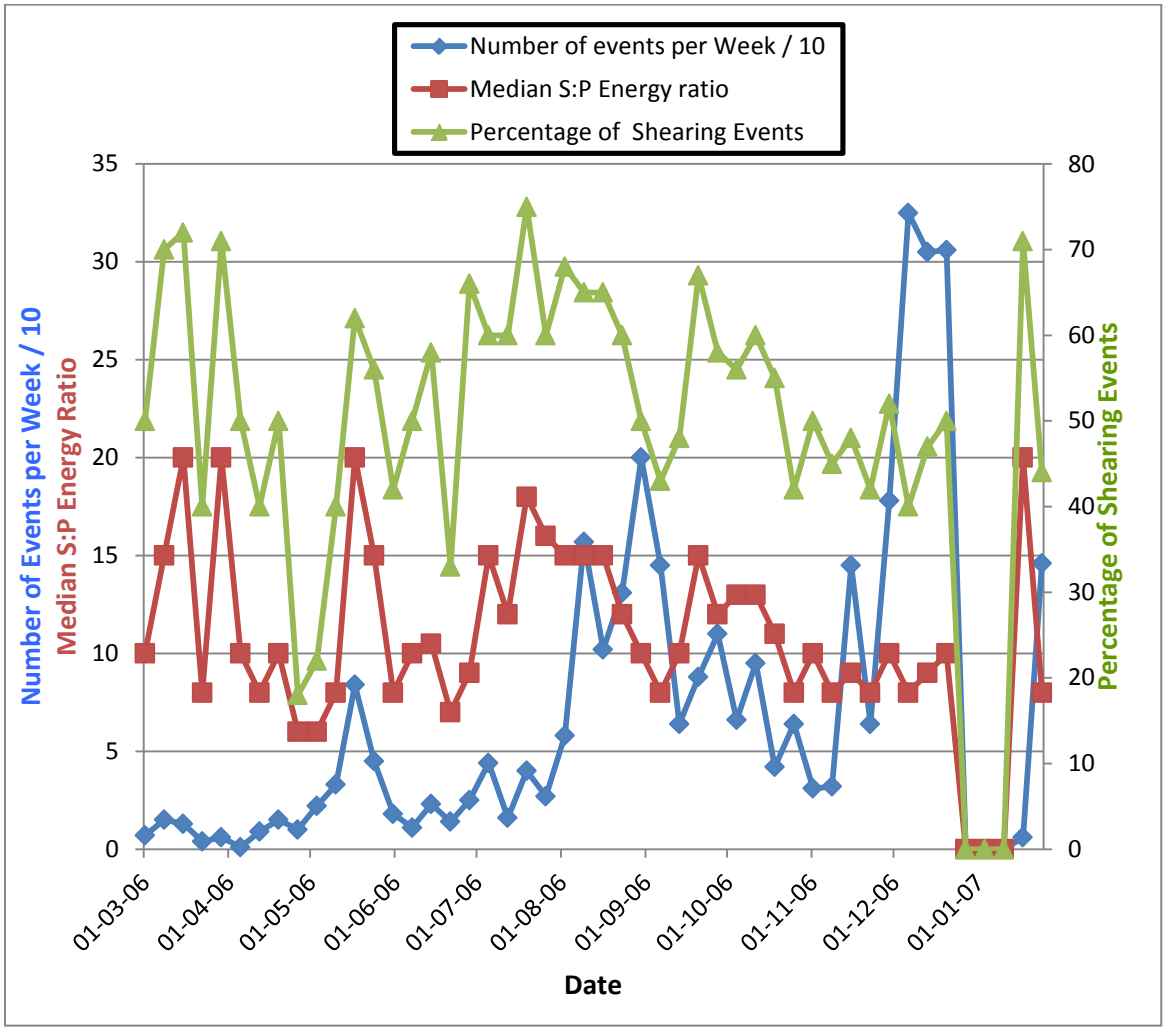

Figure 4.9 Comparison of median S:P energy ratio, weekly event rate (per 10) and percentage of shearing events during initial blasting.

4.1.4 Apparent Stress-Time History

An increasing trend in the Apparent Stress Frequency (ASF) started in July 2006 in the initial blasting period (Figure 4.10). Then, the Apparent Stress was high until mid-September 2006. The low frequency of the Apparent Stress between late August and early September 2006 was related to the weaker I30 zone. From mid-September to mid-November 2006 the total event rate decreased but the Apparent Stress Frequency was higher compared with before August 2006. The decreasing trend between October 2006 and mid-November 2006 was related to the change of seismic system sensitivity. After mid-November, the ASF increased remarkably.

The highest frequency happened in late December 2006 with frequency of 25 events per day. The spikes in the Apparent Stress Frequency coincide with an increased rate of blasting. There is a strong relation between the frequency of the Apparent Stress and stress change due to the blasting.

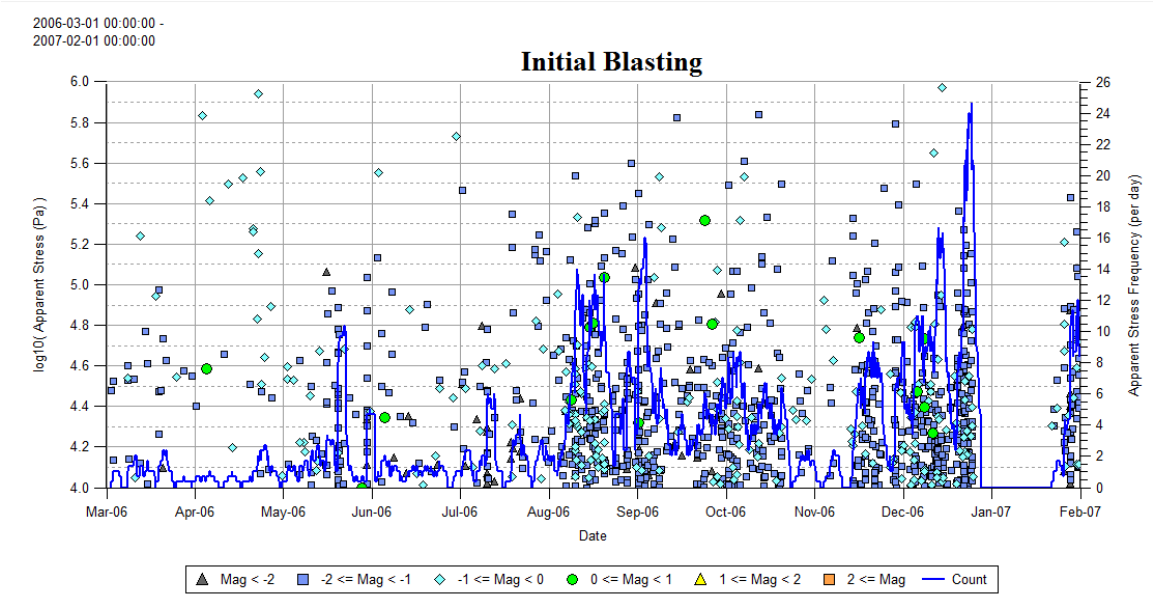

Figure 4.10 The Apparent Stress history during initial blasting.

4.1.5 Energy Index/Cumulative Apparent Volume

Except for the first two months (March and April 2006) of the initial blasting in which the EI magnitude was very high, EI was around 1.0 in all other months. The EI started to increase

when the seismogenic zone was close to the Limey unit (late July 2006).The EI started to decrease when it entered the Limey unit. A similar phenomenon happened when the seismogenic was close to I30 and Thrust domains (late August and late September 2006, respectively). For the rest of the initial blasting period, the EI was lower than 1.0. The CAV trend did not change noticeably for most of this period, but the CAV change rate, accelerated after mid-November 2006 (the slope of the Cumulative Apparent Volume trend) which is clear from Figure 4.11. The increase in the CAV value (3.0e+07 m^3) in the 2.5 months (mid-November 2006 to February 2007) was the same as the first 8.5 months (March to mid-November 2006).

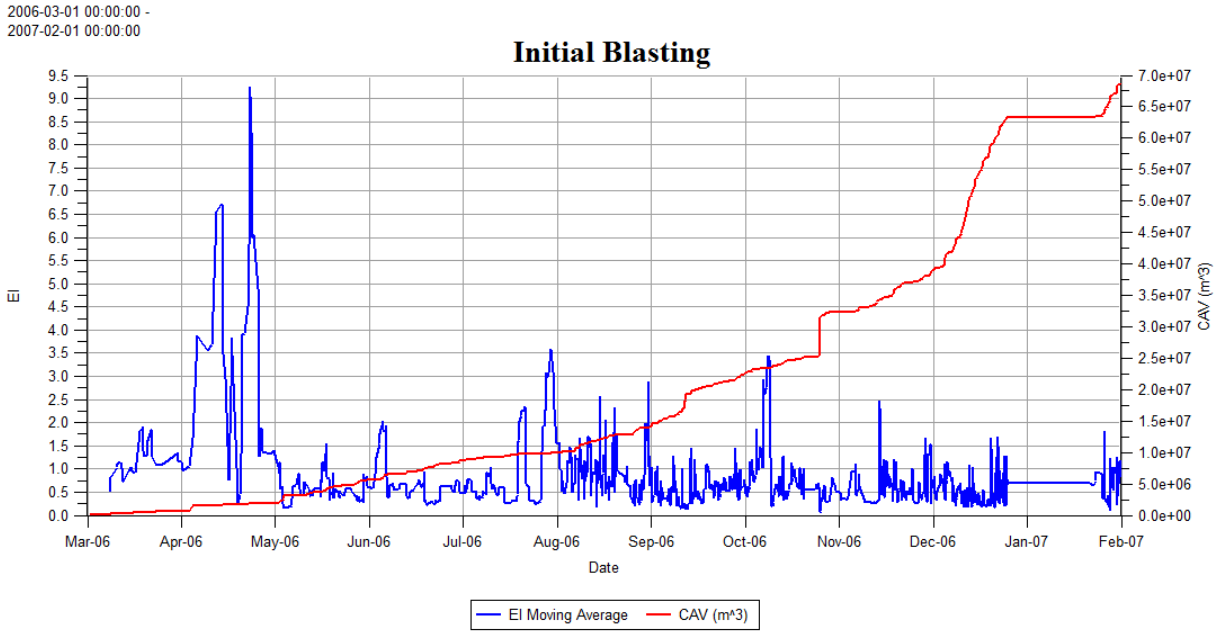

Figure 4.11 Comparison in energy index and Cumulative Apparent Volume during initial blasting.

4.1.6 Energy-Moment Relation

As shown in Figure 4.12, the large events in the selected period have non-shear type source mechanism. Also, the events with a higher seismic energy have a higher S:P energy ratio and vice versa. The slope of the relation (d-value) is 1.01 which is an indicator of a weaker rockmass surrounding the blasting area.

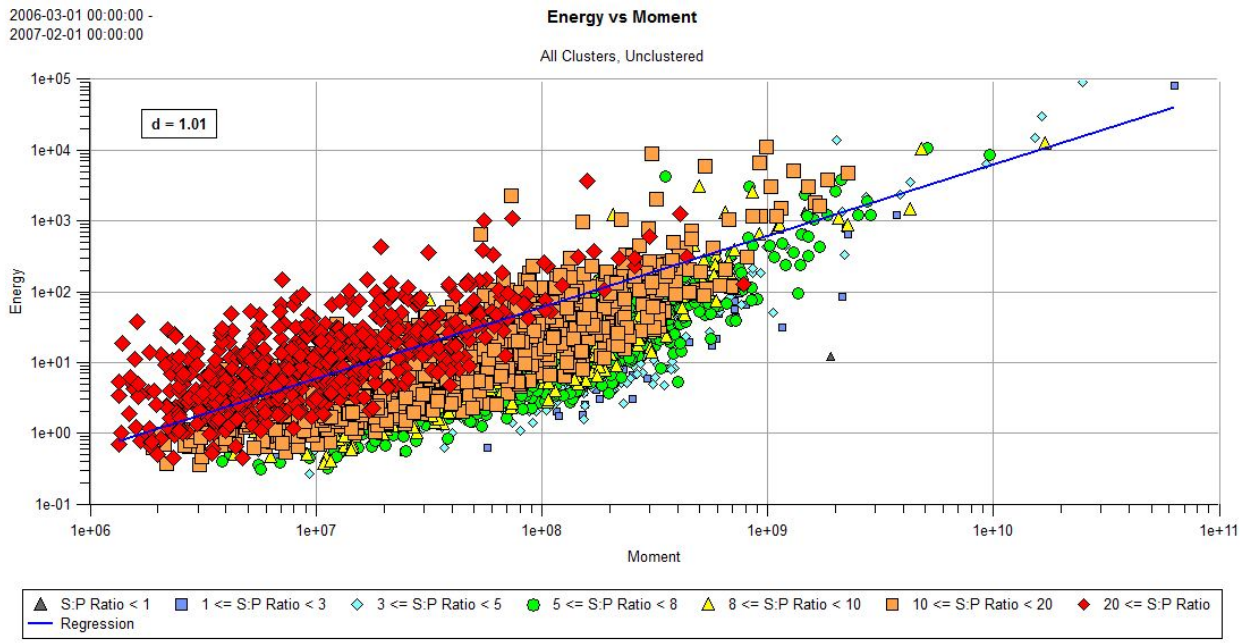

Figure 4.12 The comparison in energy moment by plotting with S:P energy ratio during initial blasting.

4.1.7 Discussion for Initial Blasting

The initial blasting is defined as the opening of an excavation within the orebody changing the state of stress in the surrounding rockmass that induces caving. Laubscher (1994) mentioned that the opening of the undercut towards the major horizontal principal stress would assist the cave initiation by reducing clamping stresses across the cave back. Brown (2003) had a different idea and noted that the opening of the first lift perpendicular to the direction of the major principal stress might help in overcoming the rockmass strength. The first lift at Telfer mine was opened in a SW-NE direction towards SE (towards the direction of the major horizontal principal stress).

More than 3400 events including 15 large events ($0< M_L<+1$) were recorded during the initial blasting at Telfer. All events had local magnitude less than 1.0 and the largest event was recorded with local magnitude 0.9. The event rate was approximately 300 events per month.

Stress change due to the first lift initial blasting was the main seismic source mechanism of the larger events. The larger events had a relatively high Apparent Stress but low S:P energy ratio (less than 3).

During the initial blasting, 52% of all events had an S:P energy greater than 10. According to the power law relation between the frequency and the magnitude of the seismic events, the recorded number of the small events was greater than large events. Therefore, smaller events were predominantly shearing events while the larger events were mainly non-shearing (stress fracturing events).

Changes in the lithology affected the event rate and seismogenic zone upward movement. The I30 reef not only reduced the event rate but also acted as a barrier and decreased the rate of the seismogenic zone upward movement.

Cook (1976) proposed the diurnal analysis which helped in finding the source of seismicity in the mines. He noted that seismicity directly related to the stress change from mine blasting occurs directly after mine blasting. Seismicity related to the geological structures often had little temporal relation to the mine blasting. During the initial blasting at Telfer mine, most of the seismic events occurred during the blast time (between 02:00 and 04:00 in the morning and between 14:00 to 16:00 in the afternoon). This would suggest that the seismicity during the initial blasting was directly associated with the stress change resulting from the mine blasting.

During initial blasting, 757 events with Apparent Stress greater than 30 kPa were recorded (22% of the all events). Proportionally, the Apparent Stress of the initial blasting events was very high compared with other caving periods. The Apparent Stress of some events reached 300 kPa in this period where such events were likely due to stress change from initial blasting.

The Cumulative Apparent Volume during the initial blasting was approximately 6.9e+07 m^3 with a rate of 6.2e+06 m^3 per month. In this period, the rate of the CAV was strongly related to the blasting.

4.2 Cave Initiation Rockmass Failure Mechanisms

It is interpreted that the cave initiation began apparently in February 2007 and continued approximately until October 2007. From the location of the seismogenic zone in February 2007 (approximately between 4760 and 4820 mRL), it can be determined that the zone has entered into the Host domain.

In October 2007, the seismogenic zone was located between 4840 and 4950 mRL. The seismogenic zone had progressed just into Zone 3 during the cave initiation.

In the first three months of the cave initiation (February to April 2007), the seismogenic zone did not progress very far. It was located mostly between 4770 and 4825 mRL. In May 2007, the cave back was asymmetrical. As shown in Figure 4.13 (in June 2007), the plan view of the seismogenic zone showed that the concentration of the events on the north-west side of the first lift diminished and the seismogenic zone migrated to the east side of the first lift (Figure 4.14). This was expected, as the direction of the first lift opening was moving to the east at that period.

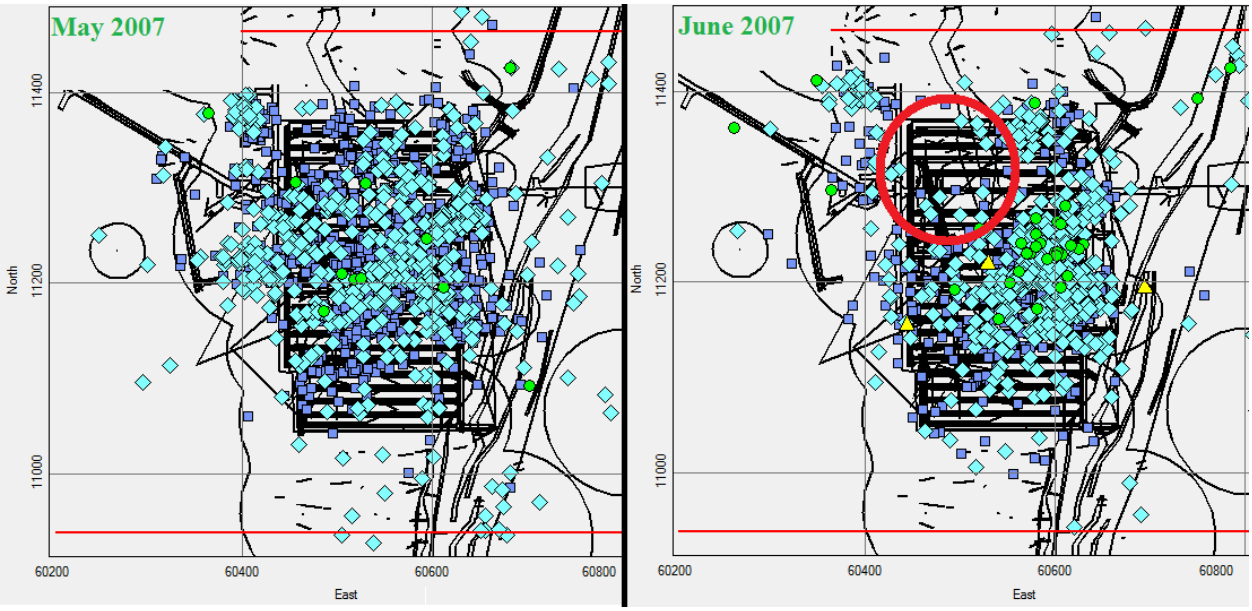

Figure 4.13 Migration of the event to the east of the first lift, plan view.

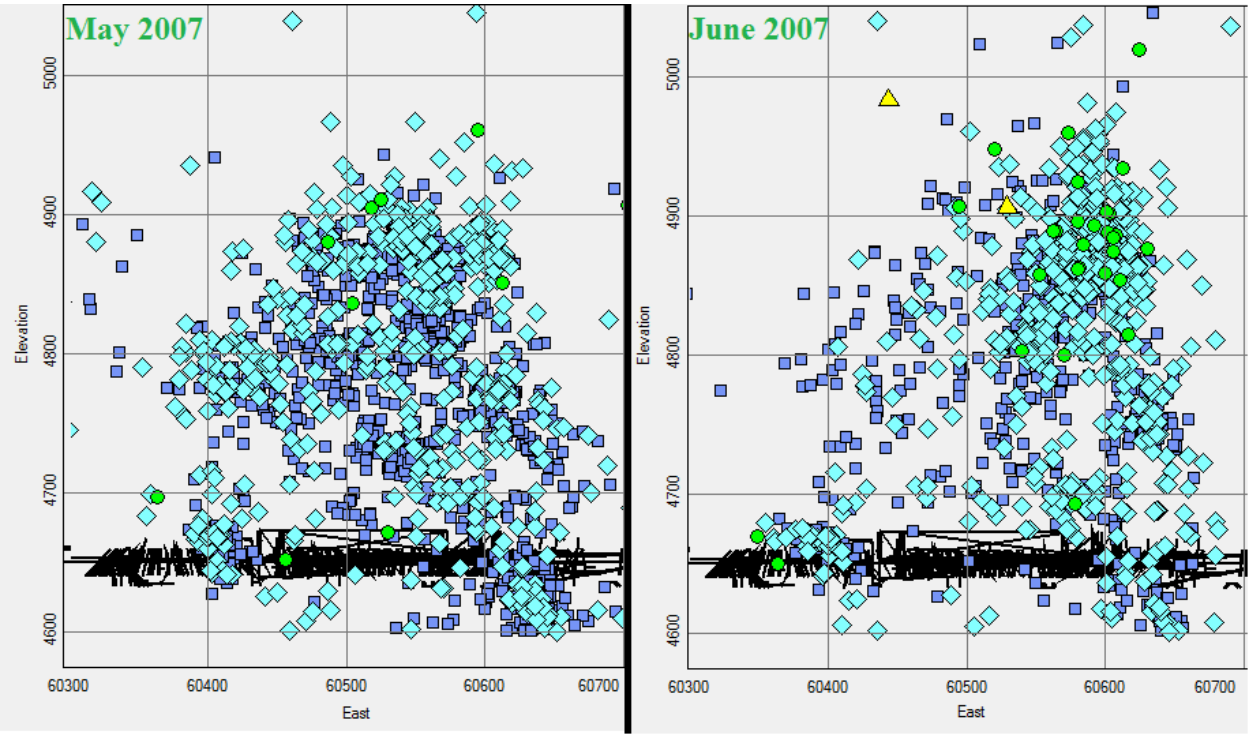

Figure 4.14 Change in the cave apex location (migration to the east), May and June 2007.

After June 2007 very few events were recorded on the north-west of the cave foot print.

Plotting the cave shoulder events according to their S:P energy ratio showed that the events with high S:P energy ratio (S:P >10) and the events with the low S:P (S:P <3) energy ratio occurred frequently on the east side of the first lift. In other words, the stress fracturing was the dominant seismic source mechanism on the east side of the first lift while shearing was the dominant seismic source mechanism on the west side. This trend in the seismic source mechanism became clear in the cave apex events after September 2007 (Figure 4.15). Although the Graben fault was located far from the first lift, the stress caving tendency on the east side of the first lift was due to the effect of the Graben fault which reduced the RMR value on the east side of the cave zone compared with the west side.

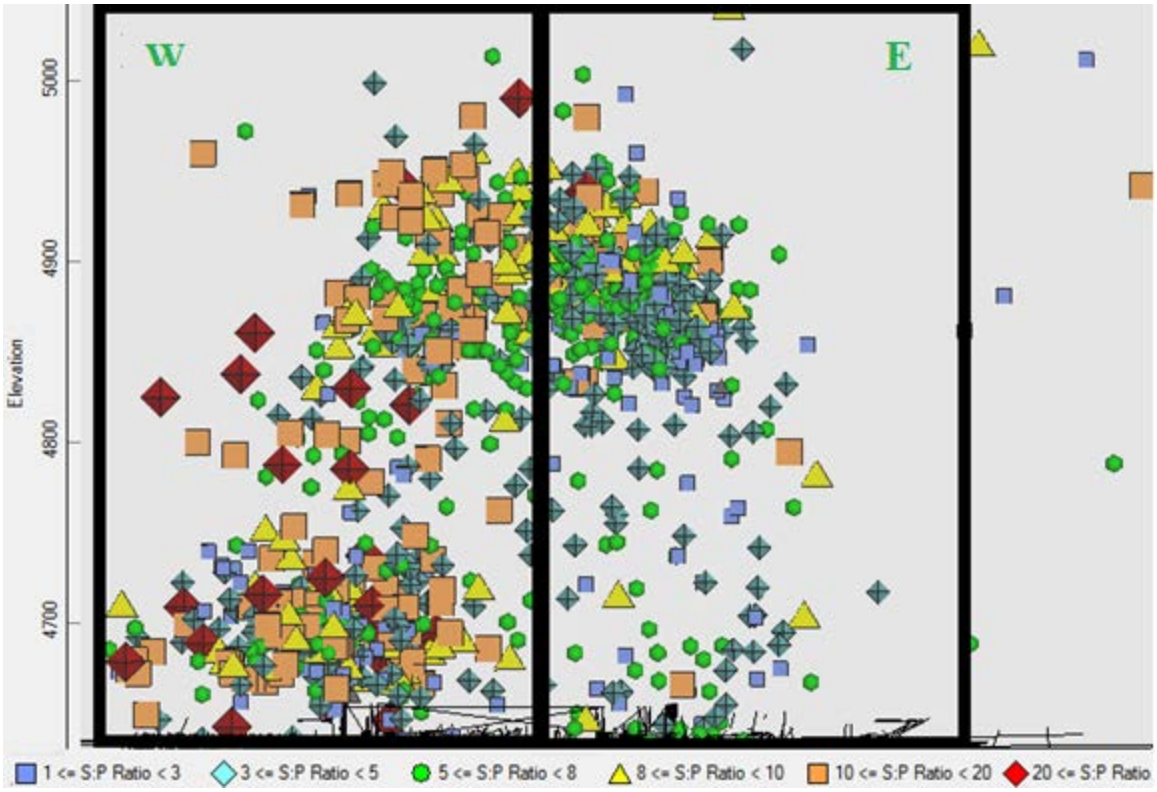

Figure 4.15 Different S:P energy ratio of the event on the west and east of the first lift, looking south.

The investigation of the cave back slope on the west and the north-west of the first lift indicated that the west slope of the cave back during the initial blasting and the cave initiation was approximately between 45º and 60º (Figure 4.16). More than 30% of the events in the mentioned area had an S:P energy ratio greater than 10 (only 8% of the events had S:P energy ratio less than 3).

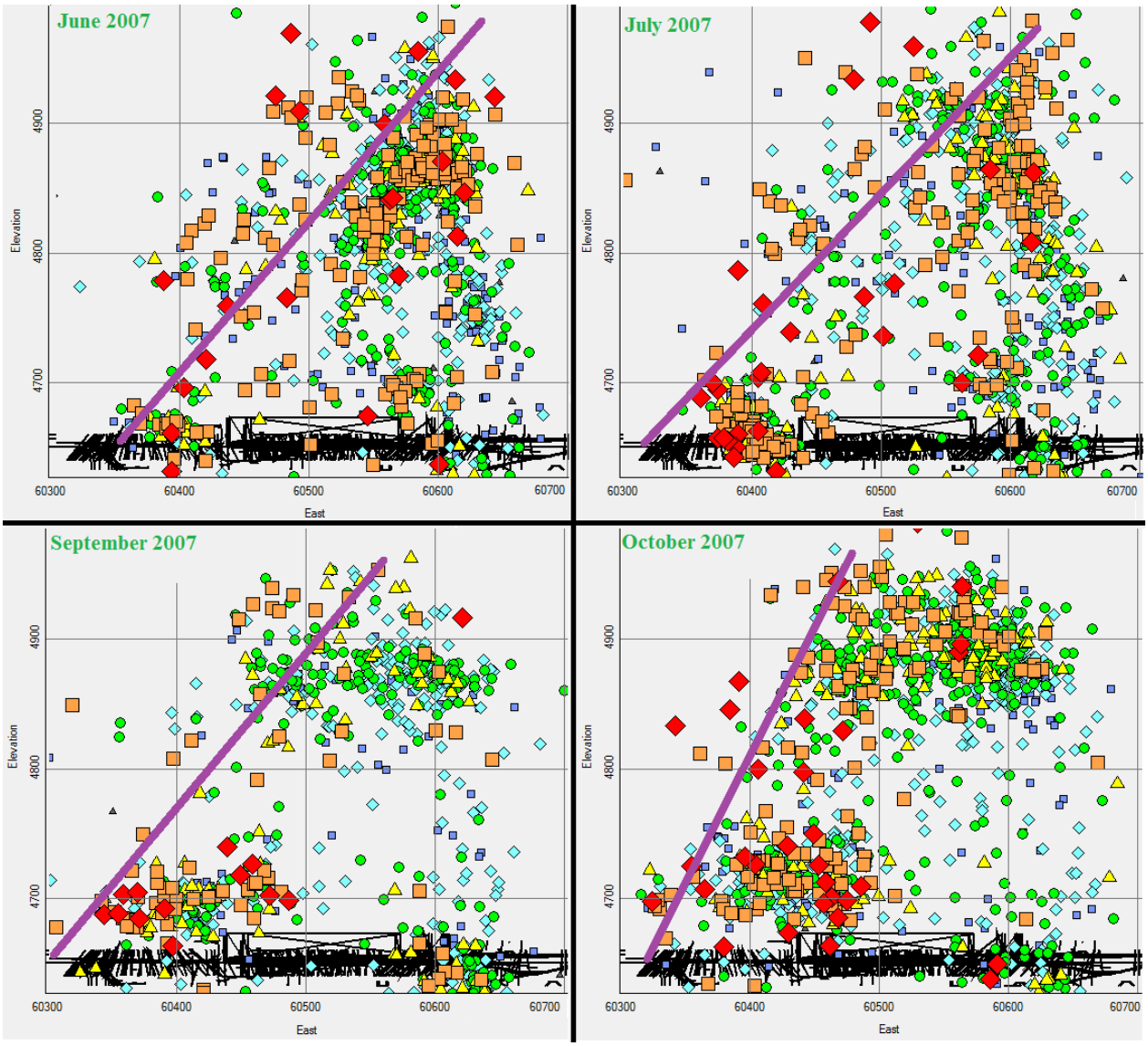

Figure 4.16 Control of the west side of the cave back with bedding planes, during cave initiation, events are plotted by S:P energy ratio.

High S:P energy ratio events were the dominant on the west side of the cave. It could be concluded that the cave back on the west area of the first lift was controlled by shear failure, likely along bedding planes.

4.2.1 Magnitude- Time History Analysis

Almost 10,000 events including 11 large events (+1< M_L <+2) were recorded in the cave initiation period (Figure 4.17). The large events started to occur in late June of 2007 related to the slowdown in the cave movement. The number of events between magnitude 0 and +1 also

increased significantly at this time. Seventy five percent of these events were recorded on the west side of the first lift. The overall event rate increased gradually from February 2007 to November 2007. In some months (June, July, and October) the number of large and significant events was high compared with other months. The largest event was recorded in late September 2007 with a local magnitude of 1.75. After a period of data loss in mid-April 2007, the sensitivity of the seismic system decreased until July 2007 (a similar drop in the sensitivity happened between September 2007 and October 2007). As opposed to the initial blasting period, the magnitude-time history chart no longer showed the influence of individual blasts. The event rate from mid-February 2007 to the start of October 2007 was relatively constant (except for the data loss periods in April 2007).

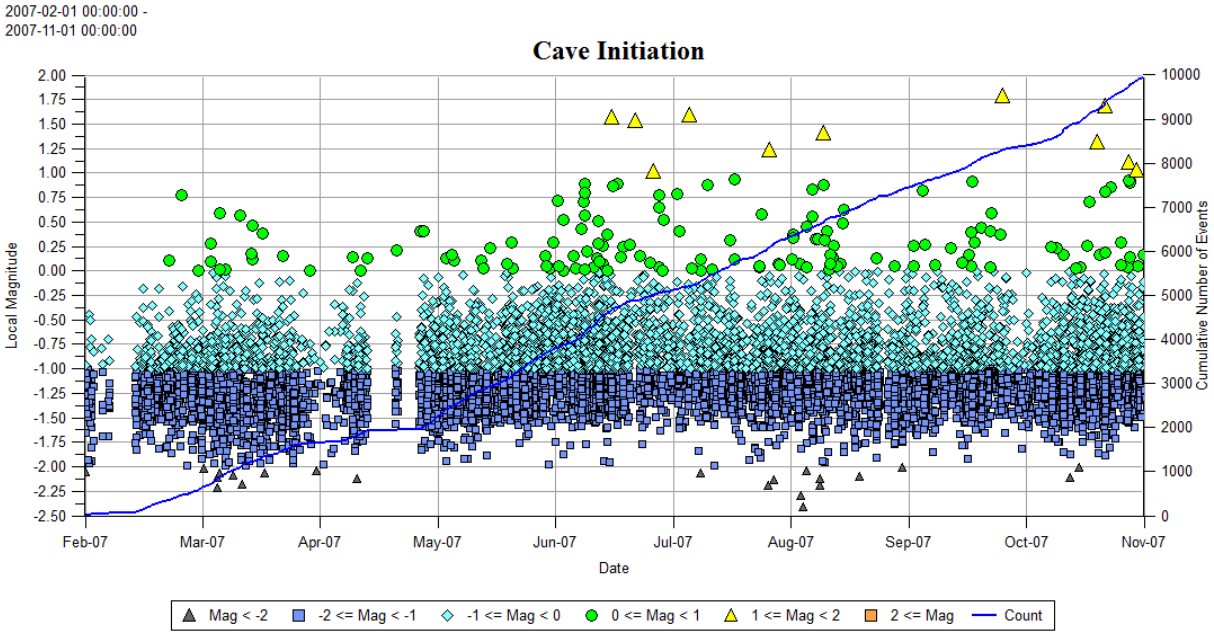

Figure 4.17 Magnitude- time history and cumulative number of events during cave initiation.

4.2.2 Frequency-Magnitude Analysis

Frequency-Magnitude analysis for the selected events during the cave initiation showed the selected events had different source mechanisms (Figure 4.18). This change in the behaviour of the events was observable after mid-June 2007. Before mid-June 200, the largest expected event from the data set was 1.2 and after that the largest recorded event was 1.9 (a good fit). There was a considerable drop in the slope of the frequency-magnitude relation, from 1.5 before mid-June

to 1.1 after mid-June. The S:P energy ratio of these two mechanisms showed that these events were similar in failure mechanism. This change in the event magnitude appeared to be related to the slowdown of the cave at 4900 EL.

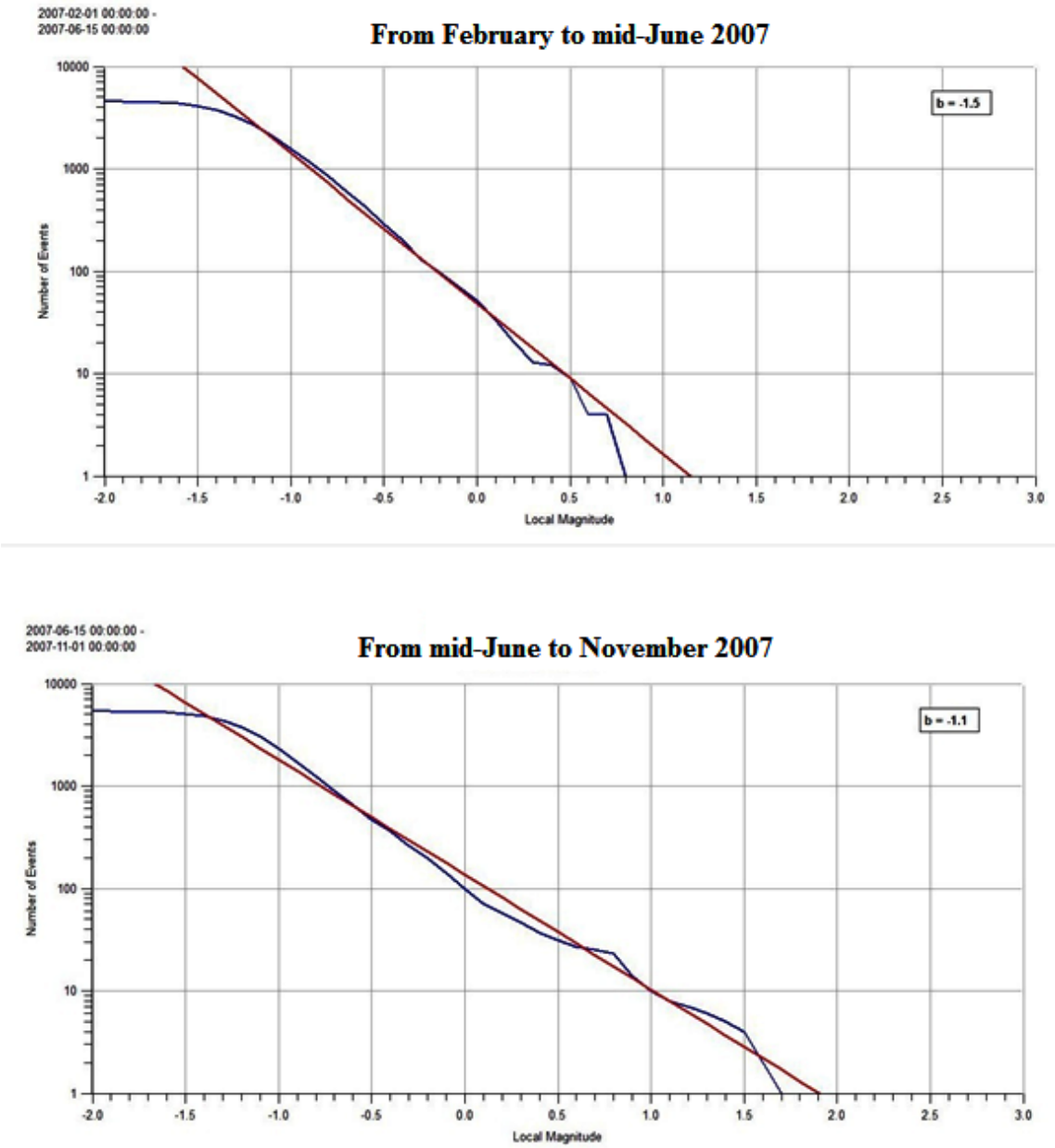

Figure 4.18 The frequency-magnitude of the events before and after mid-June 2007, during cave initiation.

4.2.3 S:P Energy Ratio Analysis

During the cave initiation, 22% and 18% of the events had S:P energy ratio less than 3 and greater than 10, respectively (Figure 4.19). There was a significant difference in the percentage of the shear type events between the initial blasting period and cave the initiation period. The percentage of the shear type events decreased from 55% to 18%. Also, the percentage of the non-shear type events increased from 9% to 22%.

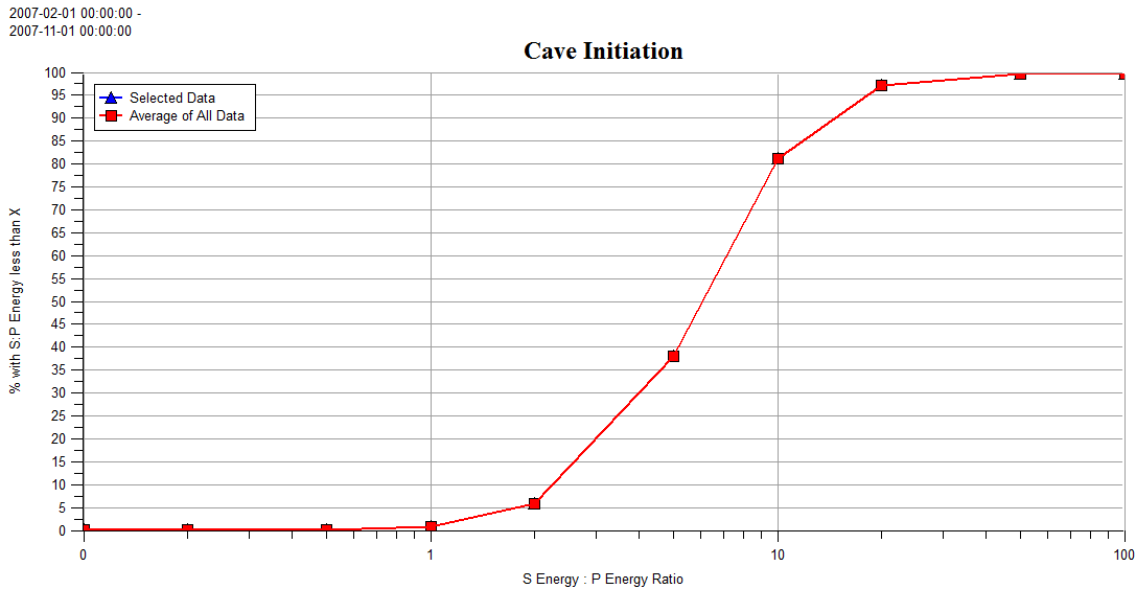

Figure 4.19 The comparison in S:P energy ratio between the all events during cave initiation.

Comparing the S:P energy ratio of the events, according to their magnitude showed that the larger events were more related to the non-shear type source of mechanisms while smaller events were related to shear type sources (Figure 4.20). There was a decrease in the percentage of the small events with S:P energy ratio greater than 10 (compared with the initial blasting period). On the other hand, the large event percentages did not change significantly.

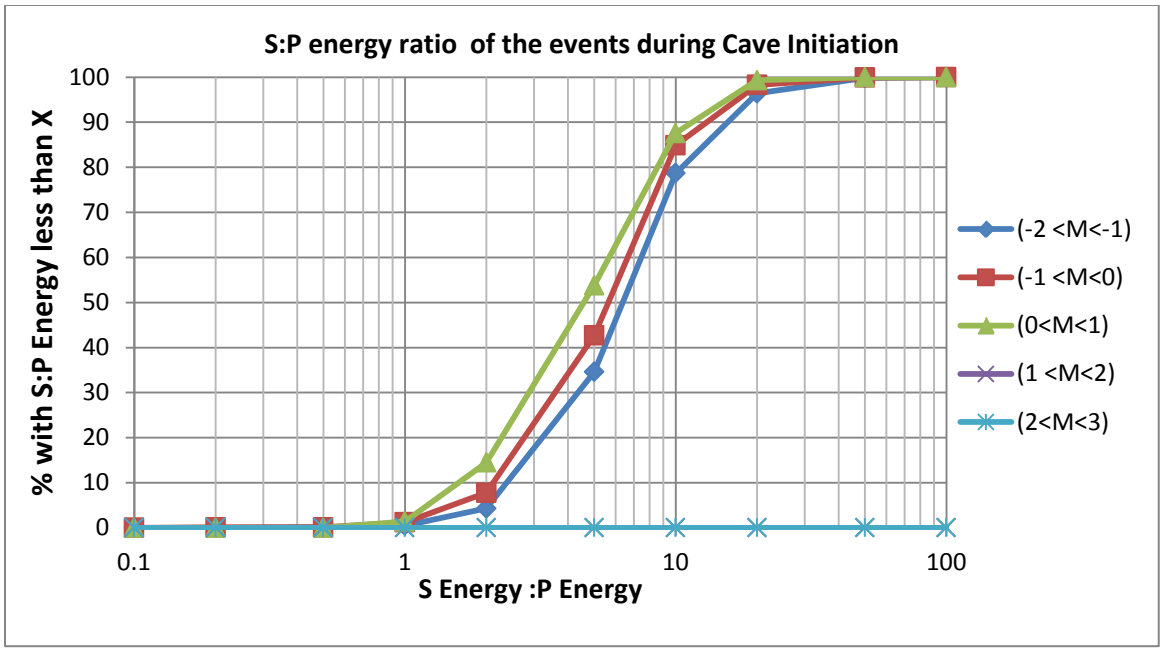

Figure 4.20 S:P energy ratio according to events magnitude during cave initiation.

Plotting the cave initiation events according to their weekly median S:P energy ratio, percentage of shearing events and event rate (Figure 4.21) showed that the median of the S:P energy was smaller than 10 in all weeks. It can be inferred that a shear mechanism was not the dominant source of mechanism anymore. The general trend showed that the percentage of the shearing events was decreasing during the cave initiation. Between late April and early June 2007, the event rate was increasing while the percentage of shearing events had a decreasing trend. This may be related to the migration of the events from the north-west to the center-east side of the first lift (a reduction of the events with shearing source mechanism due to sliding along the bedding planes).

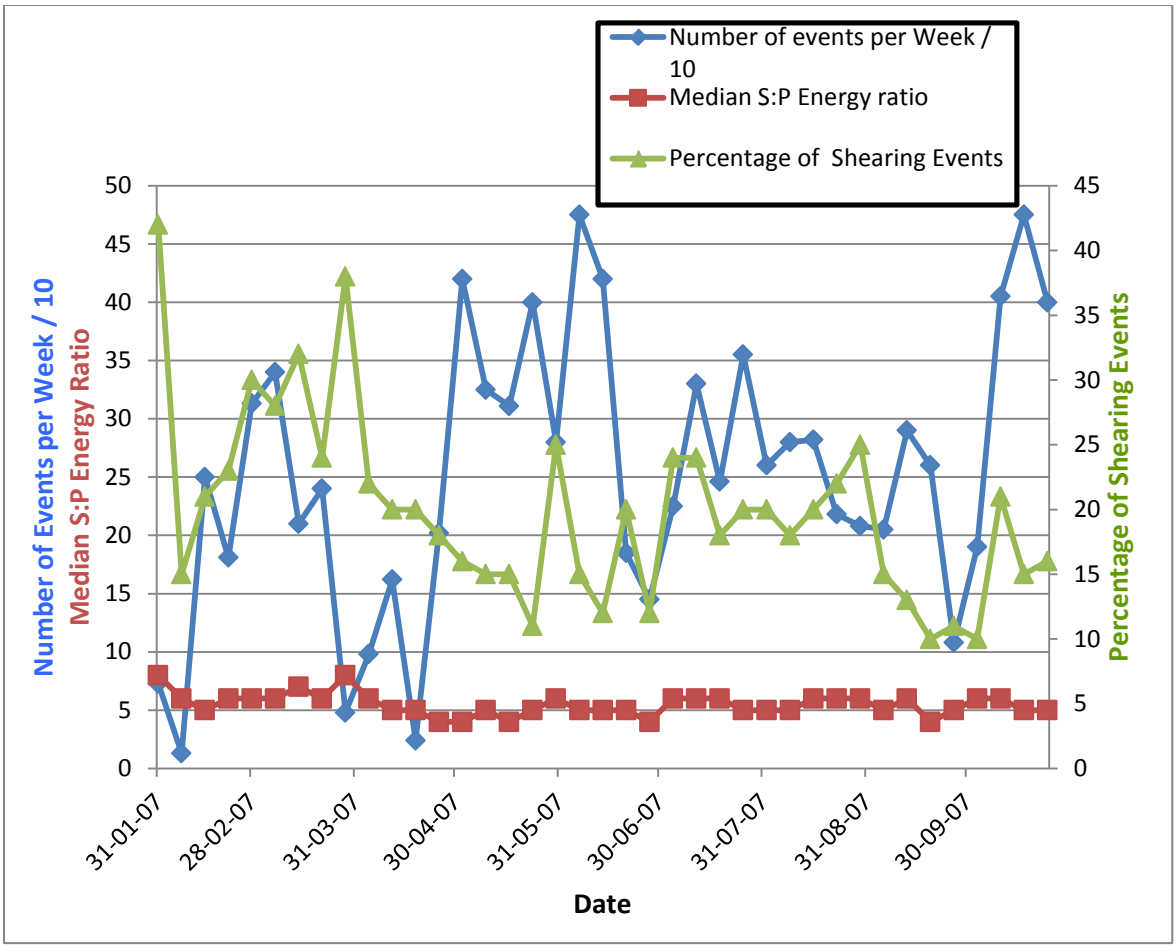

Figure 4.21 Comparison of median S:P energy ratio, weekly event rate (per 10) and percentage of shearing events during cave initiation.

4.2.4 Apparent Stress-Time History

The level of the Apparent Stress Frequency was higher during the cave initiation than that in the initial blasting period. In this group of events, most of the large events occurred during or very close to periods in which the Apparent Stress Frequency exceeded 7 events per day. The highest frequency happened in early March 2007 with frequency of 24 events per day (Figure 4.22). There was a noticeable decrease in high Apparent Stress events in the period July-September 2007 as the cave growth slowed at 4900 EL.

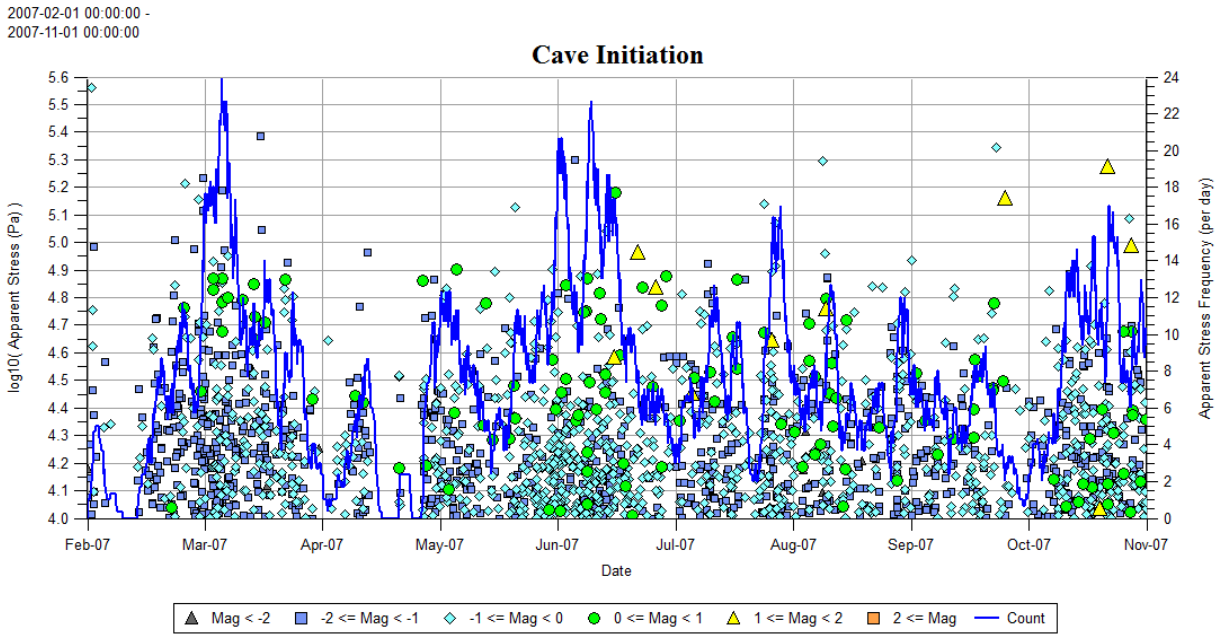

Figure 4.22 The Apparent Stress history during cave initiation.

Some important observations from Figure 4.23, Figure 4.24, and Figure 4.25 are as follows:

- The high S:P energy ratio events are at the top (leading edge) of the seismic zone, implying high stress shearing events are at the leading edge of the seismogenic zone.
- For the first few months (February to April 2007), the seismic events clearly trace the profile of the seismogenic zone from the initial blasting level on 4650 EL to the apex of the cave.
- In the last few months (August to October 2007), the seismic events are largely in the apex of the cave, no longer showing as clearly the full slope of the seismogenic zone. This is interpreted as the seismogenic zone (area of the active failure) as being largely only the apex by August to October 2007.
- There are periods of data loss in April 2007.
- Between March 2007 and May 2007, there is an upward movement of the top of the seismogenic zone from elevation 4830 EL to 4900 El.
- From May to October 2007, the seismogenic zone stalls at an elevation between 4900 EL and 4950 EL.
- High Apparent Stress events tend to be near the top of the seismogenic zone.

- High Apparent Stress events are predominantly shearing events with (almost 50% of the events having S:P >10)
- In some months high Apparent Stress events are at the north side of the cave (April, May, July, and August 2007).
- In some months (February, March, June and October 2007) the high Apparent Stress events are in the middle of the cave central around 11200 N.
- Low Apparent Stress events have much lower S:P energy ratio implying predominantly non-shearing events.
- The number of high Apparent Stress events reduces significantly in July to September 2007, potentially related to the cave slowdown around 4900 EL.

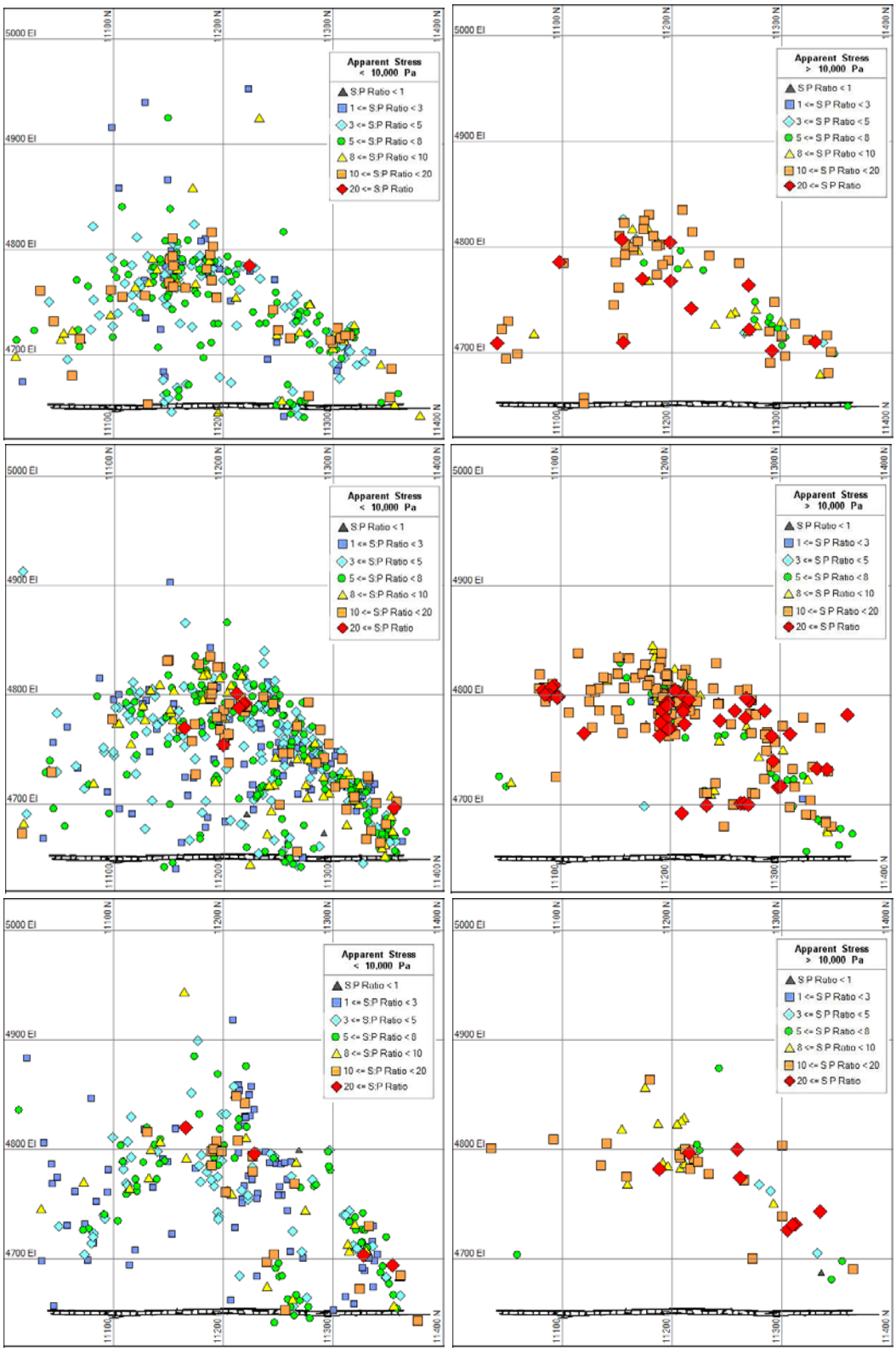

Figure 4.23 Location of events in Feb. (top), March (middle) and April 2007 (bottom). The events on the left have lower Apparent Stress (<10 kPa) and on the right have higher Apparent Stress (>10 kPa).

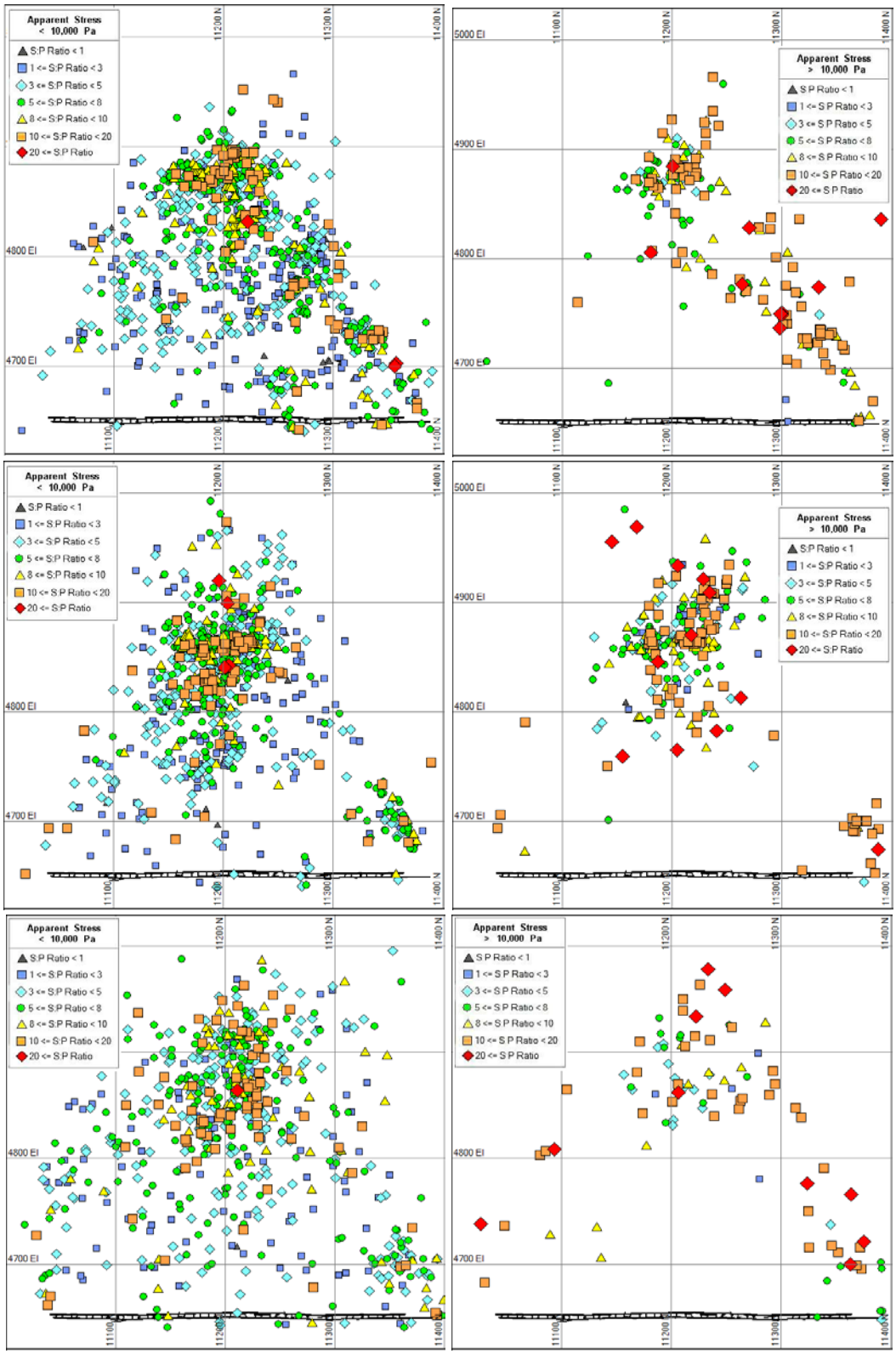

Figure 4.24 Location of events in May (top), June (middle) and July 2007 (bottom). The events on the left have lower Apparent Stress (<10 kPa) and on the right have higher Apparent Stress (>10 kPa).

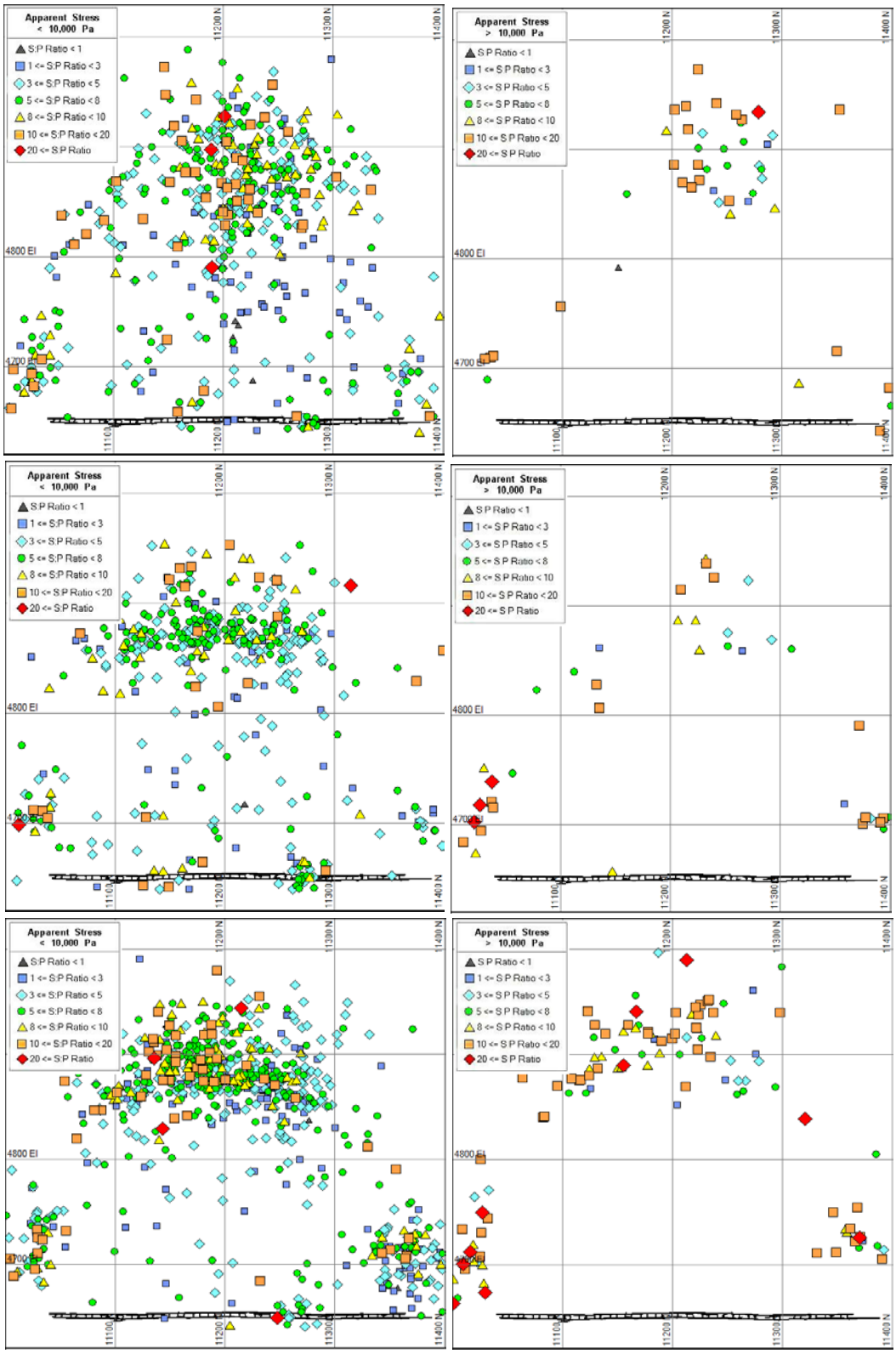

Figure 4.25 Location of events in August (top), Sept. (middle) and Oct. 2007 (bottom). The events on the left have lower Apparent Stress (<10 kPa) and on the right have higher Apparent Stress (>10 kPa).

4.2.5 Energy Index/Cumulative Apparent Volume

Similar to the Apparent Stress Frequency trend, the EI trend was high between mid-February 2007 and mid-March 2007 (entering of the seismogenic zone to Zone 3), as shown in Figure 4.26. After this period, the EI was less than 1.0 in most days of the cave initiation period (until late May 2007). Starting in late May 2007, the EI started to increase and reached to its highest magnitude in June 2007, thereafter the EI decreased again. This change in the magnitude of the EI was related to the slowdown in the migration of the seismogenic zone (Figure 4.26). The rate of change in the CAV showed a significant increase in May 2007. The rate of the CAV in the initial blasting was about 6.2e+06 m^3 per month, but this rate was 1.2e+08 m^3 per month during cave initiation.

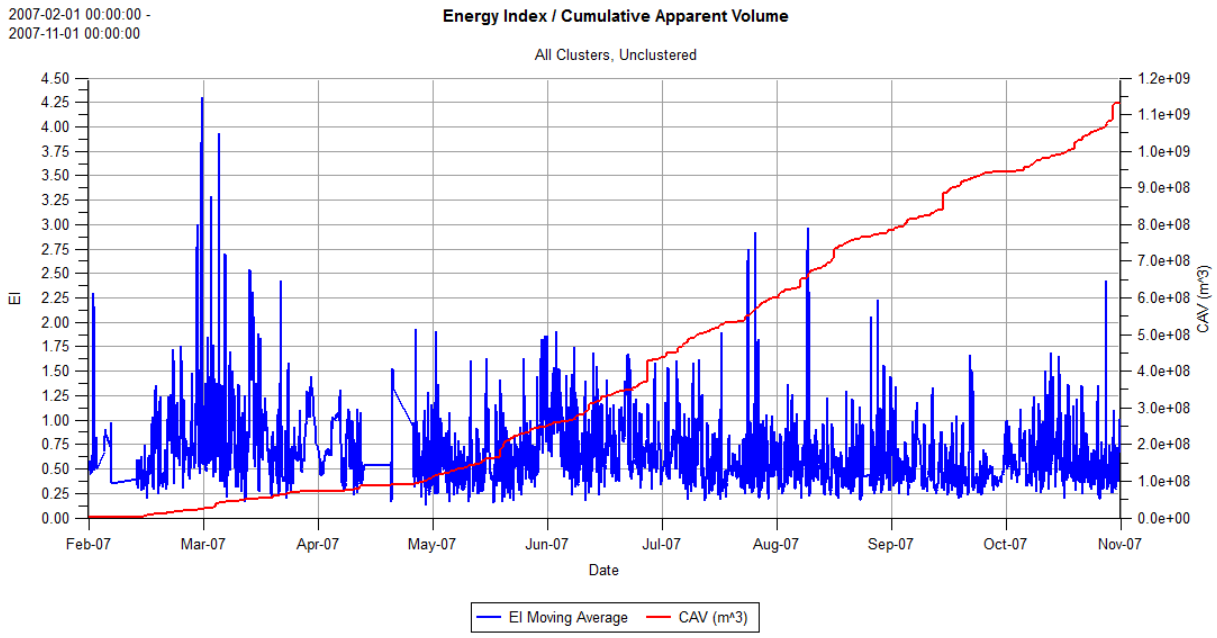

Figure 4.26 Comparison in energy index and Cumulative Apparent Volume during cave initiation.

4.2.6 Energy-Moment Relation

The large events during the cave initiation had non-shear type source of mechanism. Also the events with a higher seismic energy had a higher S:P energy ratio and vice versa (Figure 4.27).

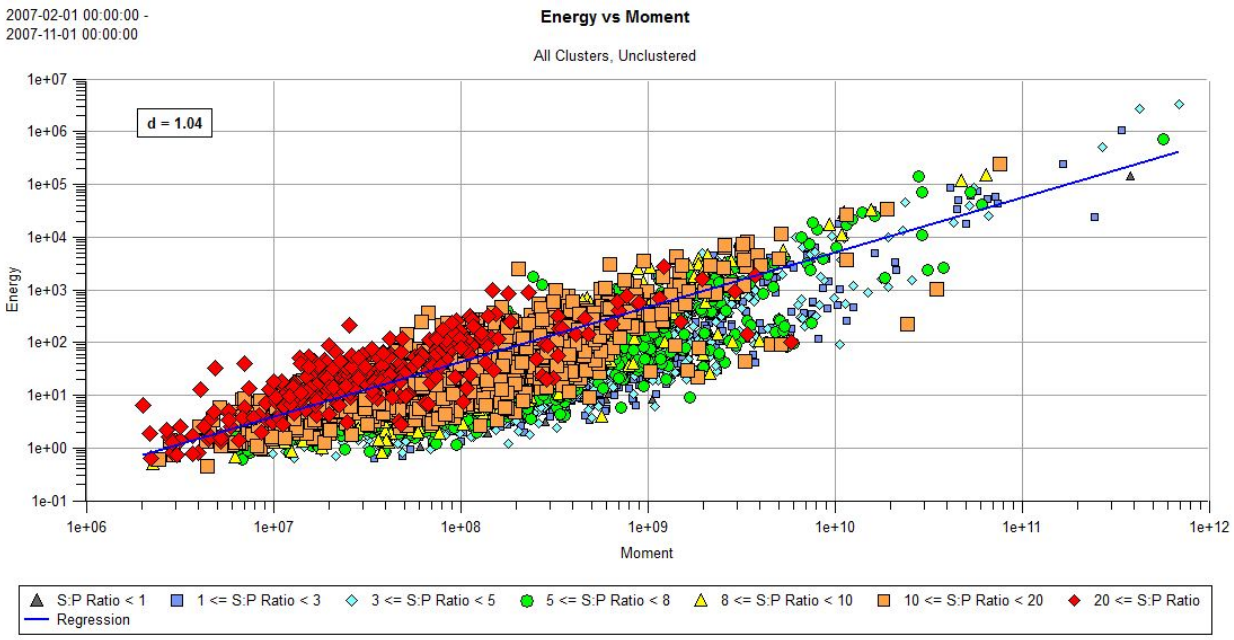

Figure 4.27 The comparison in energy moment by plotting with S:P energy ratio during cave initiation.

4.2.7 Discussion for Cave Initiation

Initiation of the cave occurs when the progression of the fracturing and rockmass weakening occur in the cave back. This happens due to the changes in the state of stress in the back of the cave and subsequently loosened rock blocks drop into the void area above the first lift (Mawdesley, 2002).

Almost 10,000 events including 11 large events ($+1< M_L <+2$) were recorded in the cave initiation period. All events had local magnitude less than 2.0 and the largest event was recorded with local magnitude 1.8. The number of events with local magnitude between 0.0 and 1.0 during the cave initiation was 10 times greater than the initial blasting period. The event rate was approximately 1100 events per month. This rate was approximately four times greater than the event rate during the initial blasting.

During the cave initiation, the frequency of events with S:P energy greater than 10 was higher on the west side of the first lift. This behaviour might be related to the sliding of bedding planes because the west side of the cave was controlled by failure along the bedding planes (shear

failure). However, the frequency of the events with S:P energy less than 3 was high on the east side (the stress fracturing was the predominant seismic source mechanism). This could be related to the effect of the Graben fault which reduced the rockmass quality on the east side of the first lift. Also, the migration of the seismogenic zone from north-west to the east could be related to the effect of the Graben fault (the cave progressed faster in the weaker zones).

Similar to the initial blasting period, most of the seismic events occurred during the blast time during the cave initiation (between 02:00 and 04:00 in the morning and between 14:00 to 16:00 in the afternoon). However, in this period the frequency of the events between the blasting times (from 4:00 am to 2:00 pm) increased that was likely related to a large proportion of events associated with the cave fracturing and movement.

During the cave initiation, 701 events (0.7% of all events) with Apparent Stress greater than 30 kPa were recorded. In contrast to the initial blasting period, all recorded events during the cave initiation had a lower Apparent Stress magnitude (300 kPa < AppStress). This behaviour could be related to the much weaker influence of the blasting on the occurrence of the recorded seismic events.

The Cumulative Apparent Volume during the cave initiation was approximately 1.1e+09 m^3 with a rate of 1.2e+08 m^3 per month. This rate was almost 20 times greater than the rate in the initial blasting period. The increase in the deformation rate was associated with the fracturing and deformation of the rockmass during the cave initiation and the increase in the movement of the seismogenic zone.

4.3 Cave Propagation Rockmass Failure Mechanisms

The cave propagation began in about November 2007 and continued until approximately October 2009. About 300,000 events including five large events (+2< M_L <+3) were recorded during cave propagation period. Almost all these large events were recorded in the cave apex and were located between 4650 and 5050 mRL. Two out of five large events had a shear source mechanism (based on S:P energy analysis). Two large events had a source mechanism related to the stress fracturing mechanism. The mechanism of the other large events was indeterminate mechanism.

Comparing the S:P energy ratio of the events according to their magnitude showed that the larger events are slightly more related to non-shear type source of mechanisms while smaller events were slightly more related to shear type sources (Figure 4.28). However, this trend of larger events as being non-shearing failure was less pronounced compared was the initial blasting period.

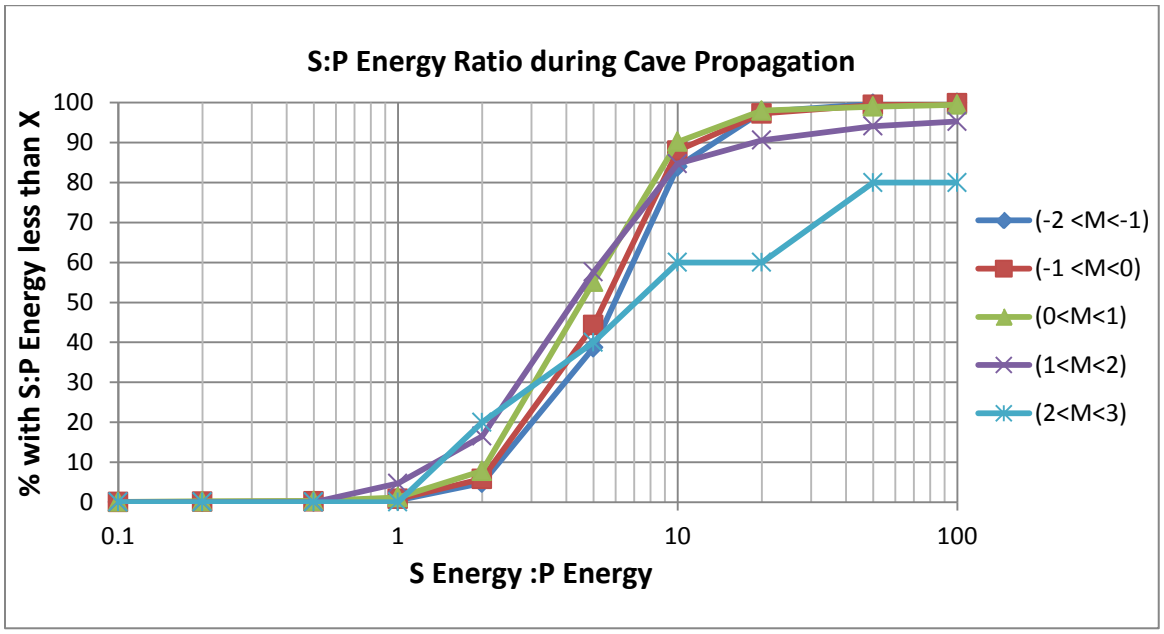

Figure 4.28 S:P energy ratio according to events magnitude during cave propagation.

Plotting the cave propagation events according to their weekly median S:P energy ratio, percentage of shearing events, and the event rate (Figure 4.29) showed that the median of the S:P energy was smaller than 10 in all weeks. In this period, changes in the event rate had no

meaningful influence on the median S:P energy ratio. The percentage of shearing events was usually between 10% and 30%.

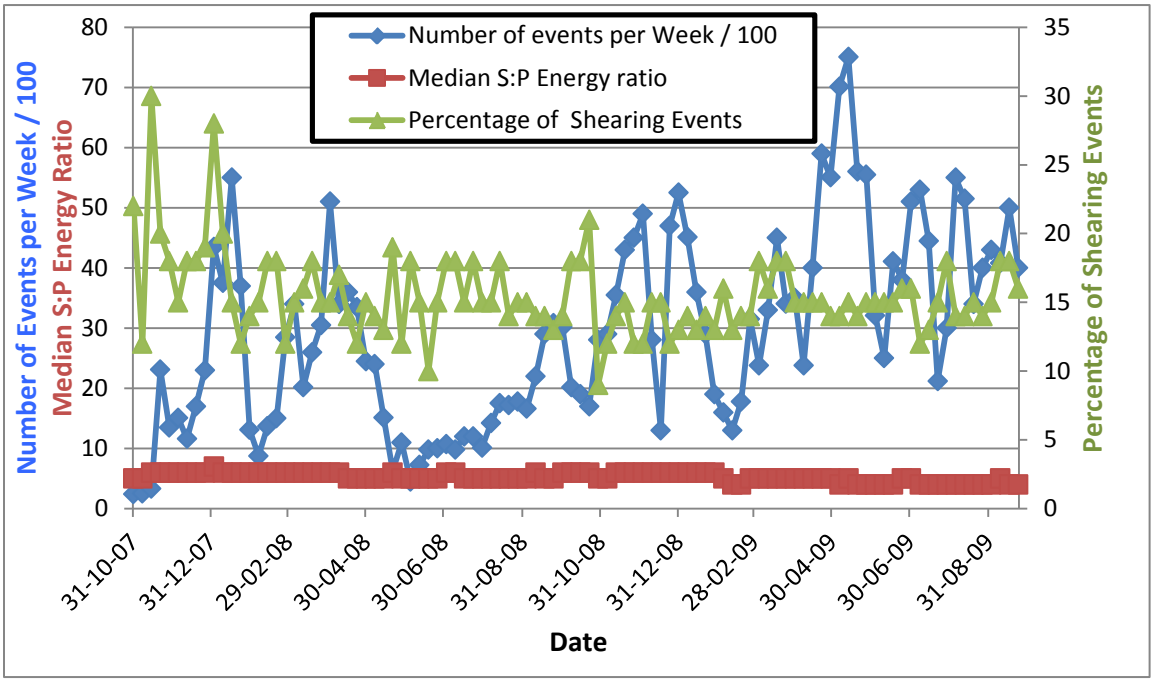

Figure 4.29 Comparison of median S:P energy ratio, weekly event rate (per 100) and percentage of shearing events during cave propagation.

The event rate changed several times due to the effects of the M50, M30 reefs and also changes in the sensitivity of the seismic system network. As a result of many variations in the event rate during the cave propagation (Figure 4.30), the history of events was divided into 4 periods:

1. Period 1- From November 2007 to February 2008.
2. Period 2- From February to May 2008 (effect of M50 reef).
3. Period 3- From May 2008 to February 2009 (effect of M30 reef).
4. Period 4- From February 2009 to October 2009 (effect of the split of the seismogenic zone).

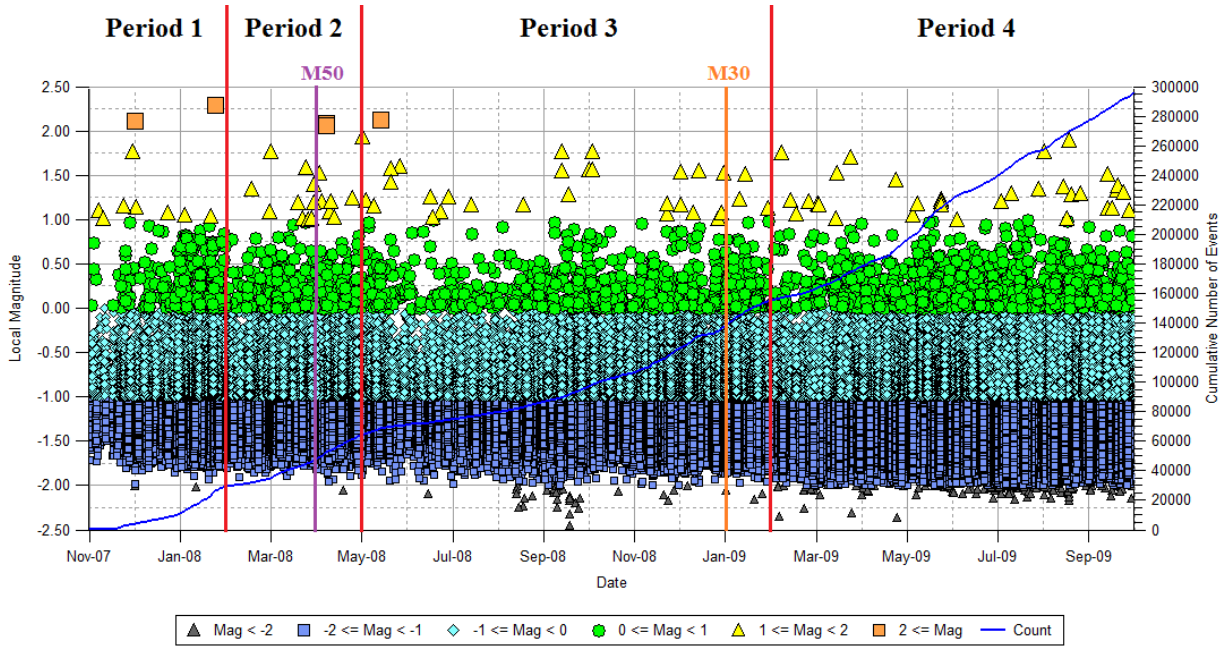

Figure 4.30 Magnitude-Time history for the events during cave propagation with 4 periods.

4.3.1 Period 1 (from 2007/11/01 to 2008/02/01)

In this period, more than 28,500 events were recorded, including two large events with local magnitude of 2.1 and 2.3 respectively in the early December 2007 and late January 2008. The seismogenic zone was approximately located around 4900 mRL in November 2007 and reached to 5000 mRL in January 2008 (with approximately 100 m thickness). The seismogenic zone was still progressing in geological Zone 3. The first interaction between the seismogenic zone's apex and the M50 happened in this period.

Figure 4.31 shows that, there was some data loss in some days in November 2007, but there was a huge difference between the event rate in December 2007 (200 events per day) and January 2008 (600 events per day). The Apparent Stress Frequency in December 2007 was 25 per day while it increased to 60 per day in January 2008.

In this period, 12% and 18% of events had S:P energy ratio less than 3 and greater than 10, respectively. These percentages remained constant for the events in December 2007 and January 2008.

The CAV in January 2008 was almost 2.5 times greater than the CAV in December 2007.

Because Zone 3 did not have a complex lithology up to 5050 mRL, according to the previously analyses (M-T, ASH, S:P and CAV), the difference between the behaviour of events in December 2007 and January 2008 could likely be related to the onset of the cave propagation.

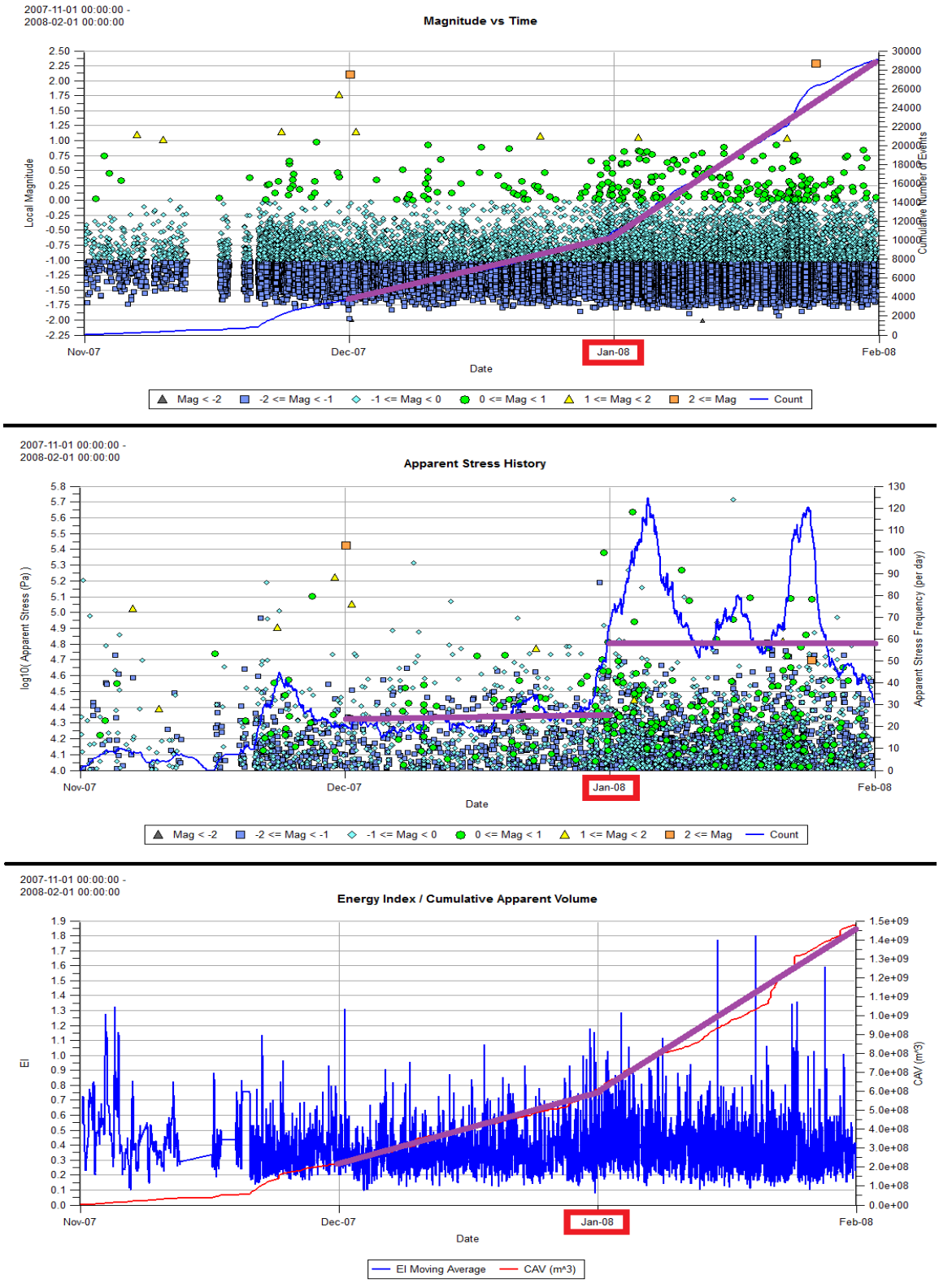

Figure 4.31 Magnitude-Time History, Apparent Stress History and EI/CAV during first Period.

4.3.2 Period 2 (from 2008/02/01 to 2008/05/01)

About 35,000 events were recorded during this period, included two large events with local magnitude of 2.1 recorded within 3 hours of each other in the early morning of April 8th 2008. The seismogenic zone's apex events were under the M50 reef in February 2008. In April 2008, the cave apex was passed through M50 and the event rate was observed to increase.

The event rates increased from 180 events per day in February 2008 to 900 events per day from March to May 2008.

In this period, 15% of the events had an S:P energy ratio less than 3 and 15% of the events had an S:P energy ratio greater than 10.

The background of the Apparent Stress Frequency in February 2008 was 30 per day while this value was 40 per day between March 2008 and May 2008.

The CAV rate in March (also April) 2008 was almost two times greater than the CAV rate in February 2008 (Figure 4.32).

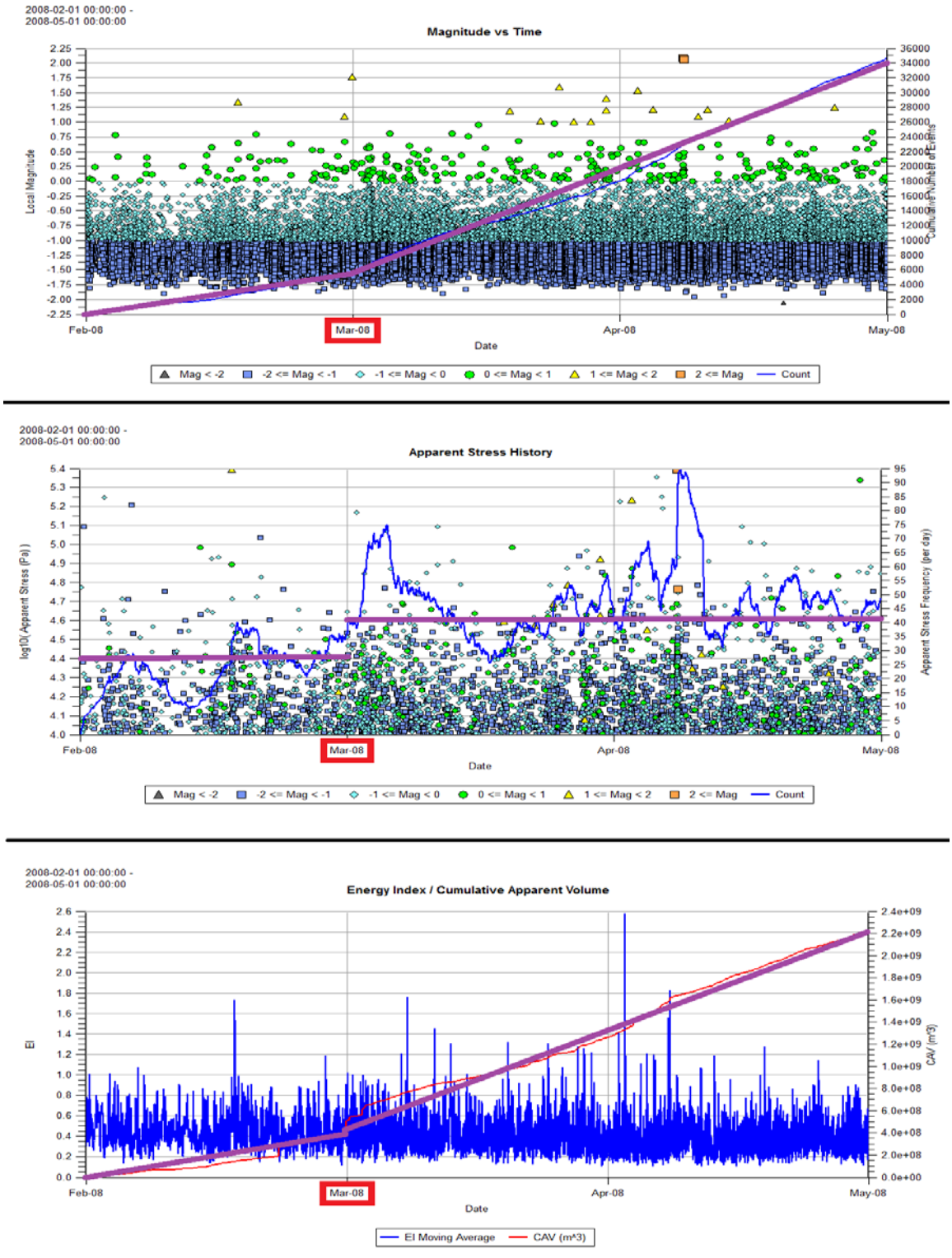

Figure 4.32 Magnitude Time History, Apparent Stress History and EI/CAV during the first Period.

4.3.3 Period 3 (from 2008/05/01 to 2009/02/01)

More than 91,000 events, including one large event with local magnitude of 2.1 in mid-May 2008, were recorded in this period. During this interval, the seismogenic zone's apex events were moving upward in the area between M50 and M30 reefs and reached to 5250 mRL in January 2009 (still propagating in Zone 3).

The seismogenic zone in May 2008 split into two separate areas. This occurred for five months from May to October 2008 (Figure 4.33). After this period, the seismogenic zone became a single integrated zone.

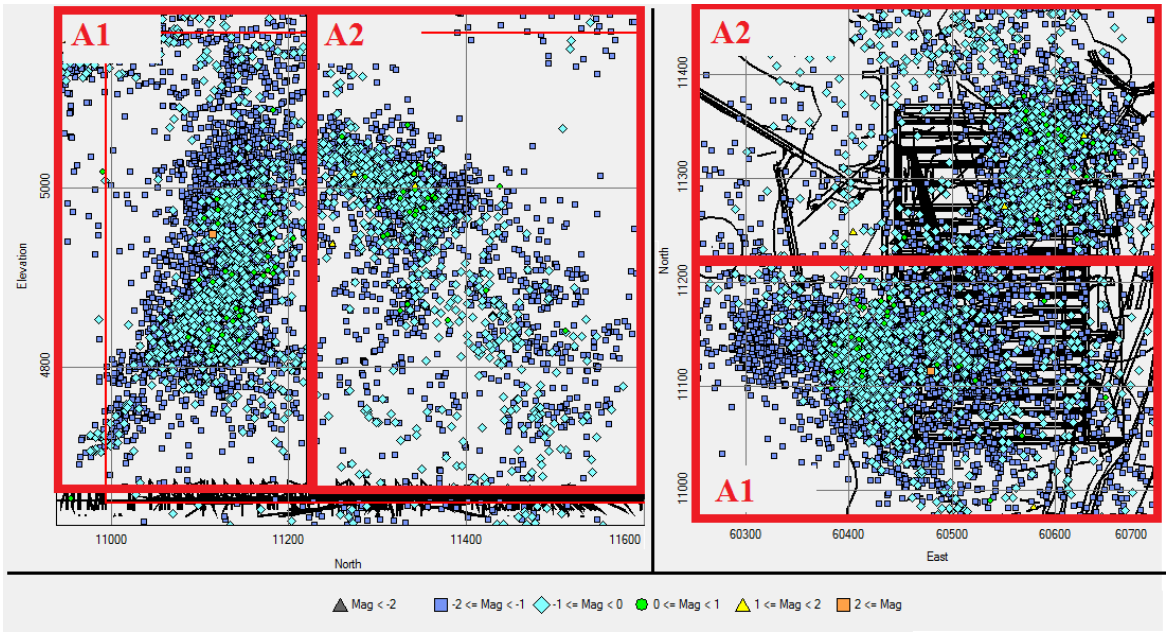

Figure 4.33 Location of the two selected group of seismogenic zone (A1 and A2) in two different views.

For assessing the behaviour of the events in the two separate zones, two groups of events A1 (a south group) and A2 (a north group) were selected (Table 4.3 and Table 4.4).

Table 4.3 Characterization of the selected events in the Group A1.

	Minimum (m)	Maximum (m)
East	60200	60800
North	10900	11230
Elevation	4650	5200

Table 4.4 Characterization of the selected events in the Group A2.

	Minimum (m)	Maximum (m)
East	60200	60800
North	11230	11600
Elevation	4650	5200

Other seismic analyses (M-T, ASH, S:P energy ratio, and CAV) showed that the events with local magnitude between 1.0 and 2.0 were recorded in Group A2 while most of the events in Group A1 had local magnitude less than 1.0. This also could be inferred from the frequency-magnitude analysis.

In Group A1, 20% of the events had an S:P energy ratios less than 3 and 15% of the events had an S:P energy ratios greater than 10. For the selected events in Group A2, 25% of the events had an S:P energy ratios less than 3, and 12% of the events had an S:P energy ratio greater than 10 (almost the same ratio for both groups). This would suggest that the seismic source mechanisms in the two areas are the same.

Both groups had roughly similar ASTH trends. Until mid-May 2008, the ASTH was high in both groups. After this time, the ASTH dropped until mid-June 2008 when it began to increase gradually rate and reached to 27 per day in both groups in the mid of October 2008.

During these five months, although the number of events recorded in Group A2 (14,000) was less than the Group A1 (15,000), the CAV in Group A2 (2.1e+09 m^3) was marginally greater than that in Group A1 (1.8e+09 m^3).

It can be concluded that there was no huge difference between the general seismological trends in the two selected groups and that they had similar behaviours (Figure 4.34, Figure 4.35, and Figure 4.36).

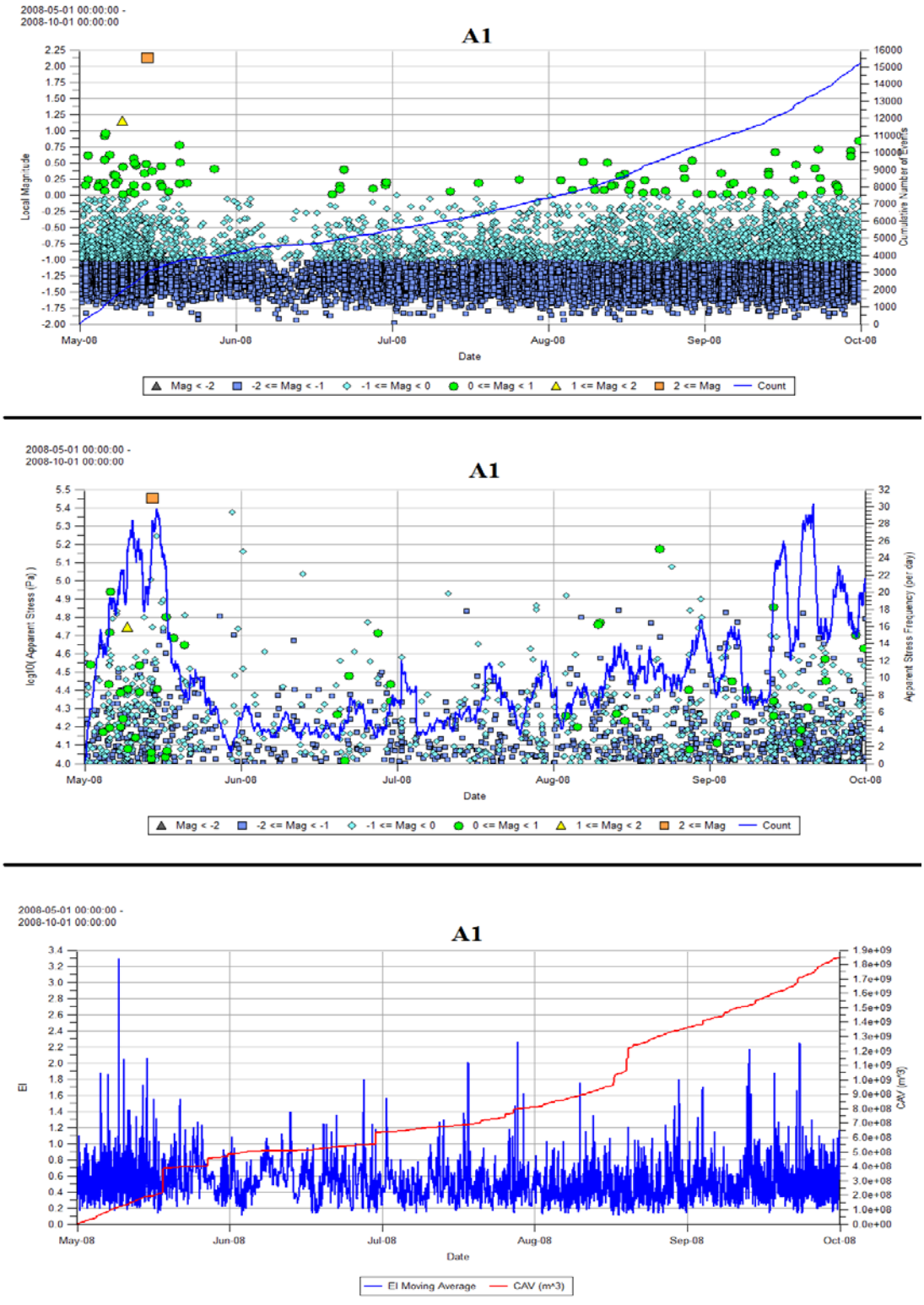

Figure 4.34 Magnitude-Time History, Apparent Stress History and EI/CAV for the two selected events during Period 3 (A1)

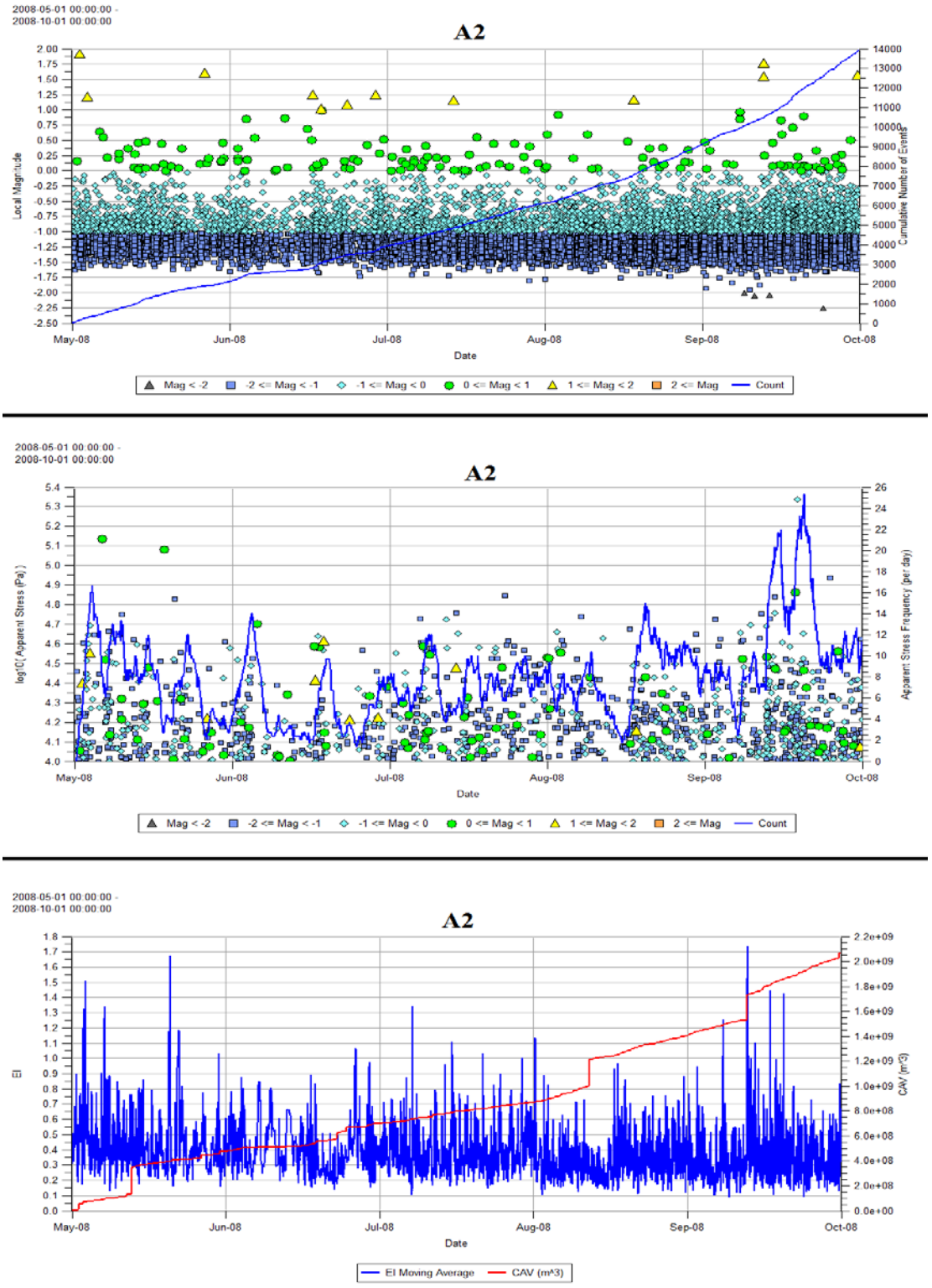

Figure 4.35 Magnitude-Time History, Apparent Stress History and EI/CAV for the two selected events during Period 3 (A2).

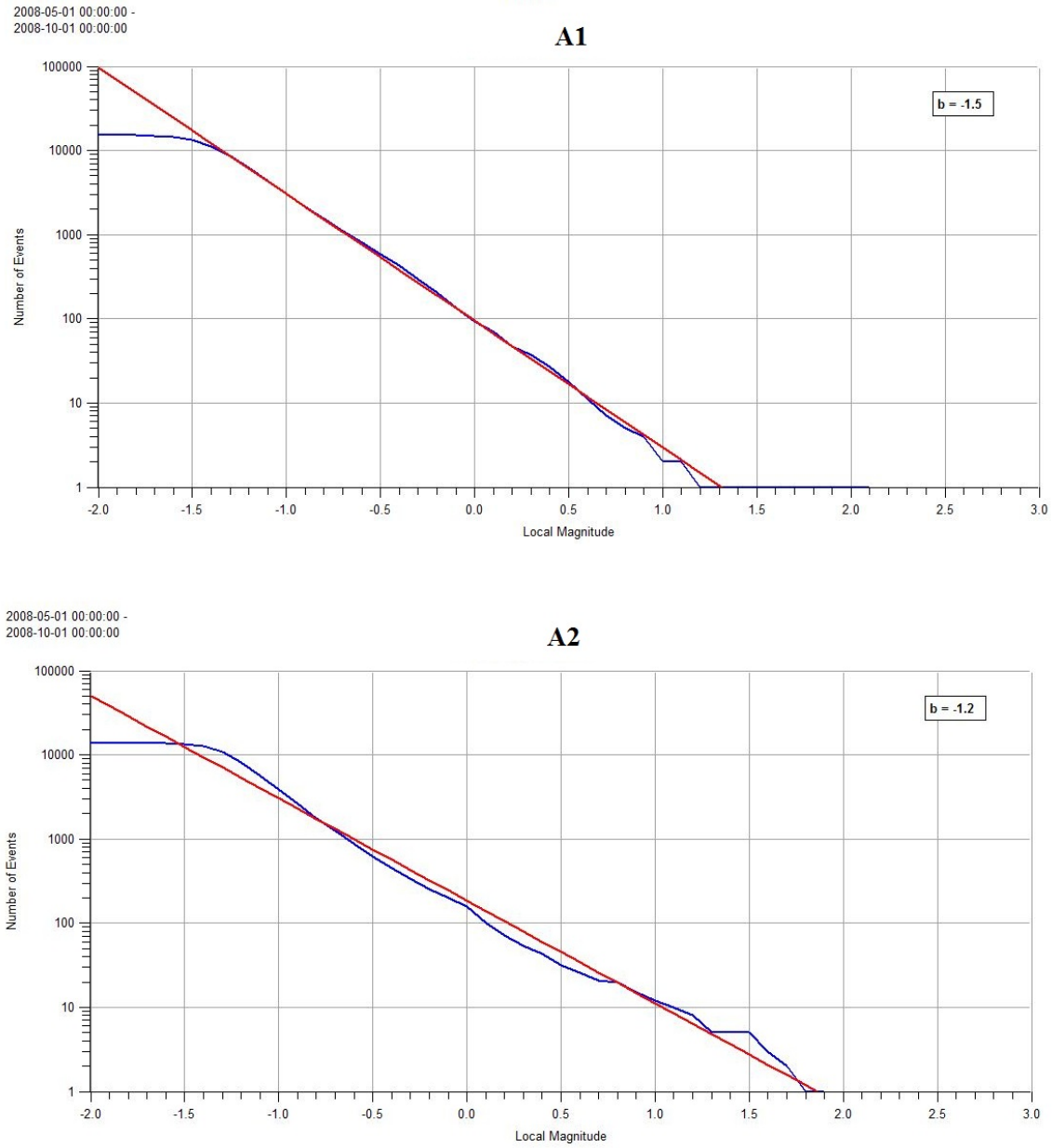

Figure 4.36 Comparison of the frequency-magnitude for the two selected events during Period 3 (A1 and A2).

In October 2008, the cave apex events entered into the area between the M50 and M30 reefs. A longitudinal projection view of the seismogenic zone showed that the events were trapped under the M30 reef and spread under the center and the south side of M30. This behaviour continued until February 2009 when the cave apex began to pass M30 (Figure 4.37).

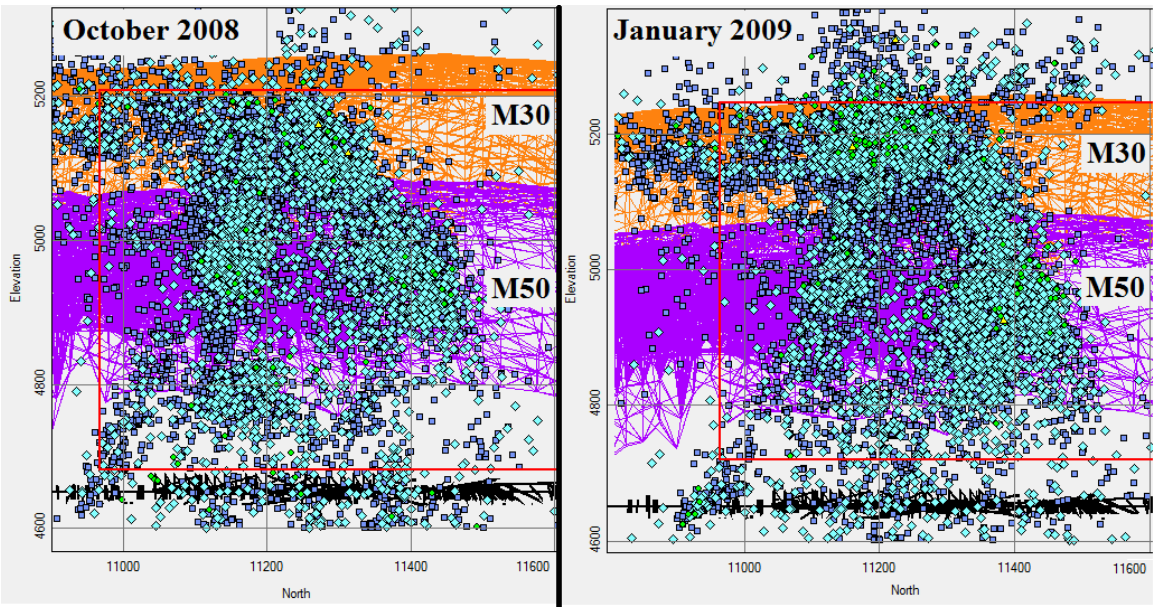

Figure 4.37 Migration of the cave apex events between the M50 and M30 in October 2008 and January 2009.

For assessing the behaviour of the events between the M50 and M30 reefs, a group of events was selected in this area from October 2008 to February 2009.

Table 4.5 Characterization of the selected events between M50 and M30.

	Minimum (m)	Maximum (m)
East	60200	60800
North	11230	11600
Elevation	5070	5250

In this group, about 32,000 events with six large events (+1< M_L <+2) were recorded. There were some missing data of the second half of December 2008. Ten percent of the events had an S:P energy ratios less than 3, and 13% of the events had an S:P energy ratios greater than 10.

The Energy-Moment plot showed an increase the slope of the relation (d=1.11) which was an indicator of the moderate rock quality in the M50 and M30 area. This value was the highest value recorded during the cave history. The CAV for the selected events reached 1.5e+09 m^3.

The general trend of the Magnitude-Time history of the events according to their S:P energy ratios showed that the events were migrating between the areas of the M50 and M30 reefs, the magnitude of the events with high S:P energy ratios was low in this period compared with other

periods. In other words, the events were more related to shearing mechanism between the M50 and M30 reefs.

4.3.4 Period 4 (from 2009/02/01 to 2009/10/01)

More than 140,000 events were recorded in this period. The seismogenic zone entered into geological Zone 2 for the first time. For a second time, starting in April 2009, the seismogenic zone split into two separate parts. This trend became clear in mid-May 2009 when the event rate changed. This separation was a good indicator for the initiation of the subsidence-type cave movement as the rockmass in that area was not competent enough to store energy and emit large seismic events. Since this time until the end of the mine's life, two separate seismogenic zones were recognizable. Similar to period 3, two groups (A1-south and A2-north) of the events were selected for more caving mechanisms assessment (Table 4.6 and Table 4.7).

Table 4.6 Characterization of the selected events in the group A1.

	Minimum (m)	Maximum (m)
East	60200	60800
North	10900	11230
Elevation	4650	5500

Table 4.7 Characterization of the selected events in the group A2.

	Minimum (m)	Maximum (m)
East	60200	60800
North	11230	11600
Elevation	4650	5500

In Group A1, the seismic system sensitivity was -1.4 while this value was -1.1 for Group A2 events. Thus, the seismic system sensitivity on the north side of the cave was lower than that in the south side (Figure 4.38). This difference in seismic system sensitivity was likely due to the location of sensors in the seismic sensor array.

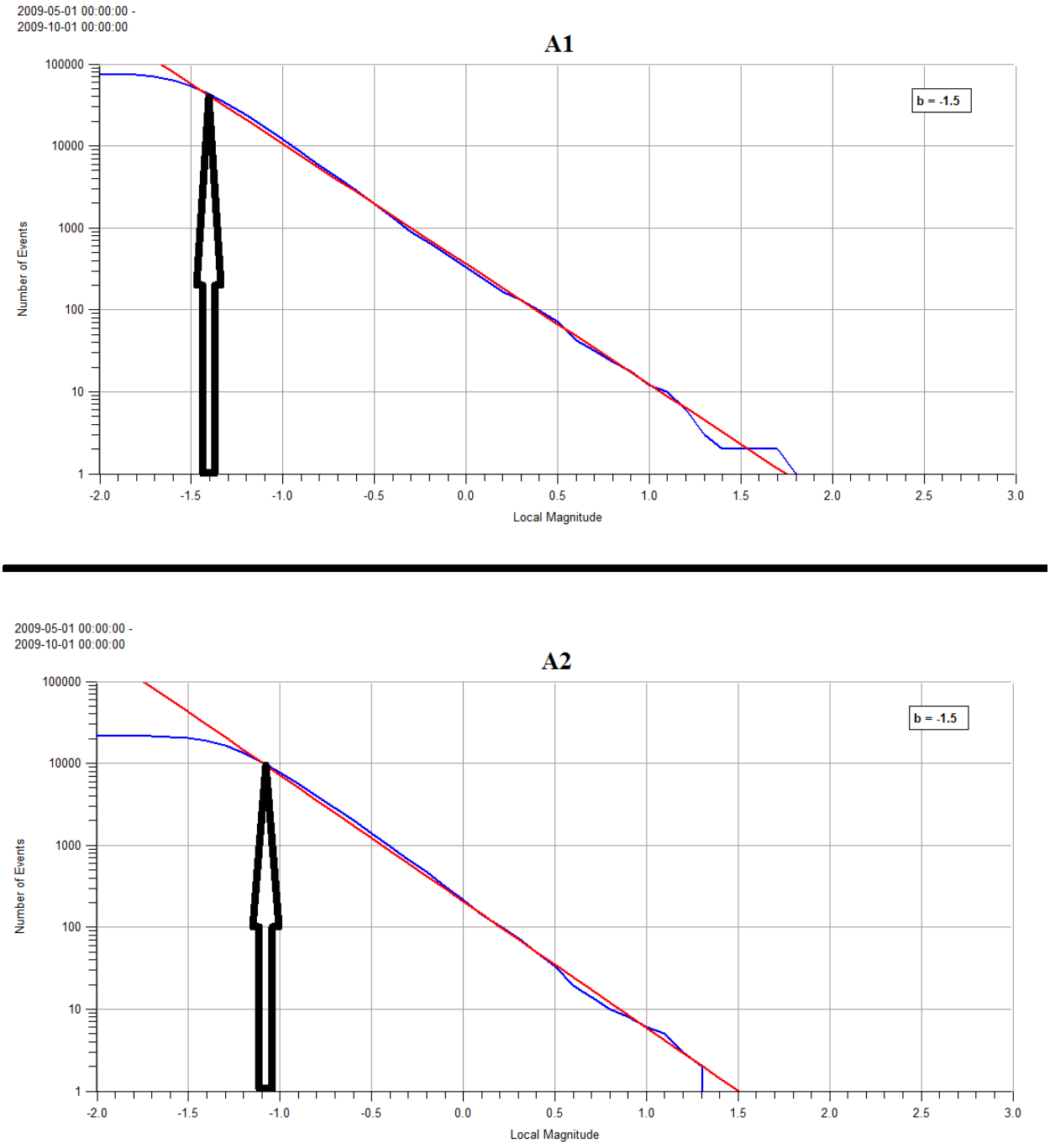

Figure 4.38 Comparison of the sensitivity for the two selected events during Period 4 (A1 and A2).

The number of events recorded in Group A1 (75,000) was almost three times greater than Group A2 (21,000). This ratio was affected by the change in the sensitivity of the seismic system network.

In Group A1, 30% of the events had an S:P energy ratios less than 3, and 15% of the events had S:P energy ratios greater than 10. For the selected events in Group A2, 40% of the events had an S:P energy ratio less than 3, and 15% of the events had S:P energy ratios greater than 10. Therefore, A2 group was slightly more related to a stress change caving mechanism compared with the Group A1.

Comparing the selected groups during Period 3 and Period 4 showed a significant increase in the events with S:P ratio less than 3 while the percentage of events with high S:P energy ratios did not change. This behaviour can likely be related to the initiation of the subsidence caving movement which was the dominant failure mechanism.

The ASTH trends in the selected groups were different. The ASTH in Group A1 increased gradually and reached its highest frequency in the second half of August 2009 with 100 events per day and the background level of this group was around 35 events per day. However, the ASTH trend in Group A2, except the first month (May 2009), was lower and the ASF was 10 per day. Furthermore, although the number of the events in group A2 was less than the number of events in Group A1, the CAV in Group A1 (6.0e+09 m^3) and A2 (5.0e+09 m^3) were similar (Figure 4.39 and Figure 4.40).

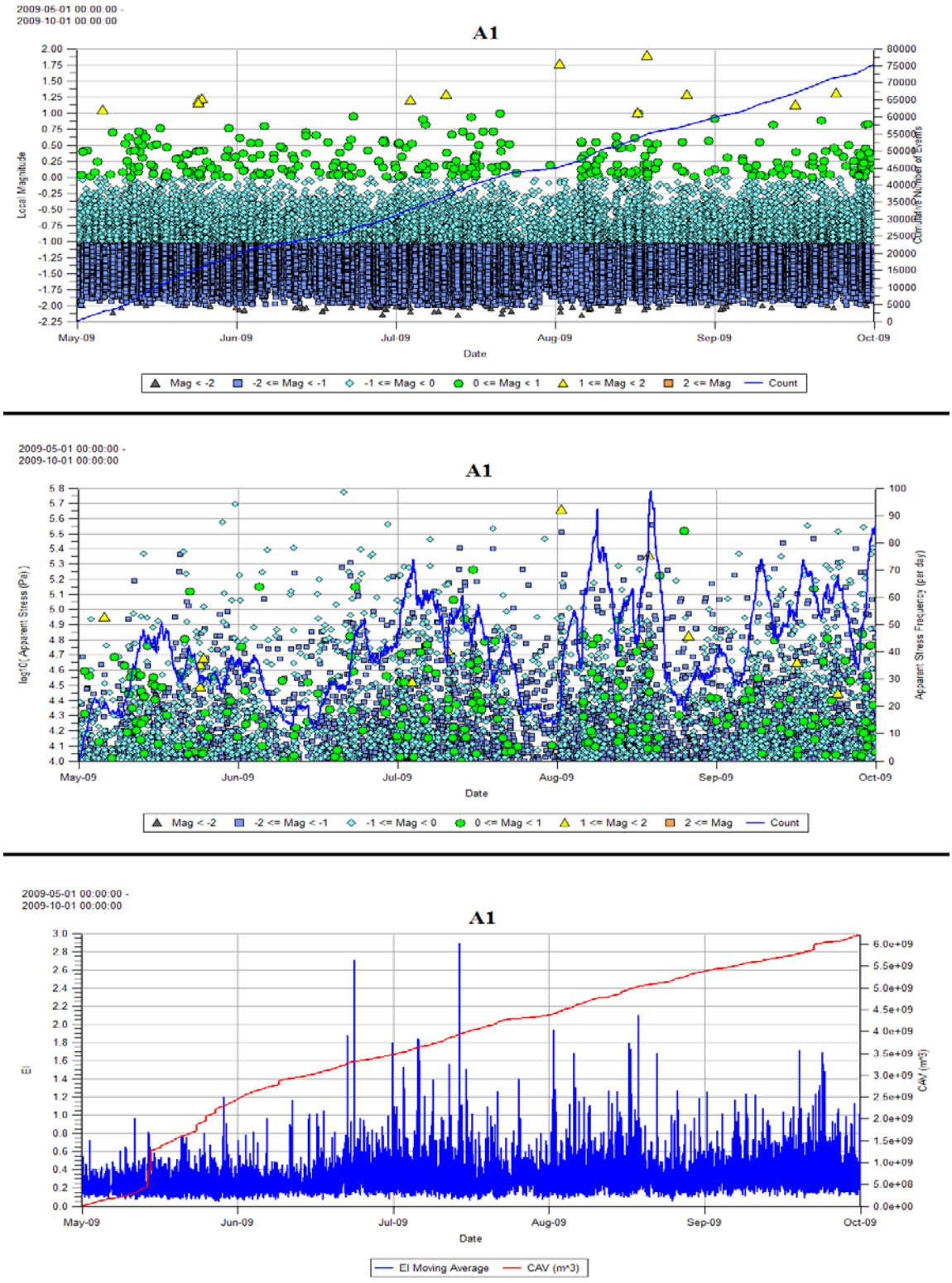

Figure 4.39 Magnitude-Time History, Apparent Stress History and EI/CAV for the two selected events during Period 4 (A1).

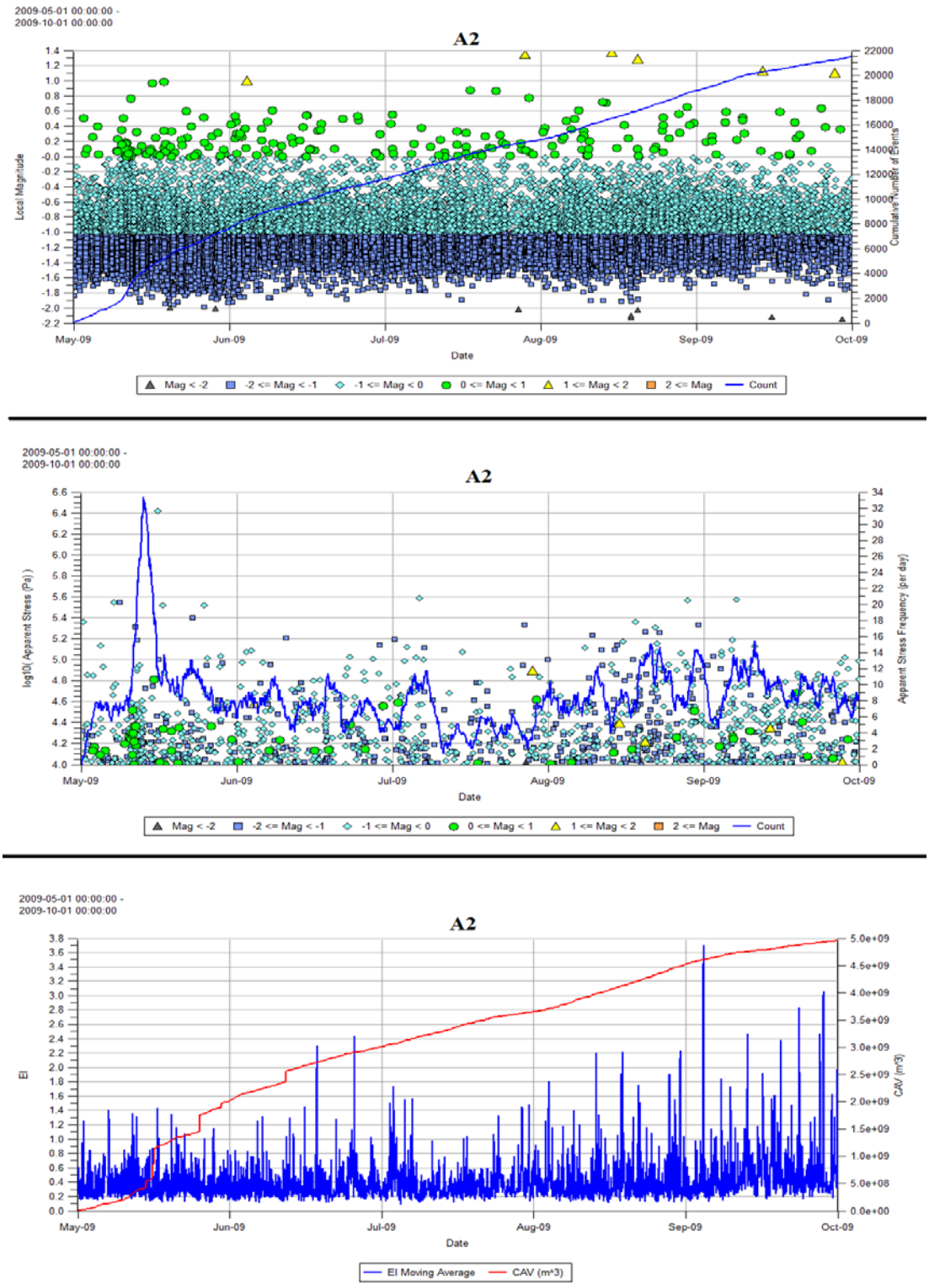

Figure 4.40 Magnitude-Time History, Apparent Stress History and EI/CAV for the two selected events during Period 4 (A2).

4.3.5 Discussion for Cave Propagation

Cave propagation is a continuous rockmass failure process in the cave back as the broken material is mucked from the bottom of the cave. During this processes, the seismogenic zone migrates due to rockmass failure ahead of the cave back.

Almost 300,000 events including five very large events ($+2< M_L <+3$) were recorded during the cave propagation period. The number of events with local magnitude between 1.0 and 2.0 during the cave propagation was eight times greater than that in the cave initiation period. The event rate was approximately 12,830 events per month. This rate was approximately 12 times greater than the event rate during the cave initiation.

The behaviour of the events during the cave propagation was not the same as the initial blasting and cave initiation periods. Generally, the events with high S:P energy ratio included both the small and large events while the events with low S:P were more related to the larger events.

The M50 and M30 reefs, similar to I30, had a very similar effect when the seismogenic zone was moving upward. The M50 and M30 reefs reduced the event rate and also the rate of the seismogenic zone upward movement.

Propagation of the cave caused the concentration of some events with very high Apparent Stress on the east side of the Graben fault, around the M50 reef, approximately 250 m above the first lift. It identified the M50 reef as a significant stress raising feature.

Subsidence-type caving started after mid-May 2009, predominantly with a stress fracturing mechanism, with the percentage of the events that their S:P <3 (fracturing events) increased to 40%.

Unlike the initial blasting and cave initiation periods, most of the seismic events in the cave propagation occurred during the day with no specific time of occurrence. This trend can be related to the events associated with the mucking rate (rather than blasting).

During cave propagation 7036 events with Apparent Stress greater than 30 kPa were recorded (2.4% of all events). After January 2009, numerous events with Apparent Stress greater than 300

kPa occurred. For the first time, the events with Apparent Stress greater than 1.0 MPa were recorded in May 2009. This behaviour is likely related to subsidence caving.

The Cumulative Apparent Volume during cave propagation was approximately 2.9e+10 m^3 with a rate of 1.3e+09 m^3 per month. This rate was almost 11 times greater than during cave initiation and approximately 210 times greater than the initial blasting period.

4.4 Breakthrough and Breakback

In the late October 2009, breakthrough happened in the west wall of the open pit (5384 mRL) within 50 m of the predicted breakthrough location (Dixon et al., 2010). Breakback occurs as the cave widens and moves outside the original footprint of the cave. In this interval (from October 2009 to November 2010), the behaviour of the events before and after of the breakthrough will be assessed. More than 120,000 events with local magnitude less than 2.0 were recorded during breakthrough and breakback.

Plotting the breakthrough and breakback events, according to their weekly median S:P energy ratio, percentage of shearing events and event rate (Figure 4.41 the median of the S:P energy was smaller than 10 in all weeks (the same as the cave initiation and propagation periods). In this period, the event rate decreased noticeably, while the percentage of shearing events increased to 30%.

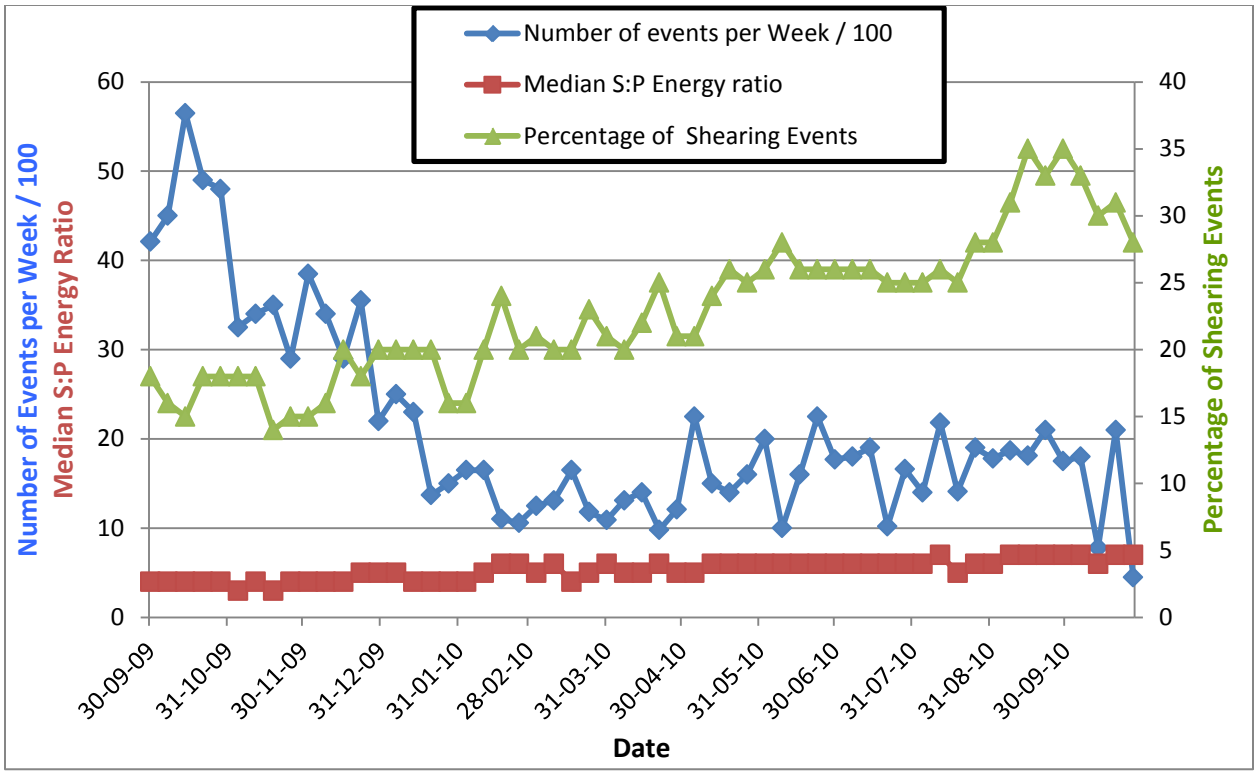

Figure 4.41 Comparison of median S:P energy ratio, weekly event rate (per 100) and percentage of shearing events during breakthrough and breakback.

During this interval the event rate changed three times. Each of these changes have been interpreted as follows (Figure 4.42):

1. Period 1 – October 2009 (Breakthrough)
2. Period 2 – From November 2009 to January 2010 (Decrease in event rate)
3. Period 3 – From January to November 2010 (Breakback). Data ends in November 2010.

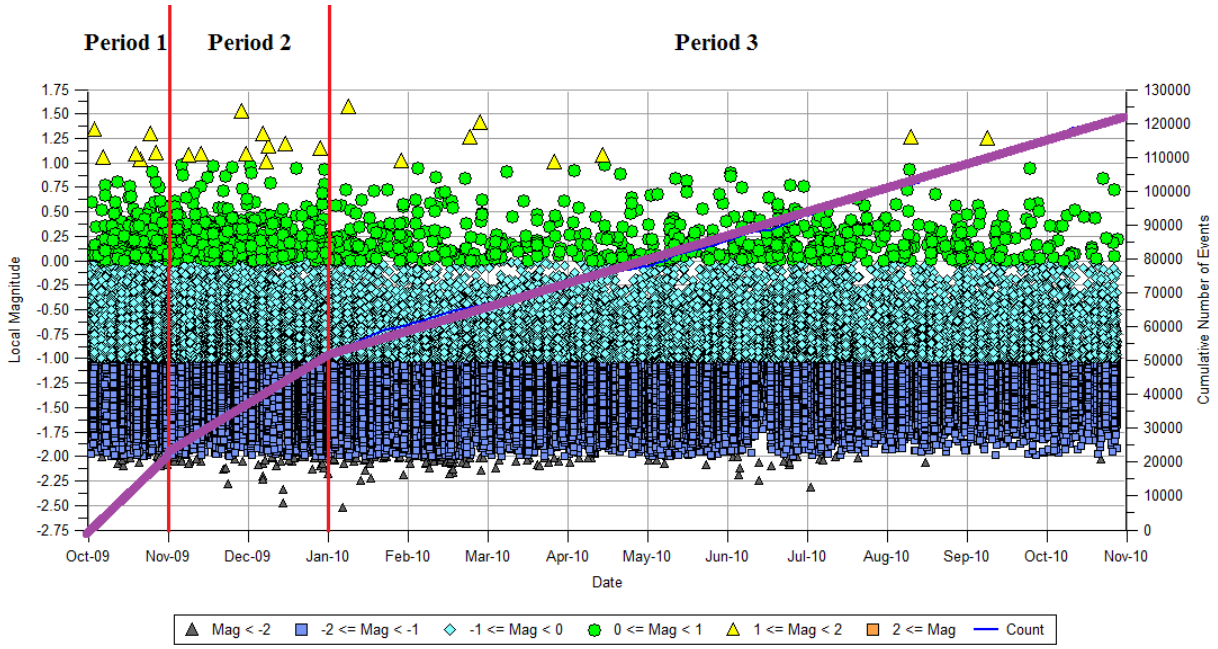

Figure 4.42 Magnitude-Time history for the events during breakthrough and breakback with 3 periods.

4.4.1 Period 1 (2009/10/01)

As shown in Figure 4.43, backfilling of the west wall was done in two phases to decrease the instability probability of the highwall. The first phase completed in May 2009, with dumping mine waste material. The second phase finished in early October of 2009 by tipping the material from 65 m above the highwall to preload bench (Dixon et al., 2010). Due to this action, the breakthrough happened 50 m away from the predicted breakthrough location, because the preload bench and the backfilled areas were competent compared with the other weathered areas of the Zone 1.

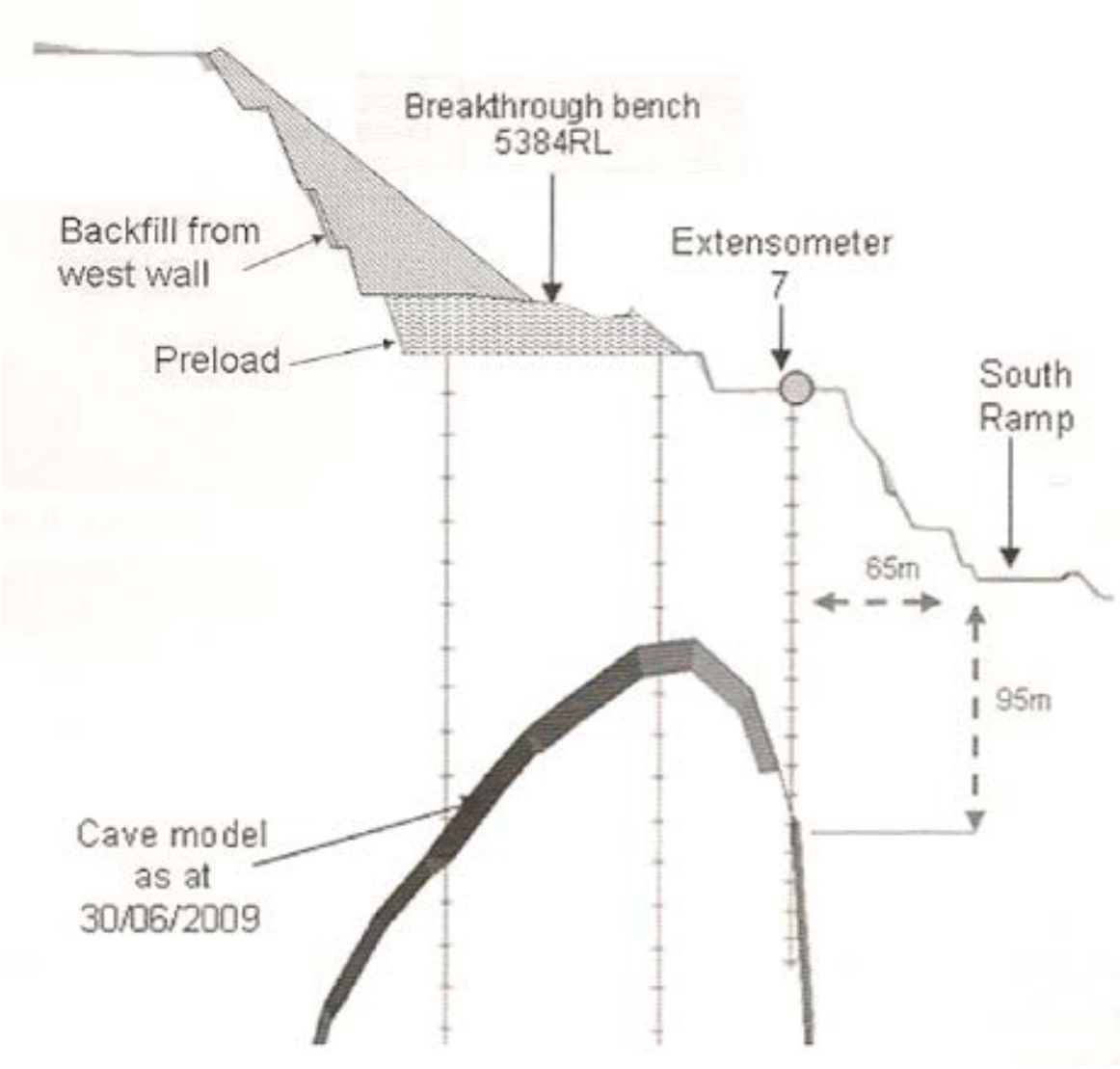

Figure 4.43 Section view showing proximity of the cave to the breakthrough bench and south ramp (Dixon et al., 2010).

From the changes in the events rate and also the Apparent Stress Frequency, it can be inferred that the seismogenic zone breakthrough happened on the 29th of October 2009. Before this day, the events rate was constant but afterwards it began to reduce.

In Figure 4.44, a Magnitude-Time history of the events in October 2009 is plotted according to their magnitude, S:P energy ratio and Apparent Stress (respectively from top to bottom). In this month, six large events ($+1 < M_L < +2$) were recorded. Four of these events were recorded between the 19th and 28th of October 2009. By evaluating other factors (S:P and ASF), it seems that in this interval, the frequency of the events with high S:P energy ratio and high Apparent

Stress is very high. After the breakthrough, the frequency of the events with high S:P energy ratio and high Apparent Stress decreased significantly. The background of the Apparent Stress frequency in October 2009 was 70 per day, while this value reached to its highest value on the 22nd of October 2009 with 105 events per day.

Due to effect of the breakthrough, the magnitude of the CAV between the 1st and 19th of October 2009 was the same as CAV magnitude between the 19th and 1st of November 2009 (1.0e+09 m^3).

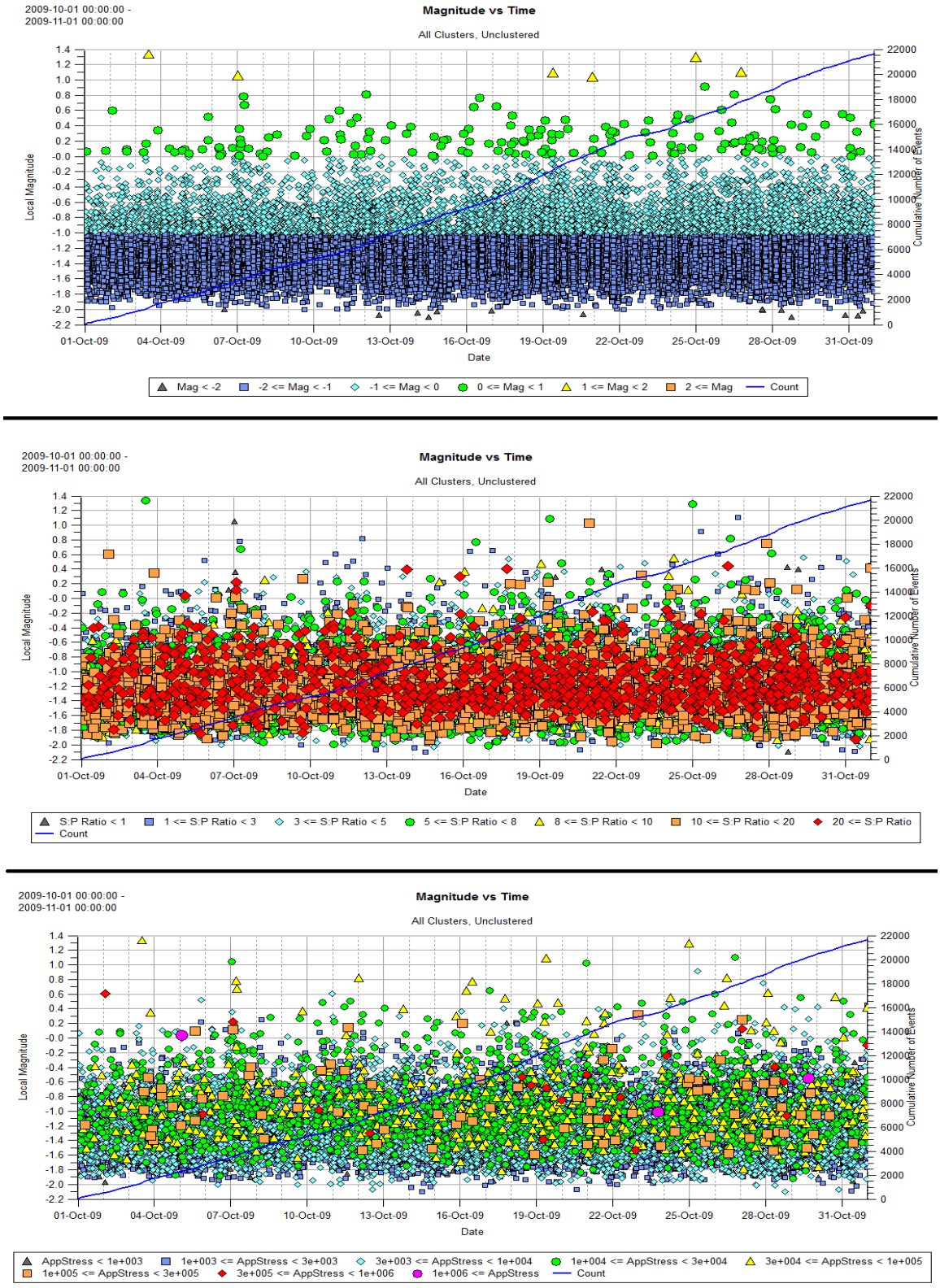

Figure 4.44 Magnitude-Time history of the events according to their magnitude, S:P energy ratio and Apparent Stress in October 2009.

In this period, 30% of all events had S:P energy ratios less than 3, and 17% of the events had S:P energy ratios greater than 10. Furthermore, comparing the S:P energy ratio of the events according to their magnitude shows that all the events with high S:P energy ratio had were similar (Figure 4.45). Thus, the mechanism is the same for all the magnitude ranges. When the magnitude of the events between -2 and 1 increased, the percentage of the events with S:P energy ratio less 3 increased slightly. The events with local magnitude between 1 and 2 showed a similar behaviour compared to smaller events, but there were only six events with magnitude over +1.

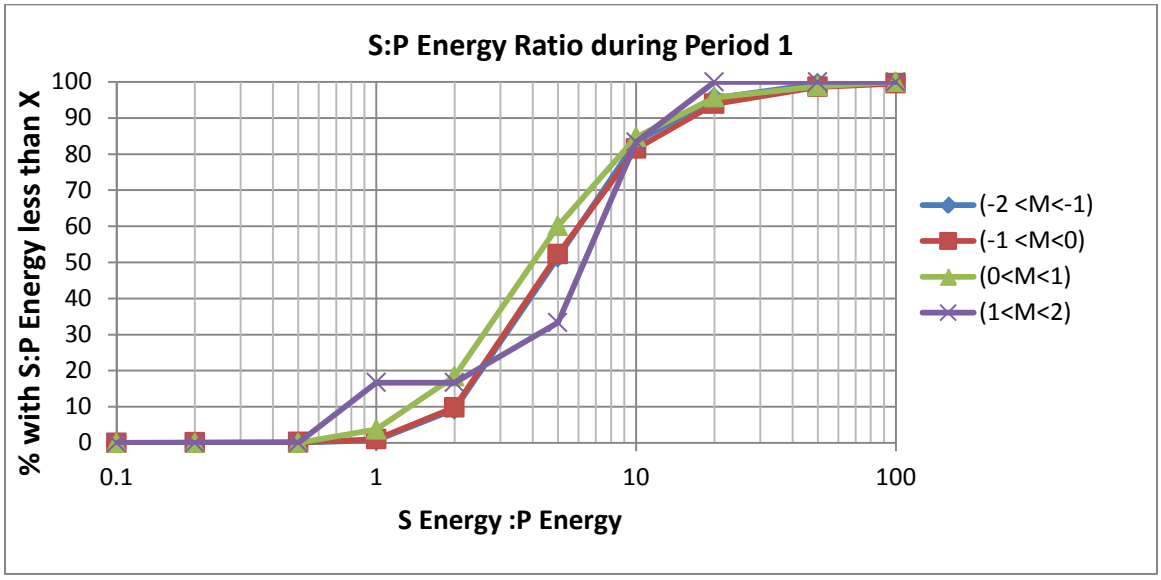

Figure 4.45 S:P energy ratio according to events magnitude during Period 1.

These assessments were done for all of the events which were recorded in October 2009. As mentioned, the seismogenic zone was divided into two separate areas (A1 and A2). Comparing the trends of Groups A1 and A2 showed that these groups did not have different behaviour. Although the number of the recorded events in the Group A2 was less than Group A1 (consequently the magnitude of the CAV and the ASF cannot be compared), the general trends of these groups in the Magnitude-Time history, the CAV and the ASH analysis were very close.

In Table 4.8 the S:P energy ratios of the groups are compared. According to the percentages, it can be inferred that the events in Group A2 are slightly more related to a non-shear source mechanism.

Table 4.8 S:P energy ratio for the Group A1 and A2 during Period 1.

	S:P Energy Ratio Range	Percentage
Group A1	S:P<3	30%
	S:P>10	16%
Group A2	S:P<3	40%
	S:P>10	20%

Figure 4.46 shows that the comparison of the S:P energy ratio of the groups according to the event magnitude. All events with local magnitude less than 1 have very similar behaviour in Group A1, while this trend cannot be seen in Group A2 (the large events are predominately non-shearing events).

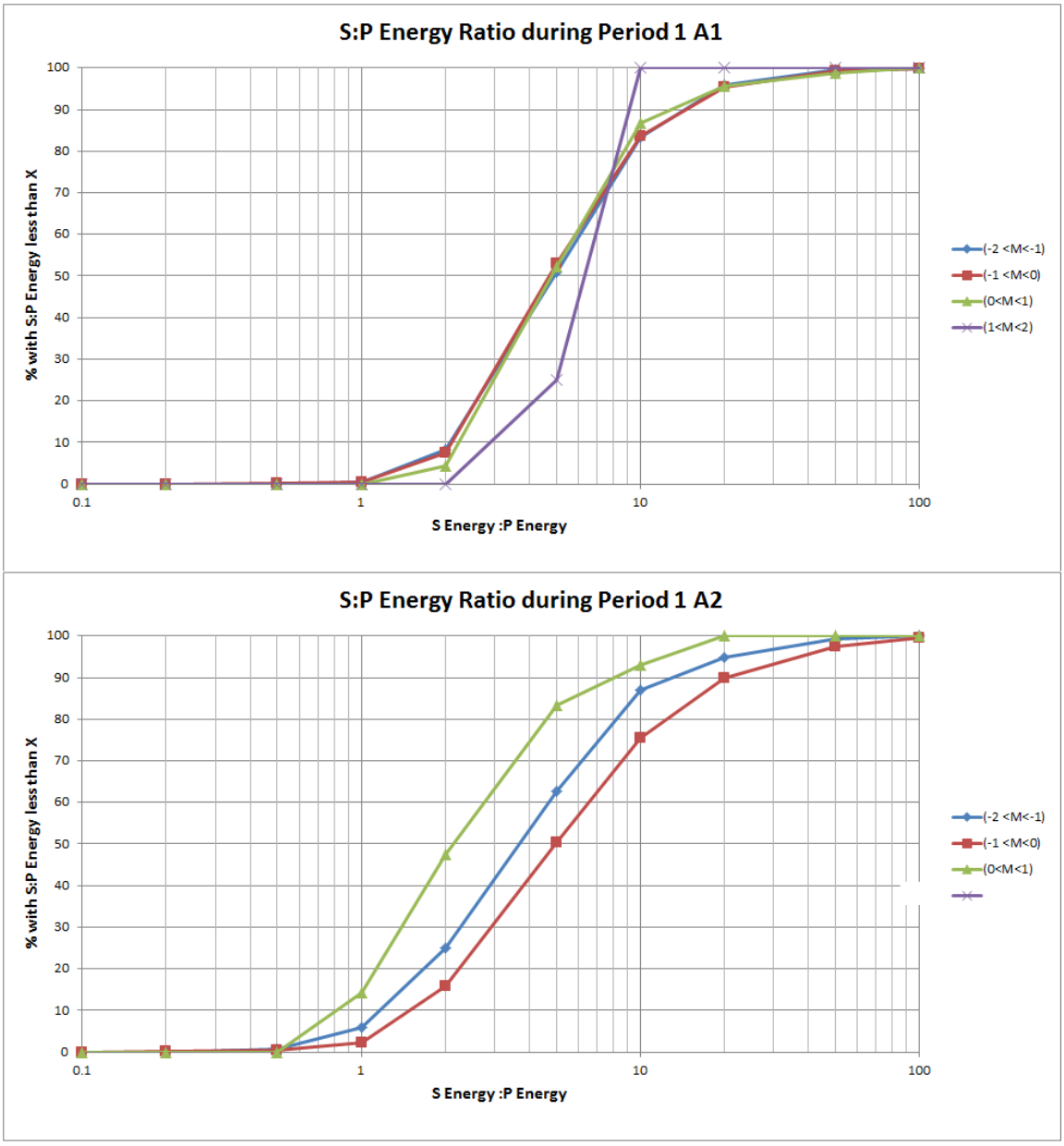

Figure 4.46 Comparison of the S:P energy ratio of the groups according to the events magnitude during Period 1.

4.4.2 Period 2 (from 2009/11/01 to 2010/01/01)

In this period, the number of the events decreased (compared to October 2009) but the rate of the events was constant during November and December 2009. Also, the two distinct seismogenic zones started to separate more quickly. This separation represents the two sides of the cave breakback into the pit.

Similar to October 2009, the Magnitude-Time history of the events in November and December 2009 is plotted according to their magnitude, S:P energy ratio and Apparent Stress (Figure 4.47). In the interval between late November and early December 2009, nine large events ($+1 < M_L < +2$) were recorded.

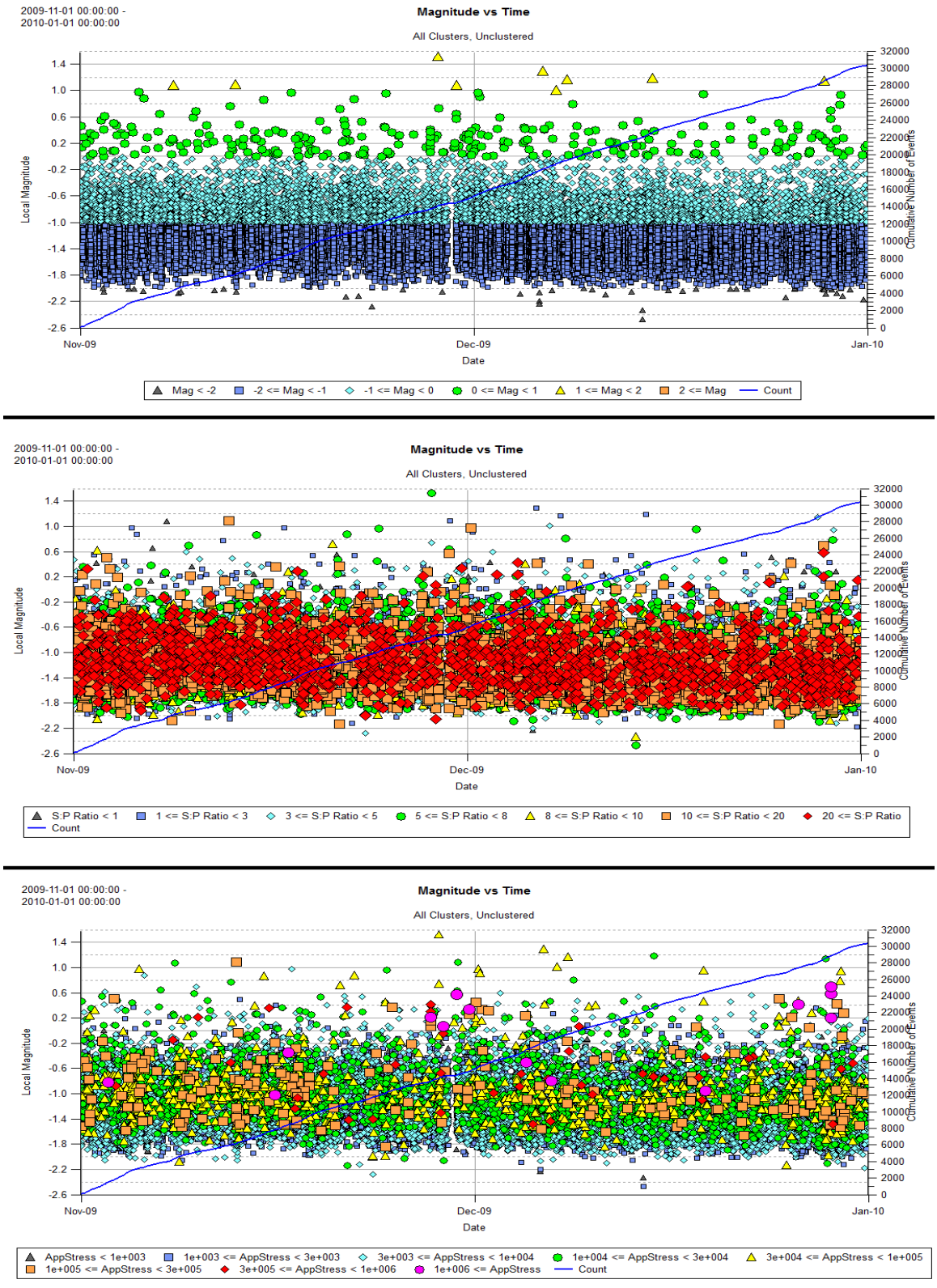

Figure 4.47 Magnitude-Time history of the events according to their magnitude, S:P energy ratio and Apparent Stress in the Period 2.

In this period, 35% of all events had S:P energy ratios less than 3 (a 5% increase compared to the previous period), and 16% of the events had S:P energy ratios greater than 10 (almost the same as the last period). Comparing the S:P energy ratio of the events according to their magnitude shows that larger events are more related to a non-shear source mechanism than smaller events. The small events are not shear (only 20%). A comparison only serves to show that one population is more or less shear than another (Figure 4.48).

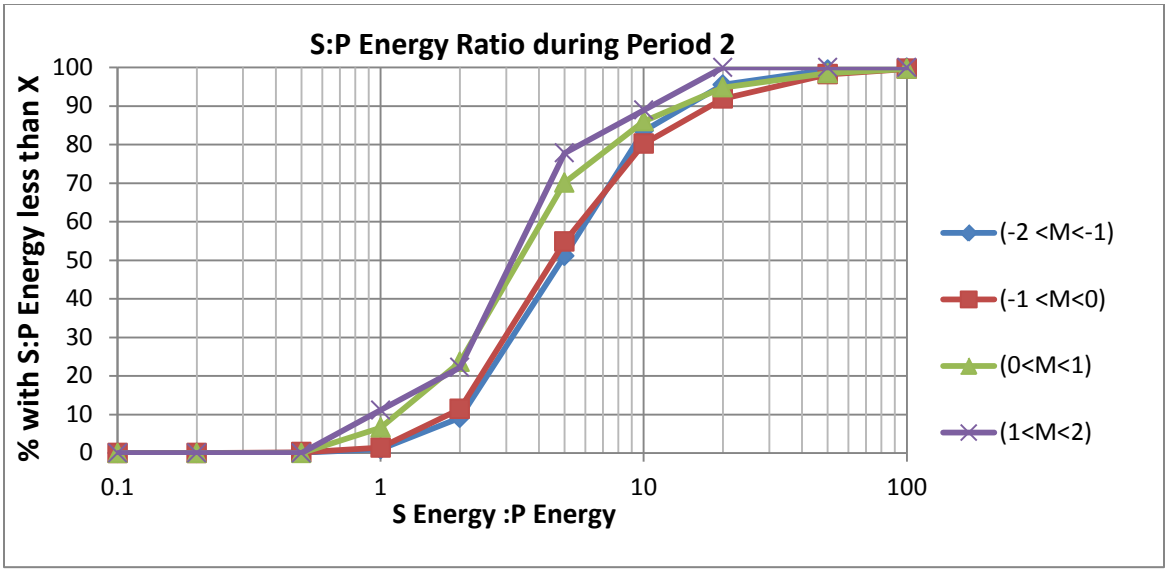

Figure 4.48 S:P energy ratio according to events magnitude during Period 2.

The background of the Apparent Stress Frequency in this period was 55 per day (reduced compared to October 2009). Between late November and early December 2009, an increase of frequency from 30 to 70 events was observed. After a drop in mid-December 2009, this value reached its highest value in late December with 100 events per day (an effect associated with the large events).

Analyzing the groups A1 and A2 events showed that the percentage of the events with low and high S:P energy in Group A1 remained constant compared with October 2009 (Table 4.9).

Table 4.9 S:P energy ratio for the Group A1 and A2 during Period 2.

	S:P Energy Ratio Range	Percentage
Group A1	S:P<3	30%
	S:P>10	16%
Group A2	S:P<3	45%
	S:P>10	17%

Figure 4.49 shows a comparison of the S:P energy ratio of the groups according to event magnitude. The events with different magnitudes in Group A1 had the same percentage for both high and low S:P energy ratio. But in Group A2, smaller events were more related to a shear type source mechanism and larger events were more related to a non-shear source mechanism.

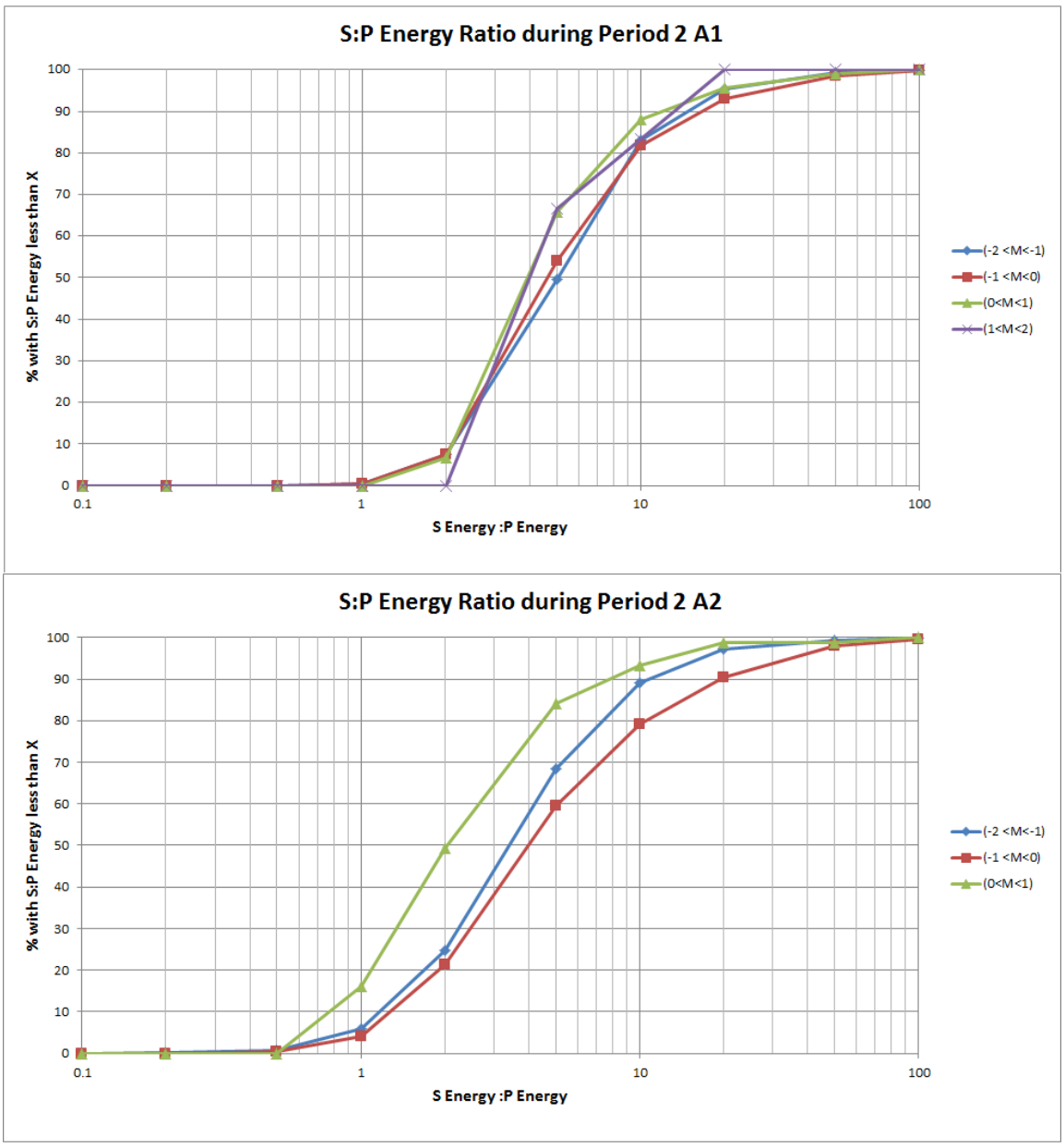

Figure 4.49 Comparison of the S:P energy ratio of the groups according to the events magnitude during period 2

4.4.3 Period 3 (from 2010/01/01 to 2010/11/01)

The event rate was essentially constant between January 2010 and November 2010, the lowest event rate for the breakthrough/breakback. Six large events (+1<M<+2) were recorded up to May 2010. The distance between the A1 and A2 seismogenic zones was initially constant but after a few months (by May 2010) some events were recorded in the elevations between 4800

and 4950 mRL (Figure 4.50). This represents the start of the breakback to the west on the lower areas of the cave.

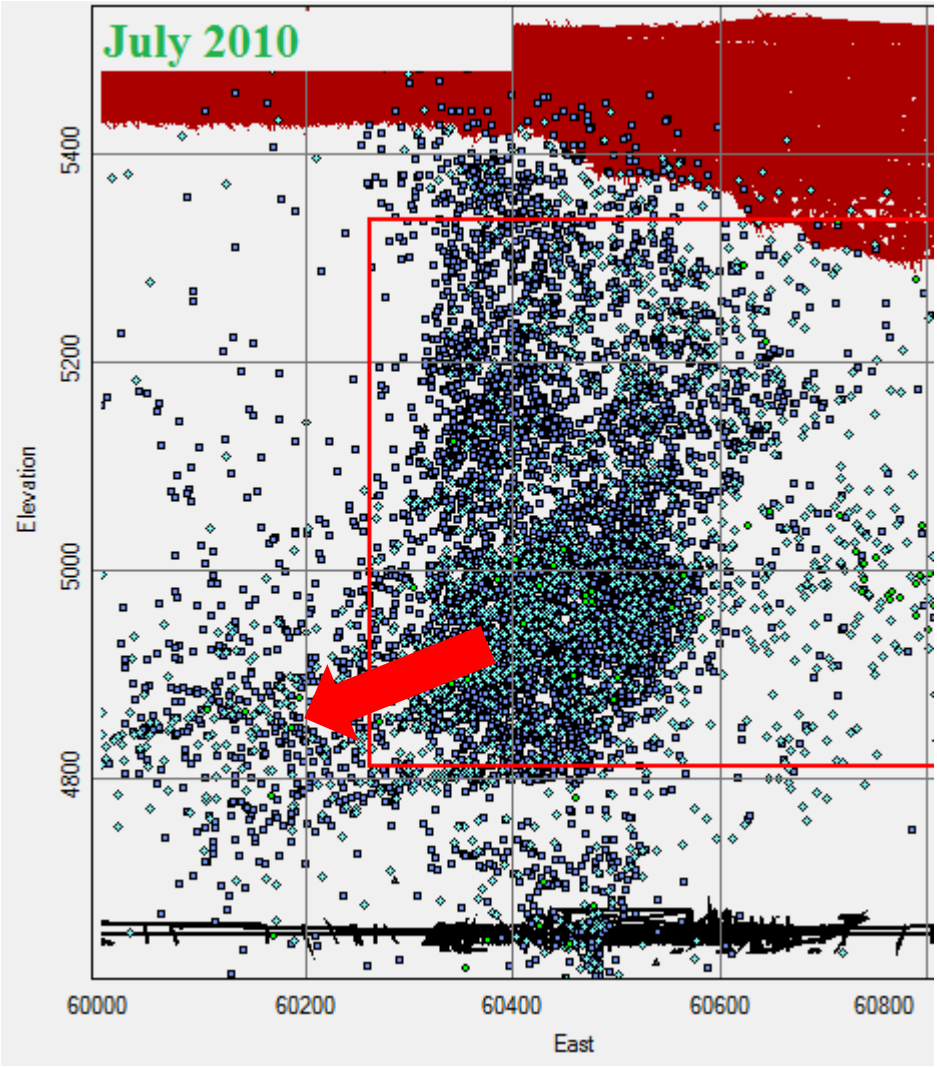

Figure 4.50 Section view the location and direction of the events in the lower part of Group A1.

From May to September 2010, the rate of lower elevation events increased. These events also migrated from the south to the west side of the side of the cave (clockwise). These events occurred at a dip angle of 40^{o} and 50^{o}. It seems these events are related to bedding plane failure. The increased event rate coincided with a decrease in the number of events recorded in Group A2. Group A2 events effectively disappeared by September 2010 (Figure 4.51), suggesting no further breakback to the north-east of the cave.

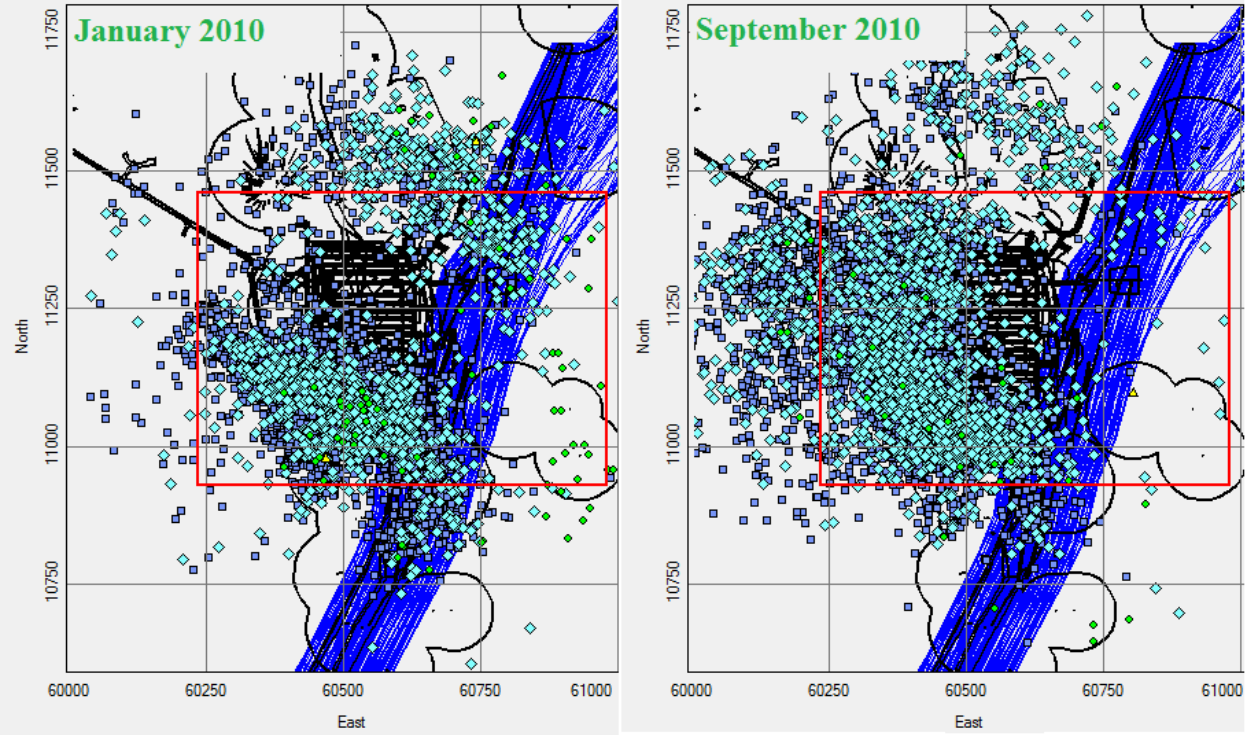

Figure 4.51 Plan view of events in January and September 2010.

In this period, 23% of the events had an S:P energy ratios less than 3, and 25% of the events had an S:P energy ratios greater than 10. A month-by-month evaluation of the ratio of the events with low and high S:P energy ratios showed that the percentage of the events with low S:P energy ratios (S:P <3) decreased from 27% to 20% while the percentage of the events with high S:P energy ratios (S:P >10) increased from 20% to 32%, indicating a trend of increasing shear source mechanism. This behaviour was due to events which were recorded in the lower part of Group A1.

The trend of the events changed after May 2010. There was a decreasing trend in ASF between January and May 2010, followed by an increasing trend between May and July 2010 and again dropped until the end of October 2010 (Figure 4.52). The CAV after May 2010 accelerated noticeably, and the CAV at end of the period (8e+09 m^3) was four times greater than the CAV before May (2e+09 m^3).

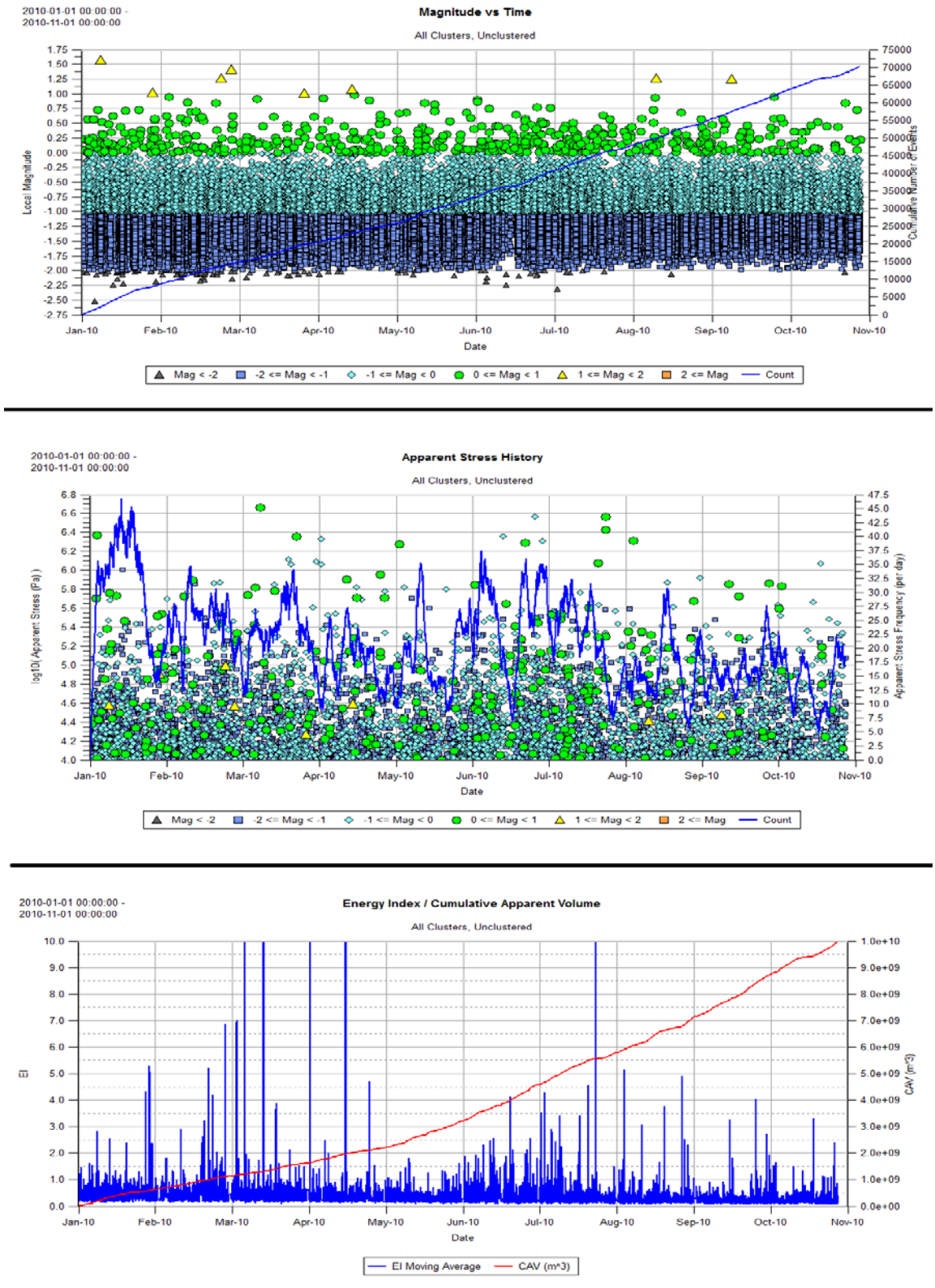

Figure 4.52 Magnitude Time History, Apparent Stress History and EI/CAV during Period 3.

4.4.4 Discussion for Breakthrough and Breakback

Cave breakthrough can be defined as the major subsidence in the open pit bottom. This significant subsidence is a vital period of the caving process (due to safety and the production factors).

More than 120,000 events with local magnitude less than 2.0 were recorded during breakthrough and breakback. The number of the events with local magnitude between 1.0 and 2.0 during breakthrough was one third compared to the recorded events during cave propagation period. The event rate was approximately 9,378 events per month. This rate was approximately 75% of the event rate during cave propagation.

Comparing the S:P energy ratio of the events according to their magnitude shows that all the events with high S:P energy ratio had similar percentages. When the magnitude of the events increased from -2 to 1, the percentage of the events with S:P energy ratio less than 3 also increased.

The seismogenic zone split into two distinct zones as it approached breakthrough into the pit. The percentage of the events with S:P < 3 (35%) was greater than the events with S:P > 10 (15%), the frequency of the events with low S:P energy ratio was higher on the north side of the breakthrough. This might be related to the smaller distance between the one of the seismogenic zones (A2) to the Graben fault compared to the other seismogenic zone (A1). On the other hand, the frequency of the events with high S:P energy ratio was higher on the south-west side. This behaviour might be related to the shearing of the bedding planes in south-west area of the cave.

Most of the events with very high Apparent Stress (> 1.0 MPa) were recorded in this period. These events had different source of mechanisms on the east side (shear) and west side of the Graben fault (non-shear).

During the breakthrough period, most of the seismic events occurred during the day with no specific time of occurrence.

During the breakthrough, 7043 events (5.9% of all events) with Apparent Stress greater than 30 kPa were recorded. The events with highest Apparent Stress (> 1.0 MPa) were recorded in this period. This suggests a higher level of induced stress associated with the breakthrough period.

The CAV during breakthrough was approximately 1.5e+10 m^3 with a rate of 1.1e+09 m^3 per month. This rate was approximately 0.8 of the CAV rate during cave propagation, but still nine times greater than the CAV rate during cave initiation and almost 178 times greater than that in the initial blasting period.

5 RELATION AMONG THE EVENT RATE/MUCKING RATE/ CAV RATE AND APPARENT STRESS

5.1 Seismic Event Rate Variations

5.1.1 Event Rate by Time Period

From March 2006 to November 2010 (from initial blasting to data ending), more than 430,000 events with local magnitude between -2 and +3 were recorded. During this period, the event rate was not constant but changed many times. Numerous factors such as mucking rate, caving periods (initial blasting, cave initiation, cave propagation and breakthrough), seismic system sensitivity, data loss and lithology, can affect the event rate.

The monthly event rate from March 2006 to November 2010 (Figure 5.1) shows that the rate of the events varied between 39 and 28,054 events per month. This variation was between 39 and 1,637 events per month from March 2006 to the October 2007. This was due to the direct influence of the mining operations and also the change in the sensitivity of the seismic network (between October and mid-November 2006). On the other hand, from November 2007 to the end of October 2010, the event rate varied between 3,571 and 28,054 events per month (due to caving progression and the effect of the lithology).

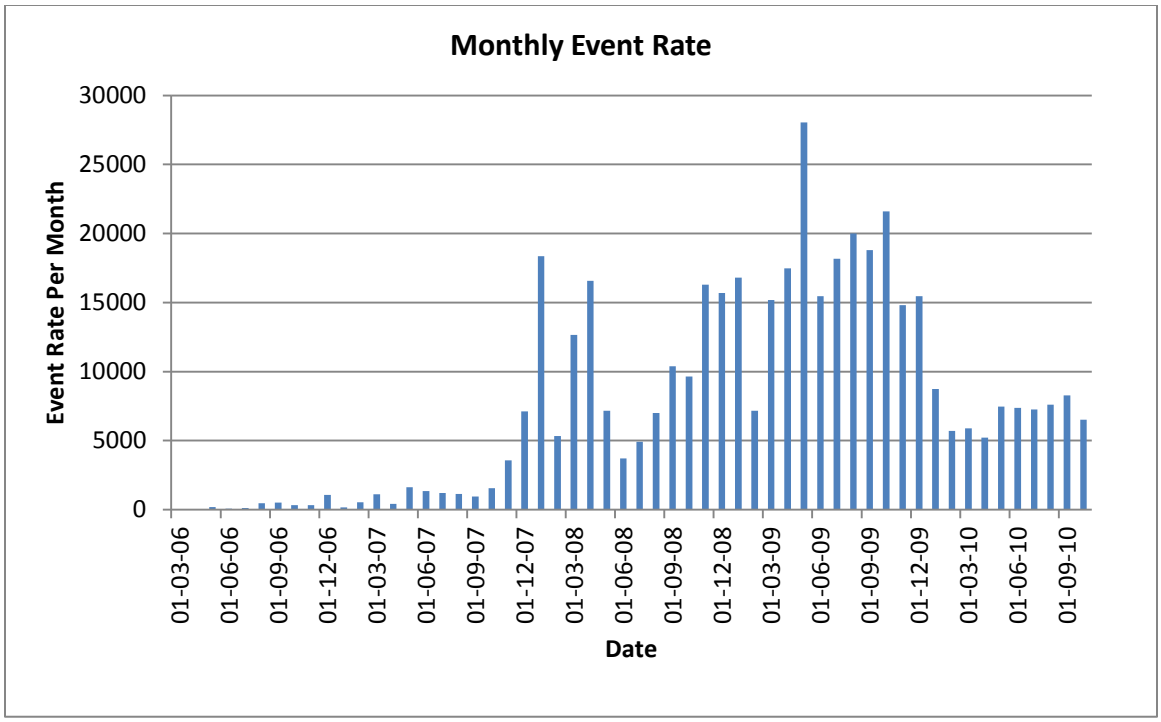

Figure 5.1 Monthly event rate.

The lowest recorded monthly event rate (in April 2006 with 39 events per month) is related to first lift opening blasts and the highest monthly event rate (in May 2009 with 28,054 events per month) is associated with cave the propagation with a maximum production rate. The low monthly event rate in January and February 2007 is related to data loss (data loss occurred several times during this period). Additionally, the decrease in the event rate in March 2007 can be related to the interaction of the seismogenic zone and the I30 reef. After one month, the seismogenic zone passed the I30 reef. Afterwards, the increase and the decrease in the event rate in January and February 2008 was related to upward movement of the seismogenic zone under the M50 reef and the entrance of the seismogenic zone's apex to the M50 reef, respectively.

The event rate reduction in May 2008 was due to the entrance of the seismogenic zone's shoulders in to the M50 reef, effectively slowing the cave and event rate. The same behaviour happened when the seismogenic zone propagated under the M30 reef from December 2008 (interaction of the seismogenic zone's apex with M30) to February 2009 (interaction of the seismogenic zone's shoulders with M30). The I30, M50 and M30 reefs were the major geological features which reduced the rate of the seismogenic zone movement. Each time the seismogenic zone passed above the mentioned reefs, the event rate increased to the previous rate.

As the seismogenic zone approached the pit bottom in May 2009, the event rate decreased because of weakness of the ground near surface. The subsequent increase in the event rate may be related to initiation of the breakback which started 5 months after cave breakthrough.

5.1.2 Event Rate by Cave Period

During cave evolution at Telfer mine, the rate of occurrence of events increased from initial blasting to cave initiation and cave propagation, but decreased from cave propagation to breakthrough and breakback. The number of recorded events during cave initiation was almost 3 times greater than that in the initial blasting period. The number of the events during cave propagation was almost 30 times greater than that in the cave initiation, and 2.5 times greater than the breakthrough and breakback periods. These ratios were not constant for the smaller local magnitude intervals. For example, the events recorded between local magnitude 0 and +1 during cave initiation was almost 10 times greater than that in the initial blasting period. The number of the recorded events during cave propagation was almost 14 times greater than that in cave initiation, and two times greater than that in the breakthrough and breakback periods.

During initial blasting, blasts were the main source of the seismic events. The number of the recorded events in each month was dependent on the blasting rate. The increase of the monthly event rate during cave initiation (compared to the initial blasting period) can be related to the opening of the first lift with a gradually increasing hydraulic radius. Therefore, the event rate during cave initiation was still discontinuous and was mainly dependent on the mining operations (expanding the first lift area).

During the cave propagation, the cave progressed continuously and caused numerous seismic events with higher magnitudes.

In the breakthrough and breakback period, the seismogenic zone was close to the weathered rock types, preconditioned ground by pit blasting (noted also at Palabora mine by Glazer and Townsend (2010) and NorthParkes by Hudyma et al. (2007b)), and also the stress free surface (bottom of the pit). Hence, the rock was not competent enough to emit high numbers of the

seismic events and consequently the event rate and magnitude decreased (compared to cave propagation period).

5.1.3 Event Rate Versus Mucking Rate

Cave mucking data is available from August 2006 to early November 2009. For assessing the monthly mucking rate, the cumulative tonnages of the mucked materials in each month was calculated. The monthly mucking rate correlates to an increasing event rate. The mucking rate varied between 124,049 and 598,880 tpm. For some days the mucking rate was zero. The longest period with zero mucking tonnage was between March 27th and April 9th 2007. The lowest mucked tonnage was in August 2006 (124,049 tpm) and the highest mucked tonnage was in October 2009 (598,880 tpm).

Comparing the event and mucking rates shows that in the first year (from August 2006 to August 2007) there was not a good relation between the two rates. Only in 4 out of 12 of the months did the increasing/decreasing trend of the mucking rate have a similar trend in the event rate. Conversely, there is a strong relation between the event rate and the mucking rate from August 2007 to November 2009. Every time the mucking rate increased the event rate increased and vice versa. This trend is true for the 23 out of 26 selected months. All of the selected months from August 2006 to August 2007 occur in the initial blasting and first half of the cave initiation periods, while the selected months from August 2007 to November 2009 occur in the late cave initiation and the cave propagation periods. It can be concluded that during the initial blasting and cave initiation periods there is weaker relation between the event and mucking rates compared for the cave propagation and breakthrough periods. In other words, the initial blasting and cave initiation events are due to blasting and expanding the first lift area, while the cave propagation and breakthrough events are more related to the mucking rate (Figure 5.2).

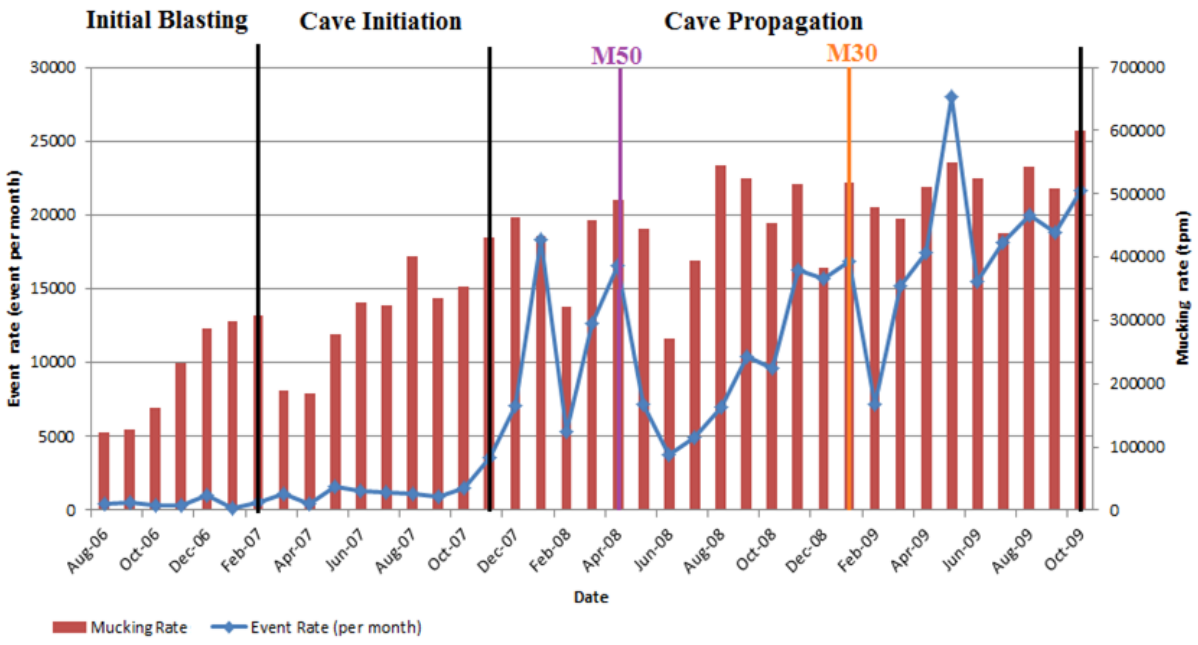

Figure 5.2 Monthly event rate versus monthly mucking rate.

5.1.4 Event Rate Versus Seismogenic Zone Movement

The seismogenic zone moved upward at different rates and thicknesses until April 2009 (5180 mRL). After April 2009, the seismogenic zone split into two distinct zones and remained in this condition until the end of October 2010.

There is a strong relation between the seismogenic zone movement and the monthly rate of events. Every time the number of the events increased, the seismogenic zone moved upward more quickly and when the monthly event rate decreased the seismogenic zone moved at lower rate.

During the initial blasting period, due to strong relation between the event rate and blasting, no clear relation can be seen between the monthly event rate and the seismogenic movement. However, during cave initiation, a close correlation of the monthly event rate and seismogenic zone is apparent. When the monthly event rate decreased, the elevation of the seismogenic remained at a relatively constant elevation (4840 mRL).

As mentioned before the seismogenic zone had to pass the M50 and M30 reef structures in the cave propagation period. A decreasing monthly event rate was observed as the seismogenic zone entered and passed through the M50 and M30 reefs. The elevation of the seismogenic zone was constant for a few months, such as February and March 2008 (due to entrance of the seismogenic zone's apex to M50), June, July and August 2008 (due to entrance of the seismogenic zone's shoulders to M50), November and December 2008 (due to entrance of the seismogenic zone's apex to M30), and January and February 2009 (due to entrance of the seismogenic zone's shoulders to M30). The M50 and M30 structures not only reduced the event rate, but also acted as a barrier for movement of the seismogenic zone (Figure 5.3).

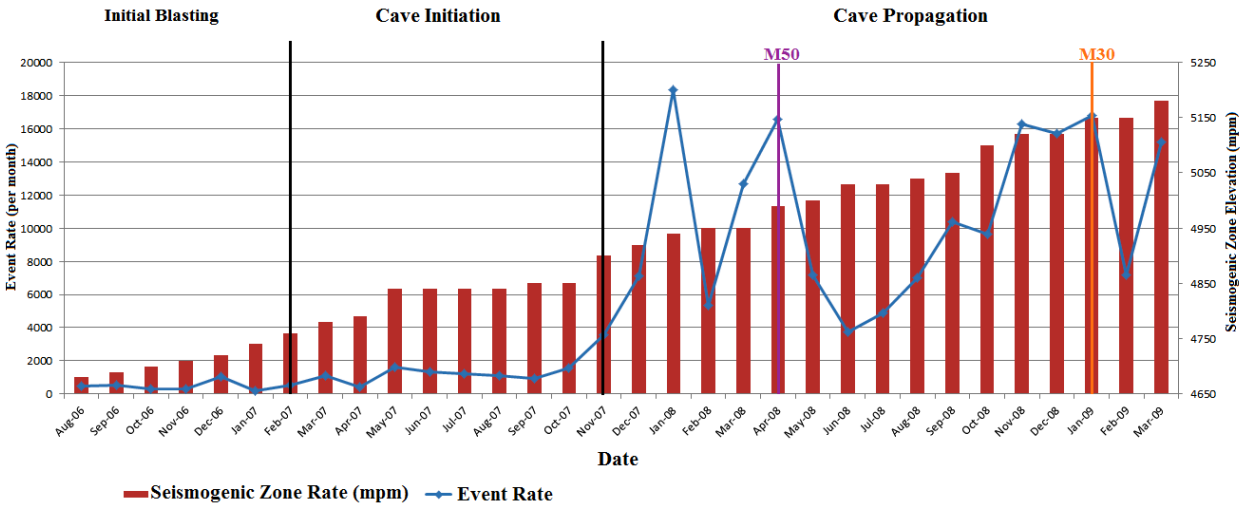

Figure 5.3 Monthly event rate versus monthly seismogenic upward moving rate.

5.1.5 Event Rate Versus Event Magnitude

During the initial blasting period, all the recorded events had local magnitude less than 1.0. In the cave initiation period, 11 events with local magnitude between +1.0 and +2.0 were recorded. There was a clear increase trend in the magnitude of the events from initial blasting to cave initiation.

After recording 15 events with local magnitude between 1.0 and 2.0, the first event larger than 2.0 happened in the first period of the cave propagation period (local magnitude 2.1). Moreover,

four other events with local magnitude between 2.0 and 3.0 were recorded during the cave propagation period.

The last event with local magnitude larger than 2.0, happened in May 2008 (period 3 of the cave propagation, the seismogenic zone entered the area between M50 and M30). After this time, all the recorded events had local magnitude less than 2.0, but the occurrence of events less than 2.0 was not constant. For example, between July and November 2009, the frequency of these events (M_L <+2.0) was very high. The highest frequency of all the events with local magnitude less than 2.0 was in period 4 (February to October 2009) of the cave propagation period. This behaviour is related to the high rate of seismogenic zone movement in May 2009 and the cave approaching pit breakthrough in October 2009.

5.2 Cumulative Apparent Volume by Cave Period/ Mucking Rate/ Seismogenic Movement

5.2.1 Cumulative Apparent Volume by Cave Period

The Cumulative Apparent Volume (CAV) rate increased from 2.0e+05 m^3 per day during initial blasting to 6.4e+07 m^3 per day in the early breakthrough period.

The CAV daily rate shows that the rate of the CAV during cave initiation was almost 20 times greater than the CAV daily rate during initial blasting. Furthermore, the CAV daily rate during cave propagation was 10 times greater than the CAV daily rate during cave initiation and 1.2 times greater than that in the breakthrough period.

Changing the rate of the CAV from daily to monthly shows the lowest CAV rate was 6.94e+05 m^3 per month which was recorded in August 2006 (early initial blasting operations) and the highest CAV rate was 2.82 e+09 m^3 per month which was recorded in the period 4 of the cave propagation.

5.2.2 Cumulative Apparent Volume Rate Versus Mucking Rate

Plotting the monthly CAV rate versus monthly mucking rate from August 2006 to November 2009 shows that there is a good relation between the two rates. Each time the monthly mucking rate increases, the monthly CAV rate also increased and vice versa. This behaviour is valid for 30 of the 38 of months. This percentage was 67% during initial blasting (4 out of 6 months), 89% during cave initiation (8 out of 9 months), and 78% during cave propagation (18 out of 23 months). Thus, the lowest consistency between the monthly CAV and mucking rates happened during initial blasting (the event CAV strongly related to blasting, instead of mucking) and the highest in the cave initiation period.

During cave propagation period, in a 3 month interval, from August to November 2008, there was an inconsistent trend between the monthly CAV and mucking rates (Figure 5.4). In this period, the seismogenic zone apex passed through the M50 reef and entered the area under the M30. It seems that the monthly CAV rate was independent of the monthly mucking rate in this interval.

Likewise, a similar trend happened from February to March 2009, when the seismogenic zone's apex passed through the M30. Although the mucking rate had a decreasing trend, the CAV rate increased. These similar behaviours appear to be related to the effect of M50 and M30 (change in lithology).

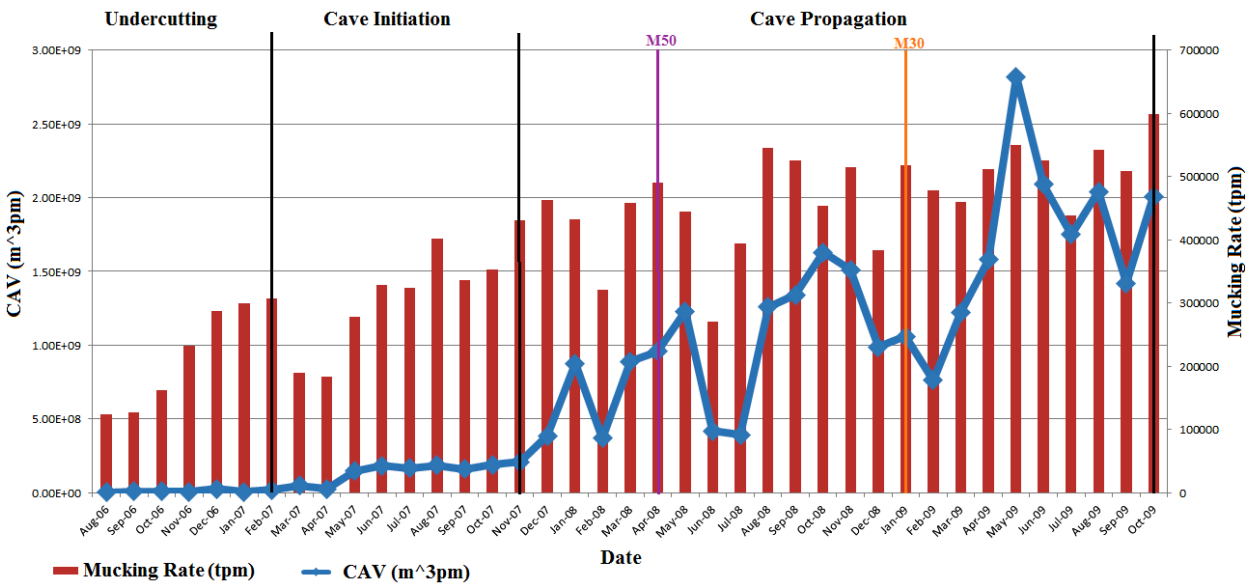

Figure 5.4 Monthly CAV rate versus monthly mucking rate.

5.2.3 Cumulative Apparent Volume Rate Versus Seismogenic Zone Movement

The monthly movement of the seismogenic zone was in good correlation with increasing and decreasing monthly rate of the CAV respectively. This correlation was visible for the 35 out of 38 of the months from August 2006 to March 2009. The first inconsistency happened during initial blasting from December 2006 to January 2007 (due to data loss). The second inconsistency happened during cave initiation in April 2007 (due to a decrease in the monthly event rate). The third inconsistency occurred during cave propagation from in February 2008 (Figure 5.5).

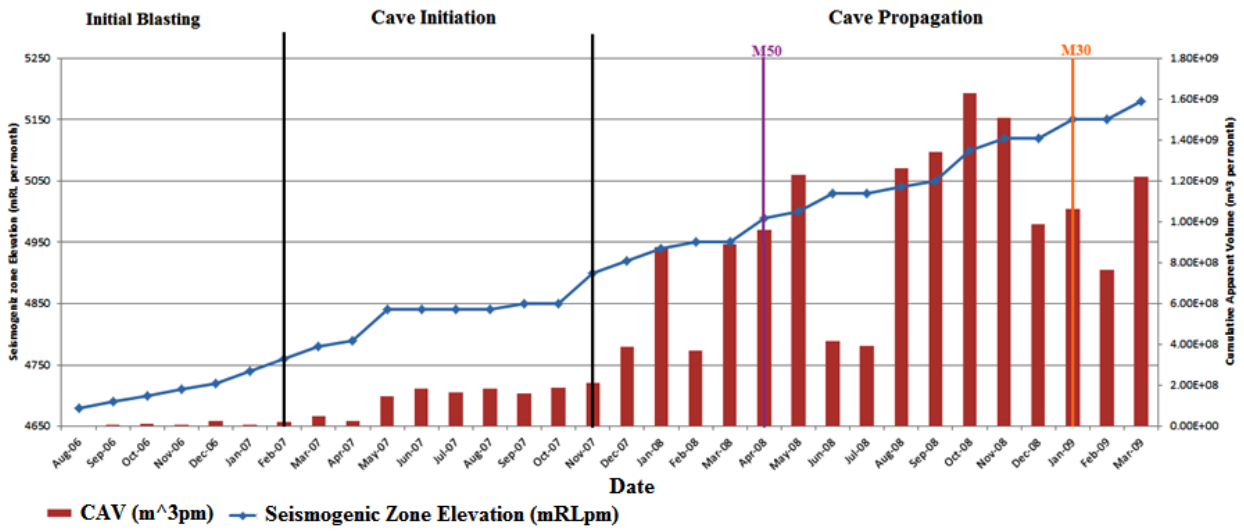

Figure 5.5 Monthly CAV rate versus monthly seismogenic zone upward movement rate.

5.3 S:P Energy Ratio of the Events

The percentage of events with S:P energy ratios greater than 10 decreased from 52% during initial blasting (shearing was the dominant source) to 15% during cave propagation.

In the breakthrough period, the percentage of the shear events increased slightly to 22%. This behaviour can be seen in the events with local magnitude less than 0 (microseismic events).

Conversely, an increasing percentage trend can be seen in the events with local magnitudes greater than 0.0 (macroseismic events). Comparing the events with S:P < 3 and S:P > 10 shows that the smaller events are more related to a shear type mechanism. As the magnitude of the events increases, the percentage of the events with S:P > 10 decreases.

After breakthrough, the larger events are more related to stress fracturing (S:P < 3).

In Period 4 of the cave propagation, the percentage of the events with S:P < 3 increased while the percentage of the events with S:P >10 was almost constant (15%) with a decreasing trend for larger events. Nevertheless, no clear trend for both events with low and high S:P energy ratio can be seen during the breakthrough.

5.4 Apparent Stress Frequency/ Seismogenic Zone Movement / Mucking Rate

The distribution of the events according to their Apparent Stress shows that between the cave initiation and the end of Period 3 of the cave propagation, almost all of the events had Apparent Stress less than 300 kPa.

The events with Apparent Stress between 100 and 300 kPa had different behaviour from initial blasting until end of the data. During initial blasting 72 events (7 events per month) were recorded, of which 93% had an S:P energy ratio greater than 10. These are high stress shearing events. From cave initiation to the end of the third period of the cave propagation, 88 events (4 events per month) were recorded. Seventy percent of these events had an S:P energy ratio greater than 10. From the third period of the cave propagation to October 2010, 991 events (48 events per month) were recorded. Similar to the initial blasting period, 93% of these events had an S:P energy ratio greater than 10. Thus, during 5 years of mining, a shear mechanism was the dominant mechanism of the events with Apparent Stress between 100 and 300 kPa.

In some periods, there was a higher frequency of occurrence of the events with Apparent Stress between 100 and 300 KPa. For instance, there was higher Apparent Stress during the initial blasting (from early August to mid-September 2006) due to progression of the seismogenic zone through the Limey unit and the I30 reef (as mentioned before, the Limey unit is the most competent rock found in the mine). During cave propagation, a second concentration of the high Apparent Stress events happened due to rapid upward movement of the seismogenic zone under M50. This phenomenon did not happen when the seismogenic zone was close to M30 (Figure 5.6).

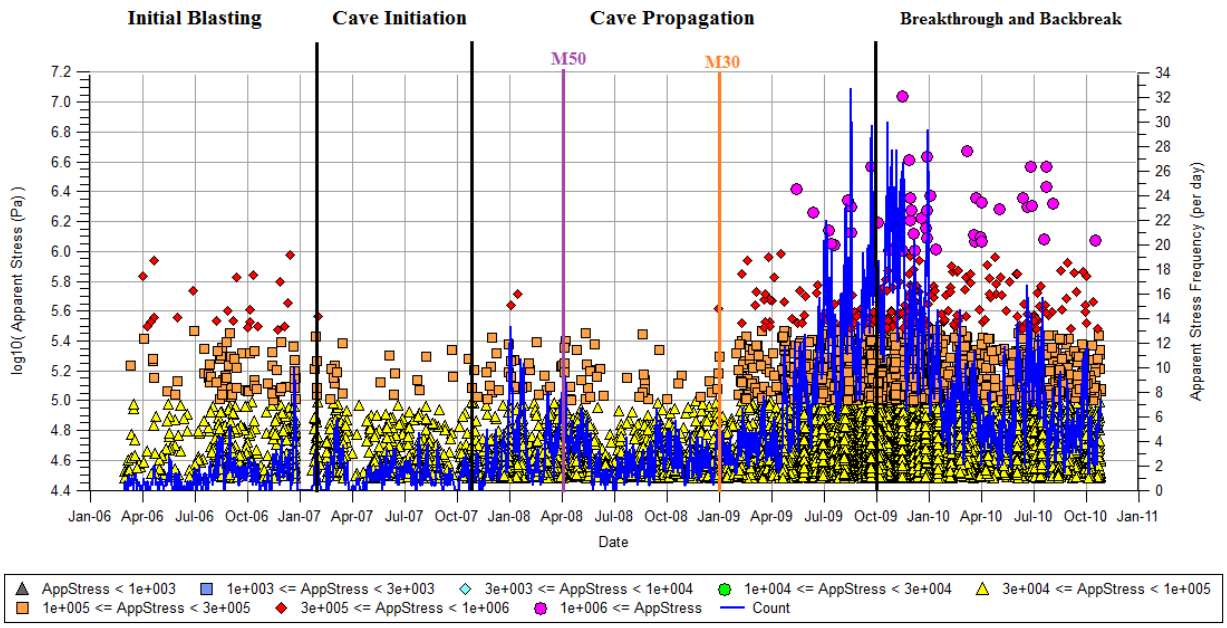

Figure 5.6 Distribution of the events according to their Apparent Stress.

There were 218 events with Apparent Stress between 300 kPa and 1 MPa, recorded from March 2006 to end of October 2010. These events were recorded primarily during two intervals, initial blasting (due to stress change from first lift opening blasts) and from December 2008 to the end October 2010 (due to high cave propagation rates).

During initial blasting, 21 events with Apparent Stress between 300 kPa and 1 MPa were recorded. All these events were less than local magnitude 0.0. Furthermore, 90% of these events had S:P energy ratios greater than 10. In other words, although blasting was the trigger for seismic events during initial blasting (stress change), the high Apparent Stress events were likely related to the sliding on the discontinuity sets.

From February 2007 to December 2008, only two events with Apparent Stress between 300 kPa and 1 MPa were recorded. These events had local magnitudes between -1.0 and 1.0 and S:P energy ratios greater than 10.

Investigation of the events with Apparent Stress between 300 kPa and 1 MPa after December 2008 shows that 194 events were recorded in this period. A plan view shows 68% of these events were recorded on the west side of the Graben fault, 4% in the Graben fault zone and 28% on the east side of the Graben fault (Figure 5.7).

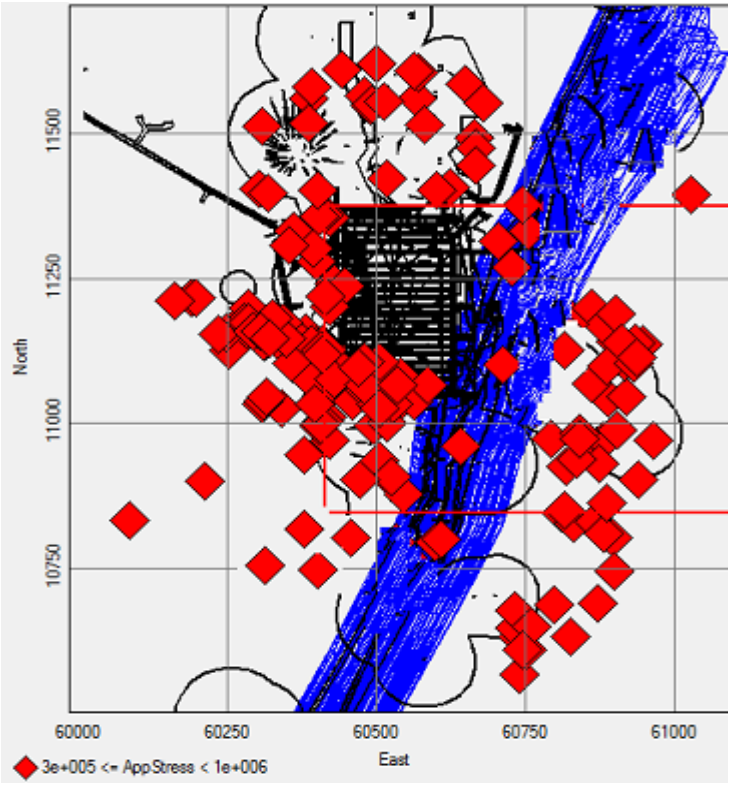

Figure 5.7 Location of the events with Apparent Stress between 300 kPa and 1 MPa in the vicinity of the Graben fault (plan view).

The events with Apparent Stress between 300 kPa and 1 MPa on the west side of the Graben fault occurred over a considerable vertical extent. This was likely due to breakback. However, the events on the east side of the Graben fault occurred in a horizontal band. These events were in the M50 reef or very close to it. It seems cave propagation caused the stress concentration around the M50 reef outside of the footprint of the cave (Figure 5.8).

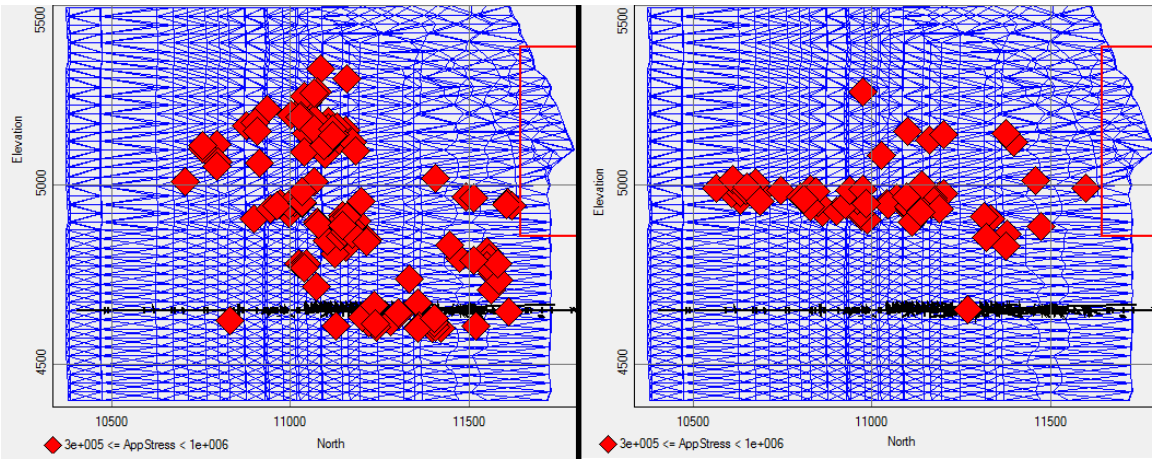

Figure 5.8 Vertical (left) and horizontal (right) location of the events with Apparent Stress between 300 kPa and 1 MPa (section).

Plotting the events on the west side of the Graben fault according to their magnitude shows that 68% of these events had local magnitude between -1.0 and 0.0 (microseismic events). Only 2% of the events had local magnitude between 0.0 and 1.0. This behaviour was different on the east side, where 65% of the events had local magnitude between 0.0 and 1.0 (macroseismic events) and 27% of the events had magnitude between -1.0 and 0.0.

Plotting events on the west side of the Graben fault according to their S:P energy ratio shows that 97% of the events have an S:P energy ratio greater than 10. This percentage for the east side events was 75%. Therefore, a shear source mechanism was the dominant failure mechanism for the events with Apparent Stress between 300 kPa and 1 MPa on both sides of the Graben fault.

Selecting a group of events starting in December 2008 and in the elevation between 4890 and 5000 mRL shows 37% of the events (300 kPa <= AppStress < 1 MPa) were recorded between these elevations. Approximately 71% of these events were recorded on the east side of the Graben fault in the vicinity of the M50 reef (stress building up around the M50 reef).

Events with the highest Apparent Stress levels (AppStress ≥ 1 MPa) were only recorded after May 2009.

A plan view of the events with Apparent Stress greater than 1000 KPa shows that 54% of these events were recorded in the east side of the Graben fault (Figure 5.9).

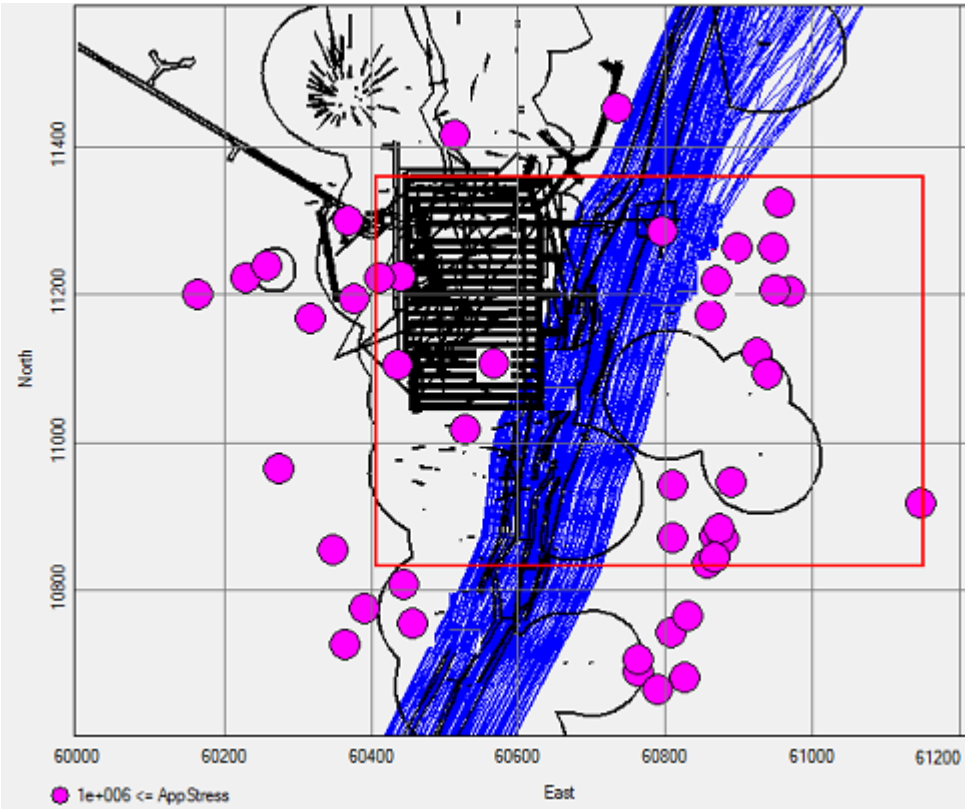

Figure 5.9 Location of the events with Apparent Stress greater than 1 MPa in the vicinity of the Graben fault (plan view).

Similar to the events with Apparent Stress between 300 kPa and 1 MPa, the events on the east side of the Graben fault occurred horizontally and in the vicinity of the M50 reef (Figure 5.10).

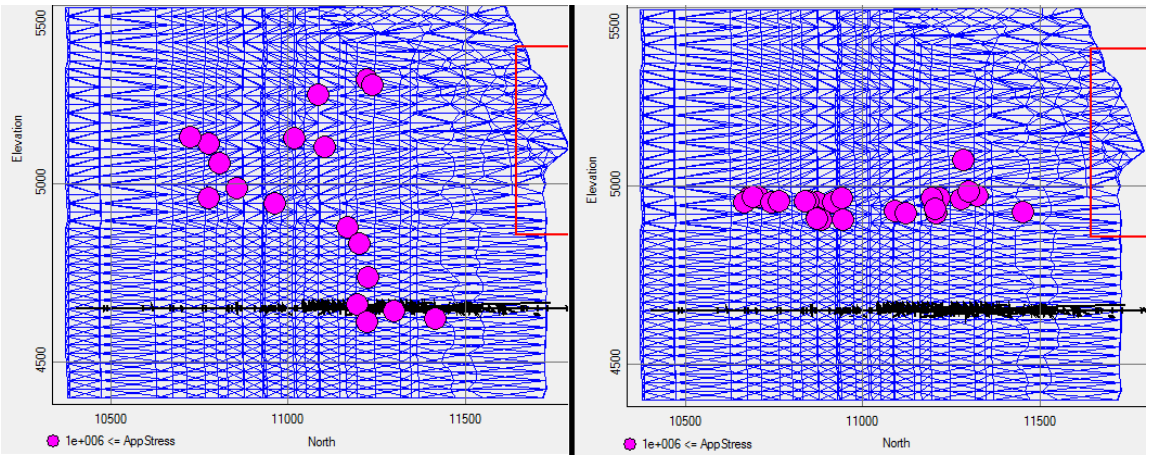

Figure 5.10 Vertical (left) and horizontal (right) location of the events with Apparent Stress greater than 1 MPa (section).

Just one event with Apparent Stress greater the 1 MPa was recorded in the Graben fault area. Presumably this lack of high Apparent Stress events was due to weak quality of the rockmass in the Graben fault zone, which was apparently not competent enough to store energy and emit events with very high Apparent Stress.

Plotting the events (AppStress $\geq$ 1 MPa) on the west side of the Graben fault according to their magnitude shows, 60% of these events had local magnitude between -1.0 and 0.0 (microseismic events). While 10% of the events had local magnitude between 0.0 and 1.0. However, 67% of the events on the east side of the Graben fault had local magnitude between 0.0 and 1.0 (macroseismic events) and 21% of the events had local magnitude between -1.0 and 0.0. Similar to the previous high Apparent Stress events, the larger events occurred on the east side of the Graben fault.

Plotting the events on the west side of the Graben fault according to their S:P energy ratio shows 95% of the events have S:P energy ratio greater than 10. This percentage for the east side events was 96%. Similarly, a shear mechanism was the dominant seismic source mechanism for the events with Apparent Stress greater than 1 MPa on both sides of the fault.

Selecting a group of events starting from December 2008 and in the elevation between 4890 and 5000 mRL, shows that 57% of the all events (AppStress $\geq$ 1 MPa) were recorded between these elevations. More than 90% of these events were recorded on the east side of the Graben fault in the vicinity of the M50 reef (stress concentration area around the M50 reef).

Plotting the monthly Apparent Stress Frequency for events with Apparent Stress greater than 300 kPa versus monthly seismogenic zone upward movement rate shows that only 53% of the selected months show a trend of increase in Apparent Stress as the seismogenic zone moves. This percentage was 50% for initial blasting, 55% for cave initiation, and 53% for cave propagation periods (Figure 5.11). There is no strong correlation between the timing of high Apparent Stress events and seismogenic zone movement.

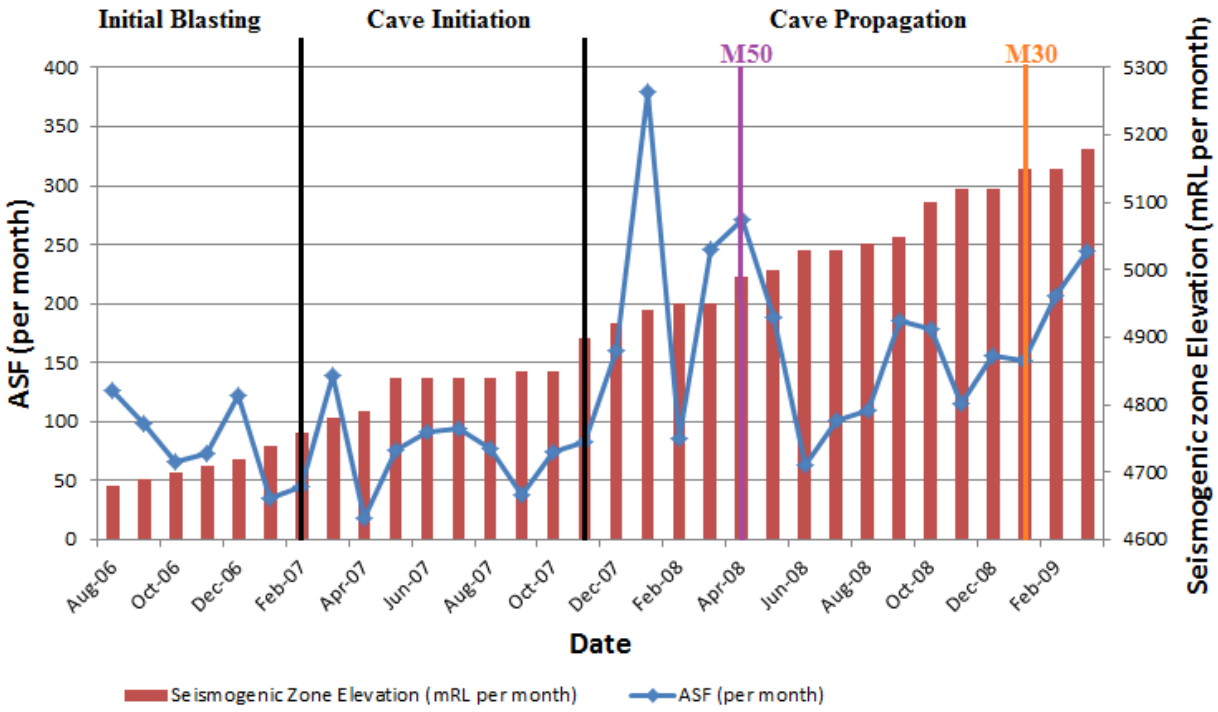

Figure 5.11 Monthly Apparent Stress Frequency rate versus monthly seismogenic zone upward movement.

Plotting the monthly Apparent Stress Frequency for events with an Apparent Stress greater than 300 kPa versus monthly mucking rate shows that 66% of the selected months have a correlation between elevated Apparent Stress and increased mucking rate. This percentage was 50% for initial blasting, 67% for cave initiation and 74% for cave propagation periods (Figure 5.12). There is a better correlation between high Apparent Stress events and the mucking rate.

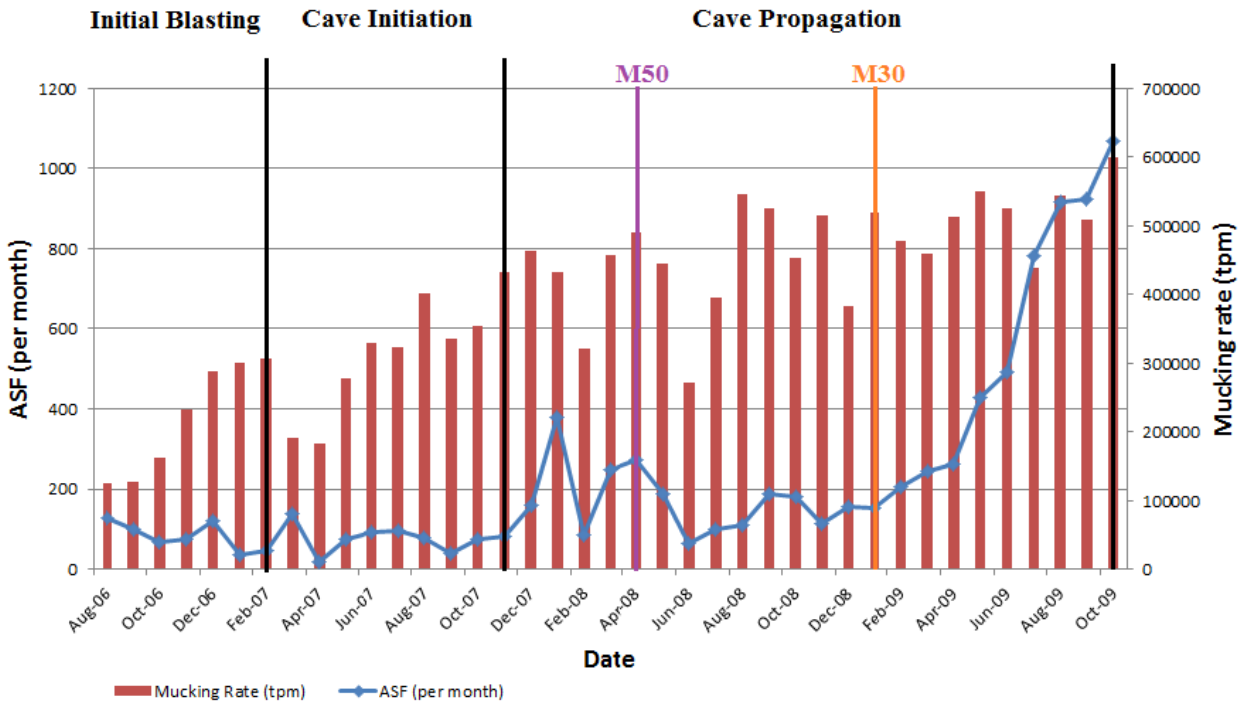

Figure 5.12 Monthly Apparent Stress frequency rate versus monthly mucking rate.

A close relation between the mucking rate and ASF is shown in Figure 5.13 during cave initiation. It can be seen that changes in the mucking rate, significantly changes the ASF trend.

S:P energy ratio of the high Apparent Stress vents with local magnitude between -1.0 and 1.0 shows that 70% of these events have S:P energy ratio greater than 10 and only 5% of these events have S:P energy ratio less than 3. Shear mechanism is the dominant source of the events with high Apparent Stress.

A different behaviour is found for events larger than magnitude 1.0. For these events, only 15% of the events have S:P energy ratio greater than 10 and 37% of these events have S:P energy ratio less than 3. The events greater than local magnitude 1.0 have a non-shearing mechanism.

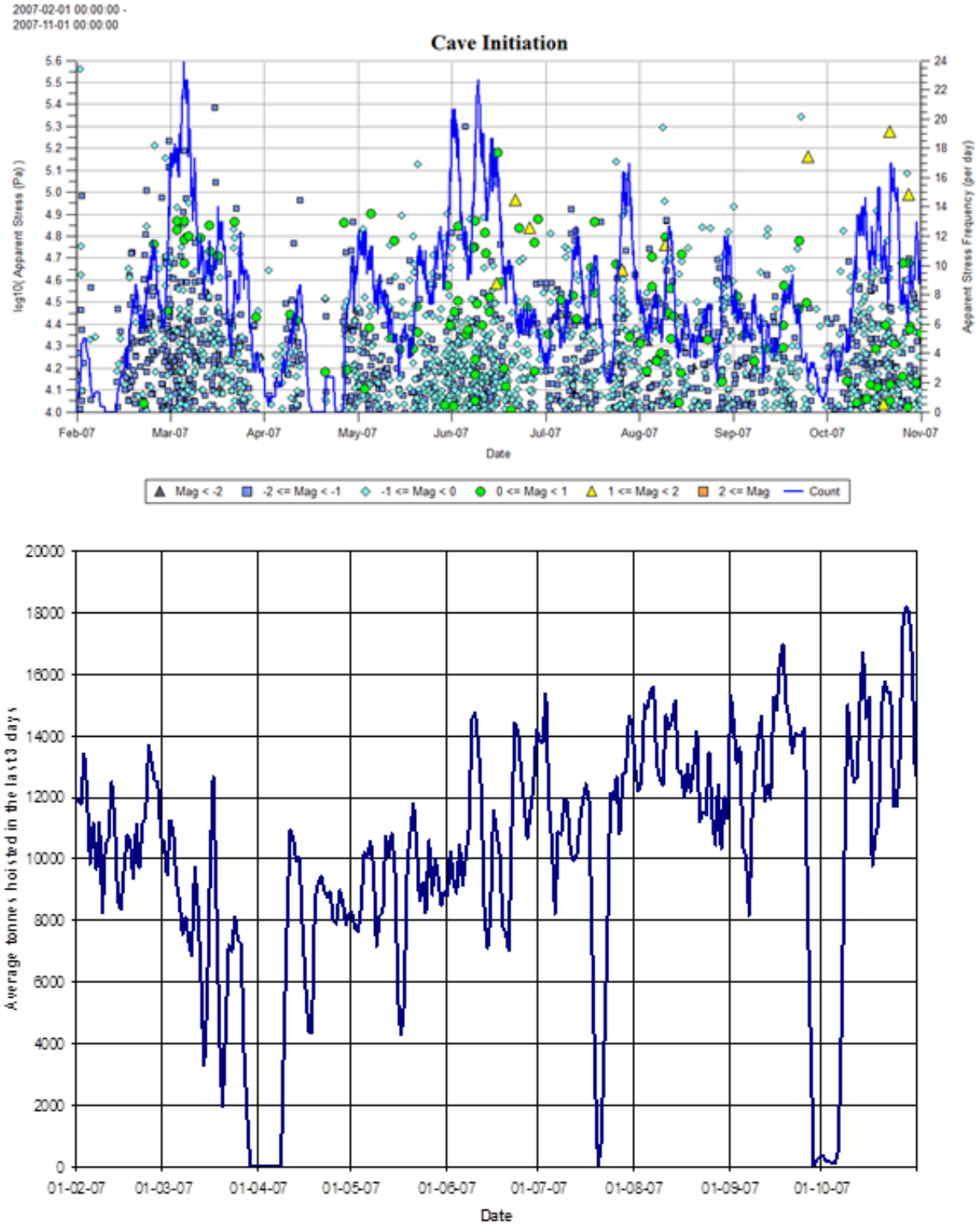

Figure 5.13 Similar relation between ASF and mucking rate during cave initiation.

6 SUMMARY AND RECOMMENDATIONS

6.1 Caving Mechanics

Numerous important observation and conclusions can be drawn about cave behaviour and cave mechanics with respect to the seismogenic zone, initial blasting, cave initiation, cave propagation and breakthrough and breakback.

6.1.1 Seismogenic Zone at Telfer

A distinct seismogenic zone was recognizable approximately 30 m above the first lift level (4650 mRL) starting in June 2006. The upward movement of the seismogenic zone had an average rate of 0.6 m per day until April 2009, when the seismogenic zone split into two separated parts.

There was a distinct apex to the cave near the centre of the cave footprint. Underneath the apex were cave “shoulders” which were always 10 to 50 m below the apex.

The thickness of the seismogenic zone changed from 10 to 120 m from June 2006 to April 2009. The lowest thickness (10 m) was recorded in late 2006 and the highest thickness (120 m) was in March 2009. The average thickness of the seismogenic zone during the initial blasting and cave initiation periods was between 20 and 40 m but it was between 50 and 100 m during cave propagation.

The thickness of the seismogenic zone under the M50 reef was approximately 100 m. Almost the same thickness was defined when the seismogenic zone was under the M30 reef. This behaviour was likely due to effect of the M50 and M30 reefs which acted like barriers and reduced the rate of upward seismogenic zone movement.

The rate of the seismogenic zone upward movement during initial blasting and the cave initiation was 0.3 and 0.5 m per day, respectively. It reached its highest rate during cave propagation with 0.7 m per day.

The rate of the seismogenic zone upward movement, when it was migrating between the M50 and M30 reefs (0.6 m per day) was approximately five times greater than the rate when it was migrating under or through the M50 and M30 reefs.

The seismogenic zone was not symmetrical during the cave evolution and it migrated from the west side of the first lift to east side, as the first lift was opened from west to east. Also, the west side of the seismogenic zone had a dip between 45º and 55º while the east side was steeper, at approximately 70º. This was largely due to the fact that the west side was controlled by shearing along the rockmass bedding.

As the cave approached breakthrough in mid-May 2009, two distinct seismogenic zones started to separate. By August 2010 the two seismogenic zones were approximately 120 m away from each other.

During the cave evolution the frequency of the macroseismic events was higher in the cave apex compared to the cave shoulders (80% of events with local magnitude greater than 2.0 were recorded in the cave apex).

6.1.2 Initial Blasting

The largest event was recorded with local magnitude 0.9. The larger events had a relatively high Apparent Stress but low S:P (less than 3). This can be related to the stress change due to first lift initial blasting.

The smaller events were predominantly shearing events, while the larger events mainly non-shearing (stress fracturing events).

Changes in the lithology affected the event rate and seismogenic zone upward movement (I30 reef).

Using Cook's (1976) diurnal analysis for events recorded during the initial blasting period at Telfer mine showed that most of the seismic events occurred directly following blast time (seismicity associated with stress change due to mine blasting).

Proportionally, the Apparent Stress of the initial blasting events was very high compared to other caving periods. The Apparent Stress of some events reached 300 kPa. These events were likely due to stress change from initial blasting.

In this period, the rate of the CAV was strongly related to blasting.

6.1.3 Cave Initiation

Cave initiation began in February 2007. The largest event was recorded with local magnitude 1.8. The seismic event rate was greater than event rate during initial blasting.

During cave initiation, the frequency of the events with S:P energy ratios greater than 10 was higher on the west side of the first lift because the west side of the cave was controlled by failure along the bedding planes (shear failure). On the east side, the frequency of the events with S:P energy ratio less than 3 was high (possibly due to the effect of the Graben fault in reducing the rockmass quality).

Similar to the initial blasting period, during cave initiation most of the seismic events occurred during blast time. But this time, the frequency of the events between the blasting times (from 04:00 am to 02:00 pm and 4:00 pm to 02:00 am) increased. This is likely related to a larger proportion of the events associated with a stress fracturing seismic source mechanism.

In contrast with the initial blasting period, all the recorded events during cave initiation had a comparatively low Apparent Stress. This behaviour can be related to the much weaker influence of the blasting on the occurrence of the recorded seismic events.

The Cumulative Apparent Volume during cave initiation was larger than that recorded in the initial blasting period. This increase in deformation rate is associated with fracturing and deformation of the rockmass during cave initiation and the increase in movement of the seismogenic zone.

6.1.4 Cave Propagation

Cave propagation is more related to mucking rate than blasting. The five largest events ($+2 < M_L < +3$) were recorded during cave propagation. The event rate was approximately 30 times greater than event rate during cave initiation.

Generally, the events with high S:P energy ratios included both the small and large events, while events with low S:P ratios were more related to the larger events, i.e. larger events were more non-shearing seismic source mechanisms.

The M50 and M30 reefs had a very similar effect as the I30 reef when the seismogenic zone was moving upward (i.e. a reduction in the event rate and the rate of the seismogenic movement).

Propagation of the cave caused the concentration of some events with very high Apparent Stress on the east side of the Graben fault, around the M50 reef, approximately 250 m above the first lift. It identified the M50 reef as a significant stress raising feature.

In contrast to the initial blasting and cave initiation periods, most of the seismic events occurred during the day with no specific time of occurrence during cave propagation. This trend can be related to the events associated with the mucking rate (rather than blasting).

For the first time, the events with Apparent Stress greater than 1.0 MPa were recorded in May 2009. This behaviour is likely related to subsidence caving.

The Cumulative Apparent Volume during cave propagation was greater than that in the cave initiation period. The rate of the CAV was strongly related to mucking rate.

6.1.5 Breakthrough and Breakback

Cave breakthrough can be defined as major subsidence in the open pit bottom. The recorded events had local magnitudes less than 2.0 during breakthrough and breakback. The event rate in this period was lower than the event rate during cave propagation.

The seismogenic zone split into two distinct zones as it approached breakthrough into the pit.

The frequency of the events with low S:P energy ratio was higher on the north side of the breakthrough (effect of the Graben fault). The frequency of the events with high S:P energy ratio was higher on the south-west side. This behaviour might be related to the shearing of the bedding planes in south-west area of the cave.

Most of the events with very high Apparent Stress (> 1.0 MPa) were recorded in this period. These events had different source of mechanism on the east side (shear) and west side of the Graben fault (non-shear).

During breakthrough period, the seismic events occurred during the day with no specific time of occurrence.

The events with the highest Apparent Stress (> 1.0 MPa) were recorded in this period. This suggests a higher level of induced stress associated with the breakthrough period.

The Cumulative Apparent Volume rate during breakthrough was lower than the CAV rate during cave propagation, but greater than CAV rate during cave initiation.

6.1.6 General Caving Mechanics

The rate of upward movement of the seismogenic zone changed from 2 to 3 m per month from initial blasting to 4 m per month during cave initiation and reached to its highest rate during cave propagation with 12 m per month.

The percentage of the events with S:P > 10 decreased from 52% during initial blasting to 15% during cave propagation. During the breakthrough period, the percentage of the shear events increased and reached to 22%. However, the percentage of the all events with S:P <3 increased from 9% during initial blasting to 22% during cave initiation, 23% during cave propagation and reached to its highest ratio with 27% during the breakthrough period.

Comparing the events with S:P <3 and S:P >10 shows that the microseismic events are more related to a shear type mechanism. While the macroseismic events are non-shear mechanism.

The highest proportion of events with Apparent Stress greater than 30 kPa was recorded during the initial blasting period. This ratio was 22% during the initial blasting, 0.7% in cave initiation, 2.4% in cave propagation and 5.9% in the breakthrough period.

During the cave initiation and most of the cave propagation, the recorded events had an Apparent Stress less than 300 kPa. The events with Apparent Stress between 300 KPa and 1 MPa were recorded during initial blasting, late cave propagation and breakthrough. The events with Apparent Stress greater than 1 MPa were recorded during late cave propagation and breakthrough. In other words, the Apparent Stress was low from initial blasting to Period 4 of the cave propagation.

The highest Cumulative Apparent Volume monthly rate was recorded during cave propagation. The CAV monthly rate during cave propagation (1.3e+09 m^3per month) was 210 times greater than that in the initial blasting (6.2e+06 m^3 per month), 11 times greater than cave initiation

period (1.2e+08 m^3per month) and almost 1.2 times greater than breakthrough (1.1e+09 m^3per month).

There was good correlation between the mucking rate and the monthly CAV rate from the initial blasting to the breakthrough periods. However, the correlation was weak when the seismogenic zone was passing through the M50 and M30 reefs.

Weak, moderate and strong correlations of the event/mucking/ seismogenic upward movement/ CAV and ASH rates in different periods of the cave evolution (from initial blasting to breakthrough) are shown in Table 6.1

Table 6.1 Correlations of the event/mucking/ seismogenic upward movement/ CAV and ASH rates in different periods of the cave evolution.

Monthly rate	**Initial Blasting**	**Cave Initiation**	**Cave Propagation**
Event rate vs. **Mucking rate**	weak	weak	strong
Event rate vs. **Seismogenic zone upward movement rate**	weak	strong	strong
CAV rate vs. **Mucking rate**	moderate	strong	strong
CAV rate vs. **Seismogenic zone upward movement rate**	strong	strong	strong
AS rate vs. **Mucking rate**	moderate	strong	strong
AS rate vs. **Seismogenic zone upward movement rate**	moderate	moderate	moderate

6.2 Application of Seismic Monitoring in Caving Mine

This thesis is a detailed investigation and application of seismic monitoring data and seismic source parameter data to understand the rockmass response in sublevel cave mining. Numerous

comments and conclusions about the seismic monitoring can be made from the work in this project.

Seismic Event Rate:

- Early in the caving, the event rate was almost completely related to sublevel cave production blasting. As cave initiation and cave propagation progressed, there was no longer a correlation between event rate and the rate of production blasting.
- The seismic event rate was useful to identify periods in which the cave slowed down, particularly associated with the M50 and M30 reefs.
- The Telfer seismic monitoring system had a sensitivity of about magnitude -1.4. This was arguably a bit too high for the first few months of the initial production blasting period, in which there was a lack of events recorded. The recorded seismic event rate can be increased by simply increasing the number of sensors monitoring the cave.
- Several weeks of data loss occurred over the four years of seismic data investigated in this project. The data loss occurred over a number of short time periods. It is believed that the data loss had a minimal effect on seismic data interpretation.
- The seismic system sensitivity decreased later in the data set, particularly as the north side of the cave approached breakthrough into the pit. This is an expected result as sensors became “blinded” by the growth of the cave zone.

Seismic Event Size:

- Event sizes were small during the initial blasting and early in cave initiation.
- During cave propagation, events with magnitude greater than 2 were recorded, similar to what was found at Palabora (Glazer and Hepworth, 2004) and North Parkes (Hudyma et al., 2007b) mines.
- The time period over which the magnitude greater than 2 events were recorded was a few months, again similar to Palabora (Glazer and Hepworth, 2004) and North Parkes (Hudyma et al., 2007b). It would appear that there is a brief period during cave propagation in which the potential for very large seismic events is elevated.
- Event sizes decreased near breakthrough and during breakback.

- The Gutenberg-Richter frequency-magnitude relation is well-behaved for all cave periods, although the b-values of 1.4 and 1.5 (during initial blasting, and early cave initiation) are higher than reported for other seismic source mechanisms.
- The largest event in any substantial population of events was well correlated with a/b from the Gutenberg-Richter frequency-magnitude relation.
- Many of the largest events recorded were spatially correlated with the leading edge of the seismogenic zone and the stiff reefs at Telfer mine.

Seismic Event Location:

- The location accuracy at Telfer was adequate to clearly identify a three-dimensional seismogenic zone of events.
- Stress raising features (M50 and M30 reefs) became active long before the seismogenic zone approached them. Essentially, stress raising stiff geological features could be proactively identified.
- Seismicity in the bottom of the pit started to react to the sublevel cave long before the seismogenic zone approached the pit bottom.
- There was a lack of seismicity in the crown pillar between the pit bottom and the cave. It is suggested that mining of the pit preconditioned the ground below the pit, preventing stress buildup and massive crown failure. This was also reported in the crown pillar below the pit at Palabora (Glazer and Hepworth, 2004) and the crown pillar between the two block caves at North Parkes (Hudyma et al., 2007b).

S:P Energy Ratio:

- It is an implicit assumption in this thesis that the S:P energy ratio of a seismic event is strongly related to seismic source mechanism. This assumption is based on past publications as outlined in Chapter 2 (Literature Review).

- There were distinct variations in S:P energy ratio in time and space recorded in the Telfer seismic data.
- There were distinct spatial variations in S:P energy ratio in the seismogenic zone, with high S:P energy ratio (shearing) events at the leading edge of the seismogenic zone. Events in the bottom half of the seismogenic zone had a much lower S:P energy ratio, suggesting that these events had a stress-fracturing seismic source mechanism.
- High S:P energy ratio events were predominant during the initial production blasting period, suggesting primarily a rockmass shearing mechanism early in the cave mining.
- S:P energy ratio was less conclusive to identify seismic source mechanism than at other caving mines. For North Parkes Lift 2 (Hudyma et al., 2007) the vast majority of events had an S:P energy ratio greater than 10. For the Telfer data, most data populations had similar proportions of shearing (S:P > 10) and non-shearing (S:P < 3) events.
- Scale dependence of S:P energy ratio was prevalent in almost all of the seismic data at Telfer. Larger events (M_L >0) typically had a low S:P energy ratio (non-shearing), while smaller events had a range of seismic source mechanisms. This highlights the need to undertake scale dependence studies for any population of seismic events.
- S:P energy ratio was a better spatial tool than temporal tool for investigating seismic source mechanism variations during the cave mining. Temporal variations were complex, making it difficult to draw conclusions.

Energy Index:

- Ideally Energy Index can be used to identify temporal and spatial variations in higher energy and lower energy events. In practice, it was hard to identify reliable trends in Energy Index within the Telfer seismic data.

Cumulative Apparent Volume:

- Previous studies (Mendecki, 1993; Mendecki, 1997) identified Apparent Volume as a measure of rockmass deformation.

- For Telfer, Cumulative Apparent Volume (CAV) within a population of events was a useful gauge of relative coseismic deformation in all the different caving periods.
- CAV was well correlated with the mucking rate of the sublevel cave.
- Changes in the CAV rate were well correlated with the rate of movement of the seismogenic zone.

Apparent Stress:

- Past research (Mendecki and van Aswegen, 2001, Simser et al., 2003) suggests that Apparent Stress is a parameter that can be used to investigate temporal and spatial changes in stress in the seismogenic zone and rockmass surrounding the cave.
- Higher than normal Apparent Stress events occur on the leading edge of the seismogenic zone, suggesting a higher level of induced stress in this area.
- Temporal variations in Apparent Stress were strongly correlated to changes in cave mucking rate. An increase in mucking rate resulted in a higher number of high Apparent Stress events. A decrease in mucking rate resulted in a lower number of high Apparent Stress events. These Apparent Stress variations could be identified very quickly, which is interesting as the events were often occurring hundreds of metres above the mucking elevation. This suggests that change in the cave draw rate has an almost immediate effect on the cave back rockmass behaviour.
- High Apparent Stress events spatially correlated with stress raising geological features (in particular, the M50 reef).
- The rate of occurrence of high Apparent Stress events was not strongly correlated with changes in the rate of movement of the seismogenic zone.
- High levels of Apparent Stress could be used to identify areas of highest induced stress, particularly in the apex of the cave at the top of the seismogenic zone.

Energy Moment Relation:

- The energy-moment relation was well-behaved for seismic events for the various caving periods.

- The largest events are clearly identifiable as having low S:P energy ratio, non-shear seismic source mechanisms.
- Higher Apparent Stress events are clearly identifiable as higher S:P energy ratio, shearing seismic source mechanisms.
- Lower Apparent Stress events are clearly identifiable as lower S:P energy, non-shearing events.

6.3 Contributions of this Work

Due to the massive rockmass deformations that occur, it is difficult to observe and monitor the failure processes in a sublevel caving mine. There are very few published accounts of the rockmass response to caving. This thesis investigates, in considerable deal, the occurrence of more than 400,000 seismic events recorded over a period of five years, as the Telfer sublevel cave propagates more than 600 m before breaking into an open pit. The author is not aware of a published example in which such an exhaustive investigation has been conducted for a caving mine.

Cave zones (zone of loosening and seismogenic zone) proposed by Duplancic (2001) for block caving can be clearly identified and monitored in the Telfer sublevel caving mine.

A methodology to identify and track the three-dimensional movement and thickness of the seismogenic zone has been proposed and used for the Telfer dataset. The methodology is based on calculating the median event elevation for space and time filtered populations of events. The mechanics of rockmass failure within the seismogenic zone at Telfer have been identified and monitored closely for variations over the course of the cave.

Four key cave periods have been identified: initial blasting, cave initiation, cave propagation, and cave breakthrough and breakback. These periods have distinct rockmass failure mechanisms, failure rates, and seismic source parameter characteristics, which have been identified and discussed in significant detail.

Variations in stress (through Apparent Stress) and deformation (through Cumulative Apparent Volume) on a local scale and on a minewide scale have been monitored in the Telfer seismic database. A number of seismological tools have been shown to be useful to understand the

rockmass response to sublevel caving. The tools inlucde: seismic event rate, seismic event size, seismic event location, seismic event timing, S:P energy ratio, Cumulative Apparent Volume, and Apparent Stress.

These seismological tools have also been used to monitor complex interactions between the cave and geological features at Telfer, such as stiff reefs and the weak Graben fault.

6.4 Recommendations for future work

Deformation is one of the criteria through which rockmass behaviour can be described in caving mines. Both seismic data and extensometer data can be used to determine the deformation of the rockmass. A brief analysis using extensometer data and seismic data was undertaken with an attempt to get better understanding of fracture behaviour and cave back location. More accurate data collection and more detailed comparison between extensometer data and seismic data is recommended to come to a more precise conclusion on estimated deformation and accuracy of methods, respectively.

Seismic source parameters were used to identify the seismic source mechanisms. Numerical modeling is another approach to reach this goal. It is recommended to compare failure criteria and stress direction, as two criteria to describe the rockmass response to caving. Consistent results from a numerical modeling analysis would help to corroborate the seismic analyses.

The formation of a fracture can be described by a seismic event source mechanism which can be determined by some methods such as first motion and moment tensor analysis. As a suggestion, the other techniques, i.e. first motion and moment tensor analysis, can be applied to Telfer data to investigate and validate seismic source mechanisms.

It is recommended to compare Telfer seismic outcomes to other caving mines to assess the employed techniques. Ideally similar results would verify the accuracy and validity of the results.

7 REFERENCES

Australian Centre for Geomechanics. (2005) MS-RAP Version 3.1 User Documentation. 237 pages.

Andrieux, P.P., Hudyma, M.R., O'Connor, C.P., Li, H., Cotesta, L. and Brummer, R.K. (2008) Calibration of large- scale three dimensional non-linear numerical models of underground mines using microseismic data. Proceedings 1st International FLAC/DEM Symposium – Minneapolis.

Boatwright, J. and Fletcher, J.B. (1984) The partition of radiated energy between P and S waves. *Bulletin of the Seismological Society of America*, Vol. 74, pp. 361-376.

Blake, W. (1987) Microseismic instrumentation. Proc. Fred Leighton Memorial Workshop on Mining Induced Seismicity, Montreal, Quebec, Canada, pp. 3-4.

Brady, B.H.G. and Brown, E.T. (1993) Rock mechanics for underground mining. 2nd edn, Chapman &Hall, Melbourne.

Brown, E.T. (2003) Block caving geomechanics. Julius Kruttschnitt Mineral Research Centre, Brisbane, pp.12-16.

Bull, G. (2002) Geotechnical feasibility-Telfer deeps document. Newcrest Mining Limited.

Burgio, N. and Diering, T. (2008) Simulating irregular cave propagation using PCBC. Proceedings 5th International Conference and Exhibition on Mass Mining, (Editors: H Schunnesson & E Nordlund), Luleå University of Technology, Luleå, pp. 1032-1042.

Butt, S.D., Calder, P.N. and Apel, D.B. (2000) The use of high frequency and minewide microseismic systems to monitor the movement of blasting induced stresses. CIM Bulletin, Volume 93, No. 1040, pp. 90-95.

Cook, N.G.W. (1976) Seismicity associated with mining. *Engineering Geology*, Vol. 10, pp. 99-122.

Dixon, R.A., Singh U. and McArthur, C. (2010) Interaction between a propagating cave and an active pit at Telfer Mine – Part II: Monitoring interaction. Proceedings 2nd International Symposium on Block and Sublevel Caving (Caving 2010), Y. Potvin (ed), 20-22 April, Perth, Australia, Australian Centre for Geomechnics, Perth, pp. 321-331.

Domanski, B. and Gibowicz, S.J. (2008) Comparison of source parameters estimated in the frequency and time domains for seismic events at the Rudna copper mine, Poland. *Acta Geophysica*, Vol. 56, No. 2, pp. 324-343.

Dowding, C.H., Su, M.B. and O'Connor, K. (1988) Principles of time domain reflectometry applied to measurement of rockmass deformation. *Int J Rock Mech Min Sci & Geomech Abstr*, Vol. 25, No. 5, pp. 287-297.

de Nicola, R. and Fishwick, M. (2000) An underground air blast – Codelco Chile – Division Salvador. Proceedings MassMin 2000, Brisbane, (Editor: G Chitomo). Australian Institute of Mining and Metallurgy: Melbourne, pp. 279-288.

Duffield, S. (2000) Design of the block cave at Northparkes E26 mine. Proceedings of MassMin 2000, (Editor: G. Chitmbo), Australian Institute of Mining and Metallurgey: Melborne, pp. 334-346.

Dunlop, R. and Gaete, S. (1995) Seismicity at El Teniente Mine. Proceedings 4th International Symposium on Mine Planning and Equipment Selection. Calgary, Canada. Balkema: Rotterdam, pp. 865-869.

Dunlop, R. and Gaete, S. (1997) Controlling induced seismicity at El Teniente Mine: the Sub6 case history. Proceedings 4th International Symposium on Rockburst and Seismicity in Mines, (Editors: S J Gibowicz and S Lasoki), Krakow, Poland. Balkema: Rotterdam, pp. 233-236.

Dunlop, R., Parraquez, R. and Zepeda, R. (2010) Using the apparent volume parameter to estimate rockmass damage. Proceeding Second International Symposium on Block and Sublevel Caving. Perth, Australia.

Duplancic, P. and Brady, B. H. (1999) Characterization of caving mechanisms by analysis of seismicity and rock stress. Proceedings 9th International Congress on Rock Mechanics, Paris, (Editors: G Vouille and P Berest). Balkema: Rotterdam, pp. 1049-1053.

Duplancic, P. (2001) Characterization of caving mechanisms through analysis of stress and seismicity. PhD thesis, University of Western Australia, Perth, Australia, 227 pages.

Franklin, J. (1990) Mine Monitoring Manual. The Canadian Institute of Mining and Metallurgy, Special Vol. 42, pp. 85-86.

Gaete, S., Dunlop, R., Parraquez, R., Parra, J.C. and Rodriguez, F. (2007) Estimation of caving back using gravity measurements at the EI Teniente mine. Proceeding First International Symposium on Block Caving and Sub-Level Caving, Cape Town, South Africa, pp. 389-396.

Gibowicz, S.J. and Kijko, A. (1994) An introduction to mining seismology. San Diego: Academic Press, 1st edition.

Gibowicz, S. J. and Lasocki, S. (2001) Seismicity induced by mining: Ten years later. *Adv. Geophys*., Vol. 44, pp. 39-181.

Giovinazzo, M. D. and Singh, D. (2010) Instrumentation and monitoring of cave initiation at Telfer Mine. Newcrest Mining Limited. Proceedings of Caving 2010, Australia.

Glazer, S. N. and Hepworth, N. (2004) Seismic monitoring of block cave crown pillar –Palabora Mining Company, RSA. Proceedings of MassMin 2004, (Editors: Karzulowicz K. and Alfaro M., A.), Minera Chilena, Santiago, Chile, pp 565-569.

Glazer, S. N. and Hepworth, N. (2007) Seismic monitoring of block cave crown pillar –Palabora Mining Company, RSA. The Southern African Institute of Mining and Mettalurgy, Symposium series S49. Chapter 15-02.

Glazer, S.N. and Townsend, P.A. (2010) Relationship between production rates, caving processes and seismicity rates at Palabora Mining Company. Proceedings of Deep Mining 2010, Australian Center for Geomechanics, Perth.

Gutenberg, B. and Richter, C.F. (1944) Frequency of earthquakes in California. *Bulletin of the Seismological Society of America*, Vol. 34, pp. 185-188.

Hartman, H.L. (1992) SME mining engineering handbook. Society for Mining, Metallurgy, and Exploration, Inc. Littleton, Colorado.

Hanks, T.C. and Kanamori, H. (1979) A moment magnitude scale. *Journal of Geophysical Research,* Vol. 84, pp. 2348-2350.

Hedley, D.G.F. (1992) Rockburst handbook for Ontario mines. CANMET SP92-1E, 305 Pages.

Hudyma, M.R. (2008) Analysis and interpretation of clusters of seismic events in mines. PhD thesis, University of Western Australia, Perth, Australia.

Hudyma, M.R. (2010) Applied mine seismology concepts and techniques. Technical notes, Laurentian University, Sudbury, Ontario, Canada.

Hudyma, M.R. and Beneteau, D.L. (2010) The Sudbury Regional Seismic Network. CIM Maintenance Engineering and Mine Operations Conference, Sudbury, Ontario.

Hudyma, M. R., Heal, D. and Mikula, P. (2003) Seismic monitoring in mines — old technology — new applications. Proceedings of the First Australasian Ground Control in Mining Conference. UNSW school of Mining Engineering, Sydney, pp. 201-218.

Hudyma, M, Potvin, Y and Allison, D. (2007a) Seismic monitoring of the Northparkes Lift 2 block cave - Part 1 Undercutting. Proceedings 1st International Symposium on Block and Sub-Level Caving, The Southern African Institute of Mining and Metallurgy, Cape Town, pp. 303-333.

Hudyma, M, Potvin, Y and Allison, D. (2007b) Seismic monitoring of the Northparkes Lift 2 block cave - Part 2 Production Caving. Proceedings 1st International Symposium on Block and Sub-Level Caving, The Southern African Institute of Mining and Metallurgy, Cape Town, pp. 335-354.

Kendricks, R. (1970) Induction Caving of the Urad Mine, *Min Congr J*, **56**(10), pp. 39-44.

Laubscher, DH. (1994) Cave Mining State of the Art. *Journal of The South African Institute of Mining and Metallurgy*, Johannesburg, pp. 279-293.

Lee, M. F., Pascoe, M. J. and Mikula, P. A. (2001) Virgin rock stresses versus rockmass strength in Western Australia's Yilgarn greenstones. Proceedings Ground Control in Mines Workshop. Chamber of Minerals and Energy: Perth.

Legge, N.B. and Spottiswoode S.M. (1987) Fracturing and microseismicity ahead of a deep gold mine stope in the pre-remnant stages of mining. Proceedings of the 6th Int. Congress on Rock Mech., Montreal, pp. 1071-1078.

Mawdesley, C. (2002) Predicting rockmass cavability in block caving mines, PhD Thesis, University of Queensland.

Maxlow, J. (2007) Newcrest Mining Limited, Telfer Geology, Reference Manual. TS-REP-DEV-0060, Internal unpublished document.

Mendecki, A.J. (1993) Real time quantitative seismology in mines. Proceedings of Rockburst and Seismicity in Mines, Kingston, August 1993, (Editor: R.P. Young). Rotterdam, A.A. Balkema, pp. 287-295.

Mendecki, A.J. (1997) Quantitative seismology and rockmass stability. Seismic Monitoring in Mines. (Editor: A.J Mendecki). Chapman & Hall, London, pp.178-219.

Mendecki, A.J., van Aswegen, G. and Mountfort, P. (1999) A guide to routine seismic monitoring in mines. A Handbook on Rock Engineering Practices for Tabular Hard Rock Mines, (Editors: A.J. Jager and J.A. Ryder). Creda Communications, Cape Town.

Mendecki, A.J. and van Aswegen, G. (2001) Seismic monitoring in mines: selected terms and definitions. Proceedings of Rockburst and Seismicity in Mines – RaSiM 5, Johannesburg, September 2001, (Editors: G. vanAswegen, R.J. Durrheim and W.D.Ortlepp). South African Institute of Mining and Metallurgy, Johannesburg, pp. 563-570.

Mikula, P.A. (1998) The Australian perspective: seismic risk management at Mt. Charlotte gold mine. Australian Centre for Geomechanics Workshop Notes Section 2, Perth, Australia.

Mikula, P.A. and Poplawski, F.P. (1995) The Australian perspective: Seismic risk management at Mt. Charlotte gold mine. Proceedings 6th Underground Operators Conference. Australian Institute of Mining and Metallurgy, Kalgoorlie, WA, pp. 79-86.

Nuttli, O.W. (1973) Seismi wave attenuation and magnitude relations for Easter North America. *J. Geophys. Res*., vol. 78, pp. 876-885.

Obert, L. (1977) The Microseismic method–discovery and early history. Proceedings. First Conference on Acoustic Emission/Microseismic Activity in Geologic Structures and Materials, Trans Tech Publications, Clausthal, Germany, pp. 11-12.

Pierce, M., Mas Ivars, D., and Sainsbury, B. (2009) Use of synthetic rockmasses (SRM) to investigate jointed rockmass strength and deformation behaviour. Proceedings of the International Conference on Rock Joints and Jointed Rockmasses, Tucson, Paper 1091.

Potvin, Y., Hudyma, M.R. and Jewell, R.J. (2000) Rockburst and seismic activity in underground Australian mines – An Introduction to a new research project. Proceedings of GeoENG 2000. Australian Institute of Mining and Metallurgy, Melbourne, Australia, UW0388.

Rauert, N.S. and Tully, K.P. (1998) Integration of a Microseismic Monitoring System in Mining the Pasminco Broken Hill Southern Cross Area. Seventh AusIMM Underground Operators' Conference,Townsville, Queensland, pp. 115-120.

Reyes-Montes, J.M., Pettitt, W.S. and Young, R.P. (2007) Validation of a synthetic rockmass model using excavation induced microseismicity. Proceedings of the 1st Canada-US Rock Mechanics Symposium: Meeting Society's Challenges and Demands, Vancouver, Canada. (Editors: E. Eberhardt, D. Stead and T. Morrison). Rotterdam, A.A. Balkema, pp. 365-369.

Richter, C.F. (1935) An instrumental earthquake magnitude scale. Bulletin of the Seismological Society of America, Vol. 25, pp. 1-32.

Rojas, E., Cavierse, P., Dunlop, R. and Gaete, S. (2000) Control of induced seismicity at EI Teniente mine, Codelco-Chile. Proceedings MassMin 2000, Brisbane, (Editors: G Chitomo). Australian Institute of Mining and Metallurgy: Melbourne, pp.775-782.

Sainsbury, B.L. (2010) Sensitivities in the numerical assessment of cave propagation. Proceedings 2nd International Symposium on Block and Sub-level Cave Mining, Australian Centre for Geomechanics, Perth, pp. 523-535.

Simser, B.P., Falmagne, V., Gaudreau, D. and MacDonald, T. (2003) Seismic response to mining at the Brunswick mine. Canadian Institute of Mining and Metallurgy Annual General Meeting, Montreal, 12 p.

SRK Consulting (2002) Report for Newcrest Mining Limited, Geotechnical Feasibility- Telfer Deeps. SRK project code NN202, Telfer Document No. TP-REP-20-GO-0094, Internal unpublished document, pp. 8-49.

Thibodeau, D. (2009) Fault slip event issue. CEMI Fault Slip Workshop, 14-15 May 2009, Toronto, Ontario.

Trenning, W. (2002) Geotechnical feasibility-Telfer Deeps. SRK project code NN202, Newcrest Mining Limited, Perth, Australia.

Trifu, C.I., Shumila, V. and Burgio, N. (2002) Characterization of caving front at Ridgeway Mine, New South Wales, based on geotechnical data and detailed microseismic analysis. Proceedings International Seminar on Deep and High Stress Mining, Perth, Section 41. Australian Centre for Geomechanics: Perth.

Turner, M H. and Beck, D A. (2002) Monitoring the onset of seismicity. Proceedings of ACG International Seminar on Deep and High Stress Mining. Australian Centre for Geomechanics, Perth.

Turner, M. and Player, J. (2000) Seismicity at Big Bell mine. Proceedings of MassMin 2000, Brisbane, (Editors: G Chitomo). Australian Institute of Mining and Metallurgy: Melbourne, pp. 791-798.

Urbancic, T.I., Feigner, B. and Young, R.P. (1992) Influence of source region properties on scaling relations for M<0 events. *Pure and Applied Geophysics*, Vol. 139, No. 3/4, pp.721-739.

van As, A. and Jeffrey, R.G. (2000) Hydraulic fracturing as a cave inducement technique at Northparkes Mines. Proceedings MassMin 2000 (Editor: G. Chitombo), AusIMM, Brisbane, pub. ser. No. 7/2000, pp. 165-172.

van Aswegen, G. and Butler, A.G. (1993) Applications of quantitative seismology in South African gold mines. Proceedings of Rockburst and Seismicity in Mines, (Editor: R.P. Young), A.A. Balkema, pp. 261-266.

Woodward, K. (2011) Investigation of block caving mechanics through the interpolation of seismic occurrence and source parameters. Undergraduate thesis, School of Civil and Resource Engineering, University of Western Australia. pp. 36- 60.

Wyss, M. and Brune, J.N. (1968) Seismic moment, stress and source dimensions for earthquakes in the California-Nevada region. *Journal of Geophysical Research*, Vol.73, pp. 4681-4694.

Appendix A

The seismogenic zone elevation and thickness at the Telfer mine in different periods, month by month. The orange line represents the bottom of the apex of the seismogenic zone for each time period.

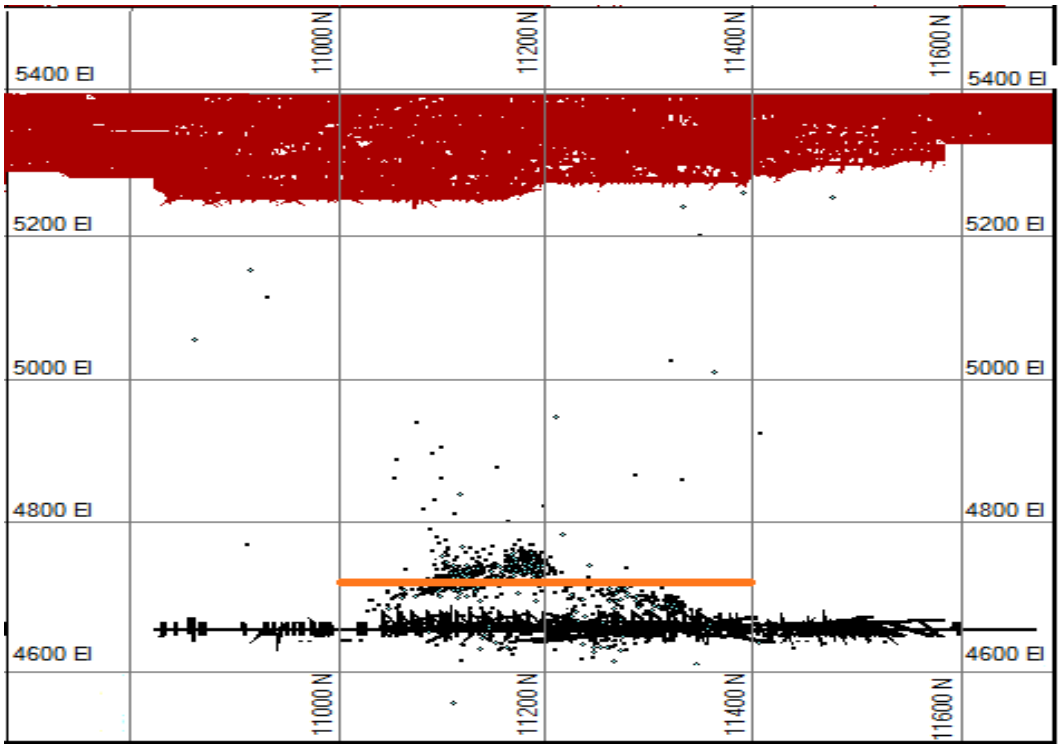

December 2006

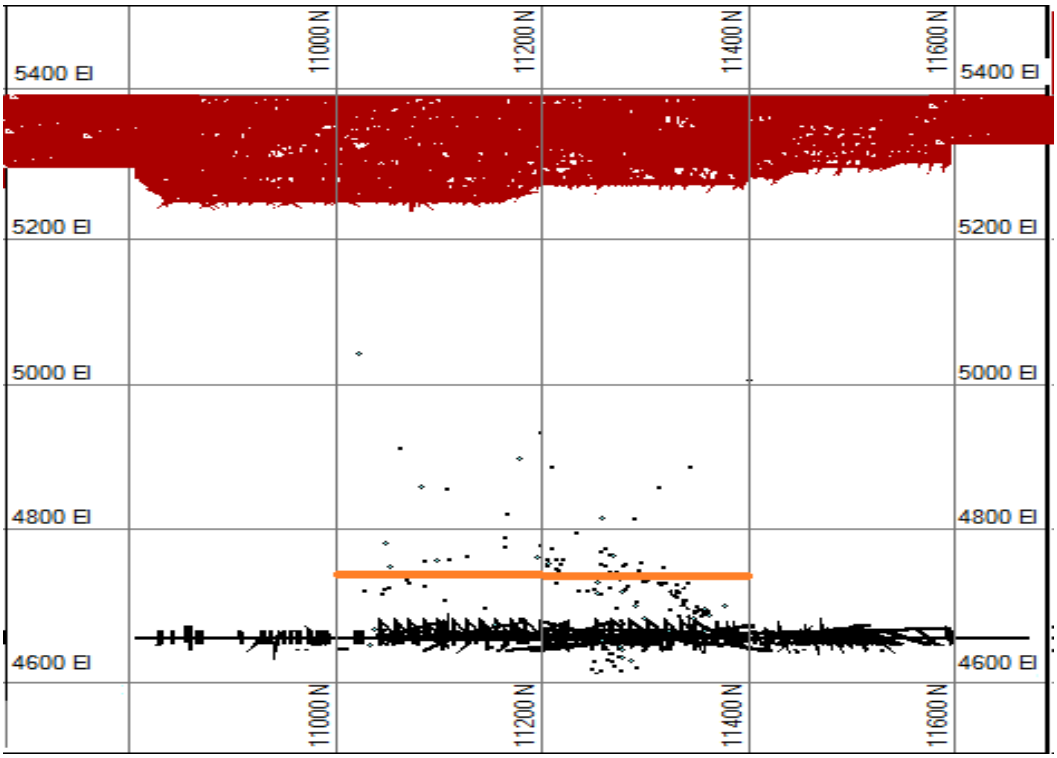

January 2006

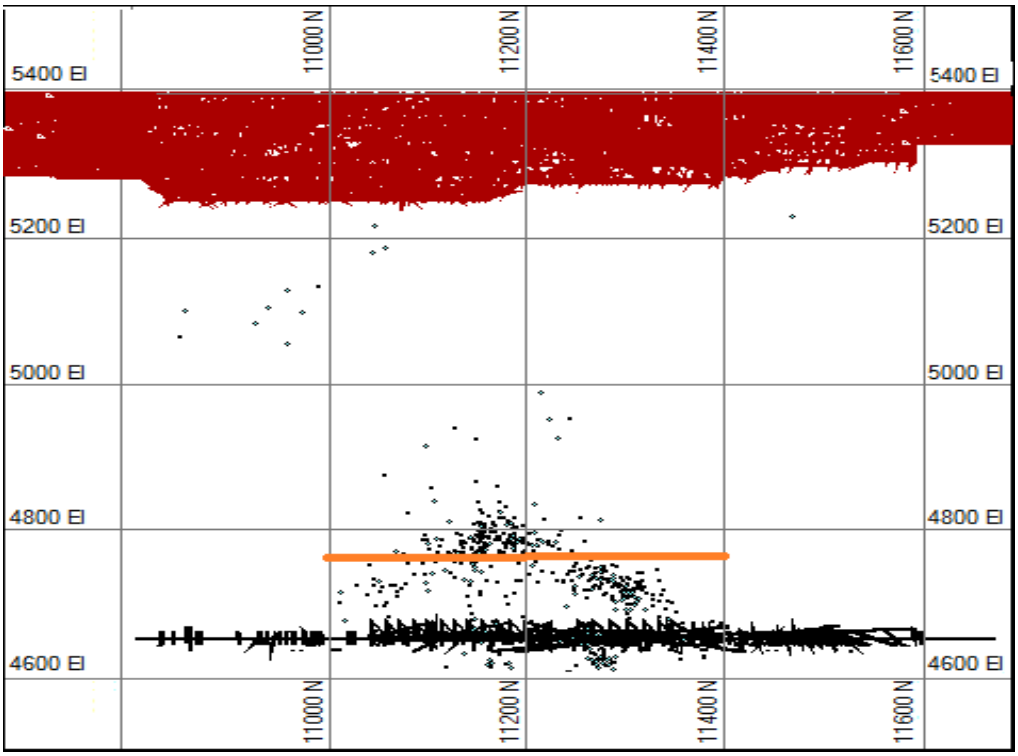

February 2007

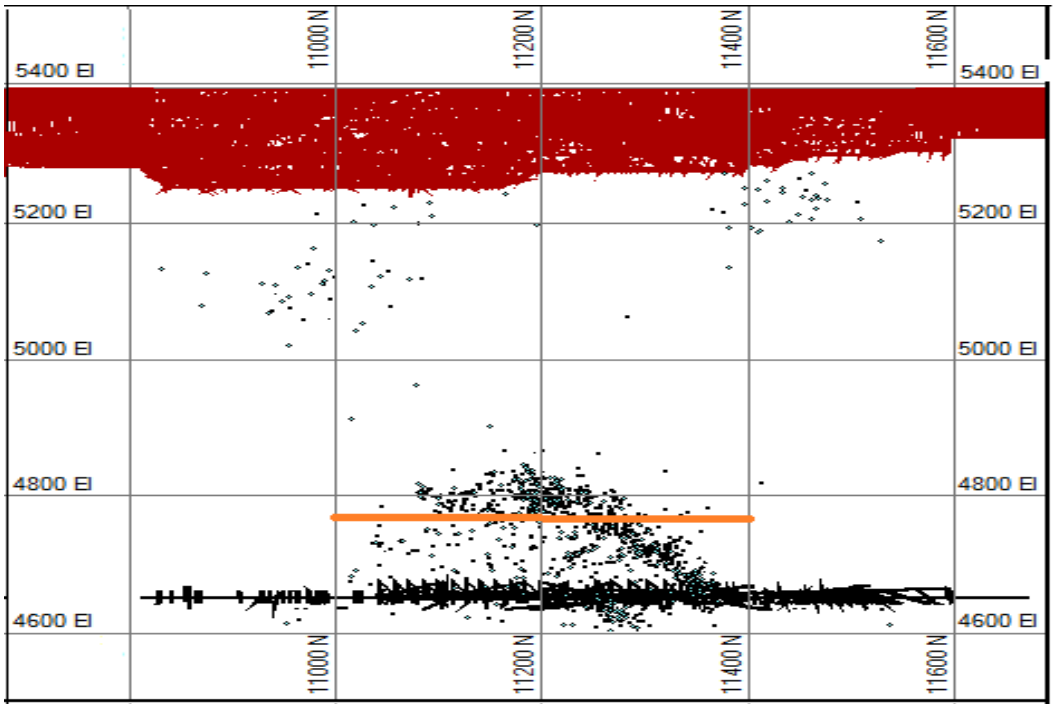

March 2007

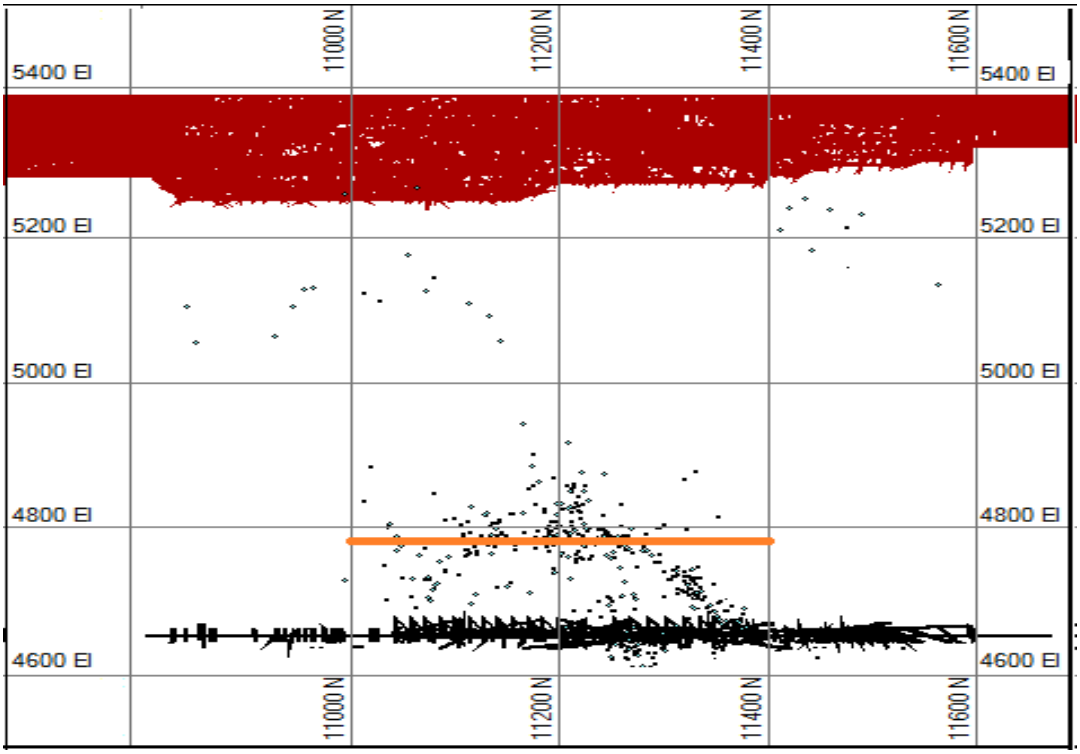

April 2007

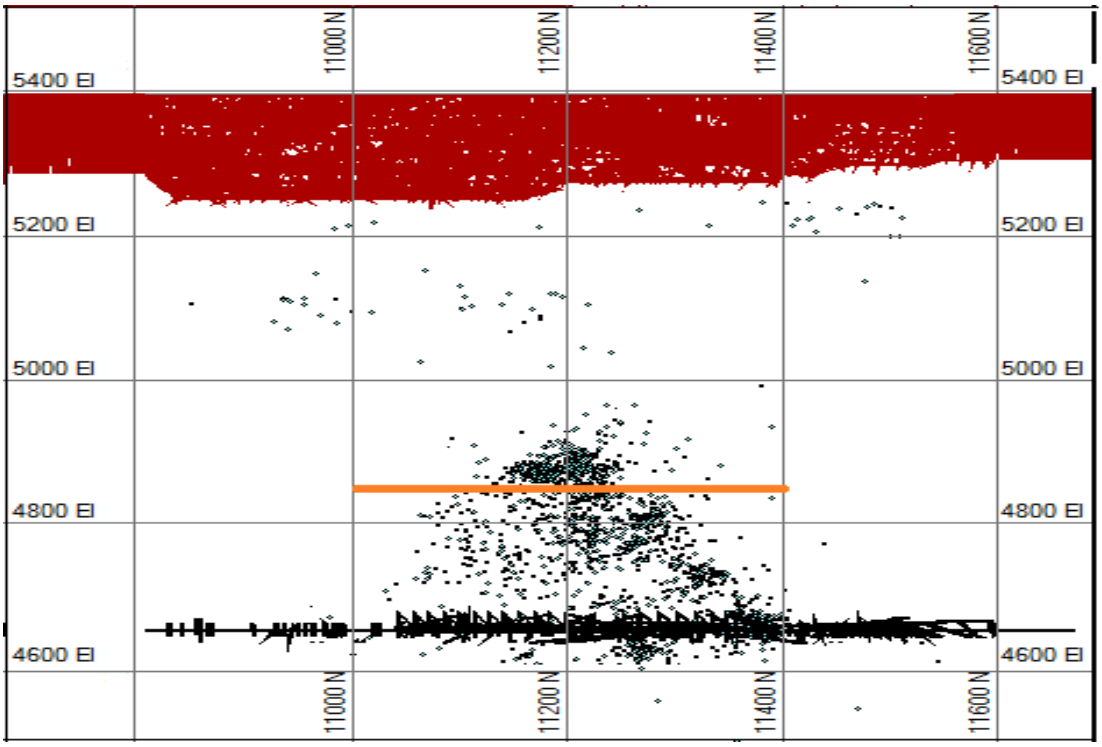

May 2007

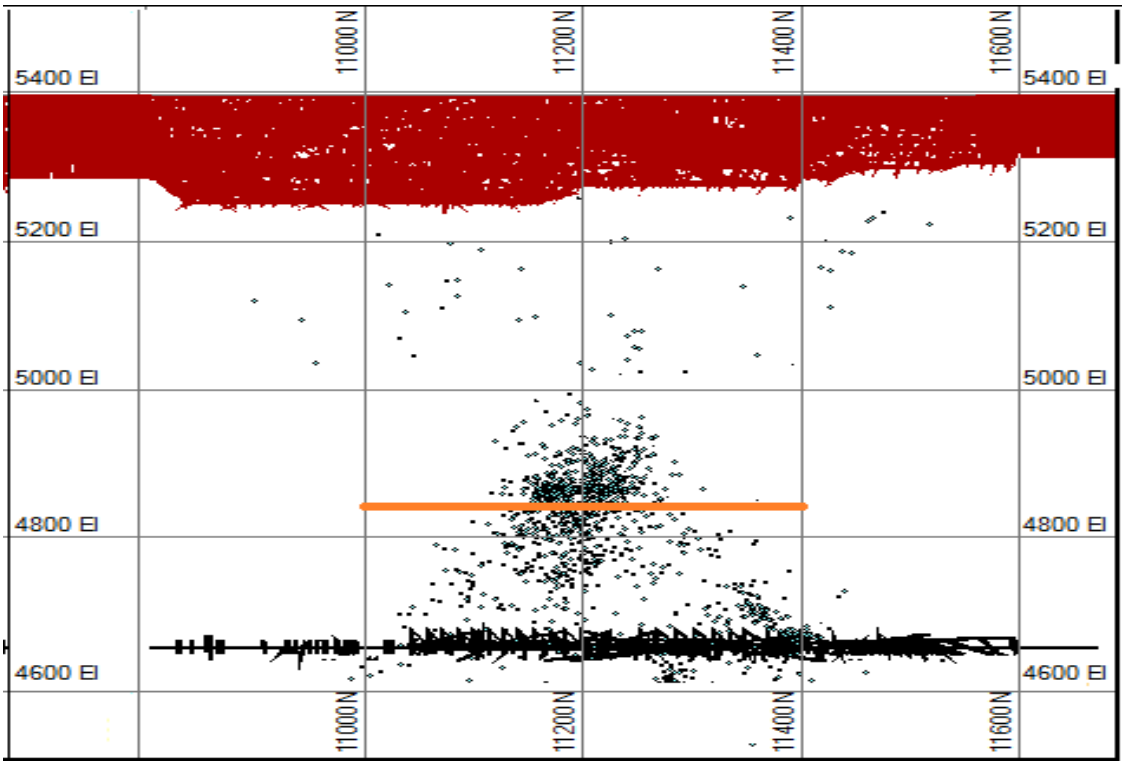

June 2007

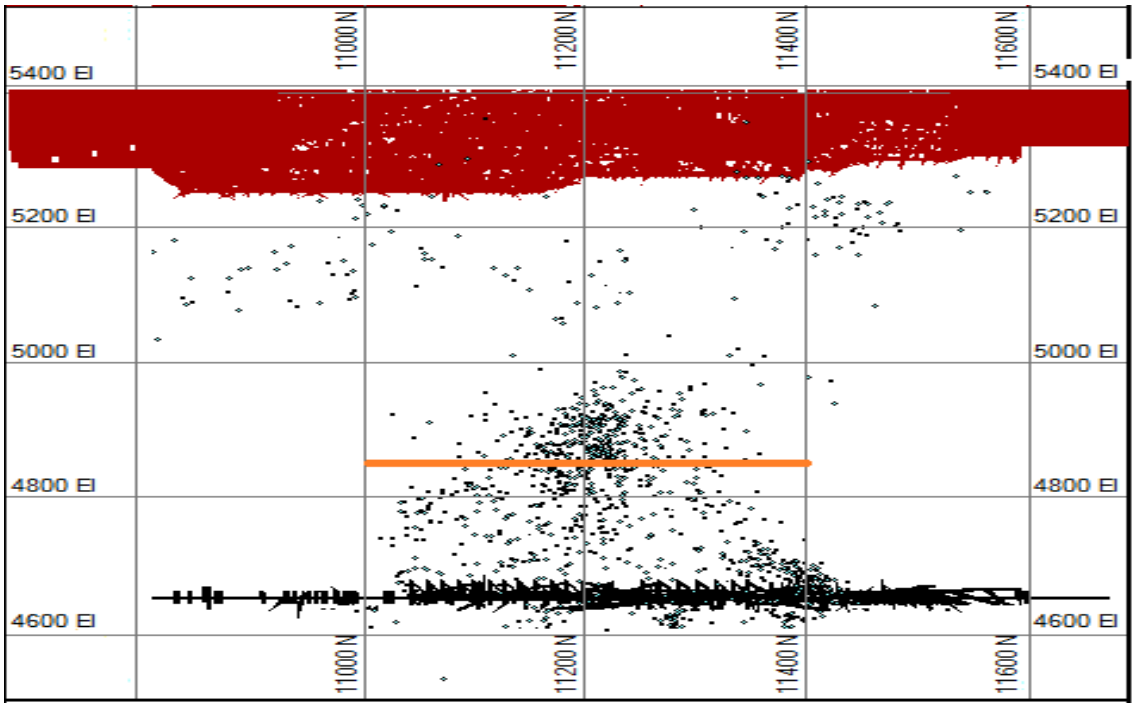

July 2007

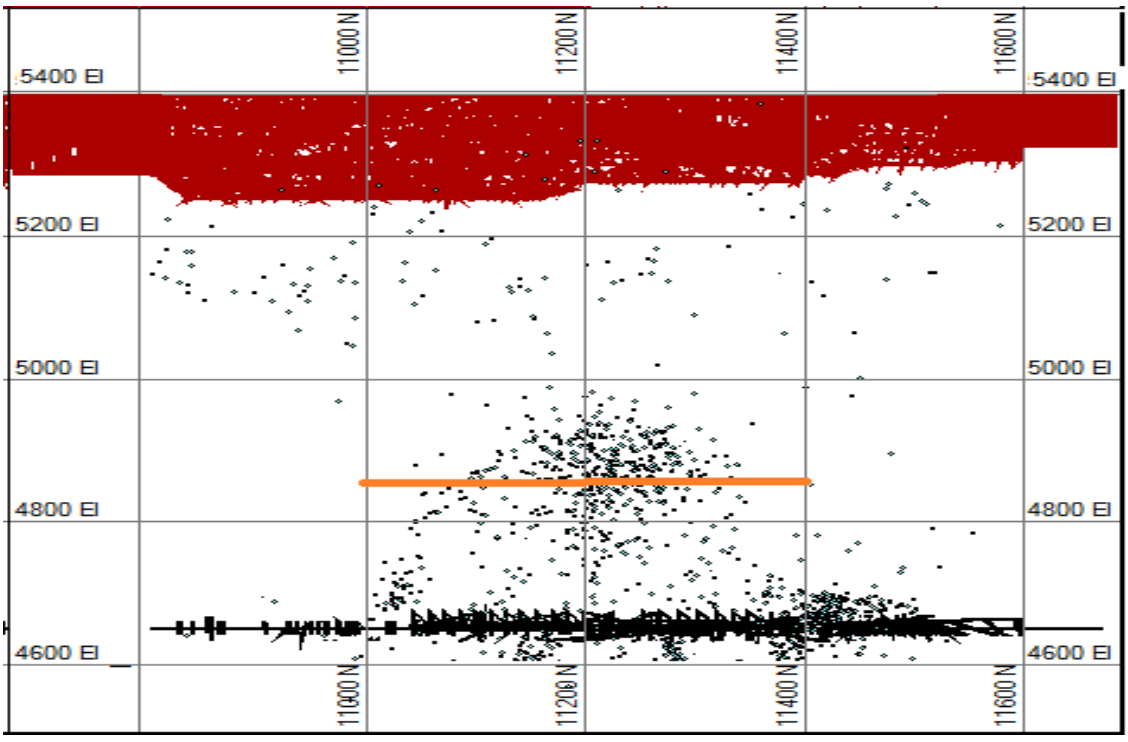

August 2007

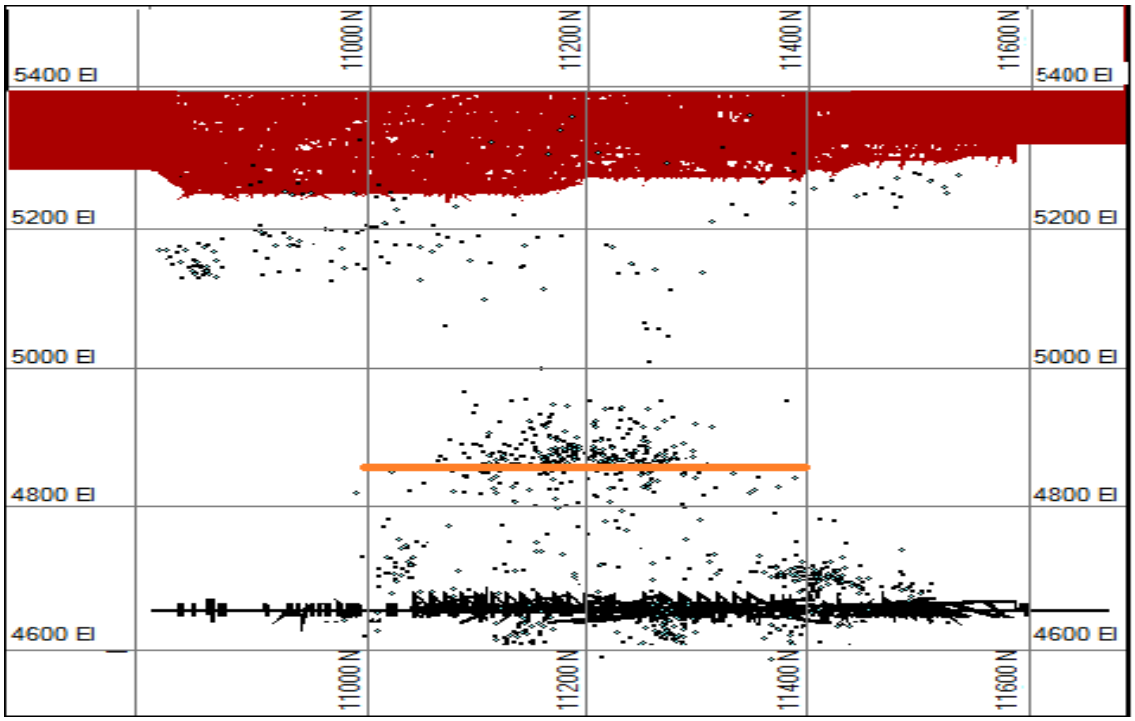

September 2007

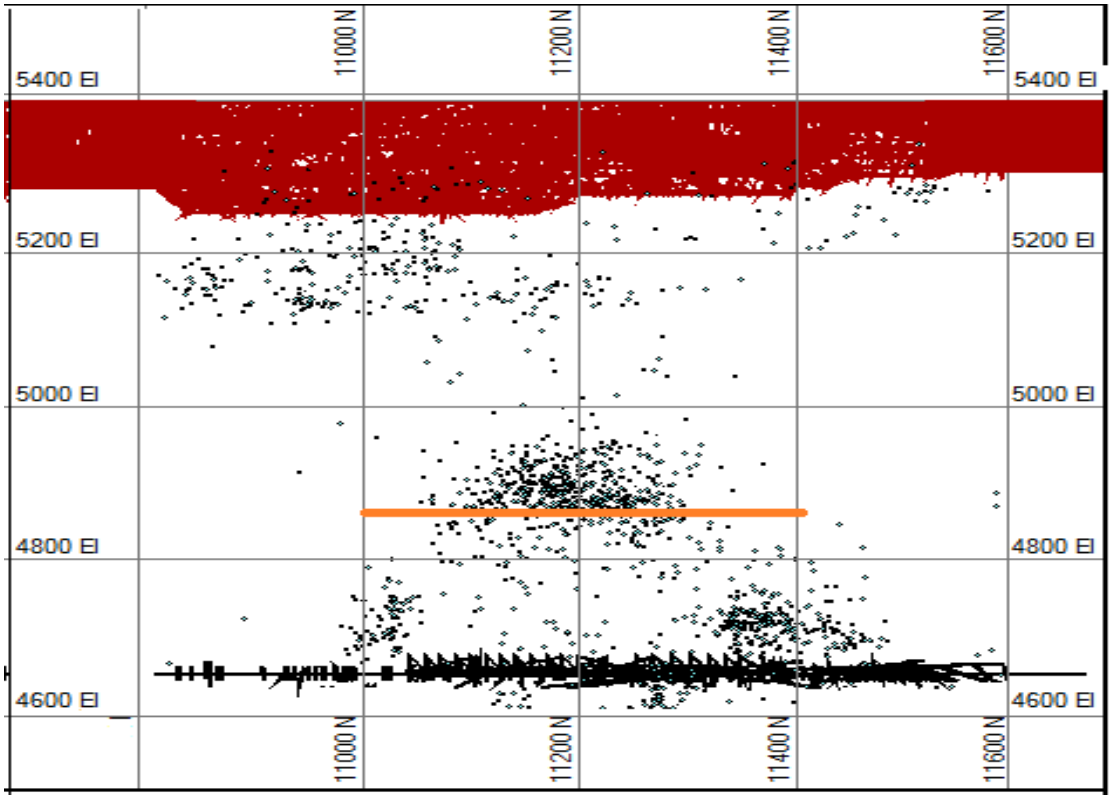

October 2007

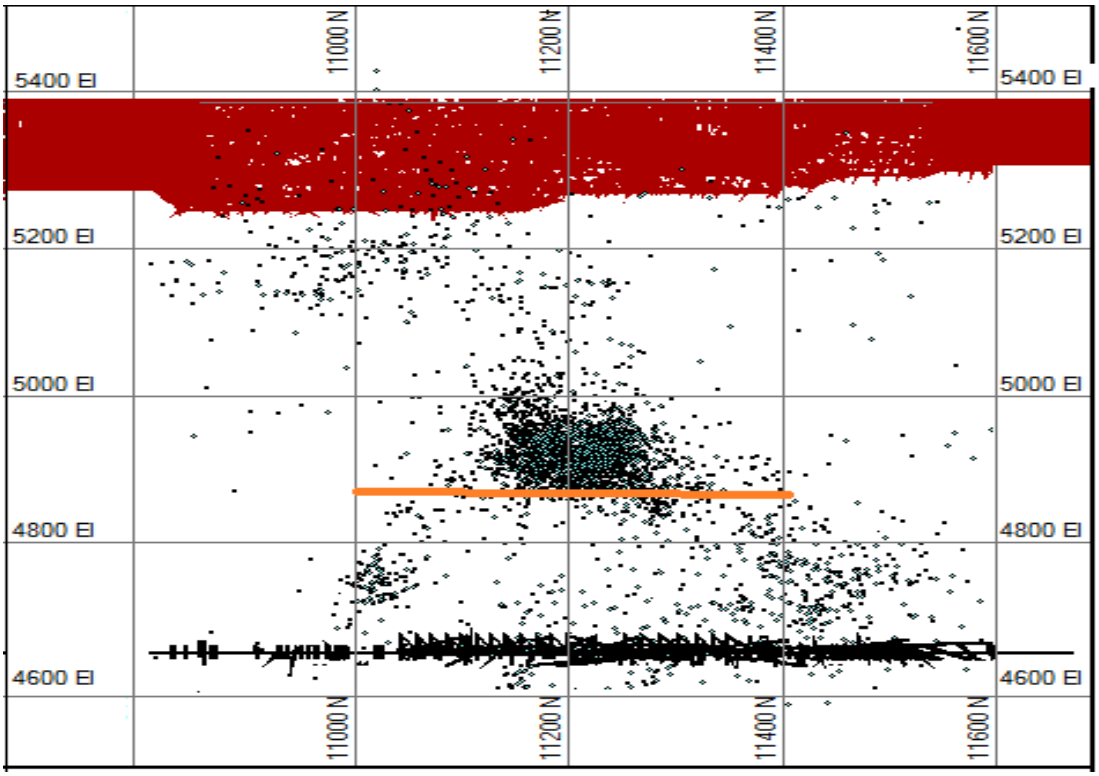

November 2007

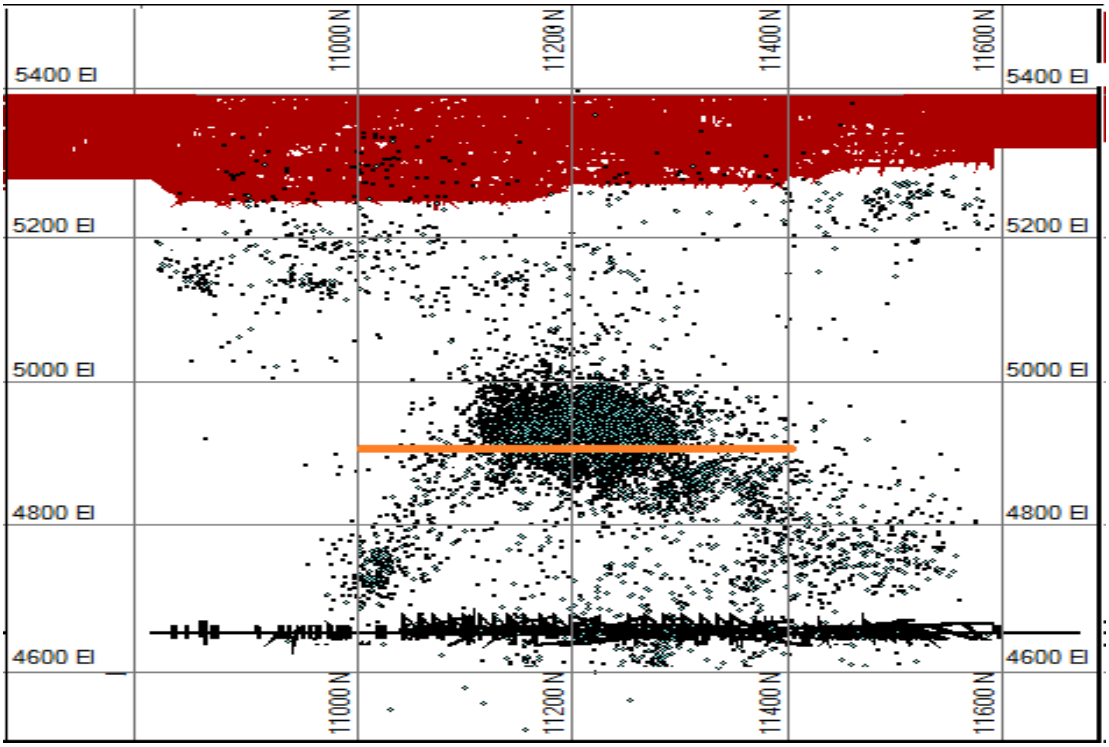

December 2007

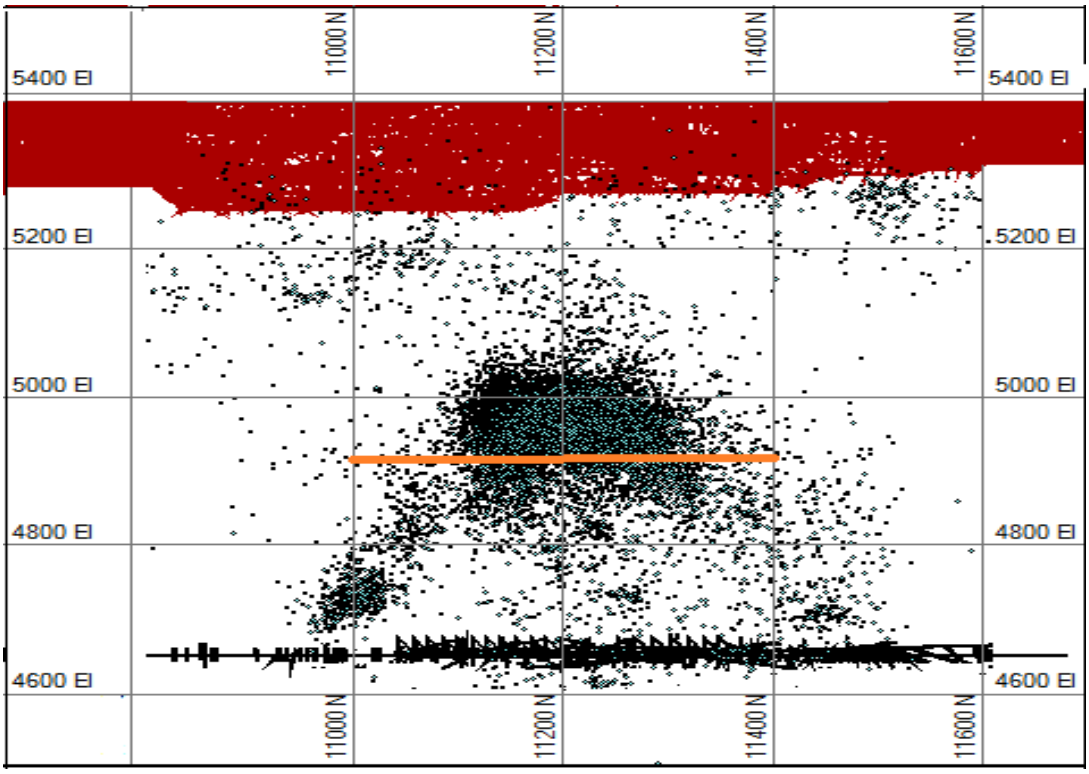

January 2008

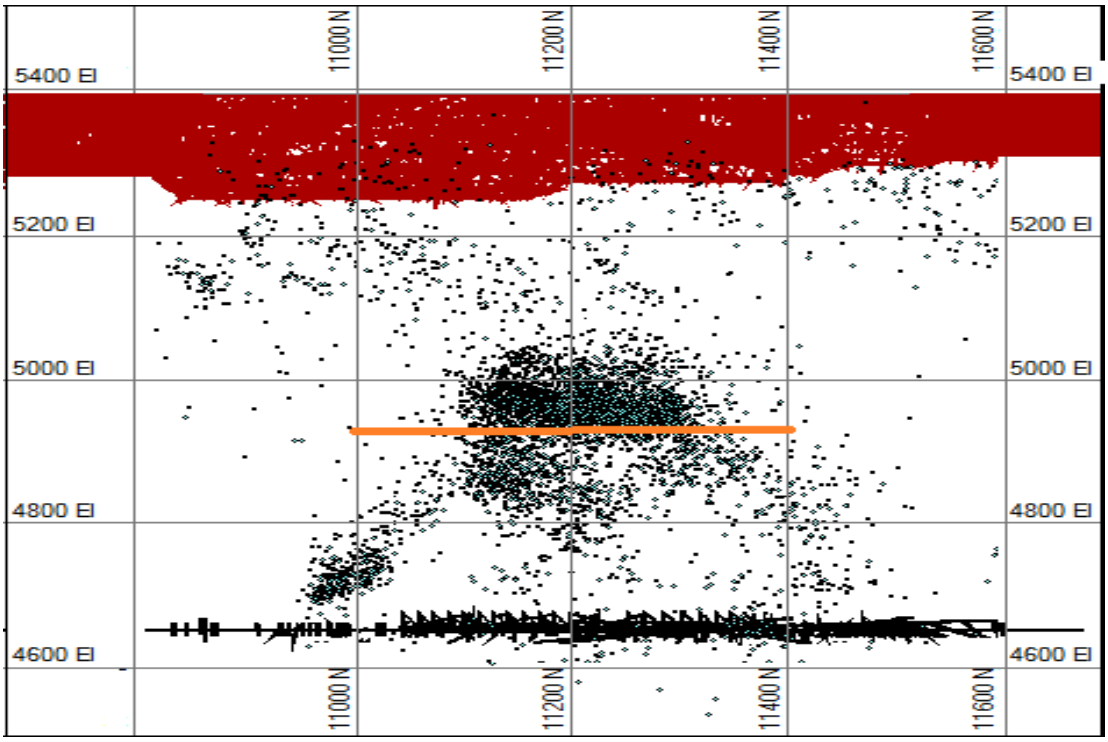

February 2008

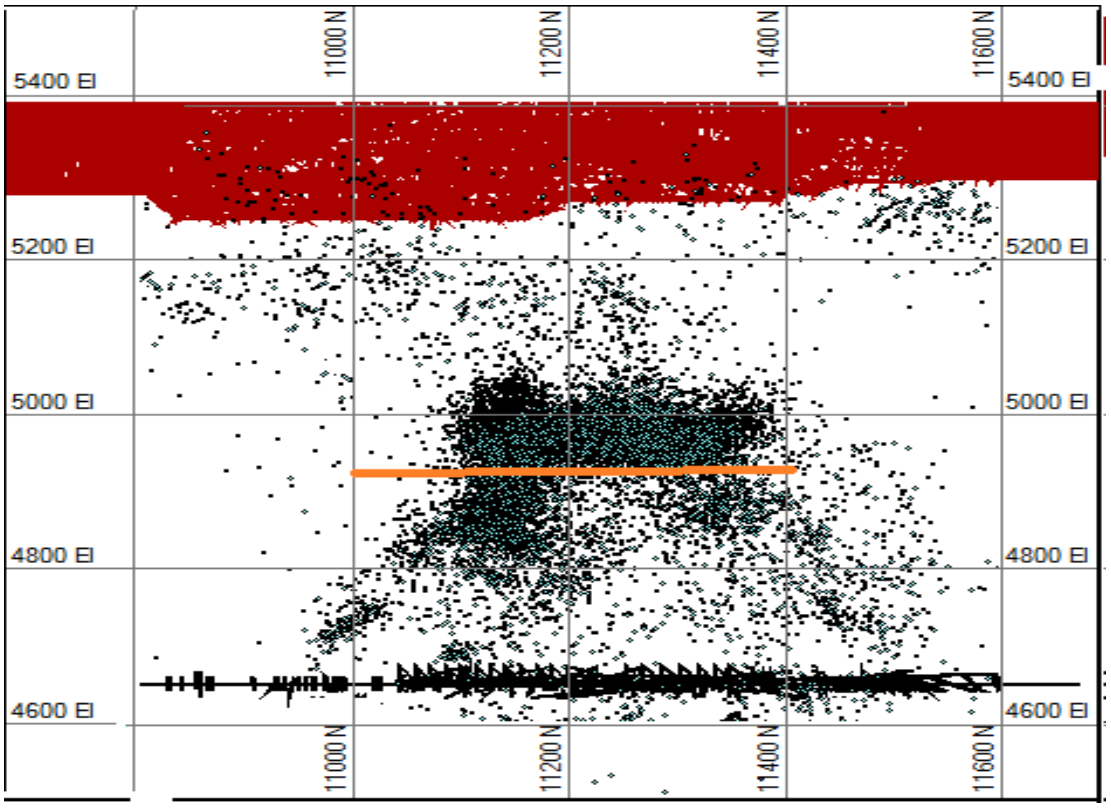

March 2008

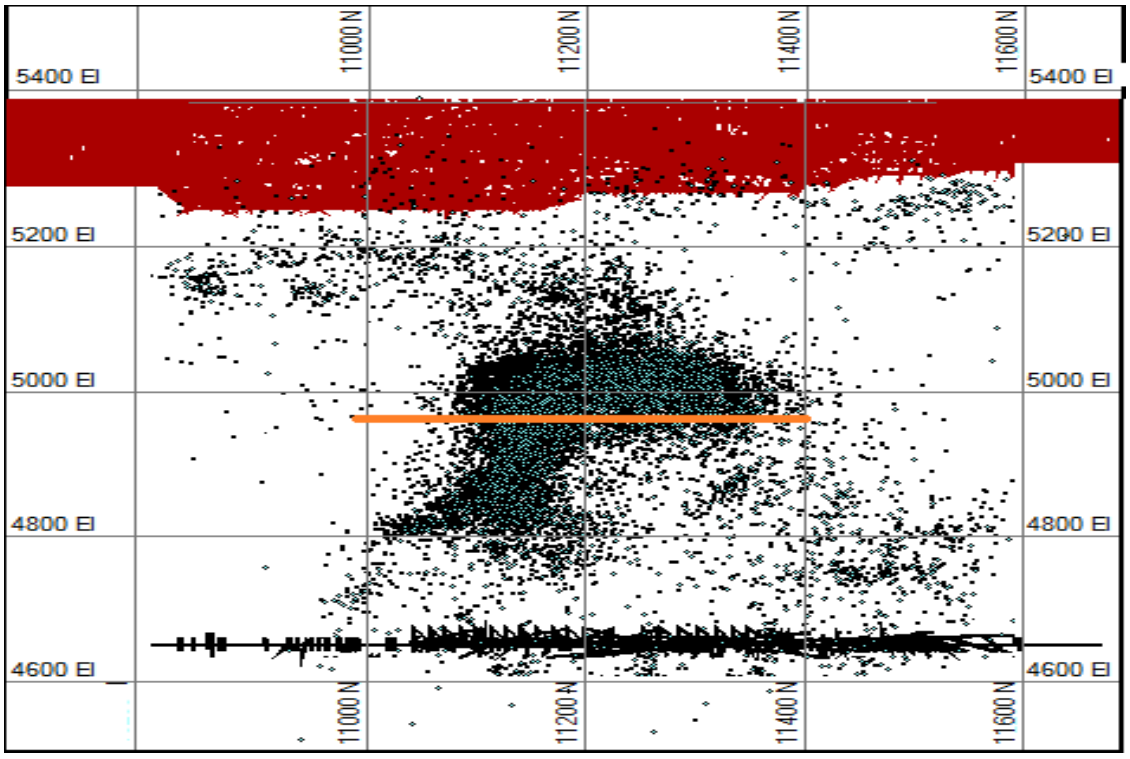

April 2008

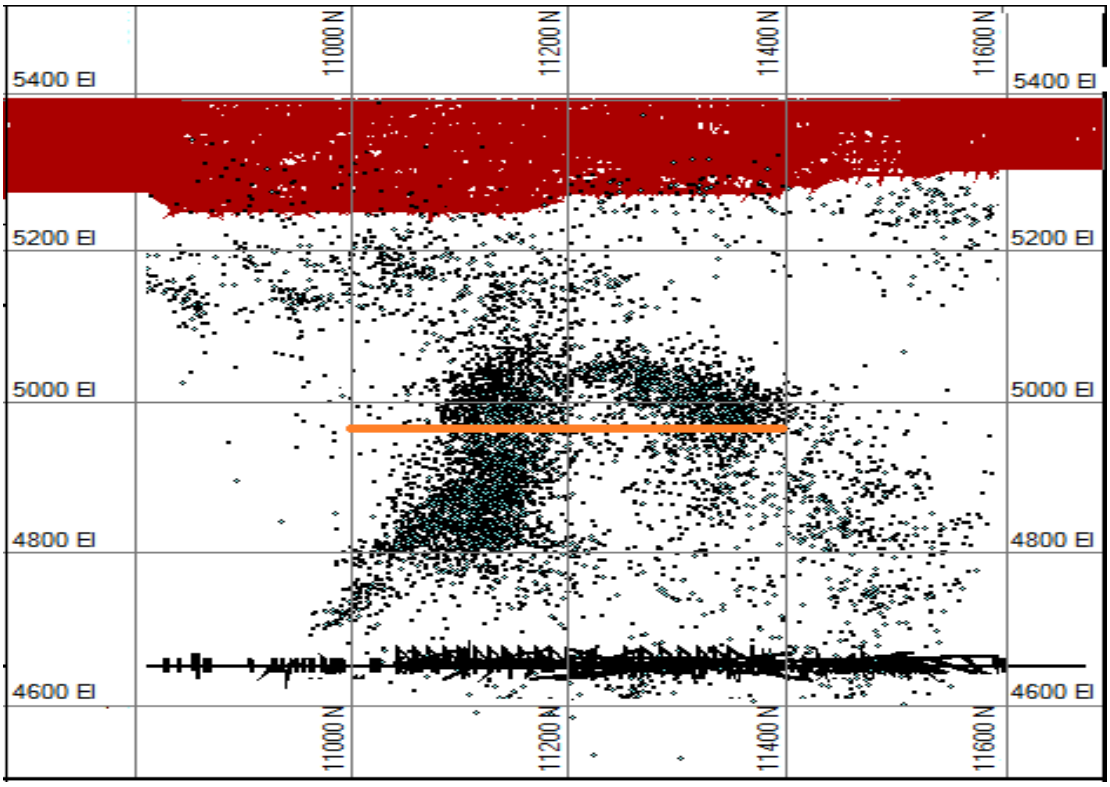

May 2008

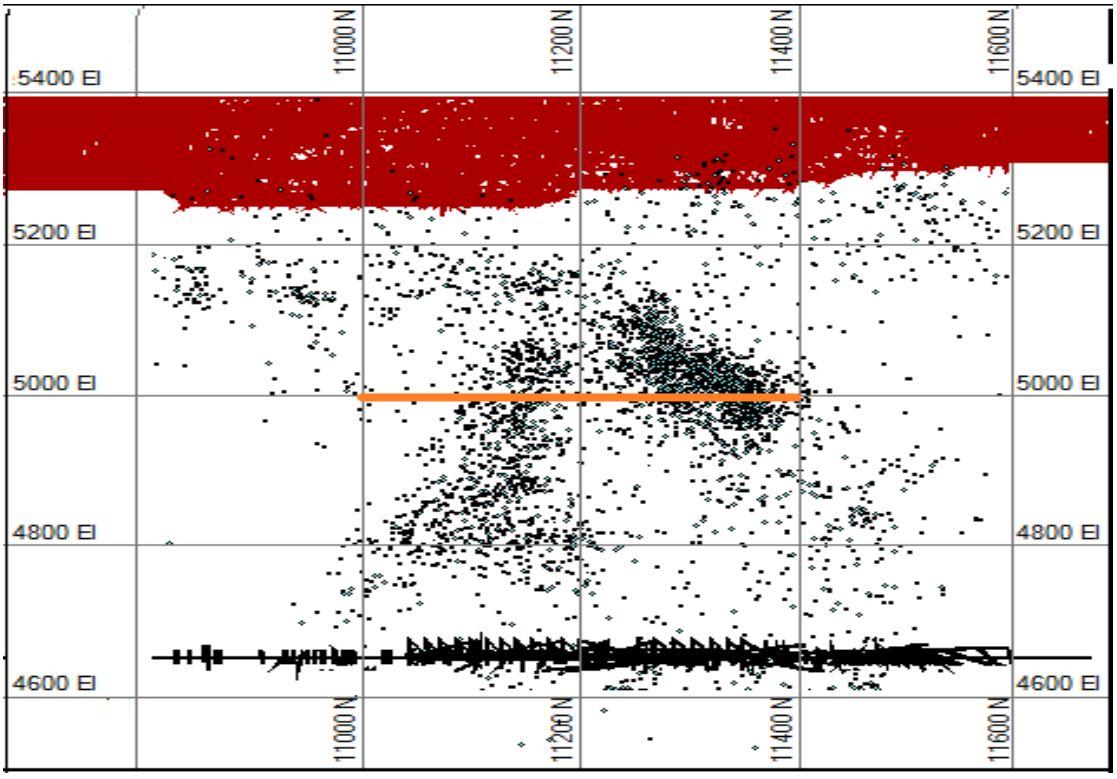

June 2008

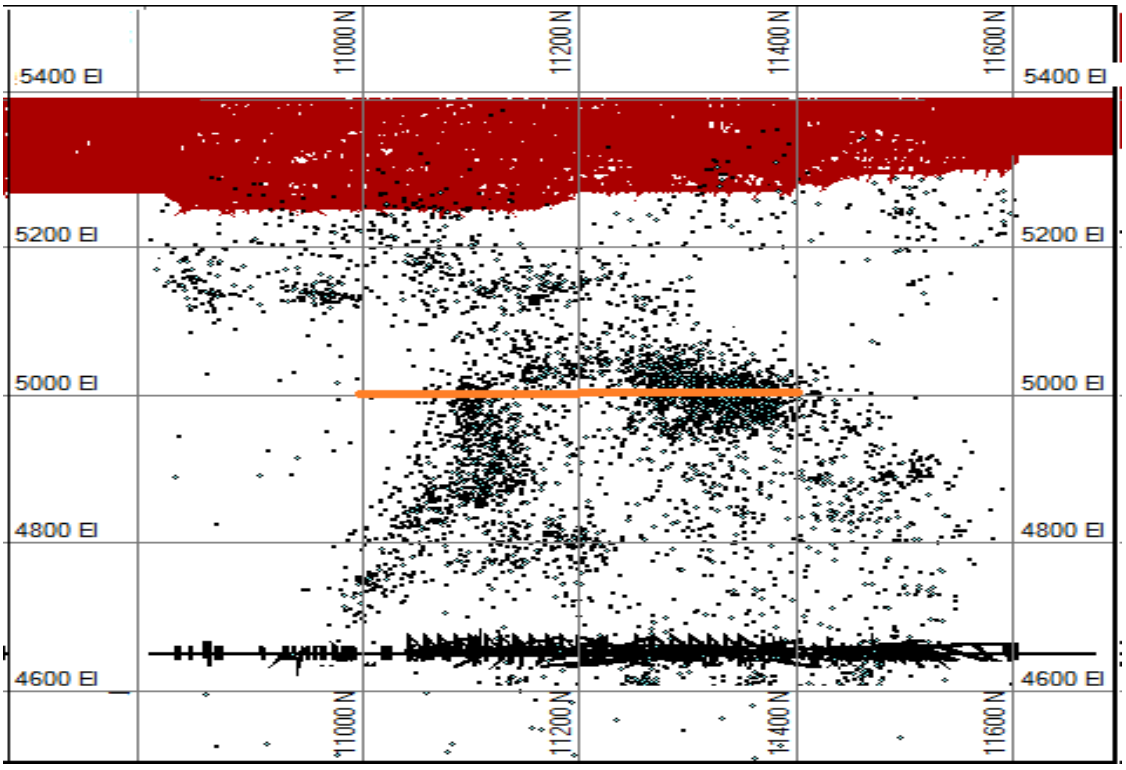

July 2008

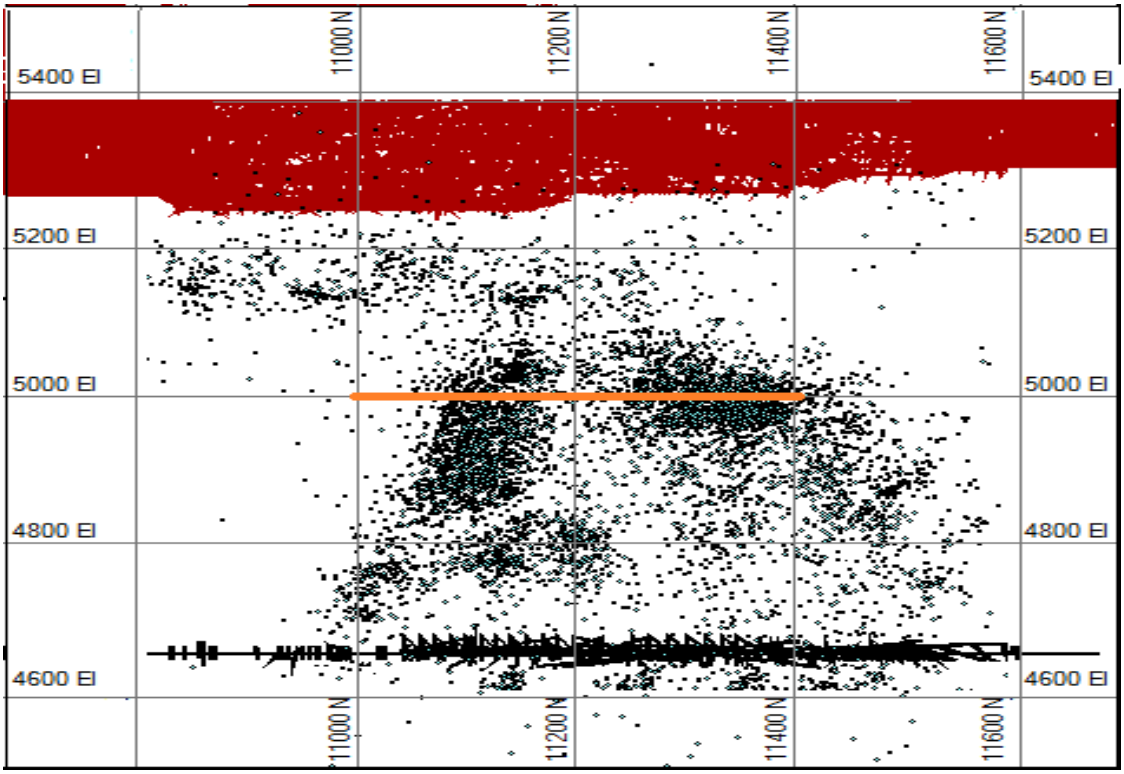

August 2008

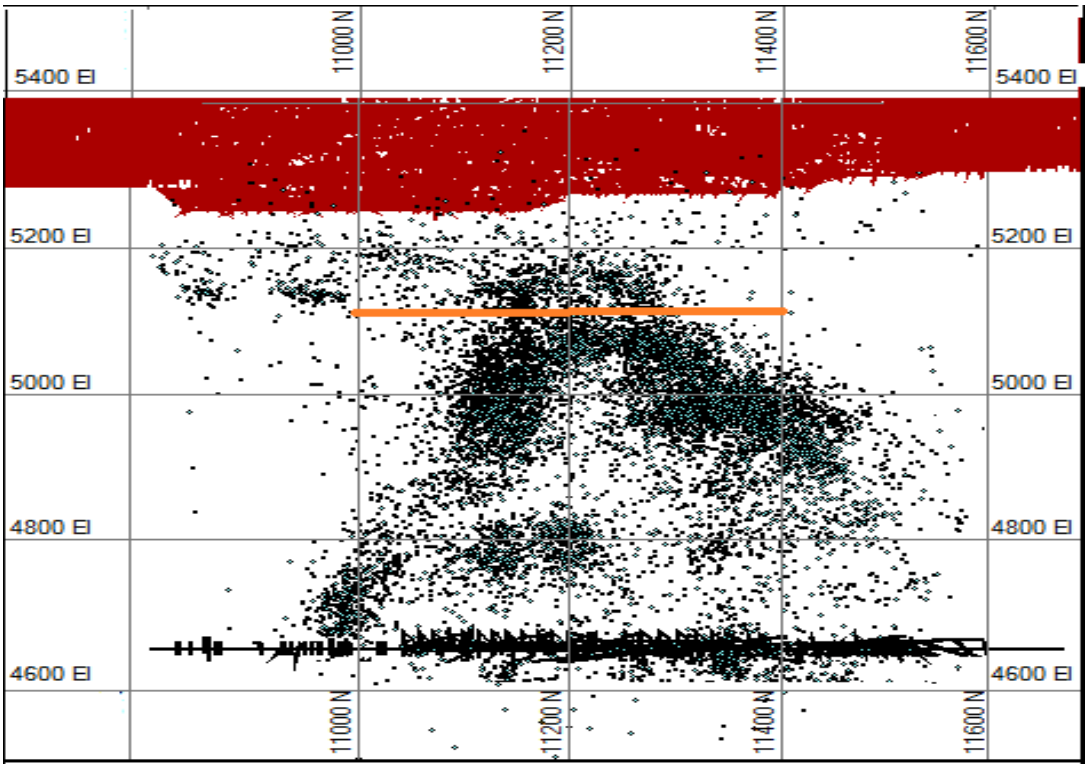

September 2008

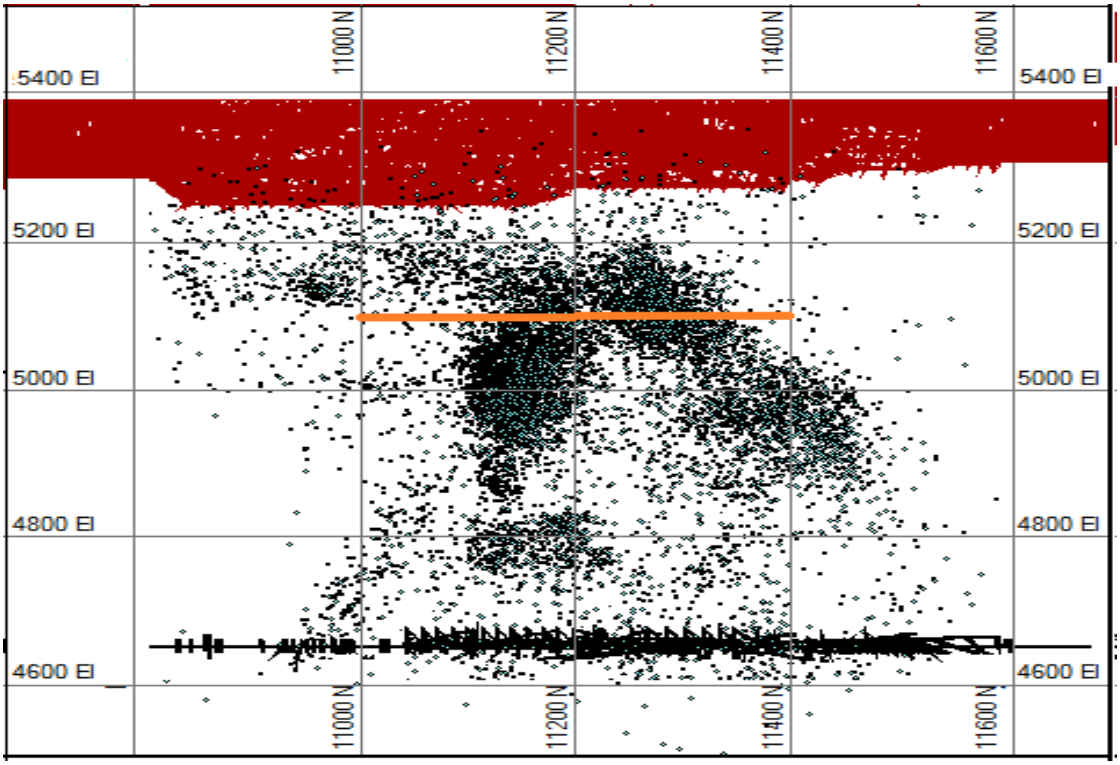

October 2008

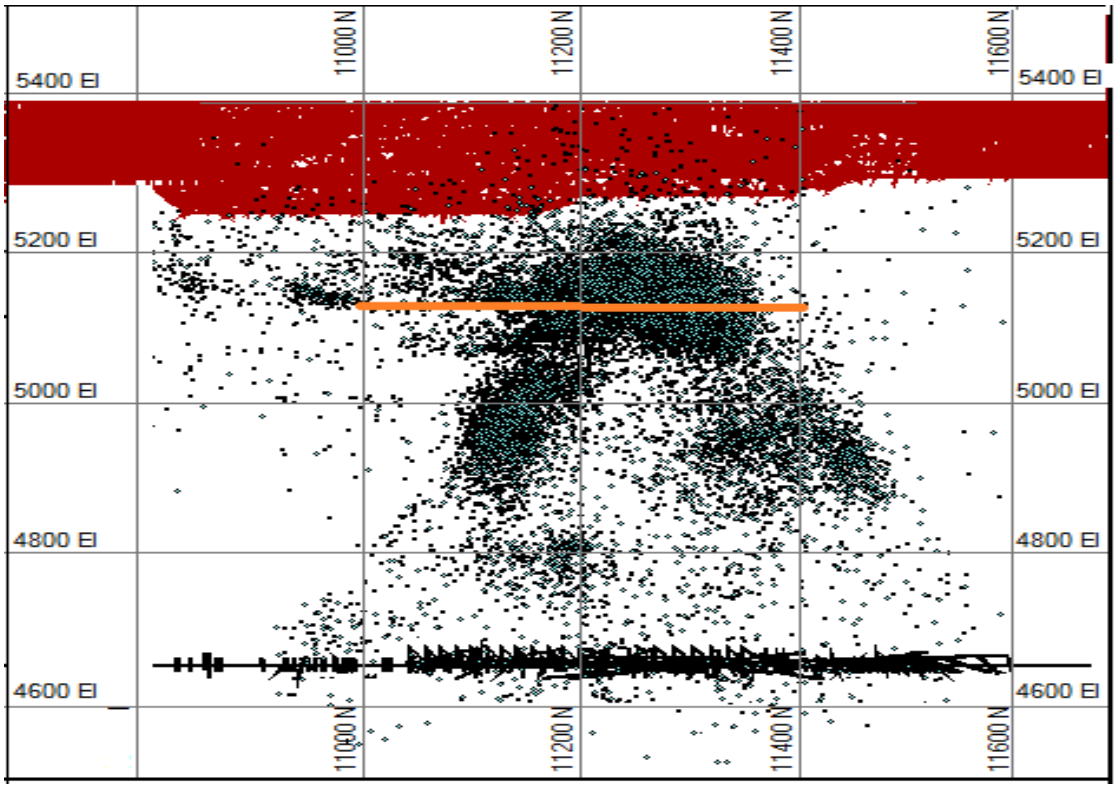

November 2008

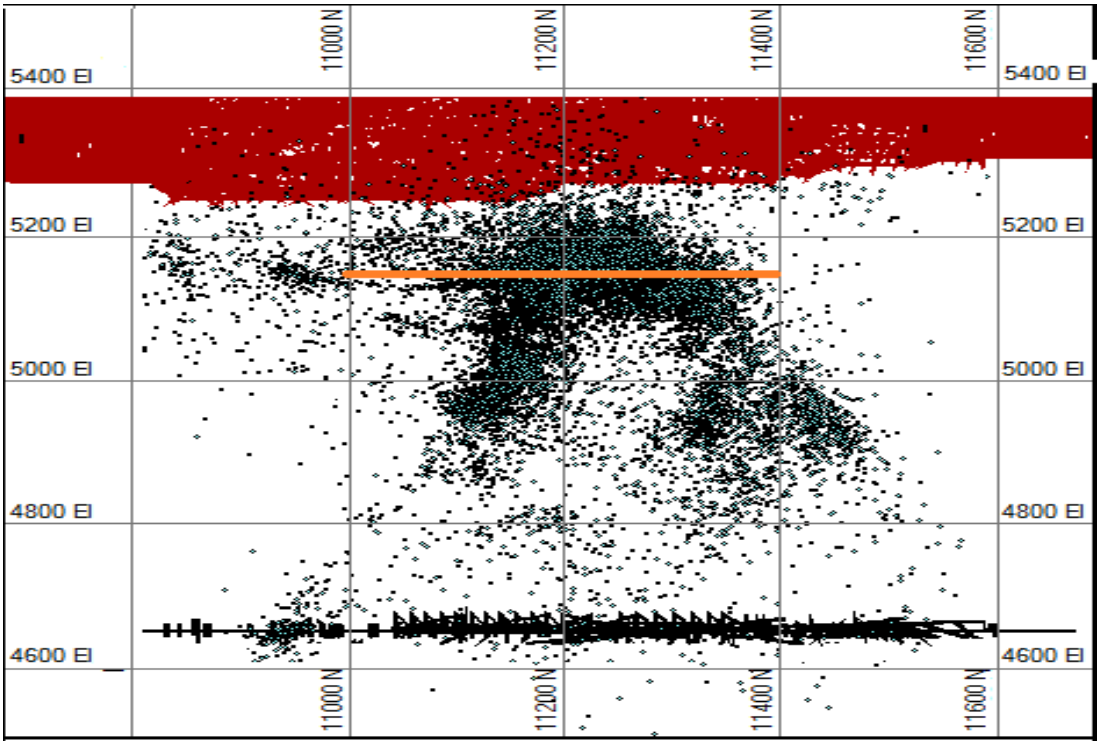

December 2008

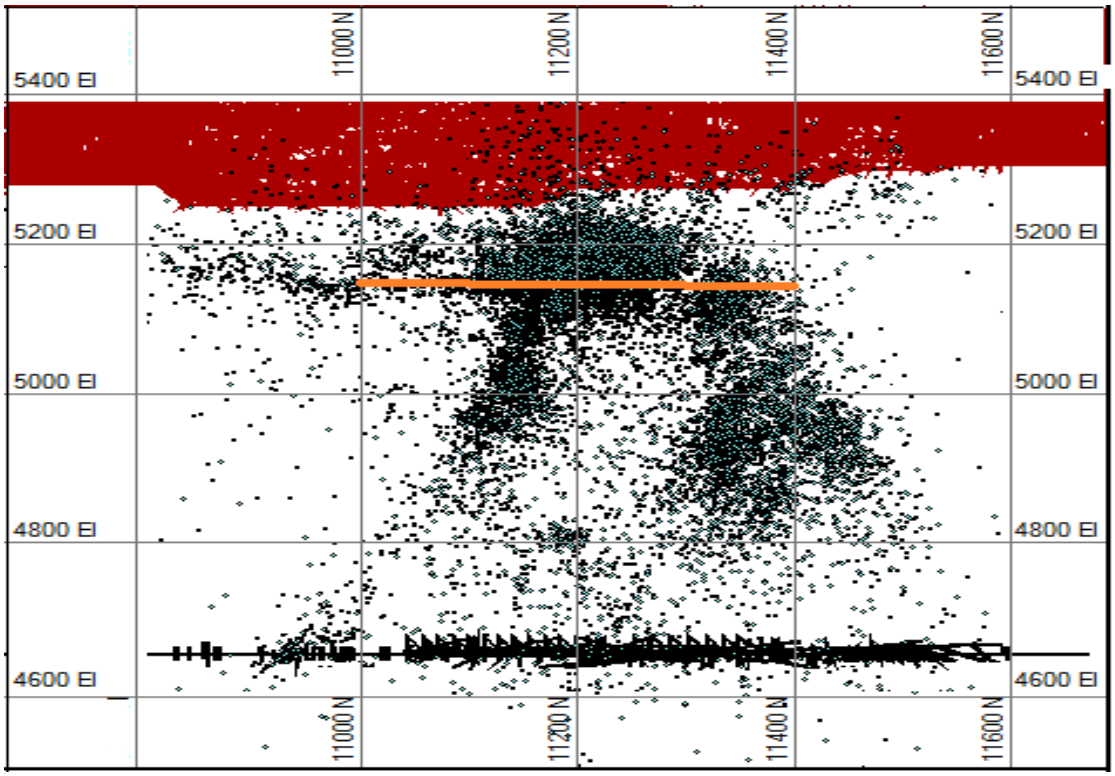

January 2009

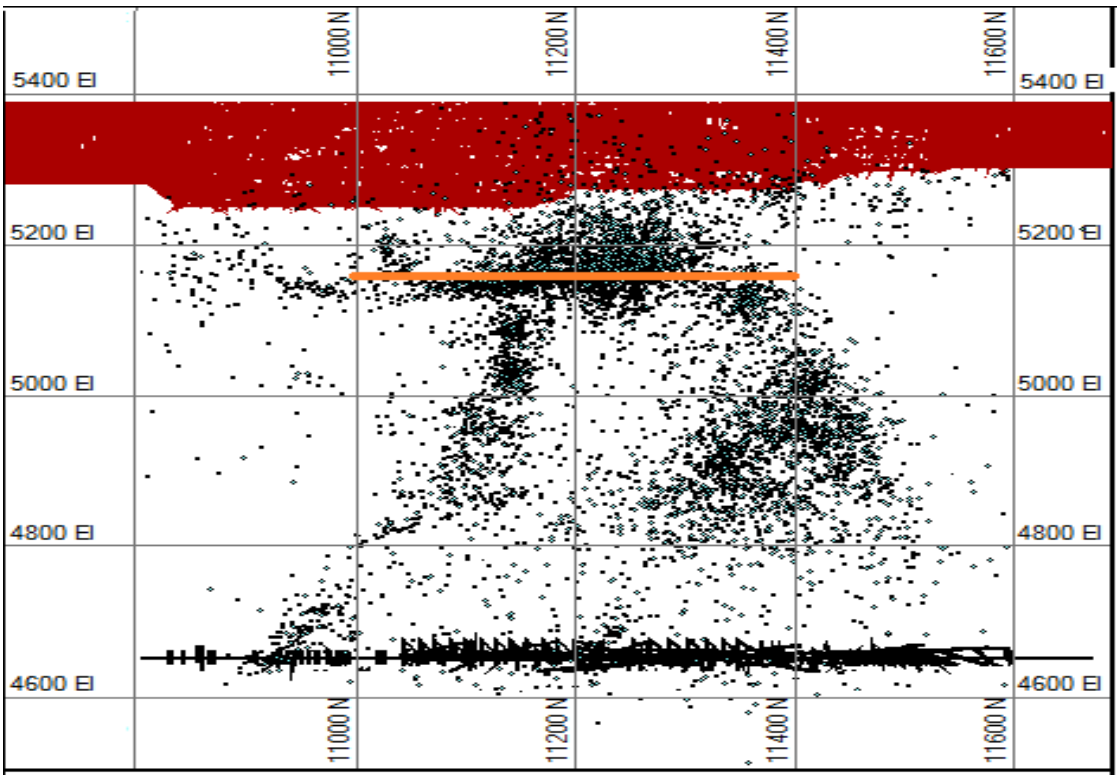

February 2009

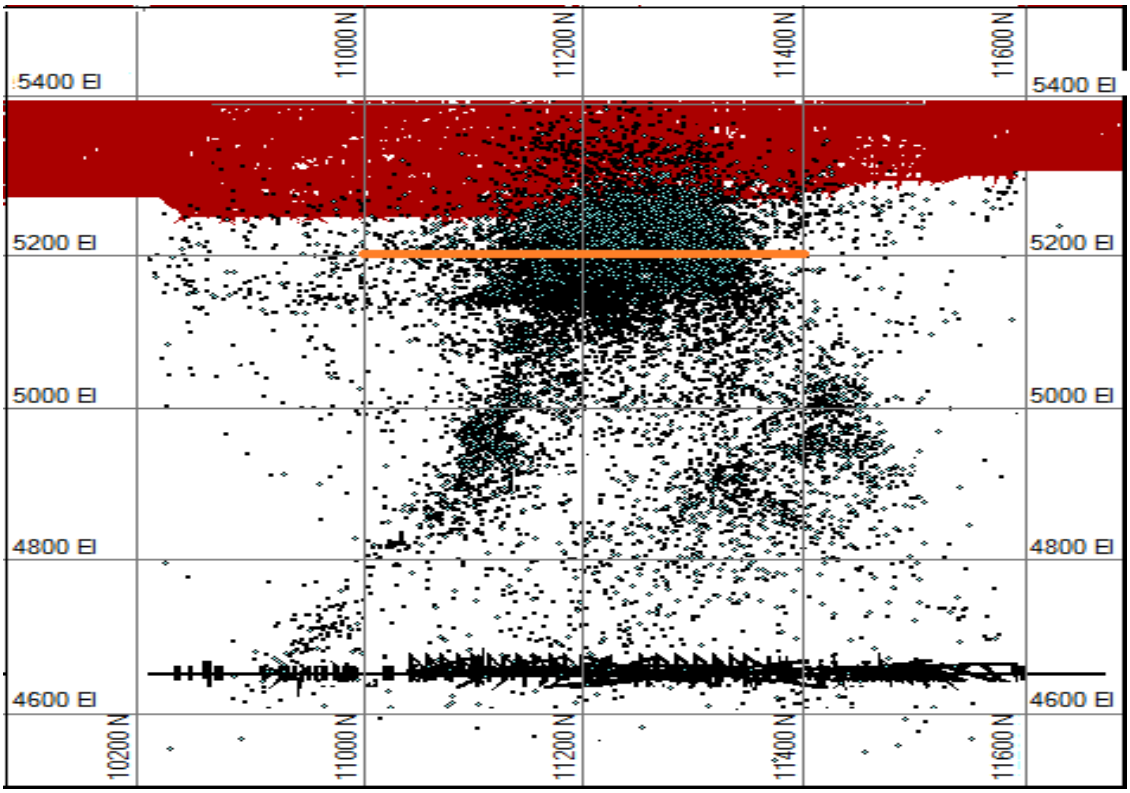

March 2009

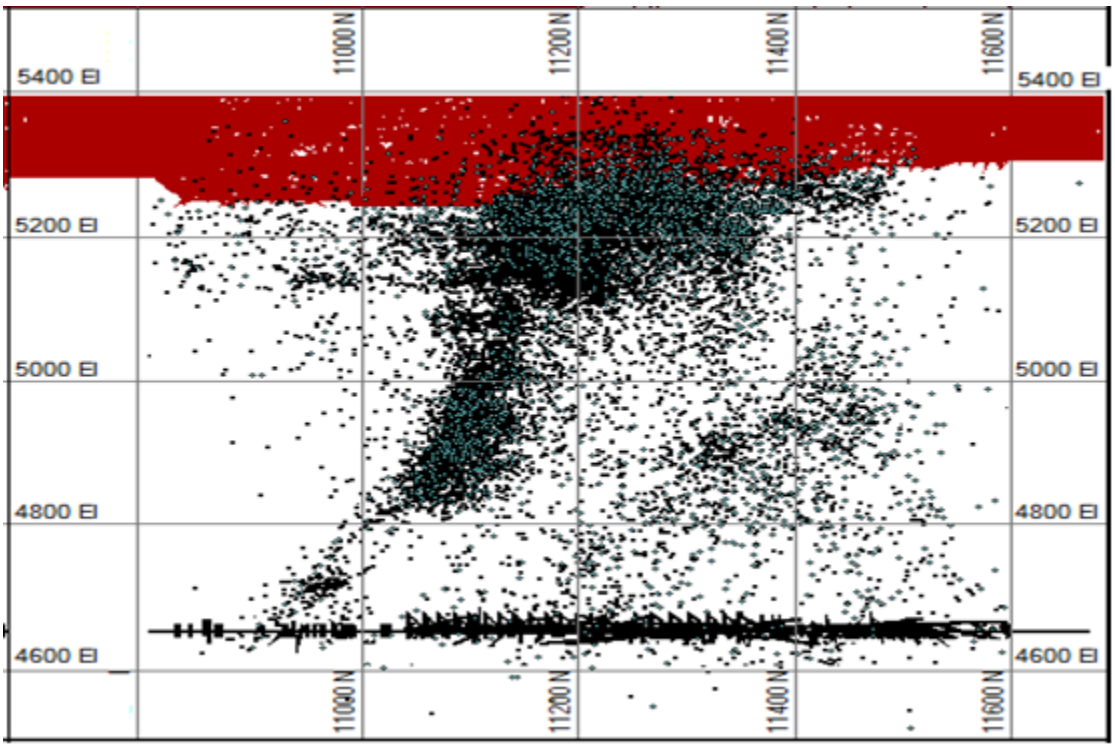

April 2009

Appendix B

The number of the events with different magnitudes in different stages of the cave evolution.

	Selected Events	Date	-2 < M < -1	-1< M< 0	0 < M < +1	+1 < M < +2	M > +2	b-value	a/b
Initial Blasting	All	Mar 06 to Feb 07	2707	587	15	0	0	-1.4	0.9
Cave Initiation	All	Feb 07 to Nov 07	6006	3751	155	11	0	-1.2	1.9
Cave Propagation	Period 1	Nov 07 to Feb 08	21467	7306	260	8	2	-1.4	2.4
	Period 2	Feb 08 to May 08	25671	8579	293	16	2		
	Period 3	May 08 to Feb 09	69898	20994	659	30	1		
	Period 4	Feb 09 to Oct 09	111774	27719	817	32	0		
	All	Nov 07 to Oct 09	228810	64598	2029	86	5		
Breakthrough and Breakback	Period 1	Oct 09 to Nov 09	16565	4870	163	6	0	-1.5	1.9
	Period 2	Nov 09 to Jan 10	23167	6826	271	9	0		
	Period 3	Jan to Nov 10	54219	15250	551	8	0		
	All	Oct 09 to Nov 10	93951	26946	985	23	0		

The event rate, mucking rate, the CAV and the Maximum of the ASF in different stages of the cave evolution.

	Date	Event Rate (npm)	Mucking Rate (tpm)	CAV (m^3 per month)	Apparent Stress (>30kPa, npm)
Initial Blasting	Mar 06 to Feb 07	301	17,600	6.2e+06	69
Cave Initiation	Feb 07 to Nov 07	1093	425,660	1.2e+08	78
Cave Propagation	Nov 07 to Oct 09	12830	464,630	1.3e+09	306
Breakthrough and Breakback	Oct 09 to Nov 10	9378	-	1.1e+09	542

S:P energy ratio comparison of the events with different magnitudes in the different stages of the cave evolution.

		Date	S:P						
				All Events	-2 < M < -1	-1< M< 0	0 < M < +1	+1 < M < +2	M > +2
Initial Blasting		Mar 06 to Feb 07	S:P <3	5%	5%	10%	22%	0%	0%
			S:P>10	52%	55%	32%	8%	0%	0%
Cave Initiation		Feb 07 to Nov 07	S:P <3	22%	18%	22%	31%	60%	0%
			S:P>10	18%	21%	15%	12%	8%	0%
Cave Propagation	Period 1	Nov 07 to Feb 08	S:P <3	12%	10%	12%	26%	18%	50%
			S:P>10	18%	20%	13%	11%	0%	0%
	Period 2	Feb 08 to May 08	S:P <3	15%	14%	16%	35%	60%	0%
			S:P>10	15%	17%	10%	7%	6%	100%
	Period 3	May 08 to Feb 09	S:P <3	17%	15%	25%	35%	25%	60%
			S:P>10	14%	16%	8%	6%	30%	0%
	Period 4	Feb 09 to Oct 09	S:P <3	30%	30%	32%	32%	47%	0%
			S:P>10	15%	15%	15%	14%	9%	0%
	All	Nov 07 to Oct 09	S:P <3	23%	20%	22%	30%	35%	30%
			S:P>10	15%	17%	12%	17%	15%	40%
Breakthrough and Breakback	Period 1	Oct 09 to Nov 09	S:P <3	30%	28%	28%	38%	23%	0%
			S:P>10	17%	17%	18%	16%	17%	0%
	Period 2	Nov 09 to Jan 10	S:P <3	35%	28%	30%	45%	47%	0%
			S:P>10	16%	16%	20%	15%	12%	0%
	Period 3	Jan to Nov 10	S:P <3	25%	22%	22%	30%	60%	0%
			S:P>10	25%	25%	28%	18%	25%	0%
	All	Oct 09 to Nov 10	S:P <3	27%	24%	25%	35%	46%	0%
			S:P>10	22%	21%	22%	18%	18%	0%